

# CIVIL ENGINEERING STUDIES

STRUCTURAL RESEARCH SERIES NO. 541



ISSN: 0069-4274

## SEISMIC DESIGN STUDIES OF LOW-RISE STEEL FRAMES

By  
SCOTT D. SCHIFF  
WILLIAM J. HALL  
DOUGLAS A. FOUTCH

A Technical Report of  
Research Supported by the  
NATIONAL SCIENCE FOUNDATION  
Under Grant No. DFR 84-19191

DEPARTMENT OF CIVIL ENGINEERING  
UNIVERSITY OF ILLINOIS  
AT URBANA-CHAMPAIGN  
URBANA, ILLINOIS  
AUGUST 1988

REPRODUCED BY  
U.S. DEPARTMENT OF COMMERCE  
NATIONAL TECHNICAL INFORMATION SERVICE  
SPRINGFIELD, VA. 22161



<b>REPORT DOCUMENTATION PAGE</b>	<b>1. REPORT NO.</b> UIUC-ENG-88-2004	<b>2.</b>	<b>3. Recipient's Accession No.</b> PB89-117642MS
<b>4. Title and Subtitle</b> SEISMIC DESIGN STUDIES OF LOW-RISE STEEL FRAMES		<b>5. Report Date</b> August 1988	
<b>7. Author(s)</b> S. D. Schiff, W. J. Hall and D. A. Foutch		<b>6.</b>	
<b>9. Performing Organization Name and Address</b> University of Illinois at Urbana-Champaign Department of Civil Engineering 205 N. Mathews Avenue Urbana, IL 61801		<b>8. Performing Organization Rept. No.</b> SRS 541	
<b>12. Sponsoring Organization Name and Address</b> National Science Foundation Washington, D. C. 20550		<b>10. Project/Task/Work Unit No.</b>	
		<b>11. Contract(C) or Grant(G) No.</b> (C) (G) DFR 84-19191	
		<b>13. Type of Report &amp; Period Covered</b> Technical Report	
<b>15. Supplementary Notes</b>		<b>14.</b>	
<b>16. Abstract (Limit: 200 words)</b> <p>In this investigation, the inelastic behavior of low-rise buildings with steel moment-resisting frames providing the lateral resistance for strong ground motions was examined. The inelastic behavior of frames is dependent on several parameters such as design base shear, beam-to-column strength ratio, moment-resisting connection behavior, nonstructural element participation, etc. The influence of these parameters was determined by performing inelastic time-history analyses.</p> <p>The direct design procedure adopted in the 1988 edition of the <u>Uniform Building Code</u> was used in the seismic design of the frames. Provisions regarding the required lateral stiffness of the frame and strength and ductility of the members were used to proportion the columns, beams and panel zones of each lateral force-resisting frame design. The inelastic behavior (maximum story drifts and shears, ductilities, energy dissipation) computed in the time-history analysis of each frame model was compared to the expected behavior characterized by the code.</p> <p>The investigation concludes with observations about the inelastic behavior of the frames with regard to the numerical modelling of the assumed load-deformation behavior. In addition, the structural performance of frames designed with the direct design procedure contained in the 1988 edition of the <u>Uniform Building Code</u> was evaluated</p>			
<b>17. Document Analysis a. Descriptors</b> Earthquake, Resistant Design, Inelastic Behavior, Dynamic Analysis, Building Codes, Structural Modelling			
<b>b. Identifiers/Open-Ended Terms</b>			
<b>c. COSATI Field/Group</b>			
<b>18. Availability Statement</b> Release Unlimited	<b>19. Security Class (This Report)</b> UNCLASSIFIED	<b>21. No. of Pages</b> 237	
	<b>20. Security Class (This Page)</b> UNCLASSIFIED	<b>22. Price</b> A15 \$36.95	





**SEISMIC DESIGN STUDIES  
OF  
LOW-RISE STEEL FRAMES**

**BY**

**SCOTT D. SCHIFF**

**WILLIAM J. HALL**

**DOUGLAS A. FOUTCH**

**A Report on a Research Project Sponsored by the**

**NATIONAL SCIENCE FOUNDATION**

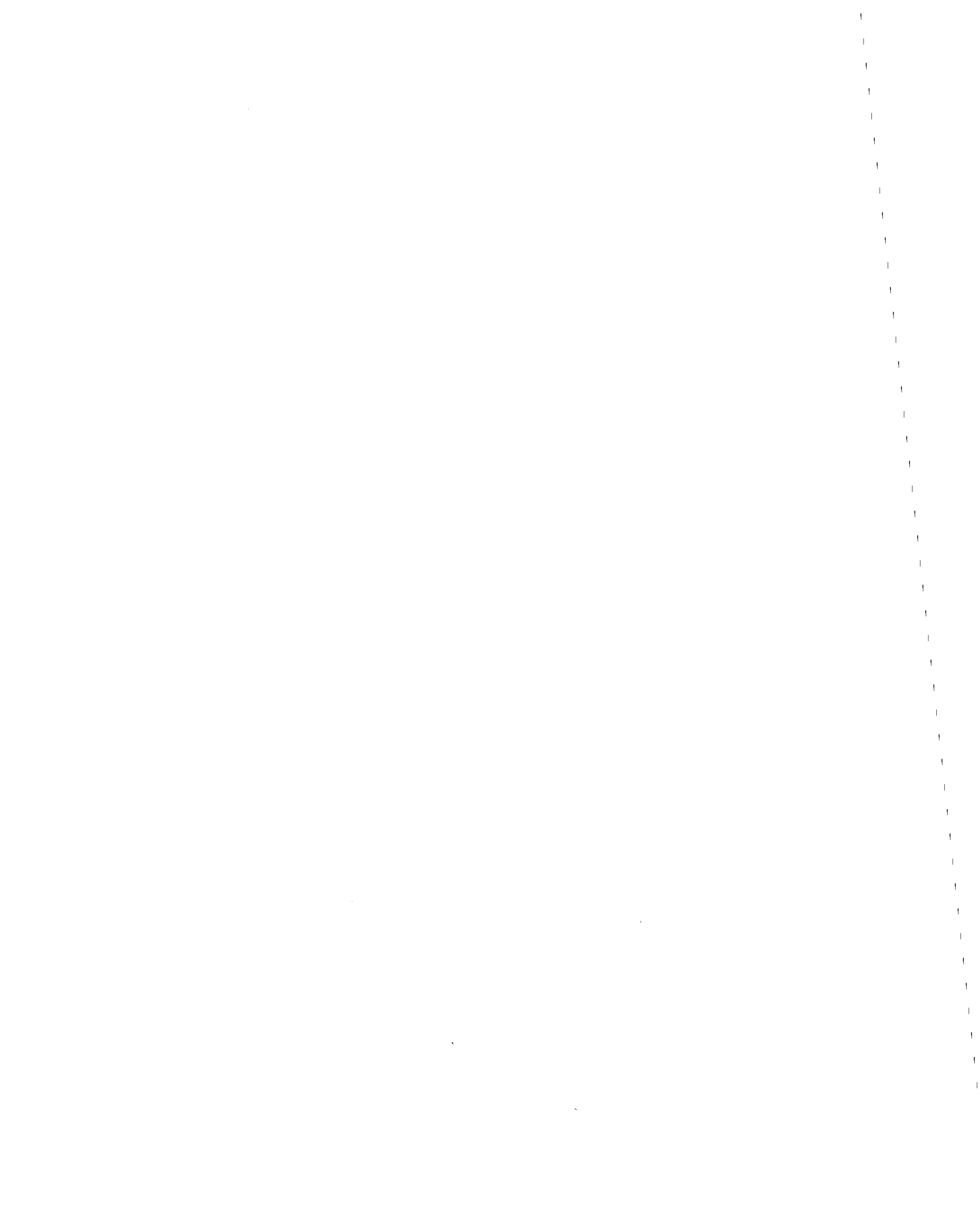
**Research Grant No. DFR 84-19119**

**UNIVERSITY OF ILLINOIS AT URBANA-CHAMPAIGN**

**DEPARTMENT OF CIVIL ENGINEERING**

**URBANA, ILLINOIS**

**AUGUST 1988**



**ABSTRACT****SEISMIC DESIGN STUDIES  
OF  
LOW-RISE STEEL FRAMES**

In this investigation, the inelastic behavior of low-rise buildings with steel moment-resisting frames providing the lateral resistance for strong ground motions was examined. The inelastic behavior of frames is dependent on several parameters such as design base shear, beam-to-column strength ratio, moment-resisting connection behavior, nonstructural element participation, etc. The influence of these parameters was determined by performing inelastic time-history analyses.

The direct design procedure adopted in the 1988 edition of the *Uniform Building Code* was used in the seismic design of the frames. Provisions regarding the required lateral stiffness of the frame and strength and ductility of the members were used to proportion the columns, beams and panel zones of each lateral force-resisting frame design. The inelastic behavior (maximum story drifts and shears, ductilities, energy dissipation) computed in the time-history analysis of each frame model was compared to the expected behavior characterized by the code.

The investigation concludes with observations about the inelastic behavior of the frames with regard to the numerical modelling of the assumed load-deformation behavior. In addition, the structural performance of frames designed with the direct design procedure contained in the 1988 edition of the *Uniform Building Code* was evaluated.

**ACKNOWLEDGMENTS**

This dissertation was prepared by Scott David Schiff and submitted to the Graduate College of the University of Illinois at Urbana-Champaign in partial fulfillment of the requirements for the Doctor of Philosophy degree in Civil Engineering. The dissertation was completed under the supervision of Professors William J. Hall and Douglas A. Foutch.

The investigation was a part of a research program sponsored by the National Science Foundation under grant NSF DFR 84-19191, "Studies Towards New Seismic Design Approaches". Any findings or recommendations expressed in this dissertation are those of the authors and do not necessarily reflect the views of the National Science Foundation. In the latter stages of preparing this dissertation, support was received from the Robert H. Anderson Fellowship in Civil Engineering and is deeply appreciated.

The numerical results were obtained using the DRAIN-2D computer program running on the Harris 800-2 machine of the Department of Civil Engineering. The post-processing of results to produce graphical plots was performed on the Department of Civil Engineering network of Apollo DN3000's and DN4000's workstations and Imagen laser printers. The authors acknowledge the usage of these computer facilities.

The authors wish to thank Professors Leonard A. Lopez, Mete A. Sozen and Narbey Khachaturian for their constructive assistance, suggestions and comments. The authors also are grateful for the contribution provided by Ms. Susan Warsaw in the preparation of the manuscript.

## TABLE OF CONTENTS

CHAPTER	Page
1 INTRODUCTION . . . . .	1
1.1 Background . . . . .	1
1.1.1 Direct Design Procedure for Seismic Forces . . . . .	3
1.1.2 Frame Design and Modelling . . . . .	7
1.1.3 Previous Work . . . . .	10
1.2 Purpose of Study . . . . .	11
1.3 Scope of Report . . . . .	12
2 APPLICATION OF DIRECT DESIGN PROCEDURE FOR STEEL FRAMES . . . . .	14
2.1 Introduction . . . . .	14
2.2 Determination of Equivalent Lateral Forces . . . . .	15
2.3 Stiffness, Strength and Ductility Requirements . . . . .	21
2.4 Equivalent Lateral Forces and Member Selections . . . . .	24
2.4.1 Five-Story Frame Designs: D1A and D1B . . . . .	26
2.4.2 Five-Story Frame Designs: D2A, D2B and D2C . . . . .	31
2.4.3 Five-Story Frame Design: D3 . . . . .	37
2.4.4 Two-Story Frame Design: D4 . . . . .	39
2.5 Summary . . . . .	41
3 ANALYSIS AND MODELLING OF FRAME STRUCTURES . . . . .	43
3.1 Introduction . . . . .	43
3.2 Analysis Approach . . . . .	43
3.3 Representation of Design Earthquake . . . . .	44
3.4 Beam-to-Column Connection Modelling . . . . .	51
3.4.1 Rigid Connection Behavior . . . . .	53
3.4.2 Flexible Connection Behavior . . . . .	57
3.5 Nonstructural Element Participation . . . . .	64
3.5.1 Linear Load-Deformation Behavior . . . . .	66
3.5.2 Trilinear Load-Deformation Behavior . . . . .	67
3.6 P-Delta Effects . . . . .	70
3.7 Development of Numerical Models . . . . .	71

	Page
4 PARAMETRIC STUDIES AND RESULTS . . . . .	74
4.1 Introduction . . . . .	74
4.2 Selection and Presentation of Output Data . . . . .	76
4.3 Influence of Ground Motion on Structural Response . . . . .	78
4.4 Development of Parametric Studies . . . . .	81
4.4.1 Investigation of Beam-to-Column Strength Ratio . . . . .	83
4.4.2 Investigation of Beam-to-Column Connection Behavior . . . . .	94
4.4.3 Investigation of Nonstructural Element Participation . . . . .	111
4.4.4 Investigation of Frame Configuration . . . . .	127
4.4.5 Investigation of Design Base Shear and P-Delta . . . . .	142
4.4.6 Investigation of Defective Connection . . . . .	163
4.4.7 Investigation of Building Height . . . . .	171
4.5 Overall Summary . . . . .	178
5 CONCLUSIONS AND DESIGN IMPLICATIONS . . . . .	181
5.1 Conclusions . . . . .	181
5.2 Design Implications . . . . .	186
APPENDIX A DETAILS OF DRAIN-2D COMPUTER PROGRAM . . . . .	191
A.1 Introduction . . . . .	191
A.2 DRAIN-2D Program Capabilities . . . . .	191
A.3 Formulation of Mass, Damping and Stiffness Matrices . . . . .	192
A.3.1 Mass Matrix . . . . .	192
A.3.2 Damping Matrix . . . . .	192
A.3.3 Stiffness Matrix . . . . .	194
A.4 Behavior of Finite Elements . . . . .	195
A.4.1 Beam-Column Element . . . . .	195
A.4.2 Beam Element . . . . .	200
A.4.3 Connection Element . . . . .	201
A.4.4 Shear Panel Element . . . . .	203
A.5 Equations of Motion . . . . .	203
A.6 Energy Expressions . . . . .	207
LIST OF REFERENCES . . . . .	217

## LIST OF TABLES

Table		Page
2.1	Uniform Dead Loads . . . . .	25
2.2	Story Weights for Five-Story Building . . . . .	25
2.3	Story Weights for Two-Story Building . . . . .	26
2.4	Lateral Forces for the D1A and D1B Designs . . . . .	29
2.5	Member Selections for the D1A Design . . . . .	30
2.6	Member Selections for the D1B Design . . . . .	31
2.7	Lateral Forces for the D2A, D2B and D2C Designs . . . . .	32
2.8	Member Selections for the D2A Design . . . . .	33
2.9	Member Selections for the D2B Design . . . . .	35
2.10	Member Selections for the D2C Design . . . . .	36
2.11	Lateral Forces for the D3 Design (Drift) . . . . .	38
2.12	Lateral Forces for the D3 Design (Stress) . . . . .	38
2.13	Member Selections for the D3 Design . . . . .	39
2.14	Lateral Forces for the D4 Design . . . . .	40
2.15	Member Selections for the D4 Design . . . . .	41
3.1	Scaling Factors for Earthquake Accelerograms . . . . .	49
4.1	Usage of Frame Designs for Parametric Studies . . . . .	81





## LIST OF FIGURES

Figure		Page
2.1	Plot of Coefficient, $C$ , for Several Soils . . . . .	17
2.2	Design Spectrum for This Study . . . . .	18
2.3	Plan View for the D1A, D1B and D2A Designs . . . . .	27
2.4	Elevation View of Frame 1 for the D1A, D1B and D2A Designs . . . . .	28
2.5	Plan View for the D2B, D2C, D3 and D4 Designs . . . . .	34
2.6	Elevation View of Frame 1 for the D2B Design . . . . .	34
2.7	Elevation View of Frame 1 for the D2C and D3 Designs . . . . .	36
2.8	Elevation View of Frame 1 for the D4 Design . . . . .	40
3.1	Unscaled Earthquake Accelerograms . . . . .	46
3.2a	Unscaled Elastic Response Spectra for Five Percent Damping . . . . .	48
3.2b	Scaled Elastic Response Spectra for Five Percent Damping . . . . .	50
3.3	Exaggerated Deformation of a Panel Zone . . . . .	52
3.4	Dimensions for Typical Interior Frame . . . . .	54
3.5	Free Body Diagram of a Typical Beam Element . . . . .	56
3.6a	Forces Acting at an Interior Panel Zone . . . . .	58
3.6b	Forces Acting on Upper Pair of Stiffeners . . . . .	58
3.7	Model for Stiffness and Strength of Panel Zone . . . . .	60
3.8	Moment-Rotation Relationship of Connection Element . . . . .	62
3.9	Attachment of a Shear Panel Element . . . . .	66
3.10	Load-Deformation Behavior of Nonstructural Elements . . . . .	67
3.11	Load-Deformation Behavior for a Story with Nonstructural Elements Attached to the Frame of the Full-Scale Test . . . . .	69
3.12a	Element Numbering for Five-Story, Five-Bay Frame . . . . .	72

	Page
3.12b	Node Numbering for Five-Story, Five-Bay Frame . . . . . 73
4.1	Typical Energy Time Histories for a Frame Model Subjected to the Scaled Earthquake Accelerograms . . . . . 80
4.2	Drift-Time Histories of First Story for Similar Modelling of D1A and D1B Frames Subjected to Three Earthquakes . . . . . 89
4.3	Shear-Drift Histories of First Story for Similar Modelling of D1A and D1B Frames Subjected to Three Earthquakes . . . . . 90
4.4	Story Drift and Shear Envelopes for Similar Modelling of D1A and D1B Frames Subjected to Three Earthquakes . . . . . 91
4.5a	Cumulative Energy Quantities for Similar Modelling of D1A and D1B Frames Subjected to Three Earthquakes . . . . . 92
4.5b	Hysteretic Energy Distributions for Similar Modelling of D1A and D1B Frames Subjected to Three Earthquakes . . . . . 92
4.5c	Hysteretic Energy Locations for Similar Modelling of D1A and D1B Frames Subjected to Three Earthquakes . . . . . 93
4.6	Drift-Time Histories of First Story for Different Connection Modelling of D1B Frame Subjected to Three Earthquakes . . . . . 100
4.7	Shear-Drift Histories of First Story for Different Connection Modelling of D1B Frame Subjected to El Centro . . . . . 101
4.8	Shear-Drift Histories of First Story for Different Connection Modelling of D1B Frame Subjected to Parkfield . . . . . 102
4.9	Shear-Drift Histories of First Story for Different Connection Modelling of D1B Frame Subjected to Taft . . . . . 103
4.10	Story Drift and Shear Envelopes for Different Connection Modelling of D1B Frames Subjected to Three Earthquakes . . . . . 104
4.11a	Cumulative Energy Quantities for Different Connection Modelling of D1B Frame Subjected to El Centro . . . . . 105
4.11b	Hysteretic Energy Distributions for Different Connection Modelling of D1B Frame Subjected to El Centro . . . . . 105
4.11c	Hysteretic Energy Dissipations for Different Connection Modelling of D1B Frame Subjected to El Centro . . . . . 106
4.12a	Cumulative Energy Quantities for Different Connection Modelling of D1B Frame Subjected to Parkfield . . . . . 107

	<b>Page</b>
4.12b	Hysteretic Energy Distributions for Different Connection Modelling of D1B Frame Subjected to Parkfield . . . . . 107
4.12c	Hysteretic Energy Dissipations for Different Connection Modelling of D1B Frame Subjected to Parkfield . . . . . 108
4.13a	Cumulative Energy Quantities for Different Connection Modelling of D1B Frame Subjected to Taft . . . . . 109
4.13b	Hysteretic Energy Distributions for Different Connection Modelling of D1B Frame Subjected to Taft . . . . . 109
4.13c	Hysteretic Energy Dissipations for Different Connection Modelling of D1B Frame Subjected to Taft . . . . . 110
4.14	Drift-Time Histories of First Story for D1B Frame with Nonstructural Elements Subjected to Three Earthquakes . . . . . 116
4.15	Shear-Drift Histories of First Story for D1B Frame with Nonstructural Elements Subjected to El Centro . . . . . 117
4.16	Shear-Drift Histories of First Story for D1B Frame with Nonstructural Elements Subjected to Parkfield . . . . . 118
4.17	Shear-Drift Histories of First Story for D1B Frame with Nonstructural Elements Subjected to Taft . . . . . 119
4.18	Story Drift and Shear Envelopes for D1B Frame with Nonstructural Elements Subjected to Three Earthquakes . . . . . 120
4.19a	Cumulative Energy Quantities for D1B Frame with Nonstructural Elements Subjected to El Centro . . . . . 120
4.19b	Hysteretic Energy Distributions for D1B Frame with Nonstructural Elements Subjected to El Centro . . . . . 121
4.19c	Hysteretic Energy Locations for D1B Frame with Nonstructural Elements Subjected to El Centro . . . . . 122
4.20a	Cumulative Energy Quantities for D1B Frame with Nonstructural Elements Subjected to Parkfield . . . . . 123
4.20b	Hysteretic Energy Distributions for D1B Frame with Nonstructural Elements Subjected to Parkfield . . . . . 123
4.20c	Hysteretic Energy Locations for D1B Frame with Nonstructural Elements Subjected to Parkfield . . . . . 124

	<b>Page</b>
4.21a	Cumulative Energy Quantities for D1B Frame with Nonstructural Elements Subjected to Taft . . . . . 125
4.21b	Hysteretic Energy Distributions for D1B Frame with Nonstructural Elements Subjected to Taft . . . . . 125
4.21c	Hysteretic Energy Locations for D1B Frame with Nonstructural Elements Subjected to Taft . . . . . 126
4.22	Drift-Time Histories of First Story for D2A, D2B and D2C Frames Subjected to Three Earthquakes . . . . . 131
4.23	Shear-Drift Histories of First Story for D2A, D2B and D2C Frames Subjected to El Centro . . . . . 132
4.24	Shear-Drift Histories of First Story for D2A, D2B and D2C Frames Subjected to Parkfield . . . . . 133
4.25	Shear-Drift Histories of First Story for D2A, D2B and D2C Frames Subjected to Taft . . . . . 134
4.26	Story Drift and Shear Envelopes for D2A, D2B and D2C Frames Subjected to Three Earthquakes . . . . . 135
4.27a	Cumulative Energy Quantities for D2A, D2B and D2C Frames Subjected to El Centro . . . . . 136
4.27b	Hysteretic Energy Distributions for D2A, D2B and D2C Frames Subjected to El Centro . . . . . 136
4.27c	Hysteretic Energy Locations for D2A, D2B and D2C Frames Subjected to El Centro . . . . . 137
4.28a	Cumulative Energy Quantities for D2A, D2B and D2C Frames Subjected to Parkfield . . . . . 138
4.28b	Hysteretic Energy Distributions for D2A, D2B and D2C Frames Subjected to Parkfield . . . . . 138
4.28c	Hysteretic Energy Locations for D2A, D2B and D2C Frames Subjected to Parkfield . . . . . 139
4.29a	Cumulative Energy Quantities for D2A, D2B and D2C Frames Subjected to Taft . . . . . 140
4.29b	Hysteretic Energy Distributions for D2A, D2B and D2C Frames Subjected to Taft . . . . . 140

	Page
4.29c	Hysteretic Energy Locations for D2A, D2B and D2C Frames Subjected to Taft . . . . . 141
4.30	Drift-Time Histories of First Story for Similar Modelling of D1B and D2A Frames Subjected to Three Earthquakes . . . . 147
4.31	Drift-Time Histories of First Story for D1B and D1B-PD Frames Subjected to Three Earthquakes . . . . . 148
4.32	Drift-Time Histories of First Story for D2A and D2A-PD Frames Subjected to Three Earthquakes . . . . . 149
4.33	Shear-Drift Histories of First Story for Similar Modelling of D1B and D2A Frames Subjected to Three Earthquakes . . . . 150
4.34	Story Drift and Shear Envelopes for Similar Modelling of D1B and D2A Frames Subjected to Three Earthquakes . . . . 151
4.35a	Cumulative Energy Quantities for Similar Modelling of D1B and D2A Frames Subjected to Three Earthquakes . . . . 152
4.35b	Hysteretic Energy Distributions for Similar Modelling of D1B and D2A Frames Subjected to Three Earthquakes . . . . 152
4.35c	Hysteretic Energy Locations for Similar Modelling of D1B and D2A Frames Subjected to Three Earthquakes . . . . 153
4.36	Drift-Time Histories of First Story for Similar Modelling of D2C and D3 Frames Subjected to Three Earthquakes . . . . . 154
4.37	Drift-Time Histories of First Story for Similar Modelling of D2C-TNE and D3-TNE Frames Subjected to Three Earthquakes . 155
4.38	Shear-Drift Histories of First Story for Similar Modelling of D2C and D3 Frames Subjected to Three Earthquakes . . . . . 156
4.39	Shear-Drift Histories of First Story for Similar Modelling of D2C-TNE and D3-TNE Frames Subjected to Three Earthquakes . 157
4.40	Story Drift and Shear Envelopes for Similar Modelling of D2C and D3 Frames Subjected to Three Earthquakes . . . . . 158
4.41a	Cumulative Energy Quantities for Similar Modelling of D2C and D3 Frames Subjected to Three Earthquakes . . . . . 159
4.41b	Hysteretic Energy Distributions for Similar Modelling of D2C and D3 Frames Subjected to Three Earthquakes . . . . . 159

	Page
4.41c	Hysteretic Energy Locations for Similar Modelling of D2C and D3 Frames Subjected to Three Earthquakes . . . . . 160
4.42a	Cumulative Energy Quantities for Similar Modelling of D2C-TNE and D3-TNE Frames Subjected to Three Earthquakes . 161
4.42b	Hysteretic Energy Distributions for Similar Modelling of D2C-TNE and D3-TNE Frames Subjected to Three Earthquakes . 161
4.42c	Hysteretic Energy Locations for Similar Modelling of D2C-TNE and D3-TNE Frames Subjected to Three Earthquakes . 162
4.43	Drift-Time Histories of First Story for D2C and D2C-D Frames Subjected to Three Earthquakes . . . . . 166
4.44	Shear-Drift Histories of First Story for D2C and D2C-D Frames Subjected to Three Earthquakes . . . . . 167
4.45	Story Drift and Shear Envelopes for D2C and D2C-D Frames Subjected to Three Earthquakes . . . . . 168
4.46a	Cumulative Energy Quantities for D2C and D2C-D Frames Subjected to Three Earthquakes . . . . . 169
4.46b	Hysteretic Energy Distributions for D2C and D2C-D Frames Subjected to Three Earthquakes . . . . . 169
4.46c	Hysteretic Energy Locations for D2C and D2C-D Frames Subjected to Three Earthquakes . . . . . 170
4.47	Drift-Time Histories of First Story for D4 and D4-TNE Frames Subjected to Three Earthquakes . . . . . 174
4.48	Shear-Drift Histories of First Story for D4 and D4-TNE Frames Subjected to Three Earthquakes . . . . . 175
4.49	Story Drift and Shear Envelopes for D4 and D4-TNE Frames Subjected to Three Earthquakes . . . . . 176
4.50a	Cumulative Energy Quantities for D4 and D4-TNE Frames Subjected to Three Earthquakes . . . . . 177
4.50b	Hysteretic Energy Distributions for D4 and D4-TNE Frames Subjected to Three Earthquakes . . . . . 177
A.1	Physical Interpretation of End Eccentricities . . . . . 196
A.2	Decomposition of Moment-Rotation Relationship . . . . . 198

	<b>Page</b>
A.3a	General Shape of Interaction Surface . . . . . 199
A.3b	Interaction Surface of Steel I-Section . . . . . 199
A.4	Idealization of Beam-to-Column Connection . . . . . 202





## LIST OF SYMBOLS

The important symbols and notations used in this dissertation are defined where they are first used in the text and given below:

- A = Cross sectional area of member.
- $\alpha$  = Reduction factor for yield stress of panel zone.
- $b_c$  = Width of column flange.
- C = Numerical coefficient to calculate design base shear for direct design procedure.
- $C_t$  = Numerical coefficient to estimate a structure's fundamental period of vibration for direct design procedure.
- DL = Axial force in column from design dead load.
- $d_b$  = Depth of beam section.
- $d_c$  = Depth of column section.
- $\delta_x$  = Relative story drift between level x and level x-1.
- EQ = Axial force in column from equivalent lateral forces of direct design procedure.
- $F_a$  = Allowable compressive stress of member.
- $F_t$  = Portion of design base shear for direct design procedure that is concentrated at top of structure.
- $F_x$  = Equivalent lateral force applied to level x for direct design procedure.
- $F_y$  = Yield stress of member.
- $\dagger$  = Frequency of vibration, in hertz.
- G = Shear Modulus of panel zone web.
- $h_{i,x}$  = Height, in feet, above the base to level i or x of structure.
- $h_n$  = Height, in feet, above the base to top level of structure.
- I = Importance factor of structure for direct design procedure.



## CHAPTER 1

### INTRODUCTION

#### 1.1 Background

Competent design of earthquake resistant structures depends on the ability to estimate the structural demand associated with the ground excitation. However, the demand on a structure from a given earthquake is dependent upon the building's supply of stiffness and strength. In seismic design, it is imperative to accurately assess the stiffness and strength of a building, so that judgement as to the worthiness (ability to withstand the demand) of the design to resist major earthquakes without endangerment of human lives can be made. This study concentrated on the assessment of stiffness and strength for low-rise steel frame buildings and the demand on the lateral force-resisting systems from severe ground motions.

A majority of buildings constructed in the United States are low-rise in nature. However, because the structural engineering portion of the total building cost is minor as compared to hi-rise construction, sophisticated techniques for the seismic design and analysis of low-rise buildings are not employed, except under unusual circumstances. Instead, practicing engineers rely on simplified design procedures that use equivalent lateral forces to represent dynamically induced forces that arise from a major earthquake to assess the adequacy of a design. Most building codes, including model building codes in the United States, contain provisions for a direct design procedure (an equivalent lateral force method) for seismic resistant design [3,4,16,23,24,43]. The more recent direct design procedures found in the building codes are based in part on principles implicitly related to elastic

response spectra for single-degree-of-freedom (SDOF) systems modified for inelastic effects, the so-called inelastic spectra [37]. Therefore an essential underlying assumption for the usage of any direct design procedure is that the dynamic response of the structure should be dominated by the first translational (lateral) mode of vibration and is relatable to the behavior of a SDOF system.

It is this underlying assumption as well as other assumptions held by the code that form the basis for this investigation. If these assumptions are valid for a building, then will the response from a major earthquake be similar to the expected response of the code and, more importantly, will the design give satisfactory performance? In contrast, if the assumptions are invalid to some degree for a building, how will the response compare to the expected response and will the design perform satisfactorily under severe ground excitation? If the usage of direct design procedures result in buildings having undesirable behavior, what modifications can be made to the direct design procedures to improve the structural performance of buildings through better design procedures. Also the seismic design requirements in the codes are, in part, related to the past performance of buildings which formed a "database" containing the actual behavior of buildings. Therefore, is it realistic to expect good performance of new building designs which are not represented in the historical database?

In the late 1970s in the aftermath of the February 1971, San Fernando Earthquake, the Applied Technology Council (ATC) developed a tentative model building code for seismic design, encompassing modern structural dynamics features [4]. The Structural Engineers Association of California (SEAOC) subsequently revised the "blue book", a building code for seismic design, by

following some of the recommended design procedures of the ATC code [43]. In addition, the Building Seismic Safety Council (BSSC) prepared for the Federal Emergency Management Agency (FEMA) the *NEHRP Recommended Provisions for the Development of Seismic Regulations for New Buildings*, this latter document is a model building code largely based on the ATC model building code [16]. The seismic design provisions in the "blue book" became the cornerstone for the latest edition of the *Uniform Building Code* (UBC), which was adopted by the International Conference of Building Officials in 1988 [24]. The *Uniform Building Code* is adopted by most municipalities west of the Mississippi River.

The provisions contained in the 1988 UBC regarding the seismic design of structures have been updated to reflect the current views for the demand on the stiffness, strength and ductility, and performance of the lateral force-resisting system for a building shaken during a major earthquake. The calculation of the design base shear and distribution of the design base shear into equivalent lateral forces are presented in a more rational format than in the previous editions of the *Uniform Building Code*. Although, the design base shear and distribution of the design base shear for a ductile steel moment-resisting frame structure having a short fundamental period of vibration are the same as that given by the 1985 UBC [23].

#### 1.1.1 Direct Design Procedure for Seismic Forces

The Structural Engineers Association of California, as well as most other structural engineers, endorse the following philosophy:

1. A building must resist a minor earthquake without damage;
2. In moderate earthquakes some nonstructural damage is allowed;

3. During a major earthquake, a building must not collapse, but some structural as well as nonstructural damage may occur.

The principal concern of building codes regarding the seismic design of a structure is life safety and not mitigation of structural or nonstructural damage. The third point given in the above design philosophy pertains to life safety, while the first two points pertain primarily to damage mitigation. Thus, the provisions given in the 1988 UBC for seismic design address the performance and survivability of a structure in the event of a major earthquake. However, it is presumed that by adequately addressing the third point, the other two points also will be satisfied.

One of the principal objectives of seismic design is to comply with this design philosophy in the most cost-effective manner. A structure could be designed to have a principally elastic response during a major earthquake which would induce distortions that cause little structural or nonstructural damage. The cost for such an elastic design probably would be economically infeasible, especially considering the rare occurrence of a major earthquake during the "lifetime" of a given building. Therefore controlled and limited inelastic behavior is permitted by the building code during the response of a structure subjected to strong ground motion. Of course, incurred damage as a result of inelastic behavior may render the structure unsuitable for further occupancy.

The response during a moderate earthquake should not cause the lateral force-resisting system to experience significant inelastic deformations or structural damage. Even so, the damage to nonstructural elements can be considerable since these elements tend to be less ductile than the lateral force-resisting system. Damage to nonstructural elements can be lessened by

isolating them from the structural frame. For instance, the attachment of exterior cladding to the structural frame usually tolerates some relative lateral movement between adjacent stories to prevent the cladding from necessarily being a part of the lateral force-resisting system. However in many cases, binding of the connections or insufficient isolation from the structural frame cause the cladding to participate in the response of the structure which results in the cladding carrying shear forces.

The advantage of the direct design procedure is that the lateral loads can be determined "directly" with a very minimum of information about the properties of the structure or the expected ground excitation from future earthquakes. In the case of dynamic lateral force procedures such as modal or time-history analysis, the design process involves iteration since the lateral loads are dependent on the properties of the structure and ground motion. Since very little information is required for the direct design procedure, the method is quite general and the factor of safety for any particular design is difficult to assess.

The direct design procedure adopted by the 1988 edition of the *Uniform Building Code* is limited to the design of "regular" structures, which have relatively uniform distribution of building mass and stiffness and no major physical discontinuities in plan or elevation. The code explicitly states under what conditions a structure is classified as being irregular because the dynamic behavior is not adequately characterized by the assumed behavior considered in the direct design procedure. A dynamic analysis, either modal or time-history, is required for the design of irregular structures and may be used for regular structures.

An assumption of the direct design procedure is that the distributions of lateral stiffness and strength for a structure are proportional to the design story shears, so that the inelastic deformations (ductility demands) at each story level are fairly uniform throughout the height of the building during severe excitation. In practice, there are many reasons why the actual distributions of stiffness and strength may not be proportional to the design shear forces, which subsequently can cause nonuniform inelastic deformations over the height of the structure. If this happens, much larger story drifts than anticipated by the code may occur in a few stories and much larger member and connection ductilities will be required to dissipate the energy demand since fewer elements are sharing the load.

Although inelastic behavior of a structure is anticipated during a major earthquake, the direct design procedure involves an elastic analysis of the structure loaded with the specified combinations of dead, live and earthquake loads. As in the construction of an inelastic design spectrum, the design of a structure using a set of reduced lateral forces should generate inelastic deformations within the desired target deformation under the actual loading. The stability and survivability of a structure during a major earthquake is presumed to be ensured when the story drifts and member forces from the direct design procedure are less than the allowable values given by the code.

The direct design procedure of the code provides a method to calculate equivalent lateral forces and check the adequacy of a design. However, the overall lateral force-resisting scheme is left to the structural engineer to devise. The code also dictates that the structural model for design and analysis must be able to represent the behavior of the structure to the



level needed to adequately predict the significant feature of the structural response. However, the code gives no guidance as to how to predict and model the structural behavior.

### 1.1.2 Frame Design and Modelling

When labor costs were small in comparison to material costs, the least expensive design generally required the least amount of material. However as labor costs have increased more rapidly through the years since, the fabrication, erection and inspection costs have had a greater contribution in arriving at the total cost of the design. Therefore the least-weight design may not necessarily be the least-cost design.

The stiffness and strength requirements of a frame may allow the column sections to become lighter in the upper stories of typical buildings, but from a cost point of view it may be more economical to continue a column section through adjacent stories. The cost of the additional "unneeded" material is offset by the reduction in required column splices and in time of construction. Typically, the length of a section available from the mill dictates the change in sections for a column line. Also, it may be less expensive to use the same section for all the columns of a story and the same section for all the beams of a story, since fewer details are required for the connections and since repetition of fabrication and better bulk pricing of material are achieved.

In years past, all of the frames in a steel frame building generally were designed with moment-resisting connections to resist lateral forces. This approach provided the greatest amount of redundancy and locations for dissipation of hysteretic energy for a building. Presumably this approach

also provided a greater margin of safety. However, to reduce the number of moment-resisting connections required and construction time it has become increasingly popular for only the perimeter frames to be designed to resist lateral forces. The connections of the interior frames are assumed to be pinned, and thus the interior frames resist only vertical forces of their tributary area. In fact, some structural engineers in Southern California are further reducing the number of moment-resisting connections by employing long bay spacings and even restricting the number of bays (sometimes to a single bay) in the perimeter frames that resist lateral forces.

The reduction in total number of moment-resisting connections for a structure has two main drawbacks. The first disadvantage is there probably will be a reduction in the overall strength of the structure. Even though all of the designs will have to satisfy the requirements of the code, the ability to match more closely those requirements will be with designs using fewer members to resist lateral loads. The lateral stiffness and strength are not independent since rolled I-sections are used as the columns and beams. Therefore, an unaccounted for additional margin of safety for the strength of the structure is reduced creating more inelastic behavior under severe ground excitation. The other disadvantage of reducing the number of moment-resisting connections is the decrease in redundancy of the structure. Under excitation from a major earthquake, inelastic deformations of the lateral force-resisting system may cause damage and eventual failure of the members or connections because of the necessity to dissipate a lot of energy in a few locations. The inability to redistribute the forces because of lower redundancy also may lead to greater instability of the structure.

The modelling of the load-deformation behavior for a steel frame typically is derived from the stiffness and strength of the columns and beams. The beam-to-column connections are assumed to be infinitely rigid, which means that there is no relative rotation between the columns and beams framing into a joint. The lengths of the column and beams are based on the member centerline-to-centerline dimensions of the frame. The contribution of the nonstructural elements, such as cladding, interior frames, interior walls, etc., to the load-deformation behavior of the structure is ignored in the modelling of the structure.

Even though shear stresses within the panel zone cause distortions, the stiffness and strength of beam-to-column connections generally are not considered in the analysis of a frame. The flexibility of the panel zones is compensated for in an analysis by using the centerline-to-centerline dimensions for the lengths of the members instead of the clear spans. More important to the load-deformation behavior of the structure is the yield strength of the panel zone. If the panel zone yields prior to yielding of the columns or beams, the moment acting at the ends of the columns or beams may never reach their yield moment.

Nonstructural elements are those building elements which are not designed to contribute to the structural capacity of the building. Even though the stiffness and strength of nonstructural elements generally are ignored in the design process, these elements can participate in the dynamic and, for that matter, in the static response when insufficient isolation from the structural system exists. Because the nonstructural elements do interact with the structural frame, the dynamic behavior of the building can be quite different from the behavior of just the bare structural frame.

Typically, only the so-called structural members are considered in the direct design procedure.

### 1.1.3 Previous Work

The direct design procedures detailed in codes for the United States have evolved over the past eighty years. In the beginning, the design base shear was simply a percentage of the building weight without regard to the properties of the structure. Many investigators have contributed in the years since to revise the direct design procedures into a more rational format, which is dependent on the load-deformation relationship of the structure, soil-structure interaction and desired response [7,12,20,21,31,35,36]. Still, the evolution of the direct design procedures is not completed since investigations into the current design procedures reveal deficiencies in the performance of seismically designed structures [4,8,10,11,14,19]. As an example, the deformations and ductility demands are larger than expected or desired for structures designed in accordance with the current direct design procedures.

In recent years significant attention has been given to the behavior of moment-resisting connections under large distortions [6,15,27,28,29,30,38,39,40]. This research has produced methods for estimating the stiffness, strength and hysteretic energy dissipation capacity of the panel zone. The inclusion of the behavior of connections in a finite element model of a frame can result in better prediction of the overall load-deformation relationship.

The behavior of nonstructural elements and the contribution to the overall stiffness and strength of the structure also is a current research

topic [5,13,26,42,45,46,47]. This research has shown that nonstructural elements can significantly increase the stiffness of a building and affect the dynamic properties of the structure. The assessment of the stiffness and strength contribution of nonstructural elements is difficult, since degradation occurs after repeated cyclic motion.

## 1.2 Purpose of Study

To design efficient and effective structures to resist strong ground excitation, a direct design procedure must consider the actual dynamic behavior of the structure. In addition, the modelling of a structure must sufficiently predict the load-deformation behavior to ensure that results from an analysis of a structure predict the actual demand on the structure. The purpose of this study is to determine the relationships between seismic design and response and between modelling and response for low-rise steel frame structures. If the direct design procedure contained in the 1988 edition of the *Uniform Building Code* can be modified to be more sensitive to the actual behavior of structures, then the performance of structures under severe excitation should improve.

Low-rise steel frames, designed in accordance with the direct design provisions of the 1988 edition of the *Uniform Building Code*, were studied to identify the above relationships. It was foreseen that the considerable inelastic deformations allowed by the code for ductile steel frames may result in significant disparity between the assumed behavior of the code and the actual response of the frame under severe excitation. Several finite element models of each frame design were developed for usage in dynamic

time-history analyses to investigate the influence of various parameters on the structural performance of the steel moment-resisting frames.

The parameters selected for this investigation featured the latitude allowed by the code in the direct design procedure for a moment-resisting steel frame. The influence of beam-to-column strength ratio, beam-to-column connection behavior, participation of nonstructural elements, configuration of lateral force-resisting frame, design base shear level and building height on the dynamic response and behavior were studied. In addition, a lateral force-resisting frame with only one bay was selected to investigate the influence of defective moment-resisting connections.

### 1.3 Scope of Report

An overview of this investigation has been discussed in this first chapter. Background information and the extent of previous research related to seismic design and inelastic behavior of steel frame structures indicate a need to further study the relationship between direct design procedures and dynamic response. Understanding this relationship may lead to better seismic performance of lateral force-resisting designs.

The application of the direct design procedure contained in the 1988 edition of the *Uniform Building Code* for the steel moment-resisting frames considered in this investigation are given in Chapter 2. Some deviation concerning the column-to-beam strength ratio, design base shear level and frame configuration are given in this code and these aspects were explored in the frame designs.

The modelling and analysis procedure for the steel frames are presented in Chapter 3. Modelling of a structure's load-deformation behavior required

making assumptions regarding the individual behavior of the elements. The finite element mesh of the frame models and modelling the beam-to-column connections and nonstructural elements for the time-history analyses are explained in this chapter. Several historical ground excitation records, representative of the design earthquake, were used in the time-history analyses as the base motion. An explanation for the scaling algorithm for the earthquake accelerograms is given in this chapter.

The development, results and conclusions for each of the parametric studies are presented in Chapter 4. The selection of the results from the time-history analyses used to quantify the inelastic behavior of the frame models also are addressed. Each parametric study was developed to determine the influence of a particular parameter on the inelastic response. The results of the parametric studies are discussed and presented in graphical form. The conclusions of each parametric study focus on the importance or influence of the parameter.

The overall conclusions related to the design, modelling and analysis of steel frame structures are detailed in Chapter 5. Since one of the goals of this study was to improve the seismic performance of structures through better design, recommendations for the direct design procedure of the 1988 edition of the *Uniform Building Code* also are given.

## CHAPTER 2

## APPLICATION OF DIRECT DESIGN PROCEDURE FOR STEEL FRAMES

## 2.1 Introduction

Structural engineers practicing in Southern California were consulted for this study to ascertain the current state for the design of low-rise steel frame structures. Frame designs in this study were usually consistent with the state of practice for low-rise steel frame structures constructed in a highly seismic region. However, some frame designs were chosen to bound a range for a particular parameter being investigated and may not represent current practice or even "good" practice for seismic design.

In this study, steel moment-resisting frames along the perimeter of the structure provided the lateral force resistance and stability. These frames were designed to resist seismic induced forces in accordance with the direct design procedure contained in the 1988 edition of the *Uniform Building Code*. Provisions pertaining to both torsional and orthogonal (bidirectional ground excitation) effects were ignored in the seismic design of these frames since the lateral load-deformation behavior for the time-history analyses of each structure was represented by planar modelling of the moment-resisting frames in a specified direction. The inclusion of torsional or orthogonal effects in the direct design procedure probably would have increased the lateral stiffness and strength of a frame but would have given misleading results (unconservative) from the time-history analyses of this investigation.

The first step in the direct design procedure is to determine the design base shear and vertical distribution of the base shear. A static elastic analysis of the structure, loaded with the gravity forces and



equivalent lateral forces, is then performed to determine story drifts, member forces and overturning moments. The story drifts and member forces are checked for code compliance with the lateral stiffness requirements of the moment-resisting frame and strength and ductility requirements of the columns, beams and panel zones.

The calculation and distribution of the design base shear for the direct design procedure of each frame design considered in this study are described in this chapter. The code provisions used to check the lateral stiffness requirements of the frame and strength and ductility requirements of the columns, beams and panel zones are explained in some detail. And finally, the motivation behind the calculation of the design base shear, the configuration selected for the lateral force-resisting frame and the rolled steel I-sections chosen as the columns and beams for each frame design are presented in this chapter.

## 2.2 Determination of Equivalent Lateral Forces

The design base shear, which is the sum total of the equivalent lateral forces applied to the structure in the direct design procedure, is given by

$$V = \frac{ZICW}{R_w} \quad (2.1)$$

The seismic zone factor,  $Z$ , represents the effective peak acceleration (EPA) of the design earthquake particular to a given site location.  $Z$  has a value of zero for regions without seismic hazard and ranges up to a maximum value of four-tenths for regions of strong seismicity. The factor,  $I$ , corresponds to the importance of the facility. Standard occupancy structures have an  $I$

value equal to unity, while essential occupancy structures have an  $I$  value equal to one and a quarter. The importance factor,  $I$ , raises the factor of safety of the design by increasing the required stiffness and strength of the structure, which will result in smaller inelastic deformations during severe ground excitation. The seismic weight,  $W$ , is the dead load plus applicable portions of live load and snow load and should correspond to the weight of the building mass that can induce inertial forces during ground excitation. The response modification factor,  $R_w$ , primarily accounts for inherent ductility and hysteretic energy dissipation capability of the lateral force-resisting system and additional, but unpredictable, strength of the nonstructural elements. The response modification factor for lateral force-resisting systems increases as the ductility increases. The design coefficient,  $C$ , is defined by

$$C = \frac{1.25 S}{T^{2/3}}, \quad (2.2)$$

where  $S$  is dependent on the soil characteristics at the site and  $T$  is the estimated fundamental period of vibration, in seconds, of the structure in the direction under consideration.

In this study, the value of  $Z$  was taken to be the maximum, four-tenths. The importance factor,  $I$ , was taken to be unity, so that the inelastic behavior was not reduced as a result of a more conservative design. The response modification factor,  $R_w$ , was taken to be twelve, since the lateral force-resisting system was assumed to be special moment-resisting space frames (SMRSF). The calculation of  $C$  was based on a value of  $S$  taken to be 1.2, which corresponds to a profile of stiff or dense soil.

Shown in Figure 2.1 are plots of the design coefficient,  $C$ , versus fundamental period of structure for each soil profile classification. The value of  $C$  generally decreases as the fundamental period of the structure increases.  $C$  has a maximum value of 2.75 for the stiff soils (types 1 and 2) and a maximum value of 2.25 for soft soils (types 3 and 4). The code allows the usage of  $C$  equal to 2.75 without regard to the fundamental period or soil profile. For long period structures, using a value of  $C$  equal to 2.75 generally is quite conservative, especially for structures founded on stiff soils.

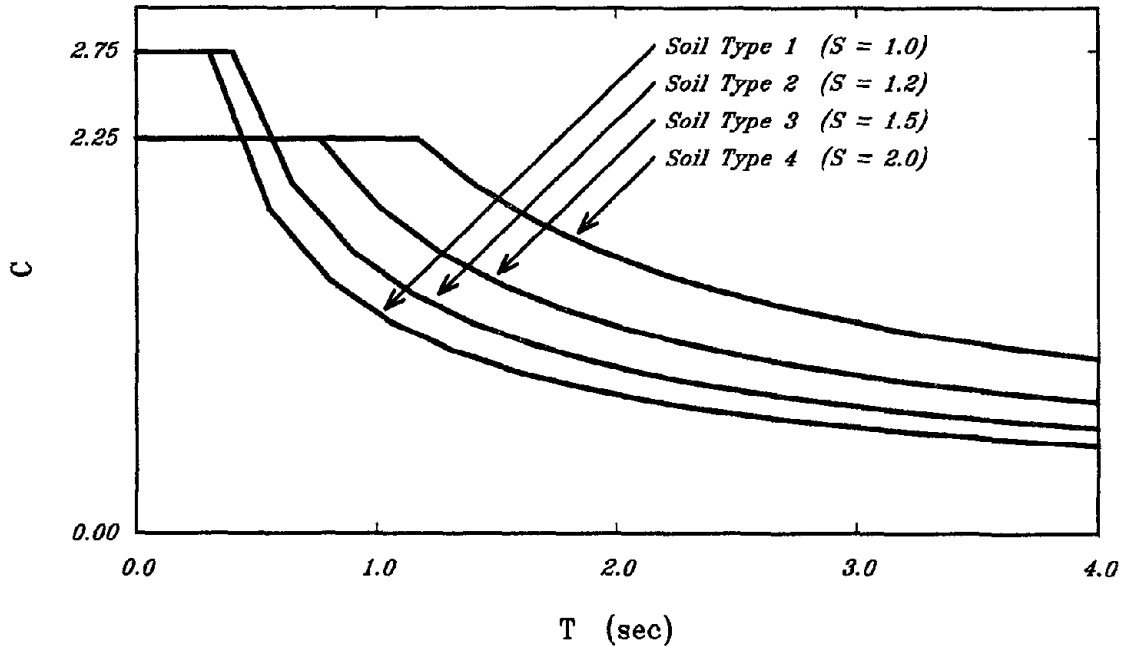


FIGURE 2.1 Plot of Coefficient,  $C$ , for Several Soils

The plots given in Figure 2.1 can be visualized conceptually in the context of elastic response spectra, which are used to anchor the design spectrum for a given soil type. The design spectrum for this study,  $S$  equal

to 1.2, is shown in Figure 2.2. The ordinate of Figure 2.2 is the design base shear given as a percentage of the building weight. Since the maximum value for  $C$  need not exceed 2.75 for soil type 2, the design base shear need not exceed 9.2 percent of the building weight. The 1988 UBC mandates that the ratio of  $C/R_w$  shall not be less than 0.075, therefore the minimum design base shear for this design spectrum in Figure 2.2 is computed to be 3.0 percent of the building weight.

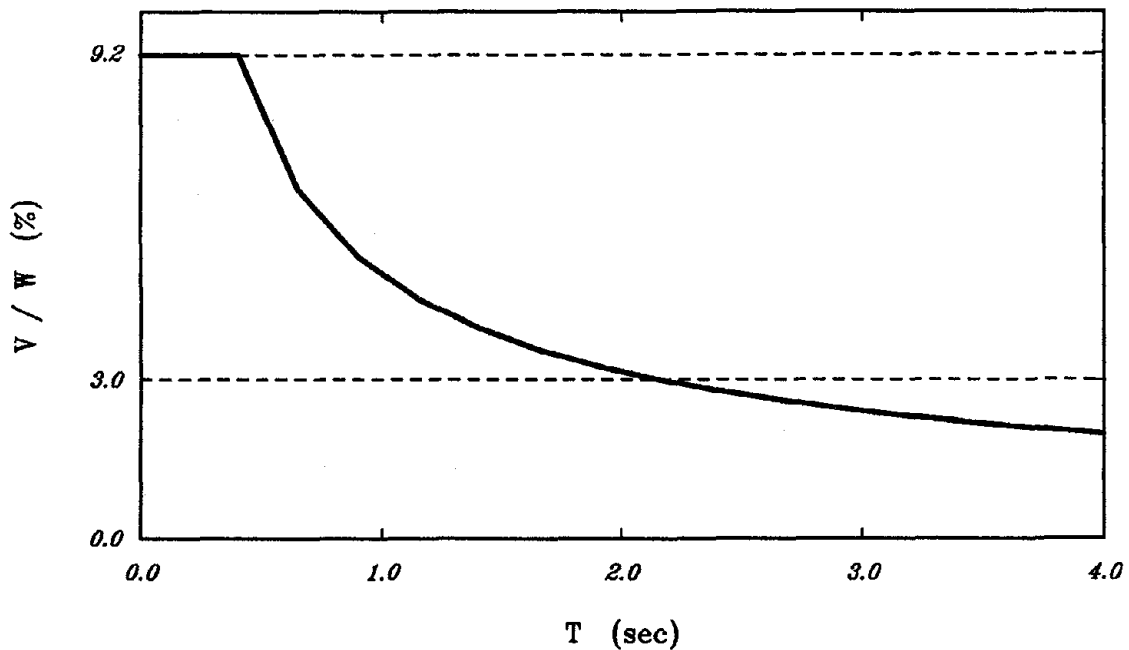


FIGURE 2.2 Design Spectrum for This Study

The product of  $ZCW$  would be the design base shear if the structure was to remain elastic from excitation by the design earthquake. Therefore the design base shear for a short period structure would need to be at least one hundred and ten percent of the building weight ( $V = 0.4 \cdot 2.75 \cdot W = 1.1W$ ). Inelastic behavior is incorporated into the direct design procedure by

dividing the "elastic" design base shear by the response modification factor,  $R_w$ . The expected story drifts, elastic and inelastic contributions, implicit in the 1988 UBC are three-eighths of  $R_w$  times the allowable story drifts.

The reduction from the "elastic" response spectrum to the design spectrum is twelve for a special moment-resisting space frame, and yet the anticipated story drifts are only four and a half times the allowable story drifts. The difference between these two factors is inconsistent with the inelastic design spectra concepts applied to single-degree-of-freedom systems [37], which generally form the basis for current direct design procedures. One explanation for this discrepancy is that  $R_w$  accounts for other factors such as the additional, but unpredictable, strength of nonstructural elements, rather than just the innate ductility of the lateral force-resisting system.

Since the fundamental period of a structure is generally unknown at the onset of the design process, the following equation is given in the code to estimate the fundamental period for the initial design phase:

$$T = C_t (h_n)^{3/4} , \quad (2.3)$$

where  $C_t$  is equal to 0.035 for steel frames and  $h_n$  is the height, in feet, to the top level of the structure. However, if the value of  $C$  is taken to be equal to 2.75, then an estimated fundamental period is not needed to obtain a design base shear.

The estimated fundamental period given by Equation 2.3 usually is shorter than the actual period of the structure. An expression that was drawn through the recorded test data of fundamental period of vibration for

instrumented steel frame buildings shaken during the 1971 San Fernando earthquake is similar to Equation 2.3, except that the coefficient, 0.049, is used instead of 0.035 [4,16]. The lower value was selected for the direct design procedure, because it will tend to be more conservative by giving a larger design base shear when  $T$  is substituted into Equation 2.2.

The equivalent lateral forces or the vertical distribution of the design base shear for the direct design procedure are given by

$$F_x = \frac{(V - F_t) W_x h_x}{\sum W_i h_i} , \quad (2.4)$$

where  $F_x$  is the equivalent lateral force applied at level  $x$ ,  $W_x$  is the weight of level  $x$  and  $h_x$  is the height of level  $x$ .  $F_t$  is a concentrated force applied to the top of the structure and is given by

$$F_t = 0.07TV . \quad (2.5)$$

$F_t$  accounts for the participation of higher modes in the response of long period structures.  $F_t$  can be neglected when  $T$  is less than seven-tenths of a second (short period structures) and need not exceed twenty-five percent of the design base shear for long period structures. The distribution of equivalent lateral forces for short period structures with constant story heights and weights linearly increases from zero at the base to a maximum value at the roof. This distribution corresponds to an assumed linear shape for the first lateral mode of vibration. Thus, the dynamic response of the structure should be dominated by the first mode, so that the distribution of the design forces resemble the maximum story shears obtained during severe ground excitation. The effect of  $F_t$  shifts the vertical distribution of the

base shear towards the upper levels of the structure, which translates to larger story shears in the upper stories and more overturning moment.

### 2.3 Stiffness, Strength and Ductility Requirements

The direct design procedure entails performing a static elastic analysis of the structure loaded with any applicable loading combinations containing earthquake loads. To safeguard against collapse of the structure during the design earthquake, the direct design procedure has two components - a drift design and a stress (strength) design - which together are assumed to ensure stability of the structure by controlling the story drifts and inelastic behavior of the structural members.

The computed story drifts for a structure of less than sixty-five feet in height shall not exceed

$$\delta_x = \frac{0.04 \ell_x}{R_w} \leq 0.005 \ell_x, \quad (2.6)$$

where  $\delta_x$  is the maximum allowable story drift of level  $x$  and  $\ell_x$  is the story height of level  $x$ . The maximum allowable story drift ratio (story drift divided by story height) for a special moment-resisting space frame (SMRSF) for which  $R_w$  is equal to twelve is computed to be one-third of a percent.

For special moment-resisting space frames designed in accordance with the provisions of the 1988 UBC, the maximum story drift as a result of excitation from the design earthquake are expected to be four and a half ( $0.375R_w$ ) times  $\delta_x$  or one and a half percent of the story height. In fact regardless of lateral force-resisting system, the expected maximum story drift ratios are one and a half percent. This is because the smaller story

drift multiplier for a less ductile system (smaller  $R_w$ ) is offset by a larger allowable story drift. Many provisions in the code are based on the expected maximum story drifts. For instance at the expected maximum story drift, the deformation compatibility of all framing elements not required by design to be part of the lateral force-resisting system shall have adequate vertical load-carrying capacity when displaced to this level, separation of adjacent buildings shall eliminate contact at this level so that pounding is prevented during excitation and connections shall allow for this level of story drift. Acceptable performance of the structure beyond the one and a half percent story drift ratio is not regulated by the code must be avoided if collapse of the structure is to be prevented during severe excitation.

Some of the strength requirements ensure that the calculated stresses in the columns and beams from the design forces are less than an allowable level. The interaction equations contained in the code, which are identical to the equations contained in the *AISC Manual of Steel Construction* [2], were used to check the design stresses. In this investigation, the loading combination of live, dead and earthquake loads controlled the designs, even though the allowable stresses for this load combination were increased by a factor of one-third. The calculated stresses in the columns of the lateral force-resisting frames from vertical dead and live loads were small compared to the stresses from the lateral forces because the tributary area for vertical loads was much smaller than the tributary area for lateral forces.

The code also contains provisions regarding minimum computed strength of the columns. The axial force capacity of the columns must be greater than the axial forces arising from the design earthquake as a result of overturning effects of the structure. The compressive strength of each



column must satisfy

$$(1.0) DL + (0.8) LL + (0.375 R_w) EQ \leq 1.7 F_a A \quad (2.7)$$

and the tensile strength must satisfy

$$(0.85) DL + (0.375 R_w) EQ \leq F_y A , \quad (2.8)$$

where  $DL$  is the axial force from the dead loads,  $LL$  is the axial force from live loads,  $EQ$  is the axial force from the equivalent lateral forces,  $F_a$  is the allowable compressive stress,  $F_y$  is the yield stress and  $A$  is the cross sectional area.

The strength of the panel zone must have the capacity to resist the prescribed shear forces applied to the panel zone. The minimum shear strength of the panel zone is derived from the beam bending moments as a result of the loading combination of gravity loads plus 1.85 times the equivalent lateral forces. However, the panel zone need not have the shear strength to develop more than eighty percent of the sum total of plastic moment for the beams framing into the joint.

Additional ductility requirements for special moment-resisting space frames (SMRSF) are provided to ensure that the structure can experience significant inelastic deformation without non-ductile failure modes. If the ductility requirements for a special moment-resisting space frames are not satisfied, then the moment-resisting space frame is classified as ordinary. The response modification factor,  $R_w$ , for an ordinary moment-resisting space frame is eight. The beams and columns of a special moment-resisting space frame must be capable of forming plastic hinges without any local buckling of the flanges or web.

The determination of the equivalent lateral forces in the direct design procedure is rather straight forward. Once the lateral force-resisting system and height of the building is selected, and the soil profile of the site is determined, the design base shear can be calculated. Because so little information is required for a design, the factor of safety for any building could have much variance depending on the actual behavior of the structure in comparison to the design assumptions.

#### 2.4 Equivalent Lateral Forces and Member Selections

All structures considered in this study had plan dimensions of 144 feet by 108 feet and had story heights of 14 feet for the first story and 12 feet for the upper stories. The perimeter moment-resisting frames were used to resist the lateral forces and provide lateral stability of the entire structure. The interior frames resisted vertical forces from the gravity loads of their individual tributary area. Since the inelastic behavior of moment-resisting frames in the direction parallel to the 144 foot dimension (the long direction) was of interest in this investigation, only those columns, beams and connections resisting lateral forces in these frames were designed and studied. In fact, only one of the exterior frames needed to be modelled because of the assumed symmetry of the structure. One-half of the design base shear for the direction under consideration was resisted by each exterior frame. The floor and roof decks were assumed to be rigid enough to transfer the inertia forces in the center of the building to the exterior frames in the event of an earthquake.

The uniform dead loads listed in Table 2.1 were used in the weight calculations of each structure. The total seismic weight for buildings

typically is calculated from the dead loads and full partition load. The partition load should account for any live load acting on the structure. The story weights, given in Table 2.2 for a five-story model and Table 2.3 for a two-story model, were determined from the plan area of the floors or roof and the vertical tributary area of the exterior cladding.

TABLE 2.1 Uniform Dead Loads

Roof	Concrete Slab with Decking	42 psf
	Mechanical and Electrical	16 psf
	Ceiling	5 psf
	Structural	15 psf
	Insulation and Membrane	11 psf
	Total	89 psf
Floor	Concrete Slab with Decking	42 psf
	Mechanical and Electrical	16 psf
	Ceiling	5 psf
	Structural	20 psf
	Partitions	20 psf
	Total	103 psf
Facade	Cladding (exterior wall area)	5 psf

TABLE 2.2 Story Weights for Five-Story Building

$W_5$ (roof)	$(144)(108)(0.089) + 2(144 + 108)(6)(0.005) = 1399$ kips
$W_4$	$(144)(108)(0.103) + 2(144 + 108)(12)(0.005) = 1632$ kips
$W_3$	$(144)(108)(0.103) + 2(144 + 108)(12)(0.005) = 1632$ kips
$W_2$	$(144)(108)(0.103) + 2(144 + 108)(12)(0.005) = 1632$ kips
$W_1$	$(144)(108)(0.103) + 2(144 + 108)(13)(0.005) = 1635$ kips
$\Sigma$	7930 kips

TABLE 2.3 Story Weights for Two-Story Building

$W_2$ (roof)	$(144)(108)(0.089) + 2(144 + 108)(6)(0.005) = 1399$ kips
$W_1$	$(144)(108)(0.103) + 2(144 + 108)(13)(0.005) = 1635$ kips
$\Sigma$	3034 kips

Three different design base shear levels were used for the design of the five-story structures. The D1 series had a design base shear based on an assumed value of  $C$  equal to 2.75. The D2 series had a design base shear based on the estimated fundamental period of vibration for the building. The D3 series was based on more realistic value for the fundamental period of vibration determined from the calculated fundamental period of vibration for one of the frames in the D1 series. A design base shear based on the estimated fundamental period of vibration for the two-story building was used in the D4 series.

#### 2.4.1 Five-Story Frame Designs: D1A and D1B

The plan view of the structural layout for either the D1A or D1B frame designs is shown in Figure 2.3. The bay spacing in both directions is 18.0 feet, which probably is smaller than used in practice for typical steel frame buildings of today. The elevation view of Frame 1 (or Frame 7) is shown in Figure 2.4. The five-story building is classified as a "regular" structure since the distribution of mass through the height of the building is fairly uniform and there are no irregularities in plan or elevation. In fact, the building is symmetric in both stiffness and mass, thus eliminating any "calculated" torsion. In accordance with trends in practice and to

simplify the loading condition for the corner columns, biaxial bending can be eliminated by using pinned connections for the attachment of the beams in Frames 1 and 7 to the corner columns. The pinned connections were placed in Frames 1 and 7, because these frames had more bays than the Frames A and I of the perpendicular direction. Since the lateral force-resisting is the same in both direction the design base shear for each direction also is the same. The interior beam-to-column connections in the end bays of Frames 1 and 7 also were pinned because moment-resisting connections were not needed to satisfy the lateral stiffness and strength requirements of the frame. Therefore, the beams in the two end bays resist only vertical gravity loads and do not contribute to the lateral stiffness or strength of the frame.

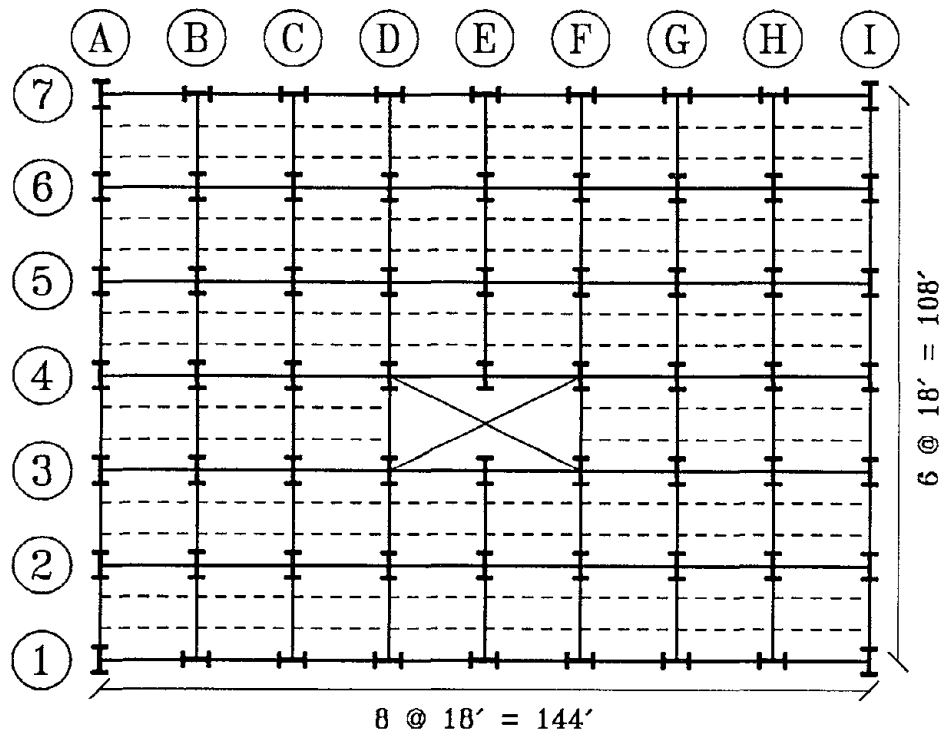
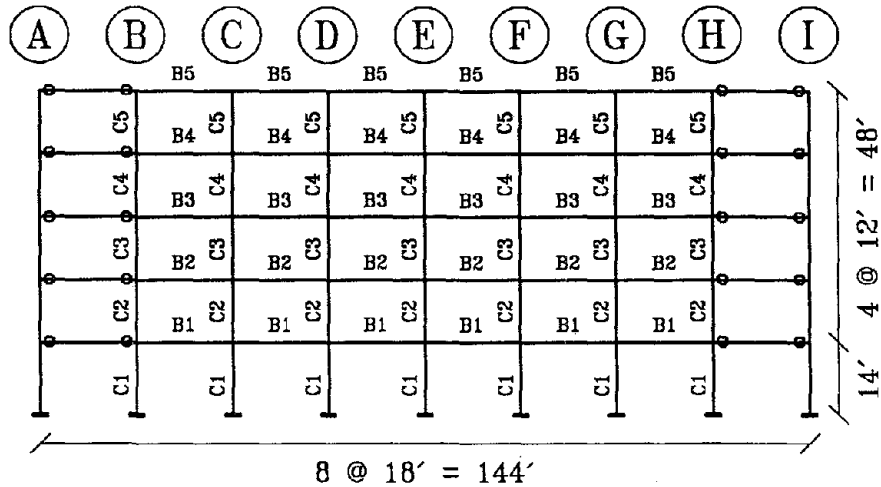


FIGURE 2.3 Plan View for the D1A, D1B and D2A Designs



*Note: ○ = Pinned Connection*

FIGURE 2.4 Elevation View of Frame 1 for the D1A, D1B and D2A Designs

In the D1A and D1B frame designs, the calculation of the design base shear was based on an assumed value of  $C$  equal to 2.75 (allowed by the code), even though a value of  $C$  based on the estimated fundamental period was smaller. Thus, the design base shear was 9.2 percent of the building weight. The usage of such an assumed value of  $C$  is generally conservative, especially for structures having an estimated or actual fundamental period longer than 0.5 seconds. Since the structure was designed with a base shear larger than the design base shear established from the estimated fundamental period, a stiffer and stronger structure than would be required if  $C$  was based on the fundamental period was necessary. Since stiffer structures typically attract more base shear during excitation (as illustrated by the calculation of  $C$ ), the additional margin of safety due to the conservative value of  $C$  is unclear. The design base shear and equivalent lateral forces for these designs are shown in Table 2.4.

TABLE 2.4 Lateral Forces for the D1A and D1B Designs

$T = 0.035(62)^{3/4} = 0.77 \text{ sec}$ (Estimated) $C = 2.75$ (Assumed) $V = 0.4(1.0)(2.75)(7930)/12 = 727 \text{ kips}$ ( $V/W = 0.092$ ) $F_t = 0.07(0.77)(727) = 39.2 \text{ kips}$					
Story Level	$W_x$ (kips)	$h_x$ (ft)	$W_x h_x$ (k-ft)	$\frac{W_x h_x}{\sum W_i h_i}$	$F_x^*$ (kips)
5	1399.	62.	86738.	0.29	241.0
4	1632.	50.	81600.	0.28	189.8
3	1632.	38.	62016.	0.21	144.3
2	1632.	26.	42432.	0.14	98.7
1	1635.	14.	22890.	0.08	53.2
$\sum$	7390.		295676.		727.0

\*  $F_s$  includes  $F_t$ 

**D1A Frame** - The member selections for the lateral-force resisting frames were controlled by the lateral forces of the seismic design, rather than the live loads and dead loads. To satisfy the lateral stiffness requirements the in-plane bending stiffness (moment of inertia) of the columns was important to controlling the drifts. The I-sections selected for the columns were deeper than normal to provide as much stiffness as possible for the given cross sectional area. The I-sections chosen for this frame design are shown in Table 2.5. These sections satisfied the lateral stiffness requirement, and matched as closely as possible the strength requirements. Smaller column and beam sections were chosen as allowable through the height of the structure. In general, the columns and beams were stronger than necessary, because lateral stiffness, not the strength of the members, controlled the design of the frame. I-sections having sufficient moment of inertia (stiffness) exceeded the requirements for the strength of

the section. Although, the shear capacity of the panel zones as a result of the column web thickness was not sufficient and doubler plates were needed. The dynamic behavior of this design was "strong beam-weak column", because the sum of the yield moments for the columns at a connection was generally less than the sum for the beams. The yield moment of each column was based on the interaction between the moment and axial force acting on the column (see Appendix A).

TABLE 2.5 Member Selections for the D1A Design

Story Level	Column Section	I (in <sup>4</sup> )	M <sub>p</sub> (in-k)	Beam Section	I (in <sup>4</sup> )	M <sub>p</sub> (in-k)
5	W21x44	843.	3430.	W18x40	612.	2820.
4	W21x68	1480.	5760.	W24x62	1550.	5510.
3	W21x101	2420.	9110.	W24x84	2370.	8060.
2	W21x111	2670.	10040.	W24x94	2700.	9140.
1	W21x111	2670.	10040.	W24x94	2700.	9140.

**D1B Frame** – The D1B frame was similar to the D1A frame, except that stronger columns of roughly the same stiffness were chosen to transform the dynamic behavior to be "strong column-weak beam". The column sections of the D1B frame were not as deep as the columns of the D1A frame. The cross sectional area, and consequently the unit weight per foot, of the columns increased considerably to acquire a section with the same moment of inertia. The I-sections chosen for this design are shown in Table 2.6. Again, the column and beam sections were reduced as allowable in the upper stories of the structure.



TABLE 2.6 Member Selections for the D1B Design

Story Level	Column Section	I (in <sup>4</sup> )	M <sub>p</sub> (in-k)	Beam Section	I (in <sup>4</sup> )	M <sub>p</sub> (in-k)
5	W14x74	796.	4540.	W18x40	612.	2820.
4	W14x120	1380.	7630.	W24x62	1550.	5510.
3	W14x176	2140.	11520.	W24x84	2370.	8060.
2	W14x193	2400.	12780.	W24x94	2700.	9140.
1	W14x193	2400.	12780.	W24x94	2700.	9140.

The inelastic behavior of the D1A and D1B frames was investigated in a parametric study to determine the influence of the beam-to-column strength ratio since this was principal difference between these two frames. The D1B frame also was used in parametric studies of beam-to-column connection behavior, nonstructural element participation and design base shear level.

#### 2.4.2 Five-Story Frame Designs: D2A, D2B and D2C

The value of  $C$  for the D2A, D2B and D2C frame designs was based on the estimated period given by Equation 2.3 for the sixty-two foot high, steel frame structure, instead of the conservative value of  $C$  equal to 2.75. Each of these D2 frame designs had a different configuration for the lateral force-resisting system. The design base shear was the same for each design, because the estimation of the fundamental period was independent of frame configuration. The design base shear and equivalent lateral forces for all three designs are shown in Table 2.7. The design base shear for these three frames was 5.9 percent, which is approximately two-thirds of the design base shear corresponding to a value of  $C$  equal to 2.75. The columns and beams of the lower three stories were each of the same section as were columns and

beams of the upper two stories. Therefore, both the story drifts and stresses from the direct design procedure were generally less than the allowable limits.

TABLE 2.7 Lateral Forces for the D2A, D2B and D2C Designs

$T = 0.035(62)^{3/4} = 0.77 \text{ sec}$ (Estimated) $C = 1.25(1.2)/(0.77)^{2/3} = 1.78$ $V = 0.4(1.0)(1.78)(7930)/12 = 470 \text{ kips}$ ( $V/W = 0.059$ ) $F_t = 0.07(0.77)(470) = 25.3 \text{ kips}$					
Story Level	$W_x$ (kips)	$h_x$ (ft)	$W_x h_x$ (k-ft)	$\frac{W_x h_x}{\sum W_i h_i}$	$F_x^*$ (kips)
5	1399.	62.	86738.	0.29	155.8
4	1632.	50.	81600.	0.28	122.7
3	1632.	38.	62016.	0.21	93.3
2	1632.	26.	42432.	0.14	63.8
1	1635.	14.	22890.	0.08	34.4
$\sum$	7390.		295676.		470.0

\*  $F_5$  includes  $F_t$

**D2A Frame** - The plan view of the structural layout and the elevation view of the frame configuration for the D2A design is identical to the D1A or D1B designs (see Figures 2.3 and 2.4). The smaller design base shear permitted lighter sections to be used for the columns and beams than the D1A frame. The I-sections chosen for this design are given in Table 2.8. The sections were not changed as allowed, but the same sections were used for the lower three stories and different sections were used for the upper two stories. Therefore, both the stiffness and strength requirements of some stories were exceeded. Although this selection of members probably is more representative of actual practice.

TABLE 2.8 Member Selections for the D2A Design

Story Level	Column Section	I (in <sup>4</sup> )	M <sub>p</sub> (in-k)	Beam Section	I (in <sup>4</sup> )	M <sub>p</sub> (in-k)
5	W21x57	1170.	4644.	W21x44	843.	3434.
4	W21x57	1170.	4644.	W21x44	843.	3434.
3	W21x83	1830.	7056.	W21x68	1480.	5760.
2	W21x83	1830.	7056.	W21x68	1480.	5760.
1	W21x83	1830.	7056.	W21x68	1480.	5760.

**D2B Frame** - The plan view of the structural layout and the elevation view of the frame configuration for the D2B design is shown in Figures 2.5 and 2.6. The bay spacing of this frame was increased to 28.8 feet, while the overall length remained unchanged. The advantage of longer bay spacings was a reduction in the number of moment-resisting connections and in the number of members that need to be erected. It should be noted that bay widths of up to 40 feet in length have been used in modern steel frame construction. However, the longer bay spacings increase the effective lengths of the columns, which in turn lower the allowable stresses for the columns. Therefore, the material efficiency actually may decrease when longer bay spacing are used. The total dead weight of the D2B frame with 28.8 foot bay spacings increased by twenty percent over the D2A frame with 18.0 foot bay spacings. The increase weight and material cost of the D2B frame is offset by the savings in the fabrication and erection costs. The I-sections chosen for this design are given in Table 2.9. Again, the same sections were used for the lower three stories and upper two stories. In this design the same column depth was used throughout the height of the structure, but two different beam depths were used.

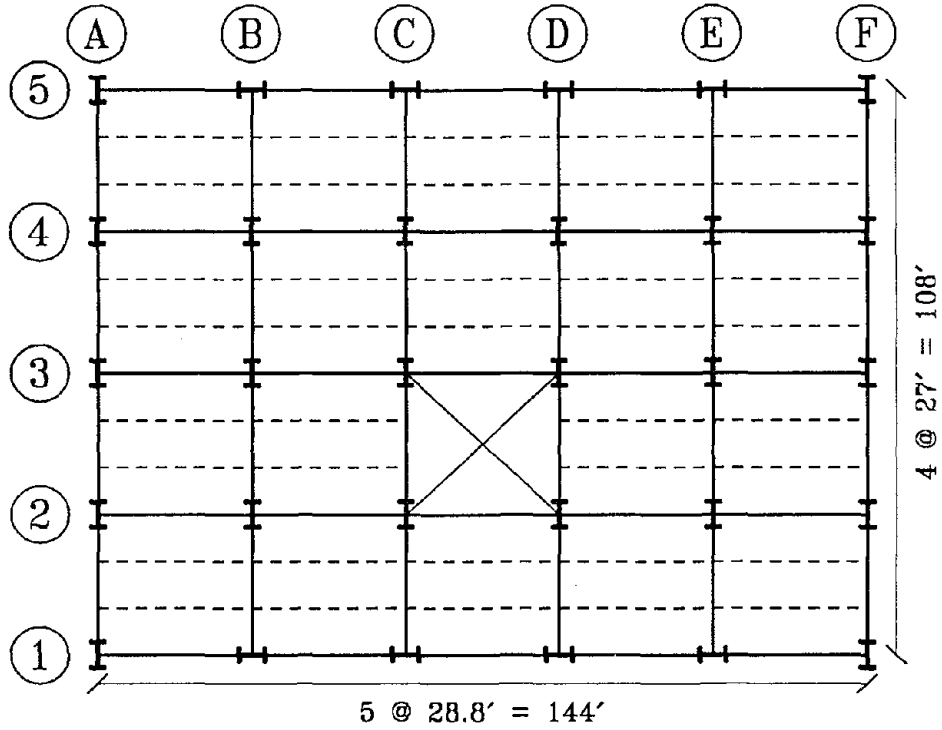
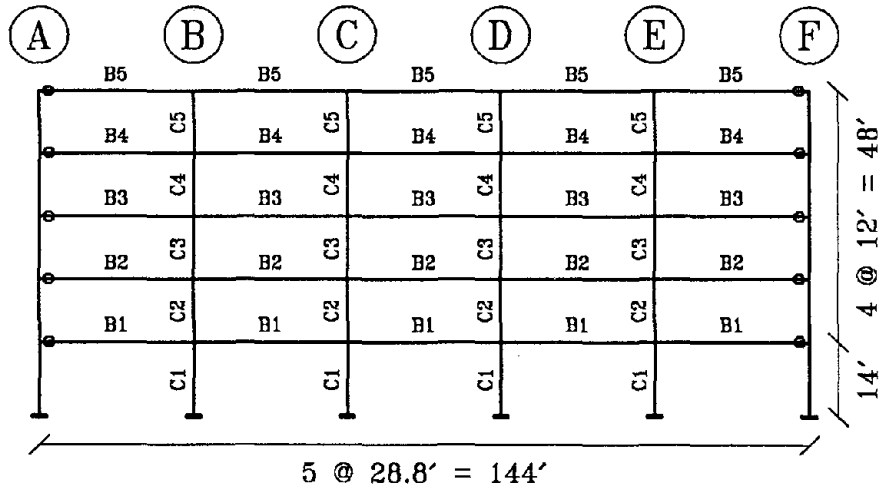


FIGURE 2.5 Plan View for the D2B, D2C, D3 and D4 Designs



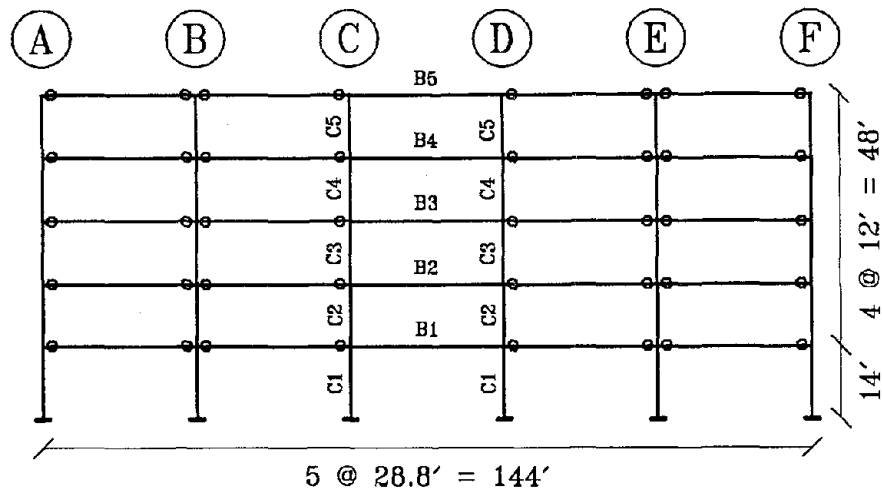
Note:  $\circ$  = Pinned Connection

FIGURE 2.6 Elevation View of Frame 1 for the D2B Design

TABLE 2.9 Member Selections for the D2B Design

Story Level	Column Section	I (in <sup>4</sup> )	M <sub>p</sub> (in-k)	Beam Section	I (in <sup>4</sup> )	M <sub>p</sub> (in-k)
5	W21x93	2070.	7956.	W24x68	1830.	6372.
4	W21x93	2070.	7956.	W24x68	1830.	6372.
3	W21x147	3630.	13428.	W27x102	3620.	10980.
2	W21x147	3630.	13428.	W27x102	3620.	10980.
1	W21x147	3630.	13428.	W27x102	3620.	10980.

**D2C Frame** - The plan view of structural layout for the D2C design is identical to the D2B design (see Figure 2.5). The elevation view of the frame configuration for the D2C design is shown in Figure 2.7. Only the center bay, which provides all of the lateral resistance and stability, has moment-resisting connections. The redundancy of the structure and possible yield locations for hysteretic energy dissipation was decreased by the elimination of moment-resisting connections. The loss of lateral strength of the frame from structural damage to a moment-resisting connection in this configuration can have a tremendous impact on the survivability of the structure. The I-sections chosen for the center bay of this design are given in Table 2.10. The same sections were used for the lower three stories and different sections were used for the upper two stories. Since only a few members are providing the entire lateral force resistance and stability, the size of these members are quite deep and heavy. In fact, architectural considerations may be necessary to allow the usage of such deep members. The member selections for the other columns and beams would be based strictly on the vertical gravity loads and would be much smaller.



*Note: ○ = Pinned Connection*

FIGURE 2.7 Elevation View of Frame 1 for the D2C and D3 Designs

TABLE 2.10 Member Selections for the D2C Design

Story Level	Column Section	I (in <sup>4</sup> )	M <sub>p</sub> (in-k)	Beam Section	I (in <sup>4</sup> )	M <sub>p</sub> (in-k)
5	W27x146	5630.	16596.	W27x146	5630.	16596.
4	W27x146	5630.	16596.	W27x146	5630.	16596.
3	W30x235	11700.	30420.	W30x211	10300.	26964.
2	W30x235	11700.	30420.	W30x211	10300.	26964.
1	W30x235	11700.	30420.	W30x211	10300.	26964.

The designs of the D2A, D2B and D2C frames for a five-story building were based on the same design procedure. The difference between the three frames was the configuration of the lateral-force resisting system. A parametric study comparing the inelastic response of the three frames was performed. The D2A and D2C frames also were used in a parametric study of

design base shear level. In addition, the D2C was used in parametric studies which examined the influence of initially defective moment-resisting connections and participation of nonstructural elements.

#### 2.4.3 Five-Story Frame Design: D3

The design base shear for the D2A, D2B and D2C designs was calculated with an estimated period (Equation 2.3) of the structure. However, the code permits  $C$  to be determined from a more realistic value for the fundamental period of the structure. The period given by Equation 2.3 is typically shorter than the calculated period of the bare structure frame, thus the design base shear is theoretically larger than necessary.

The value of  $C$  used for the drift design (stiffness requirements) is calculated from Equation 2.2, where  $T$  is the calculated fundamental period of the D2C frame. However, the code specifies the value of  $C$  for the stress design (strength requirements), may not be less than eighty percent of the value obtain by Equations 2.2 and 2.3. Therefore, the D3 design has two independent sets of equivalent lateral forces - one set for checking stiffness requirements and one set for strength requirements. The limit in the reduction of  $C$  for the stress design is to safeguard against using a value of  $T$  that is too long and results in a structure of questionable strength. One consequence of using a smaller design base shear for the drift design is that the stress design may control the selection of members and any unaccounted for additional factor of safety for the strength is eliminated. Although, the lateral stiffness of the structure is more than necessary. The design base shears and equivalent lateral forces for the drift and stress design are shown in Tables 2.11 and 2.12, respectively.

TABLE 2.11 Lateral Forces for the D3 Design (Drift)

$T = 1.48 \text{ sec}$ (Period of D2C) $C = 1.25(1.2)/(1.48)^{3/4} = 1.16$ (Full reduction) $V = 0.4(1.0)(1.16)(7930)/12 = 307 \text{ kips}$ ( $V/W = 0.039$ ) $F_t = 0.07(1.48)(307) = 31.8 \text{ kips}$					
Story Level	$W_x$ (kips)	$h_x$ (ft)	$W_x h_x$ (k-ft)	$\frac{W_x h_x}{\sum W_i h_i}$	$F_x^*$ (kips)
5	1399.	62.	86738.	0.29	112.5
4	1632.	50.	81600.	0.28	76.0
3	1632.	38.	62016.	0.21	57.7
2	1632.	26.	42432.	0.14	39.5
1	1635.	14.	22890.	0.08	21.3
$\Sigma$	7390.		295676.		307.0

\*  $F_5$  includes  $F_t$ 

TABLE 2.12 Lateral Forces for the D3 Design (Stress)

$C = 0.80(1.78) = 1.42$ (Reduction from D2C) $V = 0.4(1.0)(1.42)(7930)/12 = 375 \text{ kips}$ ( $V/W = 0.047$ ) $F_t = 0.07(1.48)(375) = 38.9 \text{ kips}$					
Story Level	$W_x$ (kips)	$h_x$ (ft)	$W_x h_x$ (k-ft)	$\frac{W_x h_x}{\sum W_i h_i}$	$F_x^*$ (kips)
5	1399.	62.	86738.	0.29	137.5
4	1632.	50.	81600.	0.28	92.8
3	1632.	38.	62016.	0.21	70.5
2	1632.	26.	42432.	0.14	48.2
1	1635.	14.	22890.	0.08	26.0
$\Sigma$	7390.		295676.		375.0

\*  $F_5$  includes  $F_t$ 

The plan view of the structural layout and the elevation view for the frame configuration for the D3 design is the same as the D2C design (see Figures 2.5 and 2.7). The D2C design was selected for recalculating the



design base shear, because dramatic changes in member sizes occur when fewer members exist in the frame. The I-sections chosen for this design are given in Table 2.13. The same section depths are used in the D2C and D3 frames, although the weights per unit length are less for the D3 frame.

TABLE 2.13 Member Selections for the D3 Design

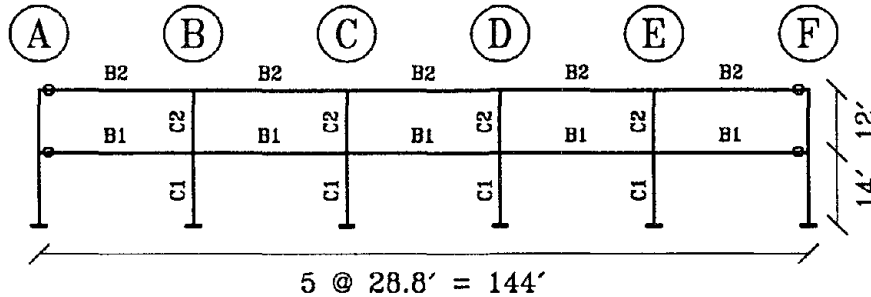
Story Level	Column Section	I (in <sup>4</sup> )	M <sub>p</sub> (in-k)	Beam Section	I (in <sup>4</sup> )	M <sub>p</sub> (in-k)
5	W27x114	4090.	12348.	W27x94	3270.	10008.
4	W27x114	4090.	12348.	W27x94	3270.	10008.
3	W30x191	9170.	24228.	W30x173	8200.	21780.
2	W30x191	9170.	24228.	W30x173	8200.	21780.
1	W30x191	9170.	24228.	W30x173	8200.	21780.

The D3 frame, single bay providing the lateral resistance and stability for the five-story structure was used in parametric studies investigating the participation of nonstructural elements and design base shear level.

#### 2.4.4 Two-Story Frame Design: D4

A two-story building, D4 design, was studied in some detail, because the fundamental period of a two-story structure is generally shorter than a five-story structure. The estimated fundamental period is located on the maximum plateau on the design spectra. The plan view of the structural layout and the elevation of the frame configuration for the D4 design is given in Figures 2.5 and 2.8. The design base shear and equivalent lateral forces for this design are shown in Tables 2.14. The I-sections chosen for this design are given in Table 2.15. The same column section was used in

both stories of the D4 frame, thus eliminating the need for any column splices. In addition, the same section was used for all of the beams in the frame. The lateral stiffness of the second stories and the strength of the members in the story were more than required by the code.



Note:  $\odot$  = Pinned Connection

FIGURE 2.8 Elevation View of Frame 1 for the D4 Design

TABLE 2.14 Lateral Forces for the D4 Design

$T = 0.035(26)^{3/4} = 0.40 \text{ sec}$ (Estimated) $C = 1.25(1.2)/(0.40)^{2/3} = 2.76$ (Use $C = 2.75$ ) $V = 0.4(1.0)(2.75)(3034)/12 = 278 \text{ kips}$ ( $V/W = 0.092$ ) $F_t = 0.0 \text{ kips}$ ( $T < 0.7 \text{ sec}$ )					
Story Level	$W_x$ (kips)	$h_x$ (ft)	$W_x h_x$ (k-ft)	$\frac{W_x h_x}{\sum W_i h_i}$	$F_x$ (kips)
2	1399.	26.	36374.	0.61	170.6
1	1635.	14.	22890.	0.39	107.4
$\sum$	3034.		59264.		278.0

TABLE 2.15 Member Selections for the D4 Design

Story Level	Column Section	I (in <sup>4</sup> )	M <sub>p</sub> (in-k)	Beam Section	I (in <sup>4</sup> )	M <sub>p</sub> (in-k)
2	W18x76	1330.	5868.	W18x65	1070.	4788.
1	W18x76	1330.	5868.	W18x65	1070.	4788.

The D4 frame design was used in a parametric study that investigated the influence of the fundamental period of vibration for a structure. Since the estimated fundamental period of the two-story structure was shorter than the five-story, the minimum design base shear level as a percentage of the building weight was larger for the two-story frame. The participation of nonstructural elements, which had the same stiffness and strength as in the five-story frames, also was investigated for the two-story frame.

## 2.5 Summary

The design of the frames for this study illustrate the wide latitude given in the code for the design of the lateral force-resisting system for a building. As is generally the case for design, there is not a "correct" solution, but many possible solutions. However depending on the design criteria, one of the designs may be preferable over other designs.

The magnitude of the design base shear was the principal difference between the D1, D2 and D3 frame designs for the moment-resisting frames of the five-story structure. The design base shear of the D1 frames was 9.2 percent of the building weight, while the design base shear of the D2 frames was 5.9 percent of the building weight. The design base shear of the D3 frame was 3.9 percent of the building weight for the drift design and 4.7

percent of the building weight for the stress. The method to calculate the design base shear for the D2 frames is typical of current practice. The design base shear for the D1 frames is conservative and, as a consequence, the expected story drifts should be less than the D2 frames. The D3 design may be unconservative because the calculated period used in the design was based only on a bare structural frame. The actual period of the structure may be greater than the estimated period given by the code, but the actual period is certainly greater than the calculated period of the trial design.

The magnitude of the design base shear used in the D4 frame design for the moment-resisting frames of the two-story structure was 9.2 percent of the building weight. The design base shear was limited by the given upper limit of the code, and therefore a larger base shear need not be used for a steel frame structure of this height.

The belief that a stiffer and stronger structure is more conservative (smaller drifts and less inelastic behavior) uses an assumption that the response spectrum of the ground motion does not increase significantly as the fundamental periods in the range under consideration decrease. For the earthquake accelerograms of this study, the elastic response spectra were fairly uniform over the frequency range of the lower modes of vibration for the various frames investigated.

## CHAPTER 3

### ANALYSIS AND MODELLING OF FRAME STRUCTURES

#### 3.1 Introduction

In order to determine the probable structural demand on the lateral force-resisting system of a building during a major earthquake, a numerical modelling of the building and an acceleration-time history of the ground motion is necessary. Since neither the "exact" load-deformation behavior of a building or the ground motion of future earthquakes is known, several alternatives for both need to be explored to determine a range in response.

The procedure to analyze the structural response and selection of the historical earthquake accelerograms are examined in this chapter. In addition, the modelling of the beam-to-column connections (panel zones), nonstructural elements and P-Delta effects are presented in some detail. This chapter also contains a discussion concerning the development of the numerical models for the time-history analyses.

#### 3.2 Analysis Approach

Inelastic time-history analyses were employed in this study to compute the dynamic response of numerical models for various frame designs excited by a set of historical ground acceleration records. The estimation of structural response to a given ground excitation with time-history analysis is computationally intensive, especially when inelastic behavior is to be considered. Much information regarding the properties and behavior of a structure is required in a time-history analysis. The solution procedure for an inelastic time-history analysis assumes that the stiffness of the

structure remains constant during each time step and that changes in stiffness only can occur between successive time steps.

The reliability of any time-history analysis is dependent on accurate modelling with finite elements of the structure's load-deformation behavior and the numerical procedure for solving the nonlinear equations of motion. The computer program, DRAIN-2D, was used to calculate the dynamic response of the frame models. The behavior of the finite (or more aptly discrete) elements used in this study which were available in the DRAIN-2D element library and the solution procedure for the equations of motion are explained in some detail in Appendix A.

### 3.3 Representation of Design Earthquake

Earthquake accelerograms, representative of the design earthquake for the 1988 edition of the *Uniform Building Code*, were used in the time-history analyses to compute the inelastic response of low-rise buildings using moment-resisting steel frames for the lateral force-resisting system. Since the ground motion of future earthquakes is unknown and nearly impossible to predict, several ground excitation records, which are plausible for a given site, generally are used to determine the probable inelastic response of a building. The adequacy of a seismic design can be judged after studying the response from each of the selected ground motions. For similar reasons, three historical earthquake accelerograms were selected to represent the design earthquake in this study. All of the frame models in this study were subjected to each of the earthquake accelerograms.

The S00E component of the 1940 El Centro earthquake, the N65E component of the 1966 Parkfield earthquake and the S69E component of the 1952 Taft

earthquake were selected for the base excitation records of the time-history analyses. These earthquake records were chosen because of the different characteristics in their ground motions. The El Centro record contains a broad frequency range of ground acceleration and has several periods of strong ground motion. The Parkfield record has a single burst of strong ground motion and is composed of lower frequency ground acceleration. The Taft record has higher frequency ground acceleration and a long duration of moderate ground motion. In these three earthquakes most of the strong ground motion occurred within the first twenty seconds of excitation. As a consequence, the time-history analyses were performed using only the first twenty seconds of ground excitation for each record. The accelerograms for each of the three earthquakes are shown in Figure 3.1.

The earthquake accelerograms needed to be scaled to about the same level of "intensity", so that the response calculated from each earthquake could be compared. In addition, the scaling of each earthquake record was supposed to produce excitation representative of the design earthquake to enable comparisons between the calculated response and the anticipated response of the code. The "design" earthquake, as characterized by various building codes, has the capability to generate significant inelastic deformations in the lateral force-resisting system - ductilities in the range of four to five for moment-resisting steel frames. An assumption in the 1988 UBC is that the chance of exceeding the intensity of the design earthquake is estimated to be ten percent in fifty years [4,16,43]. It should be noted that this definition of the design earthquake does not represent the maximum credible earthquake for the region but only the maximum probable earthquake.

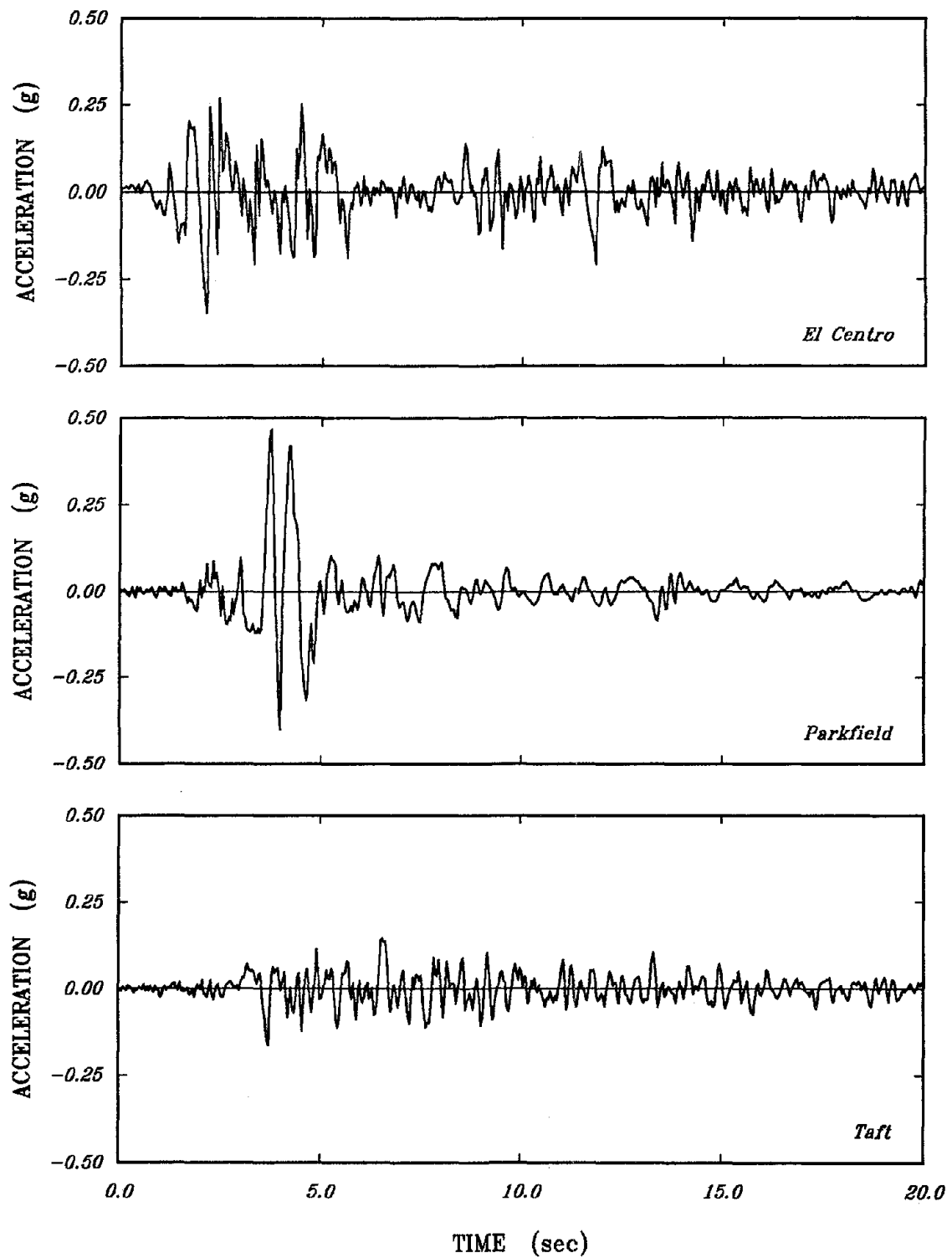


FIGURE 3.1 Unscaled Earthquake Accelerograms



A smoothed elastic response spectrum is used to anchor the design spectrum in the 1988 edition of the *Uniform Building Code*. In actuality, the code only uses equations to obtain the design base shear, but a plot of these equations can be thought of as a smoothed elastic response spectrum and a design spectrum. The smoothed elastic response spectrum, based on a five percent damped single-degree-of-freedom system, has a maximum spectral acceleration of 1.1 g for highly seismic regions (zone 4).

Nau and Hall [33] showed that a scaling procedure based on structural response, rather than peak ground motions, gave less dispersion in the responses from several records. In a more recent study [1] regarding the determination of the design earthquake, one conclusion found from this study also was that peak ground motions are not an accurate parameter to classify the intensity of a ground motion. Since the design spectrum is anchored to an elastic response spectrum, the elastic response spectra of the earthquake accelerograms were used to determine the scaling for the selected historical accelerograms. The elastic response spectra for a five percent damped single-degree-of-freedom system excited by the first twenty seconds of each earthquake are shown in Figure 3.2a along with the elastic response spectrum used to anchor the design spectrum for this investigation.

A two step procedure was used to calculate the scaling factors for the acceleration values of each earthquake accelerogram. The first step in the scaling procedure was to normalize the earthquake records, so that they all had the same spectrum intensity over a specified frequency range. The spectrum intensity is given by

$$SI_v = \int SV(f) df; \quad (3.1)$$

where  $SV(f)$  is the spectral pseudovelocity and  $f$  is the frequency in Hertz. Housner's definition of spectrum intensity has integration limits of 0.4 and 10.0 Hertz [22]. However, the integration limits used in this investigation were 0.5 and 3.0 Hertz; this range had better correlation with the natural frequencies dominating the response of the modelled frame structures and also was the region of the response spectra controlled by velocity. The spectrum intensities for each earthquake are given in Table 3.1. The values given in the column labeled " $SF_1$ " were the scale factors that resulted in equal spectrum intensities. The usage of these scale factors tended to group together the elastic response spectra. The absolute vertical position of the three spectra was determined from the second step of the scaling procedure, which shifted the spectra as a group.

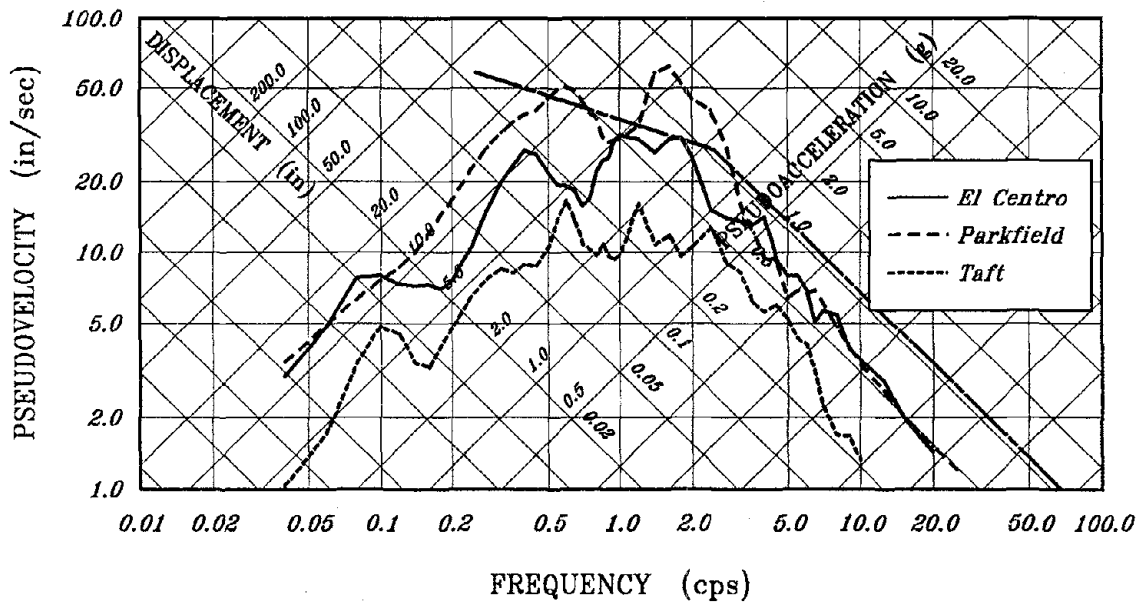


FIGURE 3.2a Unscaled Elastic Response Spectra for Five Percent Damping

TABLE 3.1 Scaling Factors for Earthquake Accelerograms

Record	$SI_v$ (in/sec <sup>2</sup> )	$SF_1$	$SI_a$ (g's)	$SF_2$	SF
El Centro	38.8	1.86	1.30	0.85	1.57
Parkfield	71.7	1.00			0.85
Taft	19.9	3.59			3.03

The second step of the scaling procedure consisted of positioning the three response spectra. A new spectrum was created by averaging at each frequency the pseudovelocities of each response spectrum scaled with the corresponding scale factor calculated in the first step of the scaling procedure. The average spectral acceleration for the new spectrum was calculated over the frequency range of 2.0 to 4.0 Hertz. The lower limit of 2.0 Hertz was roughly the location where acceleration begins to control a typical response spectrum. The upper limit was selected, because it bounded the desired frequency range and provided a wide enough frequency range for scaling. The average spectral acceleration is defined as

$$\overline{SI}_a = \frac{1.0}{4.0 - 2.0} \int_{2.0 \text{ Hz}}^{4.0 \text{ Hz}} SA(f) df, \quad (3.2)$$

where  $SA(f)$  is the spectral pseudoacceleration.

The average spectral acceleration for the average of the three scaled records was desired to be 1.1 g, maximum acceleration for elastic response envisioned by the code, but was calculated to be 1.3 g for the average of the three scaled accelerograms. Therefore, the second scale factor,  $SF_2$ , is

equal to 1.1 divided by 1.3. The final scale factors for each record, given in the column labeled "SF" in Table 3.1, are the product of the scale factors,  $SF_1$ , calculated in the first step and the scale factor,  $SF_2$ , of the second step. The final position of the scaled elastic response spectra are shown in Figure 3.2b along with the elastic response spectrum used to anchor the design spectrum. It should be noted that the Parkfield accelerogram was scaled down to the level of the design earthquake, because this record was very strong in the frequency region under consideration in this study.

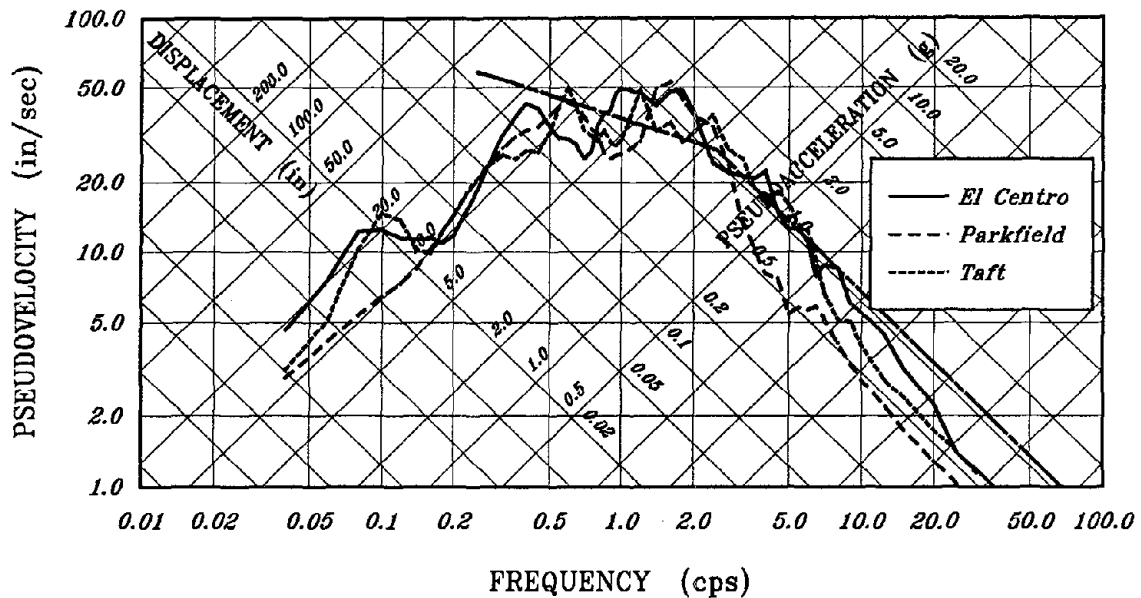


FIGURE 3.2b Scaled Elastic Response Spectra for Five Percent Damping

The maximum response quantities for a frame model with an elastic or nearly elastic response would be approximately the same as a result of excitation with each scaled record. As would be expected, the differences between the calculated responses from each earthquake accelerogram would be

more prevalent as the level of inelastic response increased. The variation in response can be judged (visually) by noting that the calculated response of the frame models in this study ranged from story drifts smaller than the design levels to story drifts larger than ten times the design levels.

### 3.4 Beam-to-Column Connection Modelling

The load-deformation behavior of a steel structural frame is dependent on the stiffness and strength of the columns and beams, and also on the stiffness and strength of the connections between the columns and beams. In one of the parametric studies for this investigation, the influence of the beam-to-column connections on the inelastic behavior was examined.

The inherent flexibility and yield strength of the beam-to-column connections affect the natural frequencies of a structure and the locations of hysteretic energy dissipation during inelastic excursions. The assumed behavior of the beam-to-column connections in the time-history analyses was dependent on the assumptions made during the modelling phase of each frame.

The panel zone of a rigid type beam-to-column connection is the length of the column located between the beam flanges at a joint. If required to satisfy the strength or stability requirements of the code, column web stiffeners and/or doubler plates can be added to the panel zone. Shear stresses are developed in the panel zone when an unbalanced moment exists between the beams framing into the joint. In the case of a single beam framing into a joint, the end moment of that beam is the unbalanced moment. Shear stresses in the panel zone cause shear deformation and possibly yielding of the panel zone. Distortion of the panel zone alters the angle between the columns and beams framing into the joint. An exaggerated view

of shear deformation in a panel zone from unbalanced beam moments applied to a typical interior beam-to-column connection is shown in Figure 3.3.

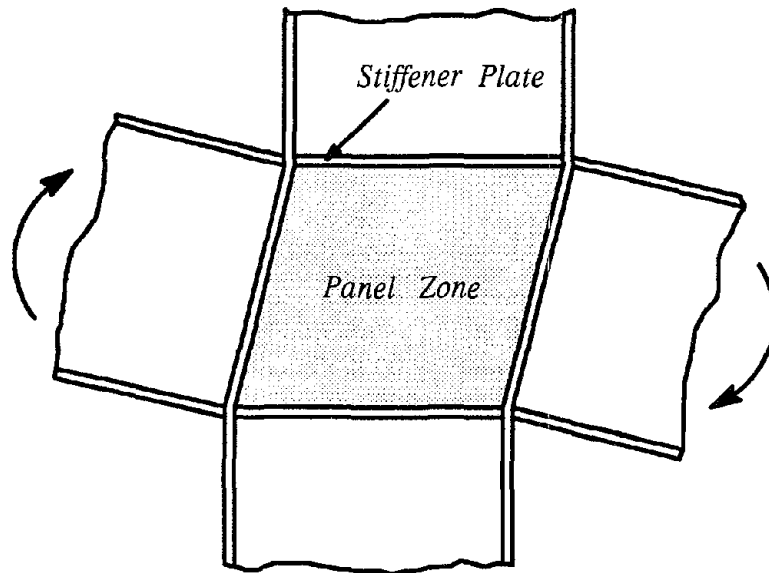


FIGURE 3.3 Exaggerated Deformation of a Panel Zone

The connection element available in the DRAIN-2D element library was utilized in the frame models so that, if desired, shear deformation in a panel zone could be modelled with a bilinear moment-rotation relationship, which is explained in Appendix A. The moment transferred by the connection element was related to the relative rotation between the ends of the columns and beams at a joint.

The parametric study of connection behavior was comprised of four models to produce a joint with different stiffness and strength. The overall behavior of a joint was dependent on the characteristics of the columns, beams and panel zone located at a joint. The physical meaning of each connection model is described next:

- 1) No Panel Zone (NPZ) model denotes a rigid connection allowing no relative rotation between the columns and beams framing into a joint and having plastic hinge locations for the columns and beams at the intersection of the member centerlines of the joint - the typical behavior for beam-to-column connections in finite element models of moment-resisting frames;
- 2) Rigid Panel Zone (RPZ) model denotes a rigid connection allowing no relative rotation between the columns and beams framing into a joint and having plastic hinge locations for the columns and beams at the connection faces of the joint;
- 3) Elastic Panel Zone (EPZ) model denotes a flexible connection allowing relative rotation between the columns and beams framing into a joint, having the elastic strength to develop the full plastic moment of the beams framing into each joint and having plastic hinge locations for the columns and beams at the intersection of the member centerlines of the joint;
- 4) Inelastic Panel Zone (IPZ) model denotes a flexible connection allowing relative rotation between the columns and beams framing into a joint, having the inelastic strength, after yielding of the panel zone web, to develop the full plastic moment of the beams framing into each joint and having plastic hinge locations for the columns and beams at the intersection of the member centerlines of the joint.

#### **3.4.1 Rigid Connection Behavior**

In both of the rigid connection models designated as NPZ and RPZ, no relative rotation occurred at a joint. In the first rigid connection model,

the influence of the panel zone was completely neglected. The flexible lengths of the columns and beams, as shown in Figure 3.4, were taken to be equal to the centerline-to-centerline dimensions. The increase in frame flexibility due to the usage of centerline dimensions is thought, in common practice, to compensate for neglecting the flexibility of the connection. The 1988 edition of the Uniform Building Code allows the deformation in the panel to be ignored, if centerline dimensions are used in the story drift calculations and the strength of the panel zone is above a specified level.

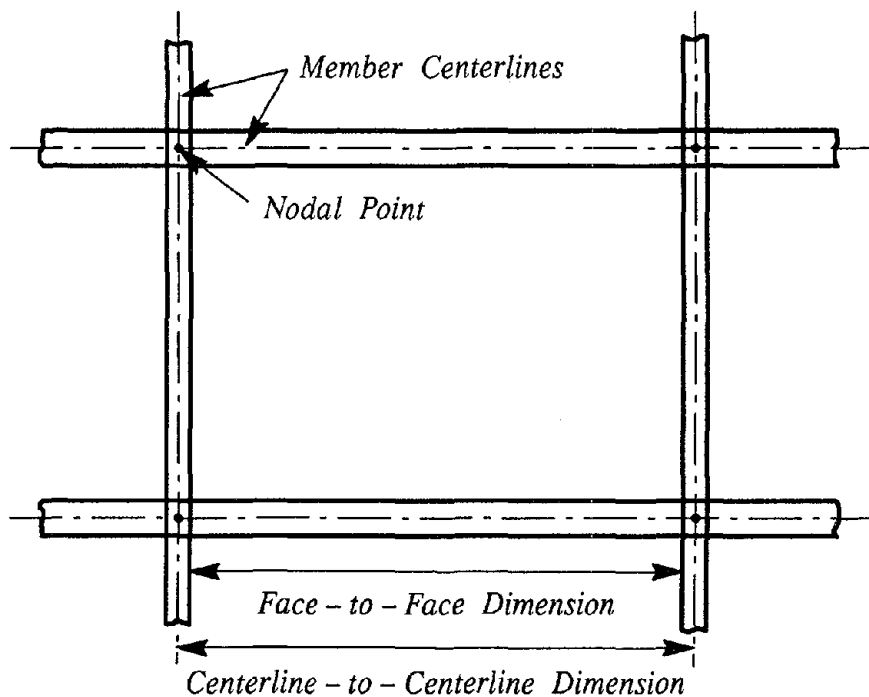


FIGURE 3.4 Dimensions for Typical Interior Frame

Yielding of a column or beam end occurred when the moment acting at an end exceeded the yield moment capacity of the section. Depending on the relative yield moments of the columns and beams at a joint, the plastic



hinge locations would either form in the column or the beam ends. However, this is not the best physical representation of the actual behavior of the connection because yielding of either the columns or the beams would occur at the connection face where the moment is maximum for the clear span portion of the beam.

The panel zone web of the other rigid connection model was assumed to be rigid. The deformation mode of the panel zone was a rigid body motion, so no yielding or deformation occurred with the panel zone region. An eccentricity at each end of the columns and beams equal to half of the column depth for the beams and half the beam depth for the columns was specified to move the plastic hinge location from the end of the member to the connection face. Therefore, the flexible lengths, as shown in Figure 3.4, of the columns and beams were taken to be equal to the face-to-face dimensions (clear span). Face-to-face dimensions produce the stiffest modelling of a frame. The increase in stiffness can be quite significant for frames with deep sections, since the lateral stiffness of a column is inversely related to the flexible length cubed.

Yielding of a column or beam at the connection face occurred when the moment at the connection face exceeded the yield moment capacity of the section. A free body diagram of a typical beam element without any forces applied along the length of the member is shown in Figure 3.5. In fact, any forces along the members are converted to equivalent nodal loads in the DRAIN-2D computer program. Since no forces are applied along the member, the shear in the member is constant and the moment varies linearly from one end to the other. Therefore, the maximum moment and any yielding always occur at an end of a member.

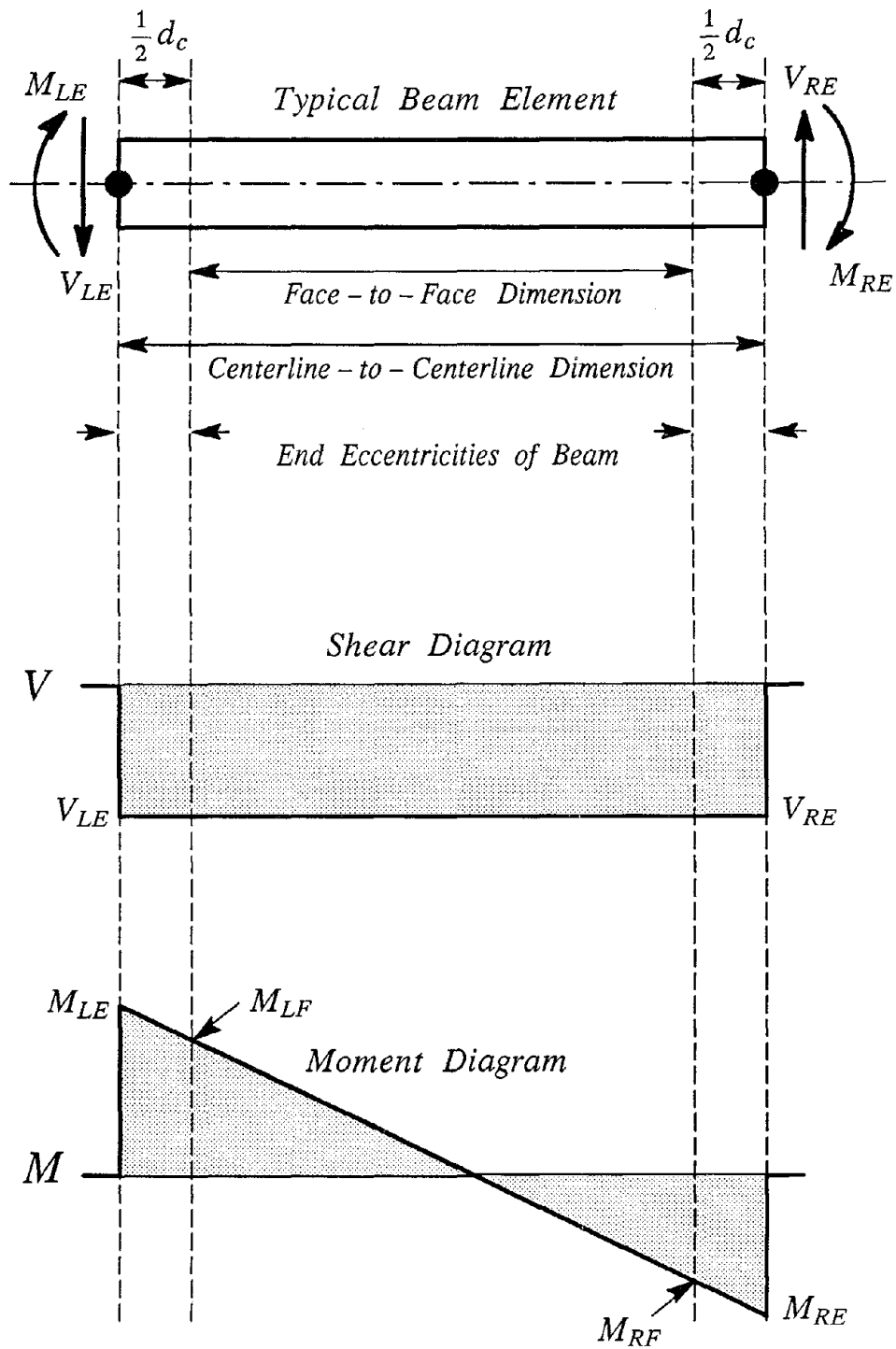


FIGURE 3.5 Free Body Diagram of a Typical Beam Element

As shown in Figure 3.5, the moment at the end of the member is applied to the node and must be in equilibrium with the other moments acting at the node. In addition, the moment at the end of a member is equal to the moment at the connection face plus the shear acting at the connection face times the distance between the end node and connection face (end eccentricity). The moment acting at the face of the connection is always less than the moment acting at the end of a member in double (reverse) curvature, which is generally the case for the columns and beams of a lateral force-resisting frame with small vertical loads. In fact, the end moments for each of the beams framing into a joint is approximately the same and acting in the same direction, because the external forces applied to the beams are relatively small compared to the lateral forces.

#### 3.4.2 Flexible Connection Behavior

The connection models designated as EPZ and IPZ were both assumed to be flexible. The forces acting at a typical interior beam-to-column connection are shown in Figure 3.6a. The forces,  $F_h$  and  $F_v$ , are the externally applied forces (inertia, static or both) to the joint. No axial forces are present in the beams of this study because the beams are assumed to be axially rigid. A free body diagram of the upper pair of web plate stiffeners for a panel zone with plate stiffeners is shown in Figure 3.6b. The shear force,  $V_{PZ}$ , acting above and below the panel zone region is resisted by the web of the panel zone and the flanges of the columns. It is quite possible that the shear strength of the panel zone can control the amount of moment that can be transferred between the columns and beams at a joint.

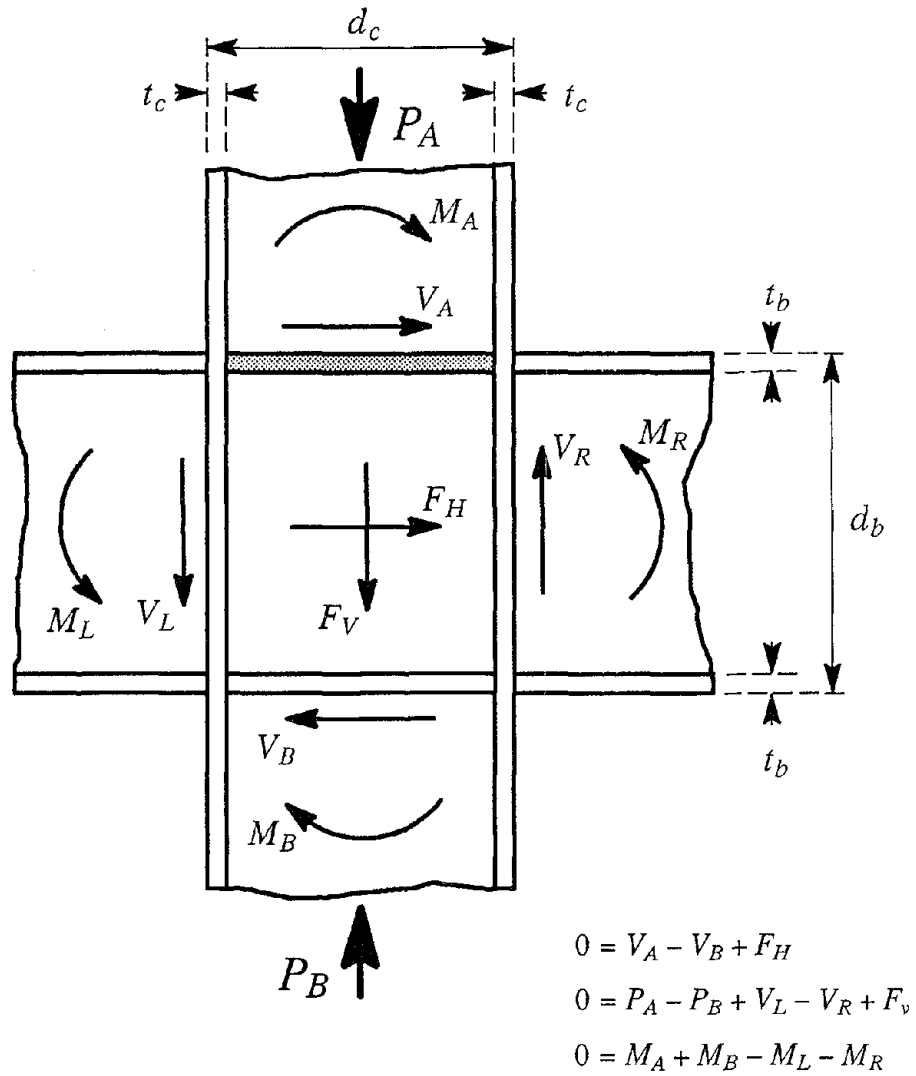


FIGURE 3.6a Forces Acting at an Interior Panel Zone

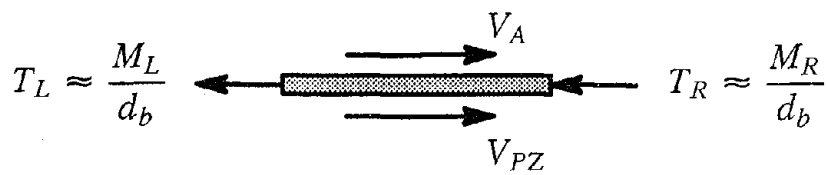


FIGURE 3.6b Forces Acting on Upper Pair of Stiffeners

The shear force couple at which yielding of the panel zone web initiates is given by

$$V_y = 0.55F_y d_c t , \quad (3.3)$$

where  $0.55F_y$  is the yield shear stress,  $d_c$  is the depth of the column and  $t$  is the thickness of the panel zone web including any doubler plates.

The model for the strength and stiffness calculations of a panel zone, shown in Figure 3.7, was developed by Krawinkler [29]. The effective shear area for the panel zone web has dimensions of ninety-five percent of the column depth and ninety-five percent of the beam depth. The panel zone web, which has an elastic-perfectly plastic behavior, yields at the shear force given by Equation 3.3. The column flanges contribute to the shear strength after yielding of the panel zone web and until the shear deformation reaches four times the yield shear strain.

The equation given in the 1988 UBC to determine the shear strength of a panel zone is based on the equation developed by Krawinkler. The maximum shear force couple that theoretically can be applied to the panel zone is given by

$$V_u = 0.55F_y d_c t \left( 1 + \frac{3 b_c t_{c_f}^2}{d_b d_c t} \right) , \quad (3.4)$$

where  $b_c$  is the width of the column flanges,  $t_{c_f}$  is the thickness of the column flanges. The first term contained in the brackets of Equation 3.4 corresponds to the strength derived from shearing of the panel zone web, while the second term relates to the strength contribution from bending of the column flanges at the corners of the panel zone.

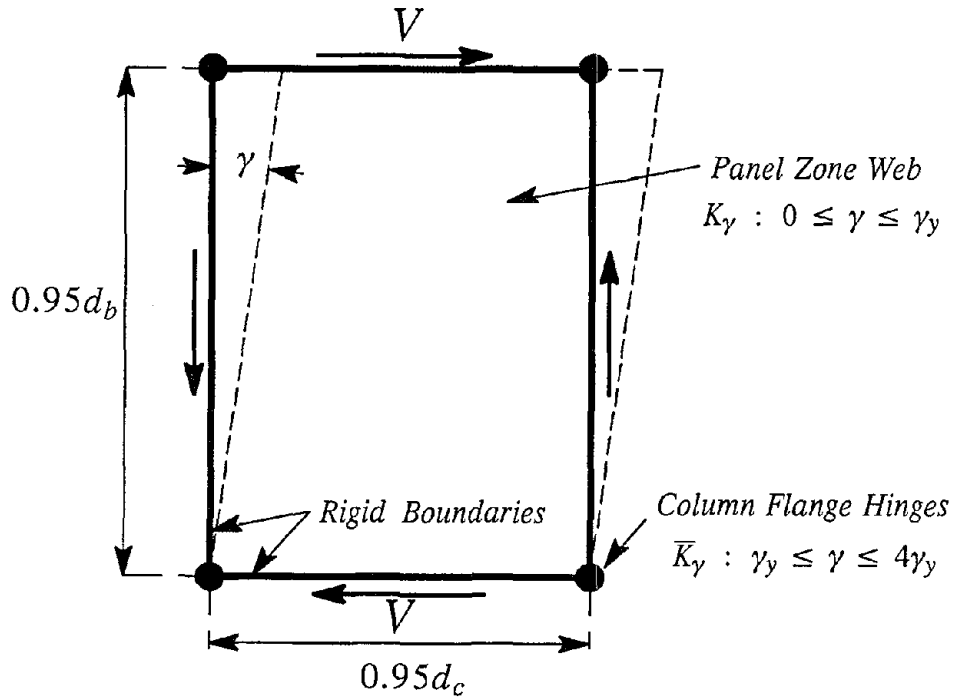


FIGURE 3.7 Model for Stiffness and Strength of Panel Zone

The behavior given by Equations 3.3 and 3.4 can be expressed with a bilinear load-deformation relationship. The elastic shear stiffness for the beam-to-column connection, which is the elastic stiffness of panel zone web, of the bilinear relationship is defined as

$$K_\gamma = (0.95d_c)tG , \quad (3.5)$$

where  $G$  is the shear modulus of the panel zone web. The shear-deformation relationship of the panel zone web is assumed to be elasto-plastic. The strain hardening shear stiffness for the beam-to-column connection, which is the bending stiffness of column flanges, of the bilinear relationship is defined as

$$\bar{K}_\gamma = \frac{1.04 b_c t_c^2 f G}{0.95 d_b} . \quad (3.6)$$

A vertical force acting above the panel zone reduces the yield shear stress of the panel zone web. The reduction factor given by von Mises yield criterion is expressed as:

$$\alpha = \left[ 1 - \left( \frac{P}{P_y} \right)^2 \right]^{\frac{1}{2}} , \quad (3.7)$$

where  $P$  is the axial column force at the design level and  $P_y$  is the yield axial force of the column. However, the reduction factor was ignored in this study, because axial design force of each column was small in comparison to the yield capacity.

Since the shear load-deformation behavior of a panel zone is modelled with a DRAIN-2D connection element (rotational spring), the shear stiffness, strain hardening and strength of the beam-to-column connection are converted into moment-rotation relationships. As shown in Figure 3.8, the relative rotation between the columns and beams framing into a joint is the same as the shear deformation in the panel zone. The relative rotation between the columns and beams framing into a joint is related to the moment transfer. The rotational elastic stiffness of the connection element is defined by

$$K_\theta = (0.95 d_b) K_\gamma = (0.95 d_b)(0.95 d_c) t G . \quad (3.8)$$

The rotational strain hardening stiffness of the connection element is expressed as

$$\bar{K}_\theta = (0.95 d_b) \bar{K}_\gamma = 1.04 b_c t_c^2 f G . \quad (3.9)$$

The yield moment for the connection element is written as

$$M_{\theta_y} = (0.95d_b) V_y = (0.95d_b)(0.55F_y d_c t) . \quad (3.10)$$

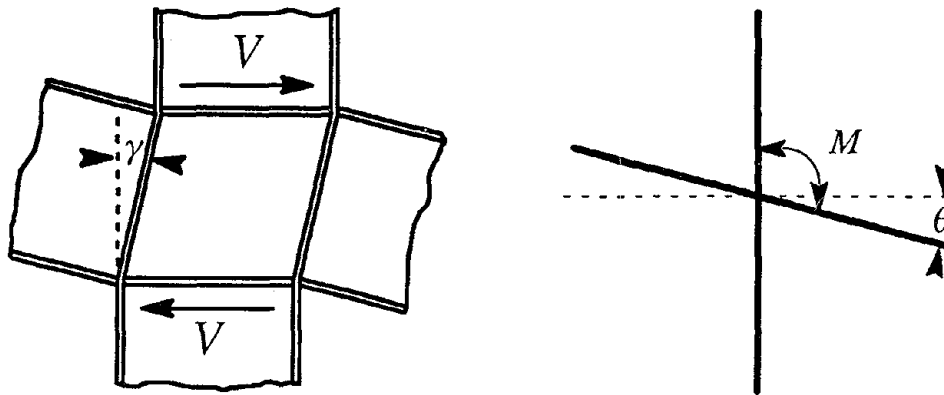


FIGURE 3.8 Moment-Rotation Relationship of Connection Element

In this study, both flexible connection models for the beam-to-column connections were designed to have the capability to transfer an unbalanced beam moment equal to the sum total of the plastic moment of the beams. The design shear force couple acting above and below the panel zone from the unbalanced beam moment is defined as

$$V_{req} = \frac{\sum M_{pb}}{0.95d_b} , \quad (3.11)$$

where  $\sum M_{pb}$  is sum total of the plastic yield moment of the beams and  $0.95d_b$  is the effective depth of the beams framing into the joint.

The first modelling of the panel zone for a flexible connection had the strength required to develop the full plastic moment of the beams derived entirely from the panel zone web. Therefore, the beam-to-column connections



virtually remained elastic during the ground excitation. The panel zone web thickness was determined from Equation 3.3, where  $V_y$  was equal to the shear force given by Equation 3.11, and can be expressed as

$$t = \frac{\sum M_{pb}}{0.55F_y d_c (0.95d_b)} \quad (3.12)$$

In the other model of the panel zone for a flexible connection, the required strength of the panel zone was developed from both the panel zone web and the column flanges. This beam-to-column connection model yielded prior to developing the full plastic moment of the beams, but could develop the moment after the shear strain reached four times the yield strain. The panel zone web thickness was determined from Equation 3.4, where  $V_u$  was equal to the shear force given by Equation 3.11, and can be expressed as

$$t = \frac{\sum M_{pb}}{0.55F_y d_c (0.95d_b)} - \frac{3 b_c t_c^2 f}{d_b d_c} \quad (3.13)$$

The strain hardening ratios given by Equation 3.9 generally were less than four percent and even as low as one and a half percent. However, test results of panel zone yielding typically had strain hardening ratios of more than five percent. Thus, the strain hardening ratios in this study were assumed to be five percent, regardless of the properties of the panel zone.

The physical difference between the two flexible connections was the thickness of the panel zone web. The web thickness for the elastic panel zone was greater than the web for the inelastic panel zone. The elastic panel zone had a yield moment equal to the sum total of the plastic yield moment of the beams. However, because of the higher strain hardening ratio of the panel zone element, the majority of yielding occurred in the beams

(assuming strong column-weak beam design) rather than yielding of the panel zone web. The inelastic panel zone had a yield value less than the sum total of the plastic yield moment for the beams of a joint. Therefore, yielding occurred in the panel zones until the inelastic deformations are large enough to cause the yielding to develop in the beams.

The both flexible connection models of the panel zone had the shear strength to develop the full plastic moment of the beams framing into the joint. However, the 1988 UBC states that the strength of the panel zone need not develop more than eighty percent of the full plastic moment of the beams. If the eighty percent limitation was followed, most of the yielding at a joint would occur in the panel zone, because the panel zone would most likely not have the ability to transfer enough moment to the beams to cause them to yield.

### 3.5 Nonstructural Element Participation

The nonstructural elements in a building can be neglected, if the nonstructural elements are isolated from the lateral force-resisting frame. In most instances, especially during initial excitation, the nonstructural elements effect the response, because the nonstructural elements are not completely isolated and they possess lateral stiffness and strength as evident by actual verses calculated periods of vibration, observed damping and maximum story shears. In fact, the observed fundametal period of buildings can be significantly higher prior to any degradation of the nonstructural elements.

The stiffness and strength of the nonstructural elements (cladding, interior walls, interior frames, etc.) were not considered in the direct

design procedure for the moment-resisting frames, since the strength of the nonstructural elements was not obliged to provide any lateral resistance. The nonstructural element contribution is difficult to assess, since the nonstructural elements tend to be less ductile than the frame and, thus, yield and degrade after limited deformations. In addition, it is believed to be conservative to ignore the stiffness and strength contribution of the nonstructural elements, since the lateral force-resisting frame would be designed to resist all of the equivalent lateral forces.

Shear panel elements, available in the DRAIN-2D element library, were added to selected frame models to account for the participation of the nonstructural elements. The load-deformation behavior of the shear panel element is explained in Appendix A. The load-deformation behavior of the shear panel elements did not model any particular component or material, but was suppose to possess the composite characteristics of the relationship between the nonstructural elements and the lateral force-resisting system.

The shear panel element, as shown in Figure 3.9, was attached to the frame at the location of the beam-to-column connections. The shear panel element did not contribute to the rotational stiffness of a joint and did not impinge upon the end rotation of the columns and beams. The lateral stiffness of the shear panel element of each story multiplied by the story height was constant for all stories in a frame model, since the "same amount" of nonstructural elements was assumed to be in each story. Thus the absolute increase in lateral stiffness and strength for each story was the same, but the relative increase was much greater for the upper stories of the frame models.

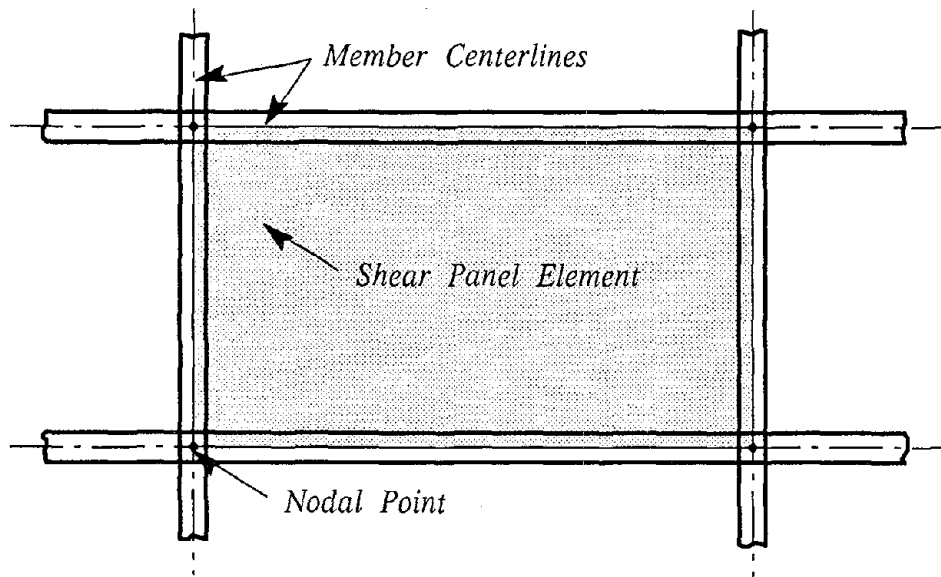


FIGURE 3.9 Attachment a of Shear Panel Element

### 3.5.1 Linear Load-Deformation Behavior

The initial attempt to determine the impact of nonstructural elements on the dynamic response of a frame employed a simple modelling for the behavior of nonstructural elements. The load-deformation behavior, as shown in Figure 3.10, was taken to be linear with a failure strain (total loss of stiffness and strength) of 0.005 inches/inch. After reaching the failure strain, the element no longer participated in the response of the frame. The desired load-deformation behavior of the nonstructural elements could be modelled with a single shear panel element per story.

The linear shear panel elements were added to the D1B design of a five-story frame. The stiffness of the linear shear panel elements was chosen to shorten the calculated fundamental period of the five-story frame to the estimated value given by the 1988 UBC. The calculated period of the bare structural system for the D1B design was around 1.25 seconds, while the

estimated period given by the 1988 UBC for a five-story building was 0.77 seconds. To obtain the desired fundamental period, the lateral stiffness of the frame model with nonstructural elements was approximately two and a half times greater than the lateral stiffness of the bare structural frame model.

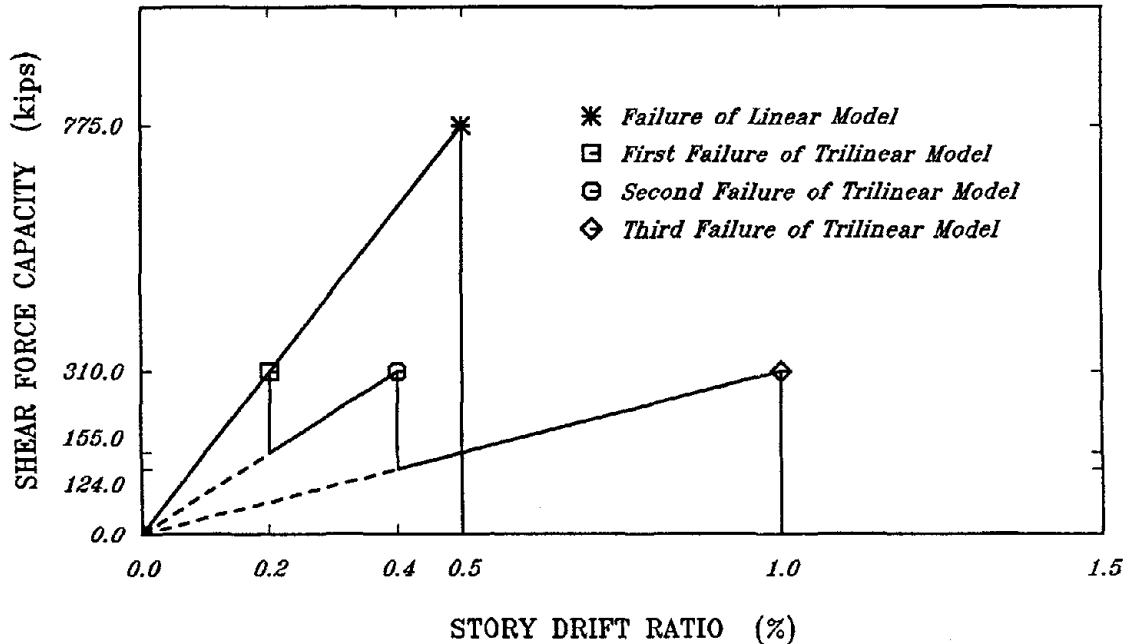


FIGURE 3.10 Load-Deformation Behavior of Nonstructural Elements

### 3.5.2 Trilinear Load-Deformation Behavior

The linear shear panel elements had a significant influence on the response of the frames. Since the failure of this element was rather abrupt, the stiffness and strength degradation of the element was refined. The load-deformation data from the Nonstructural Element Test Phase of the U.S.-Japan Cooperative Research Project on a Full-Scale Steel Test Frame [45,46,47] was used to obtain a more realistic behavior of nonstructural elements. The data from this test phase was taken from a static cyclic

loading of a six-story structure with cladding attached to the exterior frames and infill walls along the interior frame.

The test data for one of the stories is shown in Figure 3.11 for cycles of increasing deformation. The stiffness value given in each plot represent the slope of line between the maximum excursions in each direction. The hysteresis loops shown represent the load-deformation behavior of both the structural steel frame and nonstructural elements. Therefore, some of the degradation is due to the frame, but most of it is due to the deterioration of the nonstructural elements. The contribution of the bare steel frame for this story was estimated from the results of another story in the frame without nonstructural elements.

Instead of using one shear panel element per story, three elements having different load-deformation characteristics were used. Each of the shear panel elements had a linear load-deformation behavior and specified failure strain. The load-deformation behavior from the combination of the three shear panel elements, shown in Figure 3.10, degrades in stiffness and strength at predefined deformations. The initial stiffness of the trilinear model of nonstructural elements was identical to the initial stiffness of the linear model of nonstructural elements. However, the stiffness was assumed to decrease by fifty percent after the shear strain reached 0.002 inches/inch, thereafter the shear strain was taken to be twenty percent of the initial value until the shear strain reached 0.004 inches/inch and finally at a shear strain of 0.01 inches/inch the trilinear nonstructural element was assumed to fail. Unloading after a failure (degradation) of a nonstructural element occurred along the dashed line to the origin.

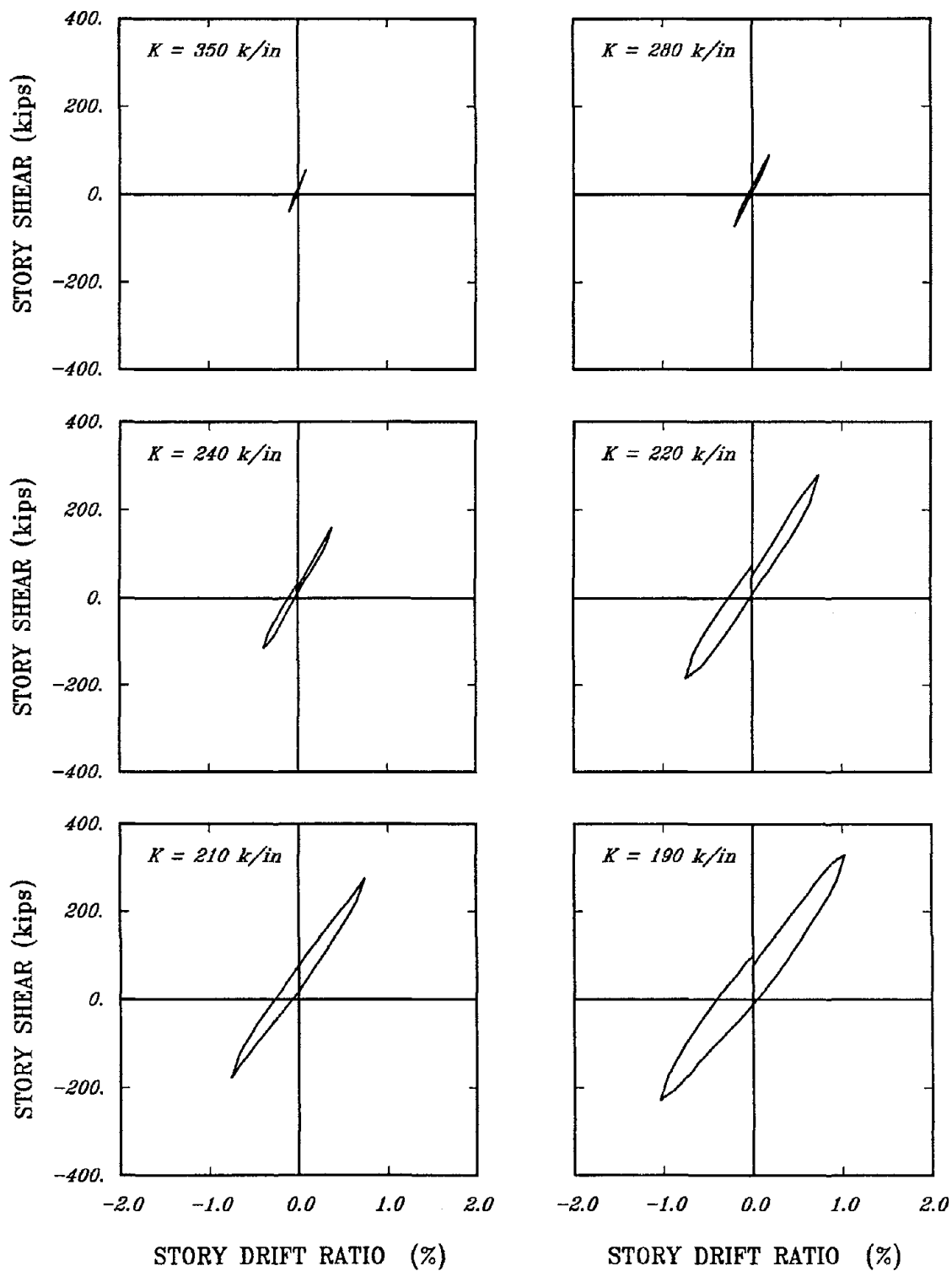


FIGURE 3.11 Load-Deformation Behavior for a Story with Nonstructural Elements Attached to the Frame of the Full-Scale Test

The trilinear nonstructural elements were added to the D1B design of a five-story frame to examine the influence of this assumed nonstructural element behavior. In addition, the trilinear nonstructural elements were added to the other frame models, so that the responses of these models with and without nonstructural elements could be compared.

### 3.6 P-Delta Effects

P-Delta effects were not accounted for in the direct design procedure of the moment-resisting frames in this study, because the provisions of the 1988 edition of the *Uniform Building Code* stipulate that structures located in zones 3 and 4 of the Seismic Zone Map for the 1988 UBC and satisfying the drift limitations of the code need not consider P-Delta effects. However, P-Delta effects, arising from the instability of the interior frames, were investigated in this study.

In low-rise structures in which all of the frames are resisting lateral forces, P-Delta effects generally are not of concern, because the axial compressive forces in the columns are not large enough to cause significant second order displacements. However, the structures in this study utilized moment-resisting frames along only the perimeter to resist the lateral forces. The interior frames having only pinned beam-to-column connections provided no lateral resistance or stability and were designed to carry the gravity loads of their tributary area. Therefore, the exterior frames not only provided the lateral resistance for the structure, but also acted to stabilize the displaced interior frames through diaphragm action of the floor and roof slabs.



To determine if P-Delta effects were significant, the time-history analyses of some of the frame models were performed with and without the inclusion of P-Delta effects. As an approximate means to account for P-Delta effects, the lateral stiffness of the stories were reduced, so that larger story drifts were required to maintain equilibrium of the deflected structure. The modelling of P-Delta effects could be thought of as applying at each time step an additional shear force at each story level equal to the total weight acting on the story times the story drift divided by the story height. One advantage of the approximation of P-Delta effects with this type of modelling is that no iteration to determine the P-Delta forces is required within a time step.

### 3.7 Development of Numerical Models

Since a frame model could have many variations, the development of a generic numerical model which could be used by all models would be desired, so that the interpretation of the results would be easier. Thus in some models, elements that were not necessary to model the desired behavior were used. For instance, in frame models with rigid beam-to-column connections, a connection element was not necessary, but could be used if the rotation stiffness and yield moment was large in comparison to the other elements.

The element numbering scheme, shown in Figure 3.12a, was used for all frame models of this configuration. The columns and beams of an exterior frame, including the members not resisting lateral forces, were represented in each frame model. Connection elements, were used in the frame models to attach the columns to the beams at the moment-resisting connections. The stiffness and strength of the connection elements were dependent on the

desired behavior of the beam-to-column connection. Shear panel elements for the linear behavior of nonstructural elements are shown as the shaded region in each story. In the case of the trilinear behavior for nonstructural elements, three shear panel elements per story were used.

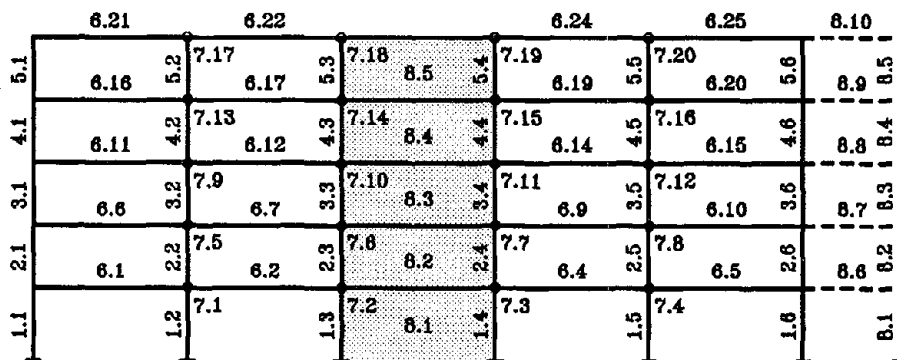


FIGURE 3.12a Element Numbering for Five-Story, Five-Bay Frame

The columns in the additional bay, shown with dashed lines, carried the vertical forces necessary to obtain P-Delta effects. The element stiffness matrix for each of the columns in the additional bay included geometric stiffness contributions. As a consequence of the columns in the additional bay having pinned end connections, no lateral stiffness resulted from the material stiffness of the columns. The overall lateral stiffness of each column was negative if the axial force in the column produced compression and positive if the axial force in the column produced tension. The compressive force acting in a P-Delta column was equal to the weight of the story levels located above the column. When P-Delta effects were ignored, the axial force in each column was zero, and the P-Delta bay provided no contribution to the overall lateral stiffness of the stories. The beams of

the additional bay acted as a link to transfer the stabilizing forces from the actual frame to the P-Delta columns.

The node numbering scheme, shown in Figure 3.12b, also was used for all frame models of this configuration. A pair of nodes was required at the connection element locations. One of the nodes, designated with a "B", was the end node for the beams framing into the joint and the other node, designated with a "C", was the end node for the columns framing into the joint. The vertical translations of each pair of nodes were constrained to be identical. The horizontal translations of all the nodes in a story level were constrained to be identical, since the axial deformations of the beams were ignored. The moment transferred between the columns and beams by the connection element at a moment-resisting connection was a function of the relative rotation between the pair of nodes.

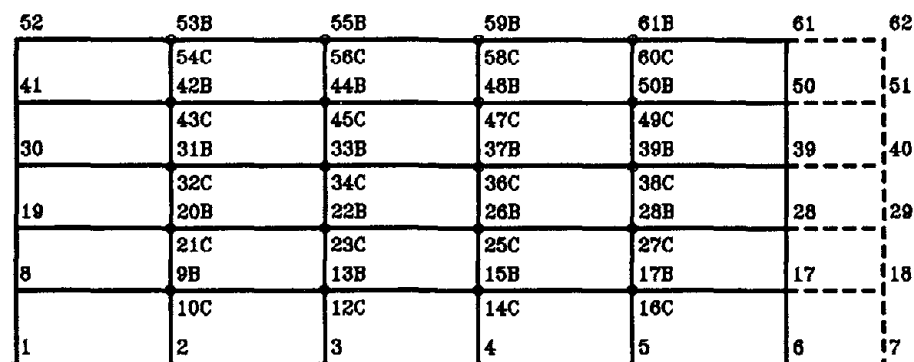


FIGURE 3.12b Node Numbering for Five-Story, Five-Bay Frame

## CHAPTER 4

## PARAMETRIC STUDIES AND RESULTS

## 4.1 Introduction

The goal of the parametric studies presented in this chapter was to determine if, and by how much, certain parameters influence the inelastic response of low-rise steel frame structures arising from strong ground motion. If it is determined that a particular parameter does impact the calculated response of a building, then this parameter may need to be considered in the design process and detailed in the mathematical model for the analysis of the structure, so that the design process is compatible with the expected behavior of the building. Therefore, improvements to direct design procedures may be needed to obtain equivalent lateral forces which correlate to the expected inertia forces produced by the design earthquake. Safe and efficient lateral force-resisting systems capable of withstanding the design earthquake are highly dependent on determining the anticipated inelastic behavior of structures, so that unnecessary safety factors can be eliminated without sacrificing life safety.

The direct design procedure given in the 1988 edition of the *Uniform Building Code* is a very simplistic approach to a complicated problem because of the difficulty in assessing the stiffness and strength of a building, and the inability to forecast the ground excitation of future earthquakes. In addition, a structural engineer generally can not justify the cost of a more detailed analysis (modal or time-history) for a low-rise building. The problem is how to maintain a simple and general design procedure and at the same time produce designs that are structurally adequate and economically

feasible. The focus of this study is to determine if the current direct design procedure of the 1988 UBC results in buildings that behave in the manner expected by the code writers and more importantly that perform satisfactorily during a major earthquake. Therefore, several parameters that may or may not be considered in the direct design procedure, but that alter the seismic behavior of a building, will be investigated to determine their influence on the structural response.

In an analytical study of this type the amount of generated output data is overwhelming. The challenge is to interpret and process the significant data, so that implications as they pertain to practical design applications and building codes can be determined. General information related to the selection and presentation of the generated data from the time-history analyses is explained in this chapter. In addition, influence of the ground motions selected for this study on the structural response is discussed in some detail. In separate sections of this chapter, the development of each parametric study, along with results and conclusions is given. The results of each parametric study focuses on the calculated response arising from strong ground motions in order to understand the inelastic behavior of the frame model. Some of the results were compared to the direct design procedures to determine if the inelastic behavior of the structure was representative of the behavior assumed in the code. The chapter has an overall summary section that reiterates the important conclusions as they relate to the performance, design or analysis of a moment-resisting frame structure of each parametric study and also includes some general conclusions about the parametric studies.

#### 4.2 Selection and Presentation of Output Data

After much deliberation, the interpretation of the results from the time-history analyses for the frame models was characterized by studying: a) the lateral displacement of each story level; b) the total horizontal shear resisted by the members of each story; c) the accumulated input energy and dissipation of the input energy; d) distribution of hysteretic energy. These quantities were selected, because the story drifts and story shears provided an overall picture as to how the structure responded to the ground excitation. In addition, the maximum story drifts and story shears obtained during each time-history analysis were compared to the allowable story drifts for the equivalent lateral forces, the maximum expected story drifts from inelastic behavior as a result of excitation with the design earthquake and the design story shears arising from the equivalent lateral forces for a special moment-resisting space frame (SMRSF). The maximum computed story drifts also were compared to the expected story drifts proposed in the 1988 UBC. The energy quantities, which were a function of the response and properties of the frame model, gave an indication as to the manner in which a structure dissipated the input energy and absorbed the hysteretic energy.

A substantial amount of data can be generated during each time-history analysis of a frame having many degrees of freedom and members. The amount of output data generated during the time-history analyses was minimized by only writing the results of every fifth time step to the output file. The time step of each analysis was 0.01 seconds, and the corresponding increment between saved data points was 0.05 seconds. Even so the analysis of such a massive volume of data constitutes a major task.

The results are presented in graphical form for easier assessment and comprehension of the response and comparison with other frame models. Most of the jaggedness contained in the traces of various plots is a consequence of only sampling every fifth time step. The corners (locations) of yielding and unloading generally are the areas that require more sampling of output data to obtain "true" values of response because the stiffness change can be very abrupt. In this investigation, the hysteretic energy distributions by elements and stories were based on the hysteretic energy dissipated by the columns and connection elements of an interior column line of a frame model and the beam ends attached to this column line. However, the hysteretic energy distributions calculated for this column line are believed to be representative of the distribution for the entire structure.

One type of plot made for each parametric study was a time history of story drift and the story shear-drift history for the first story. Only the results for the first story were plotted so that the general behavior of the structure during the analysis could be seen. Since an assumption for the direct design procedure was that the structure would experience roughly equal ductilities through the height of the structure, the behavior of the first story would be representative of all the stories. However in many of the analyses, other lateral modes than the first lateral mode had significant contributions to the response. Thus, the behavior of one story was not necessarily representative of another story.

Other plots that were made for each parametric study were envelopes of maximum story drifts and shears for each story. Although these plot gave an indication of the maximums, they did not relate the number of times that a level of ductility was reached or nearly reached during a time-history

analysis. However, the information contained in this plot can be directly related to the direct design procedure.

Bar charts were generated showing the total input energy and the dissipation into damping and hysteretic energy for each analysis. The difference between the total input and the sum total of the hysteretic plus damping energy was the kinetic and elastic strain energy associated with the structure at the end of the time-history analyses. In most instances, the difference was minimal because the ground excitations were small towards the end of the twenty seconds. Therefore, the response was diminishing at the completion of each time-history analysis.

Another bar chart that was generated showed the distribution of hysteretic energy in the selected interior column line by both elements and stories for each parametric study. In addition to this bar chart, the same information was displayed in a more graphical form for (perhaps) easier evaluation. An elevation of this interior column line was plotted along with the amount of hysteretic energy dissipated in each location. The hysteretic energy for a location was given as a dot in which the area symbolized the percentage of the total hysteretic energy dissipated at that location. These diagrams gave a clearer picture as which elements dissipated hysteretic energy and how a certain parameter possibly altered the yield pattern for a frame.

#### 4.3 Influence of Ground Motion on Structural Response

The time histories for the distribution of input energy into hysteretic (plastic strain), damping (viscous) and stored (kinetic plus elastic strain) energy for a typical five-story frame model subjected to each of the scaled



earthquake accelerograms are shown in Figure 4.1. The input energy at any point in time was the accumulated energy imparted into the structure during the excitation. The input energy increased or decreased between successive time steps, depending on whether the ground motion at that particular time was or was not opposing the motion of the structure. The hysteretic energy was the portion of input energy dissipated by inelastic deformation of the members. The damping energy was the amount of input energy dissipated through viscous damping in the structure. The difference between the input and hysteretic plus damping energy was the amount of energy stored in the structure. Since the stored energy was either elastic strain energy or kinetic energy, the stored energy was recoverable as the structure came to rest. Depending on the frequency content of the ground motion and the dominating frequencies of the structure, the stored energy at times had large oscillations. The equations implemented in the DRAIN-2D computer program to calculate the various energy quantities during the time-history analyses are given in Appendix A.

The El Centro accelerogram generally caused two regions of significant hysteretic energy accumulation separated by a period of lull excitation. The Parkfield accelerogram generated one region of substantial inelastic behavior in which the structure experienced large drift excursions during this interval, and then basically responded elastically thereafter. The Taft accelerogram gradually accumulated hysteretic energy over a considerable portion of the ground excitation. The excitation from the Parkfield record was not that strong for the higher frequency five-story frame models and the two-story frame models, because the frequency band was not as broad as in the El Centro and Taft.

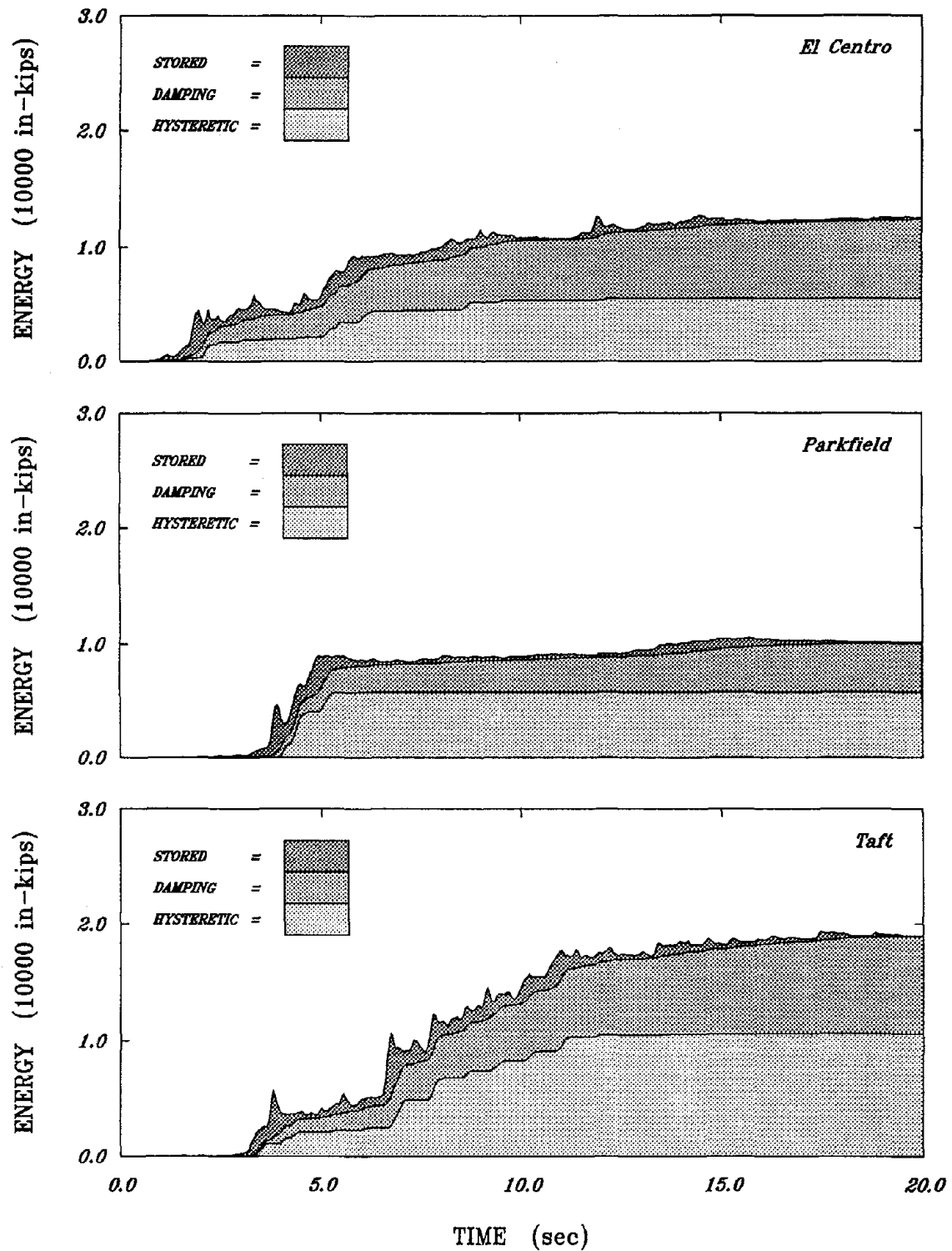


FIGURE 4.1 Typical Energy Time Histories for a Frame Model Subjected to the Scaled Earthquake Accelerograms

#### 4.4 Development of Parametric Studies

The various parametric studies undertaken in this investigation are shown in Table 4.1, along with the frame designs that were used in each study. The first parametric study, beam-to-column strength ratio, actually was "unplanned". The goal of the initial design for the five-story frame was to have a design with "strong column-weak beam" behavior, but due to the interaction between the axial forces and bending moments of the columns during the time-history analyses, the strength of the columns at a joint generally was smaller than the strength of the beams. Reselection of stronger column sections having the same lateral stiffness produced a design with "strong column-weak beam" behavior.

TABLE 4.1 Usage of Frame Designs for Parametric Studies

Parametric Study	D1A	D1B	D2A	D2B	D2C	D3	D4
Beam-to-Column Strength Ratio	*	*					
Beam-to-Column Connection Behavior		*					
Nonstructural Element Participation		*			*	*	*
Moment-Resisting Frame Configuration			*	*	*		
Defective Moment-Resisting Connections					*		
Design Base Shear Level & P-Delta		*	*		*	*	
Structure Height (Fundamental Period)				*			*

The second and third parametric studies centered on the variance of the assumed lateral load-deformation behavior of the building components which ultimately influence the behavior of the structure as a whole. The

"strong column-weak beam" frame design of the first parametric study was used as the basis for the frame models of these parametric studies. One of the parametric studies investigated the influence of the beam-to-column connection behavior for the moment-resisting connections, while the other parametric study examined the participation of the nonstructural elements in resisting lateral forces.

The fourth parametric study concentrated on the frame configuration for the lateral force-resisting system. Since the determination of the design base shear and vertical distribution of base shear is independent of frame configuration, the required lateral stiffness and strength of each frame design were approximately the same. The fifth parametric study compared the response of frame designs with identical frame configurations, but with different design base shear levels. The 1988 UBC has three methods to obtain the design base shear level for the direct design procedure.

The influence of defective beam-to-column connections was examined in the next parametric study. A frame configuration with one bay in the perimeter frames resisting lateral forces was chosen to be studied, because the impact of a couple of defective (poor quality) connections per frame could be very significant. The last parametric study pertained to the inelastic response of a two-story structure. The fundamental period of the two-story structure was in the range where the design spectra is a maximum and independent of the fundamental period for the structure.

One of the key points for this investigation was to determine if the inelastic behavior of the structure was compatible with the assumed behavior of the code. The code expects an even distribution of ductility over the height of the structure and maximum story drifts of less than one and a half

percent of the story height. Story drifts beyond this level could seriously compromise the survivability of the structure because the integrity of the connections would be questionable and second order effects may lead to even more instability.

#### 4.4.1 Investigation of Beam-to-Column Strength Ratio

The direct design procedure of the 1988 edition of the *Uniform Building Code* is not only concerned with the lateral stiffness and strength of the moment-resisting frames, but also the inelastic behavior of the frame. The 1988 UBC advocates "strong column-weak beam" design for moment-resisting frames, although under certain conditions "strong beam-weak column" design is permitted. The rotational strength ratio of the columns and beams at a moment-resisting connection must satisfy the following relationship, given in the 1988 UBC:

$$\frac{\sum Z_c (F_{yc} - f_a)}{\sum Z_b F_{yb}} > 1.0 , \quad (4.1)$$

where  $Z_c$  is the plastic section modulus of each column framing into a joint and  $Z_b$  is the plastic section modulus of each beam framing into a joint.  $F_{yc}$  and  $F_{yb}$  are the nominal yield stress of the columns and beams and  $f_a$  is the maximum axial compressive stress in a column for all applicable loading combinations.

The denominator of Equation 4.1 represents the total strength derived from the beams framing into a connection and is simply the sum total of plastic moment for the beams. The numerator of Equation 4.1 represents the total strength derived from the columns and is the "adjusted" sum total of

plastic moment for the columns. The plastic moment of a column is reduced, when a compressive axial force is present. The reduction factor,  $f_a$ , is a rather crude (simple) method to determine the portion of the total strength that can be associated with bending. A reduction factor is not needed for the beams because it is assumed that their axial forces are insignificant.

If certain beam limitations for compactness also are applied to the columns, the 1988 UBC allows the relationship given in Equation 4.1 to be ignored under either of the following conditions:

1. The compressive stress ( $f_a$ ) in the columns is less than forty percent of  $F_y$  for all applicable loading combinations;
2. The lateral shear strength of the columns in a story are fifty percent greater than the story above.

The members selected for the D1A frame satisfied the requirements of the first condition given above, and thus the "strong beam-weak column" design was permitted. Stronger columns were selected for the D1B frame to force the behavior to be "strong column-weak beam". In both of the frames, the I-sections for the columns of each story changed as required by the drift design. Therefore the distributions of the lateral stiffness and strength were quite uniform, although the strength of the D1B frame was more than required.

The axial forces in the columns of the D1A and D1B frame designs resulting from the gravity (dead and live) loads and equivalent lateral forces were relatively small. The interaction equation given in the steel material section of the code (same as AISC (1.6-2)), governing the design of steel members having a compressive stress from an applied axial force smaller than fifteen percent of the allowable axial stress, was used in lieu

of the interaction equations having the same form as AISC (1.6-1a) and AISC (1.6-1b). In accordance with the 1988 UBC, the allowable stresses are increased by a factor of one-third for loading combinations containing earthquake forces.

The primary reason for avoiding plastic hinging of the columns is the possibility of local buckling of the columns near the plastic hinge location or inelastic buckling of the entire column. Also, buckling (failure) of the columns rather than the beams will cause greater lateral instability of the frame. Since the axial forces in the columns of the D1A frame design were small, and therefore, the columns were stressed primarily in pure bending, the allowance of "strong beam-weak column" behavior was justifiable.

The finite element models of the D1A and D1B frames were typical for the modelling of moment-resisting frames since the influence of "rigid" beam-to-column connections and nonstructural elements were ignored. The centerline-to-centerline dimensions were used to define the flexible length of the columns and beams. The yielding of the columns and beams occurred in concentrated plastic hinges located at the ends of the members. However, the model did not consider degradation of the members as a result of inelastic behavior. Thus, yielding of the columns was no more catastrophic than yielding of the beams. Although if the behavior of a frame was "strong beam-weak column", then the yield moment of a column end fluctuated with the axial force acting in the column.

Comparisons of the time histories for the first story drift of the D1A and D1B frames subjected to each of the earthquake accelerograms are shown in Figure 4.2. The corresponding story shear-drift histories for the first story are shown in Figure 4.3. The response of the D1A and D1B frames

arising from each earthquake accelerogram were quite similar since, the natural frequencies of vibration for the two frames were approximately the same as a result of drift controlling the seismic design of both frames and minor inelastic deformations. As shown in the first story hysteresis loops, the inelastic deformations for the first story of the stronger D1B frame were about half as much as in the D1A frame.

The maximum story drifts and story shears obtained during each of the time-history analyses are plotted as envelopes in Figure 4.4. The maximum values for an envelope did not occur necessarily at the same time but were the maximum values calculated for each story. The envelopes for the maximum story drift ratios tended to be similar, since they all had larger drifts in the upper stories. In fact, the drifts calculated in the upper stories were around four to five times the allowable story drifts for the equivalent lateral forces in the direct design procedure and generally exceeded story drift ratios of one and a half percent expected by the 1988 UBC from inelastic behavior. Perhaps the larger ductilities occurred in the upper stories as a result of higher mode participation. The maximum story shears of the D1A frame were two times larger than the design story shears and three times larger for the D1B frame, although the absolute difference in story strength decreased towards the top level of the frame. As expected, the stronger D1B frame resisted more shear in each of the stories than the D1A frame, even though the D1A frame experienced larger drifts. The strength increase above yielding was very small even at large deformations, so consequently the yield strength dictated the maximum story shears. The actual shear strength of the frame was several times larger than the design shears as a result of the working stress design to size the members.



The total input energy quantities and dissipation thereof (hysteretic and damping) at the end of the dynamic analyses are shown in Figure 4.5a. The total input energies corresponding to each earthquake were nearly the same for both frames, although the hysteretic energy dissipated in the D1A frame was slightly less than in the D1B frame. Therefore, the larger deformations in the D1A frame were offset by the larger height of the hysteresis loops for the D1B frame.

In Figure 4.5b, the distributions of the hysteretic energy dissipated along an interior column line are shown by both elements and stories. Not surprisingly, most of the hysteretic energy is dissipated in the columns of the D1A frame which was "strong beam-weak column" design and in the beams of the D1B frame which was "strong column-weak beam" design. The hysteretic energy dissipated at the base was attributable to yielding of the column at the assumed rigid connection to the ground. The pattern in the interior column line for hysteretic energy dissipation is given in Figure 4.5c. The generally greater yielding in the upper stories and changes in locations for hysteretic energy dissipation is clearly presented in this figure.

The design base shear for the D1A and D1B frames was determined from a rather conservative value of  $C$  equal to 2.75, and yet some of the inelastic drifts arising from the "design" earthquake were still larger than expected or desired. In the case of these two frames, the I-sections required for the columns of the "strong column-weak beam" design weighed approximately seventy percent more than the columns of the "strong beam-weak column" design. In spite of the increased weight, if hysteretic energy dissipation is a good indicator of structural damage, as it is thought to be, and

stronger members can safely dissipate more hysteretic energy, then the D1B frame may be more attractive in terms of survivability than the D1A frame.

The question of whether a "strong beam-weak column" design for a frame is acceptable depends on the axial forces and bending moments acting on the columns. For the case of frames with small axial forces, there appears to be little difference between the expected deformations of the two frame behaviors. Of course, frame designs having both large bending moments and axial forces should be avoided because the interaction of the two loading conditions reduce the allowable stresses and consequently the efficiency of material for the members. One benefit of employing a perimeter lateral force-resisting system is that the perimeter frames are principally designed to resist bending moments arising from the lateral force, because the tributary areas for the gravity forces are much smaller than they are for the lateral forces. Therefore, the "strong beam-weak column" behavior seems to be permissible in lateral force-resisting schemes that use perimeter moment-resisting frames.

One other issue that should be addressed is the permanent deformations that may result from an earthquake of smaller magnitude than the "design" earthquake. It is quite possible that slight inelastic behavior may arise from a moderate earthquake. Does plastic hinging of the columns, rather than plastic hinging of the beams create larger permanent offset in the structure and restrict the possible reuse or significantly increase the cost for repair of the structure? If so, regardless of magnitude of the axial forces, "strong column-weak beam" behavior may be more advantageous to the owner of the structure, even though the initial cost can be higher.

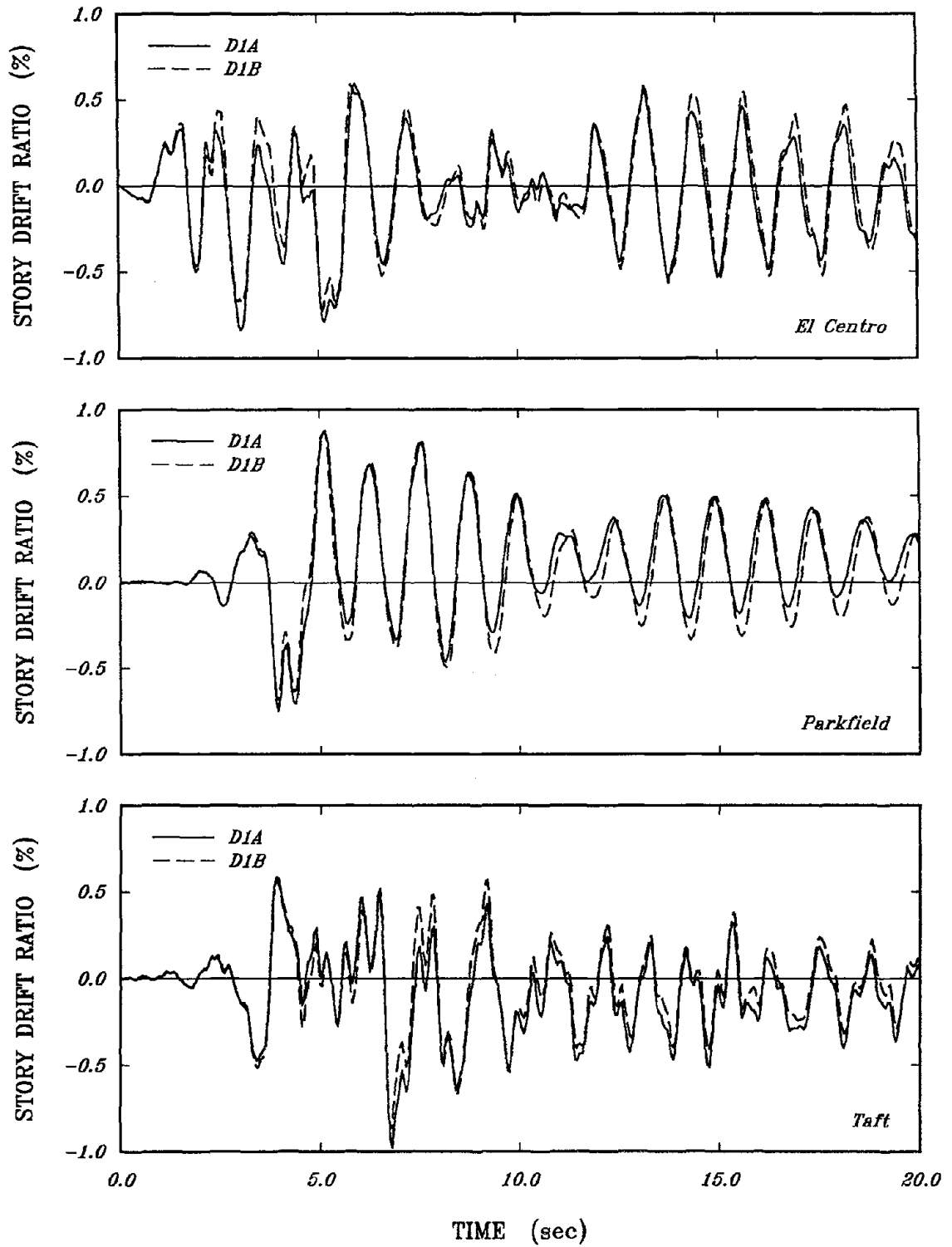


FIGURE 4.2 Drift-Time Histories of First Story for Similar Modelling of D1A and D1B Frames Subjected to Three Earthquakes

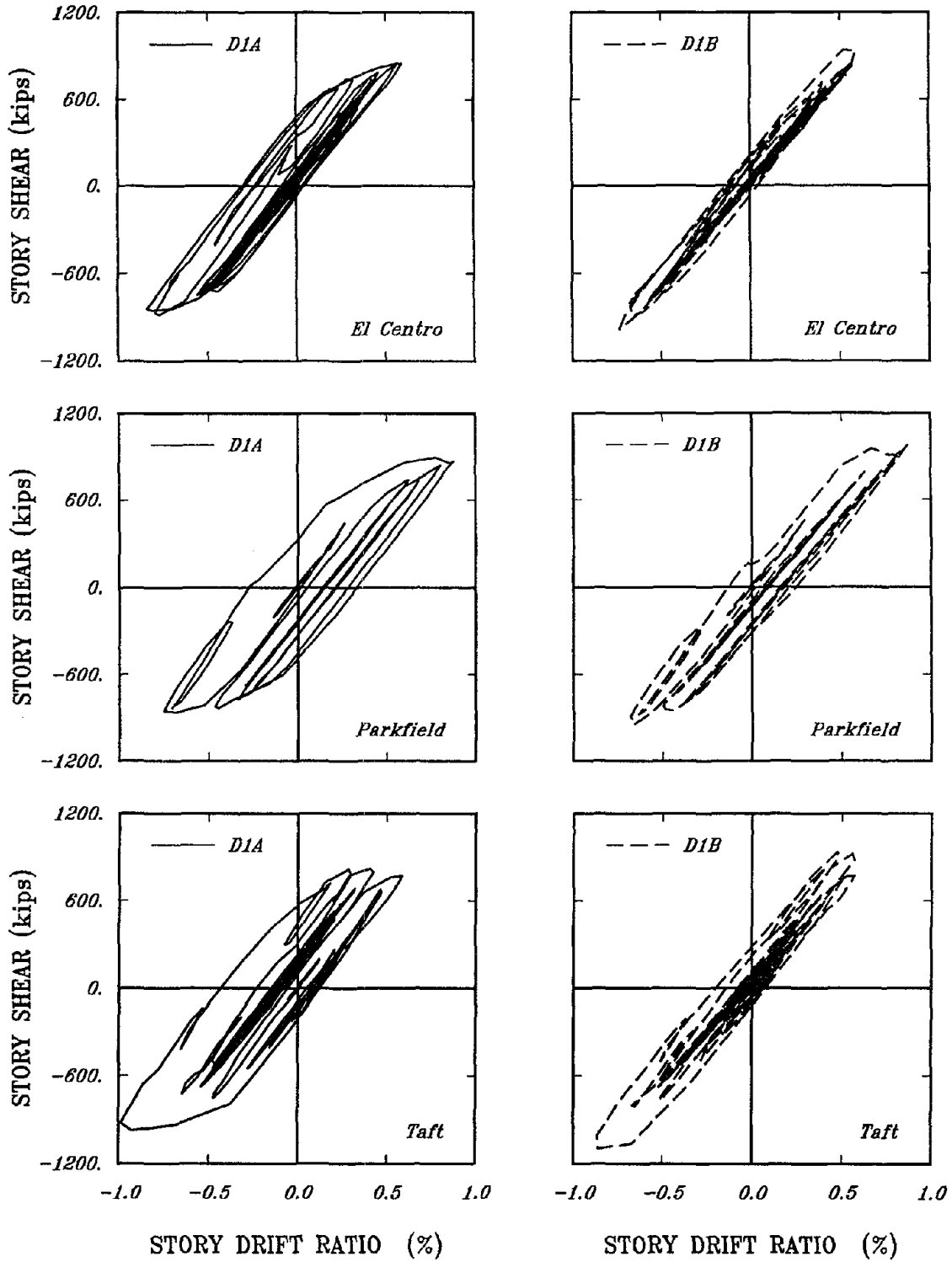


FIGURE 4.3 Shear-Drift Histories of First Story for Similar Modelling of D1A and D1B Frames Subjected to Three Earthquakes

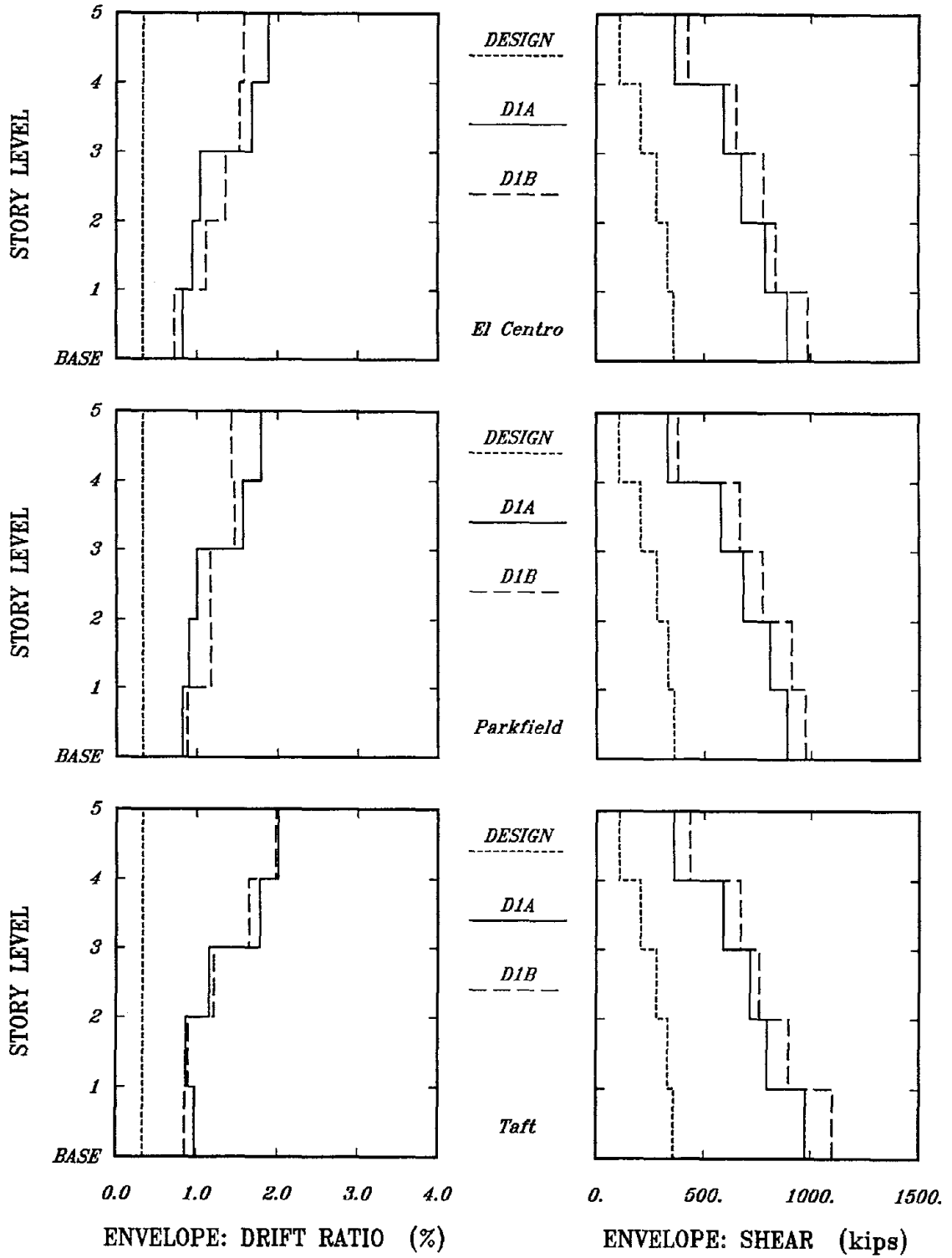


FIGURE 4.4 Story Drift and Shear Envelopes for Similar Modelling of D1A and D1B Frames Subjected to Three Earthquakes

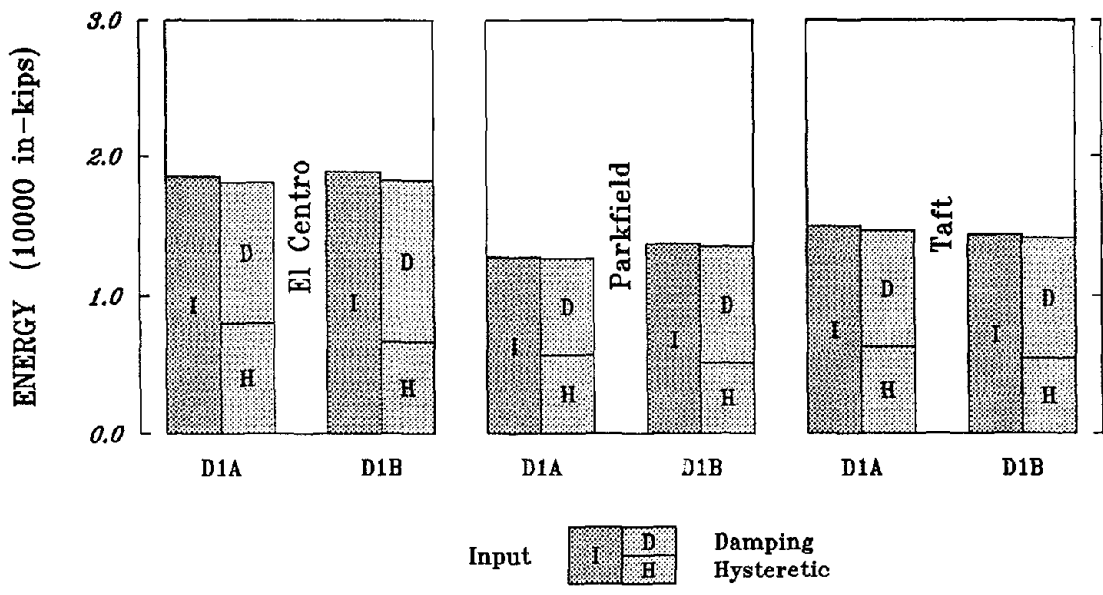


FIGURE 4.5a Cumulative Energy Quantities for Similar Modelling of D1A and D1B Frames Subjected to Three Earthquakes

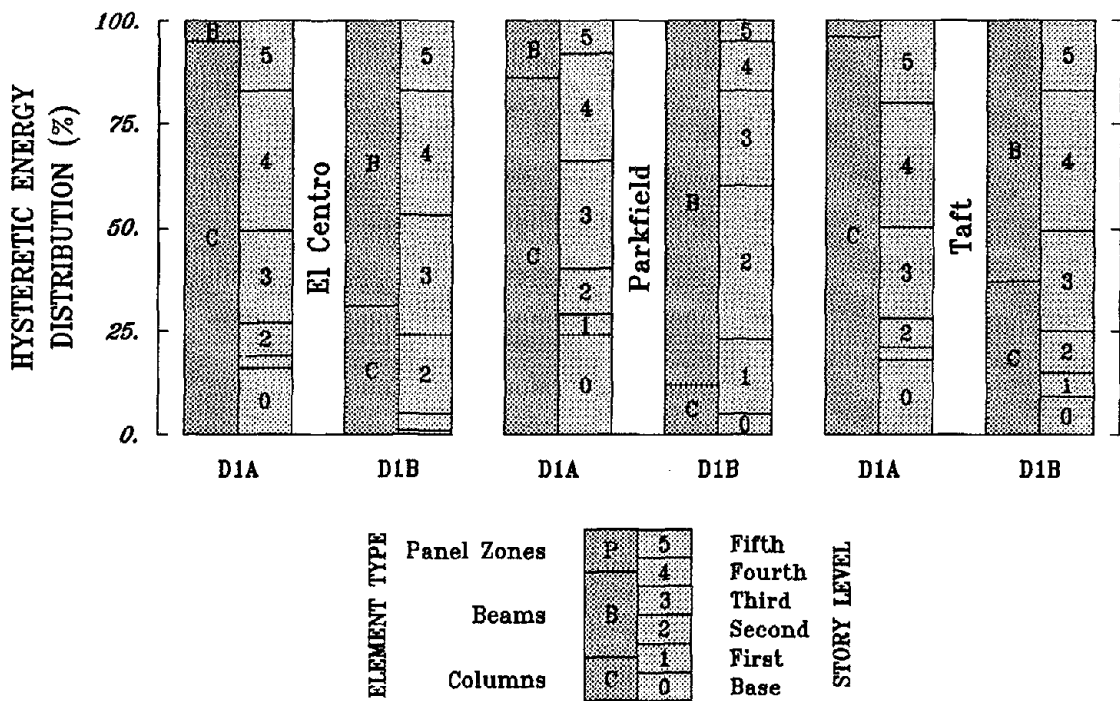
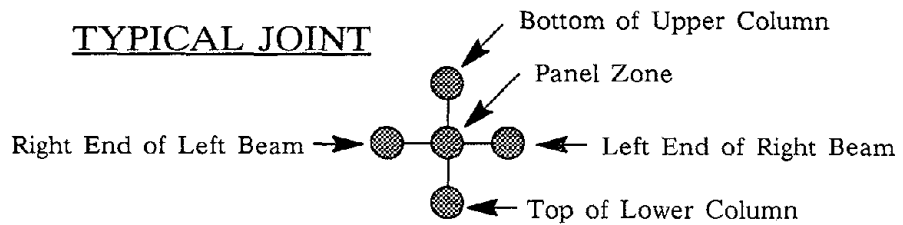
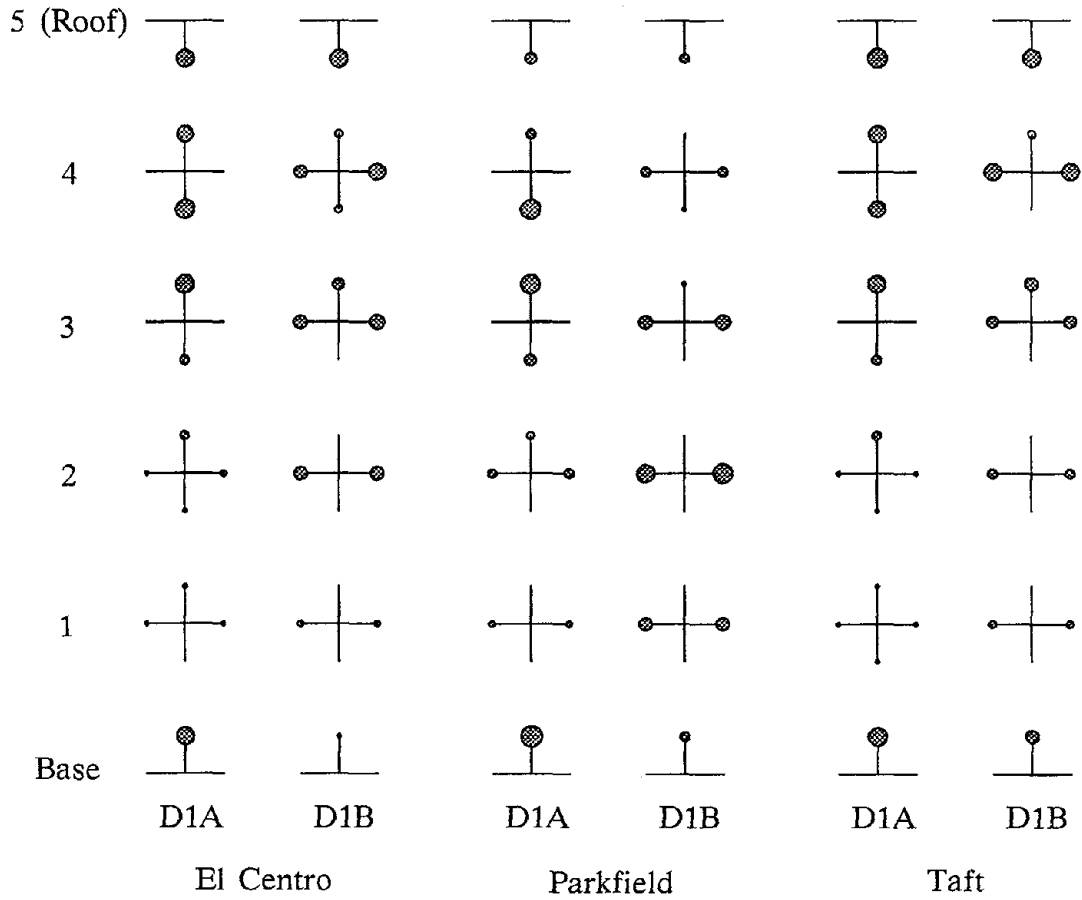


FIGURE 4.5b Hysteretic Energy Distributions for Similar Modelling of D1A and D1B Frames Subjected to Three Earthquakes



Note: Areas proportional to percentage of hysteretic energy dissipated at location.

FIGURE 4.5c Hysteretic Energy Locations for Similar Modelling of D1A and D1B Frames Subjected to Three Earthquakes

#### 4.4.2 Investigation of Beam-to-Column Connection Behavior

In the typical finite element modelling of moment-resisting steel frames, the beam-to-column connections are assumed to be rigid. However, the meaning of the term "rigid" is somewhat misleading for a beam-to-column connection, because deformation in the panel zone does occur from shear stresses that develop as a result of unbalanced beam moments. The 1988 edition of the *Uniform Building Code* requires that the drift calculations for the direct design procedure consider bending and shear contributions from the clear spans of the beams and columns, axial deformations of the columns and rotations and distortions of the panel zones. However, the drift calculations can be based on beam and column centerline-to-centerline dimensions and ignore the rotation and distortion of panel zones, if the difference between the two calculated drifts is less than fifteen percent or the strength of the panel zone can develop eighty percent of the plastic moment of the beams framing into a joint.

The 1988 UBC does not state how the contribution of the panel zone should be included in the drift calculations. However, the equation given in the code to calculate the strength of the panel zone is based on the equations developed by Krawinkler for assessing the stiffness and strength of panel zones. The drift calculations for the frame designs of this study were based on the centerline dimensions without regard to deformation in the panel zone, because the panel zones were designed to develop one hundred percent of the plastic moment of the beams framing into a joint.

The standard modelling of the D1B frame had rigid beam-to-column connections and the yielding of the columns and beams occurred at the ends of the members. Three other connection models were assumed for the D1B



frame to determine the influence of connection behavior on the inelastic response of steel moment-resisting frames. One of the connection models not only assumed that no relative rotation occurred between the columns and beams framing into a joint, but also that yielding of the columns and beams occurred at the connection faces. In other words, the panel zone was a rigid element having only rigid body motion. The remaining two connection models assumed that there was relative rotation between the columns and beams framing into a joint and that the yielding of the columns and beams occurred at the ends of the members. The difference between these two flexible connection models was principally the yield strength of the panel zone as a result of different thicknesses for the panel zone web. The panel zone of the inelastic flexible connection model yielded prior to the development of the full plastic moment of the beams, while the panel zone of the elastic flexible connection model yielded at the development of the full plastic moment of the beams. A discussion of modelling the beam-to-column connections with the finite elements available in the DRAIN-2D computer program is contained in Chapter 3.

The standard model of the D1B frame with rigid connections and yielding of the columns and beams at the ends of the members was designated D1B-NPZ (No Panel Zone). The frame model with rigid panel zones was designated D1B-RPZ. The frame model with flexible connections having the elastic strength to develop the full plastic moment of the beams was designated D1B-EPZ. The other flexible connection model having the inelastic strength to develop the full plastic moment of the beams was designated D1B-IPZ.

Comparisons of the time histories for the first story drift of the D1B-NPZ, D1B-RPZ and D1B-IPZ frames subjected to each of the earthquakes are

shown in Figure 4.6. The corresponding story shear-drift histories for the first story are shown in Figures 4.7, 4.8 and 4.9 for each earthquake. The time histories of story drift and story shear-drift histories for the D1B frame model with elastic panel zones (D1B-EPZ) were quite similar to the frame model with inelastic panel zones (D1B-IPZ) and, thus, are not given in these figures. The fundamental period of vibration for the frame model with rigid panel zones was roughly twenty-five percent shorter than the frame models with the other types of connections. As a consequence, the dominating period of the drift-time histories for the D1B-RPZ model was shorter than the other two shown. The story shear-drift histories of the D1B-NPZ and D1B-IPZ were quite similar and again this was due to the limited inelastic behavior of the frame.

The maximum story drifts and story shears obtained during each of the time-history analyses are plotted as envelopes in Figure 4.10. The maximum story drift and story shear envelopes were nearly identical for the D1B-IPZ and D1B-EPZ, thus the D1B-EPZ envelopes are not given in the figures. The maximum story drifts, especially in the upper stories, were smaller for the D1B-RPZ frame model. The story drifts were quite uniform from excitation with the Parkfield record, but the other two records produced larger drifts in the upper stories. In fact, the drifts calculated in the upper stories of the analysis with the El Centro and Taft records generally exceeded the maximum expected story drifts of one and a half percent of the story height. The maximum story shears for each of the frame models were roughly the same and usually were three times larger than the design story shears.

The total input energy quantities and the dissipation thereof are shown in Figures 4.11a, 4.12a and 4.13a for the D1B frame modelled with each of

the four connection models subjected to each of the earthquakes. The energy quantities were approximately the same, except for the D1B-RPZ model. The difference between the total input energy for the D1B-RPZ model and the other models probably could be contributed to difference in excitation due to the interaction between fundamental frequency of vibration for the structure and frequency content of the ground motion.

The distributions of the hysteretic energy by elements and stories for each of the four frame models are shown in Figures 4.11b, 4.12b and 4.13b for each earthquake record. The D1B-NPZ model had most of the hysteretic energy dissipated in the beams because of the "strong column-weak beam" design. The D1B-RPZ model had even less hysteretic energy dissipated in the columns than the D1B-NPZ, because the reduction in moment from the plastic hinge location to the end node was greater for the columns than the beams (see Figure 3.5). The distributions by stories for the D1B-EPZ and D1B-IPZ models were essentially the same. The Parkfield record tended to cause the middle stories to dissipate most of the hysteretic energy, while the El Centro and Taft records caused most of the dissipation in the upper stories. However, the distributions by elements were different for these two frames. The hysteretic energy dissipated by the columns of the D1B-IPZ and D1B-EPZ frames were approximately the same, but the relationship between the elastic strength of the beams and the elastic strength of the panel zone dictated which of these elements dissipated most of the balance of hysteretic energy for each frame. The locations of hysteretic energy dissipation for an interior column line are shown in Figures 4.11c, 4.12c and 4.13c. As shown in these figures, most of the hysteretic energy was dissipated in the upper stories.

The calculated story drift and shears from the dynamic analyses of the frame models with various connection behaviors were quite similar, except for the model with rigid panel zones. The frame model with rigid panel zones probably depicts the inelastic behavior of the individual columns and beams better than the other frame models. The plastic hinge locations for yielding of the columns or beams would most likely be located at the face of the connections where the moment is the largest (assuming no external forces along the members) for the clear span of the member. However, the total disregard for deformation in the panel zone resulted in poor modelling of the overall load-deformation behavior of the frame.

The code states that the strength of the panel zones need not develop more than eighty percent of the full plastic moment of the beams. Therefore in a "strong column-weak beam" design, the panel zone designed to this level usually will experience significant inelastic behavior before either of the beams framing into a joint yield. The bending moments acting in each of the beams at a joint are essentially the same magnitude and acting in the same direction, since the vertical forces of a perimeter frame are rather small. Research has shown that the panel zone is a good location for dissipation of hysteretic energy, except that under severe distortion of the panel zone the beam-to-column connections may fail prematurely [27,28,29,30,38,39,40].

The structural engineer is in "charge" of determining the location(s) for hysteretic energy dissipation at a joint by specifying the thickness for the web of a panel zone. If the engineer specifies the minimum strength, then the yielding generally will occur in the panel zone. However, if a thicker web is specified for the panel zone than the yielding can occur in the ends of the beams or columns depending on their relative strengths.

Since the structural engineer has the capability to determine where the yielding at a connection will take place, the required ductility can be designed into these locations so that non-ductile failures are prevented after many cycles of inelastic deformations. The provisions in the 1988 UBC encourage the strength of the panel zone to be able to develop at least eighty percent of the full plastic moment of the beams. Although at this minimum level, the panel zones will dissipate most of the hysteretic energy at a joint.

It should not be surprising that the calculated story drifts and shears were not much different for the three frame models without rigid panel zones, because once there was yielding at a joint the net result was the same - the inability to transfer moment from the columns to the beams. The placement of plastic hinge locations at the connection face should only be used if deformation in the panel zone can be accounted for in an analysis, because the stiffness of the frame would be unrealistically high. However, care must be taken in developing the numerical model for a joint so that calculated response indicates where the yielding would actually occur in the structure when subjected to a major earthquake. It would be quite difficult to model the deformation in the panel zone and force the plastic hinge locations of the columns and beams to occur at the connection faces using the finite elements currently available with the DRAIN-2D program. One limitation with the frame models developed for this investigation was the inability to account for degradation of the members and connections as a result of inelastic behavior. Perhaps yielding in the columns would cause more degradation to the overall stiffness and strength of the frame than yielding in the beams.

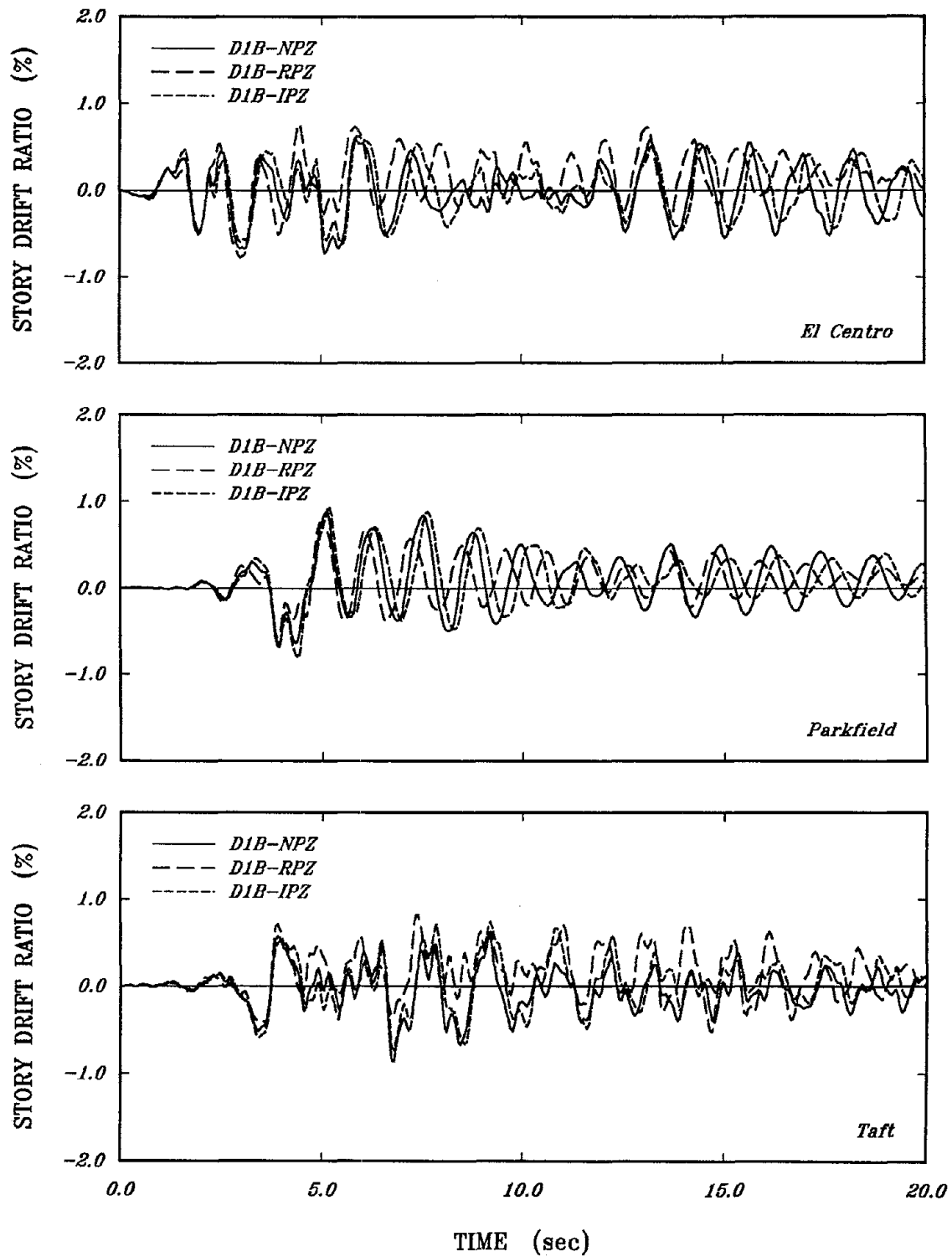


FIGURE 4.6 Drift-Time Histories of First Story for Different Connection Modelling of D1B Frame Subjected to Three Earthquakes

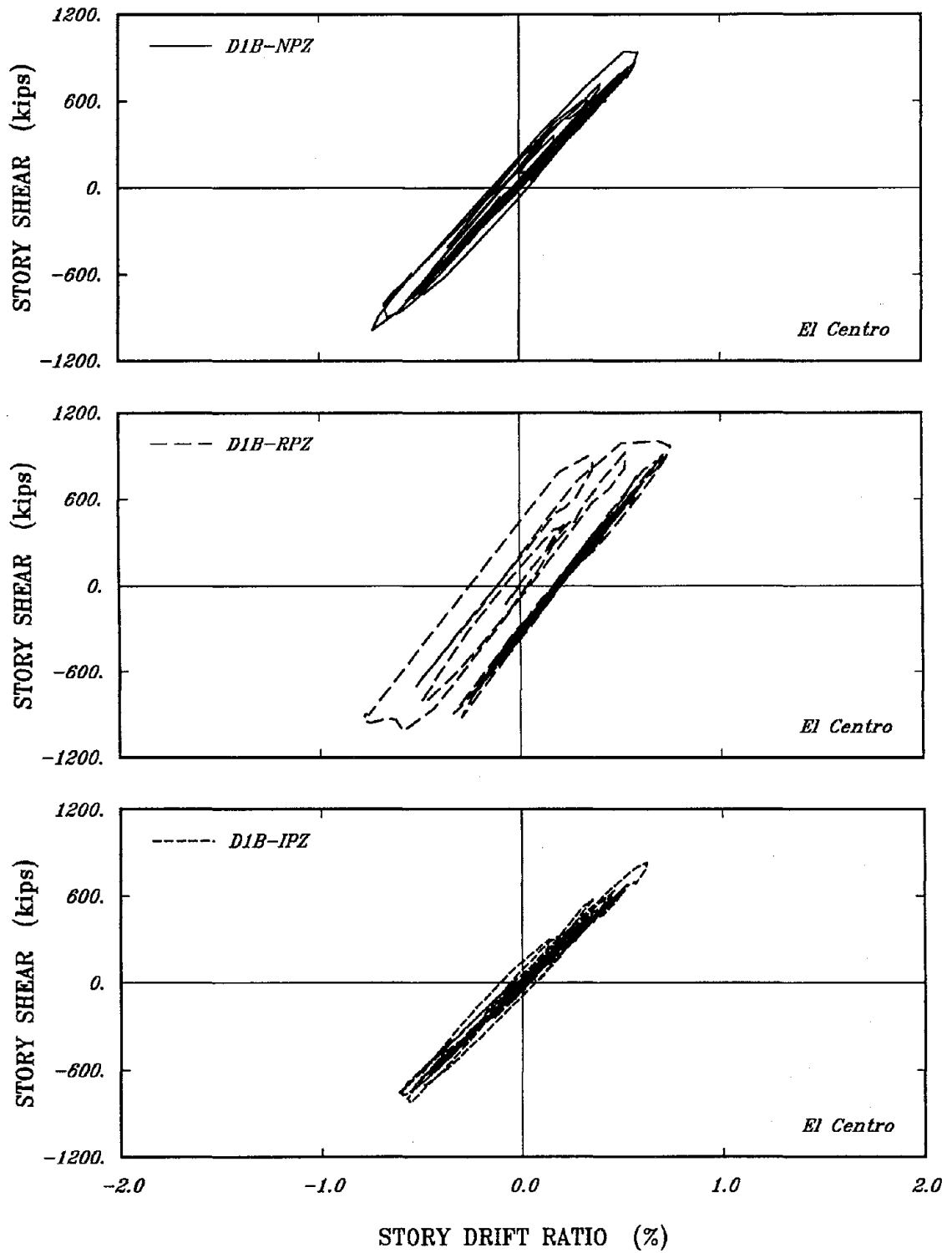


FIGURE 4.7 Shear-Drift Histories of First Story for Different Connection Modelling of D1B Frame Subjected to El Centro

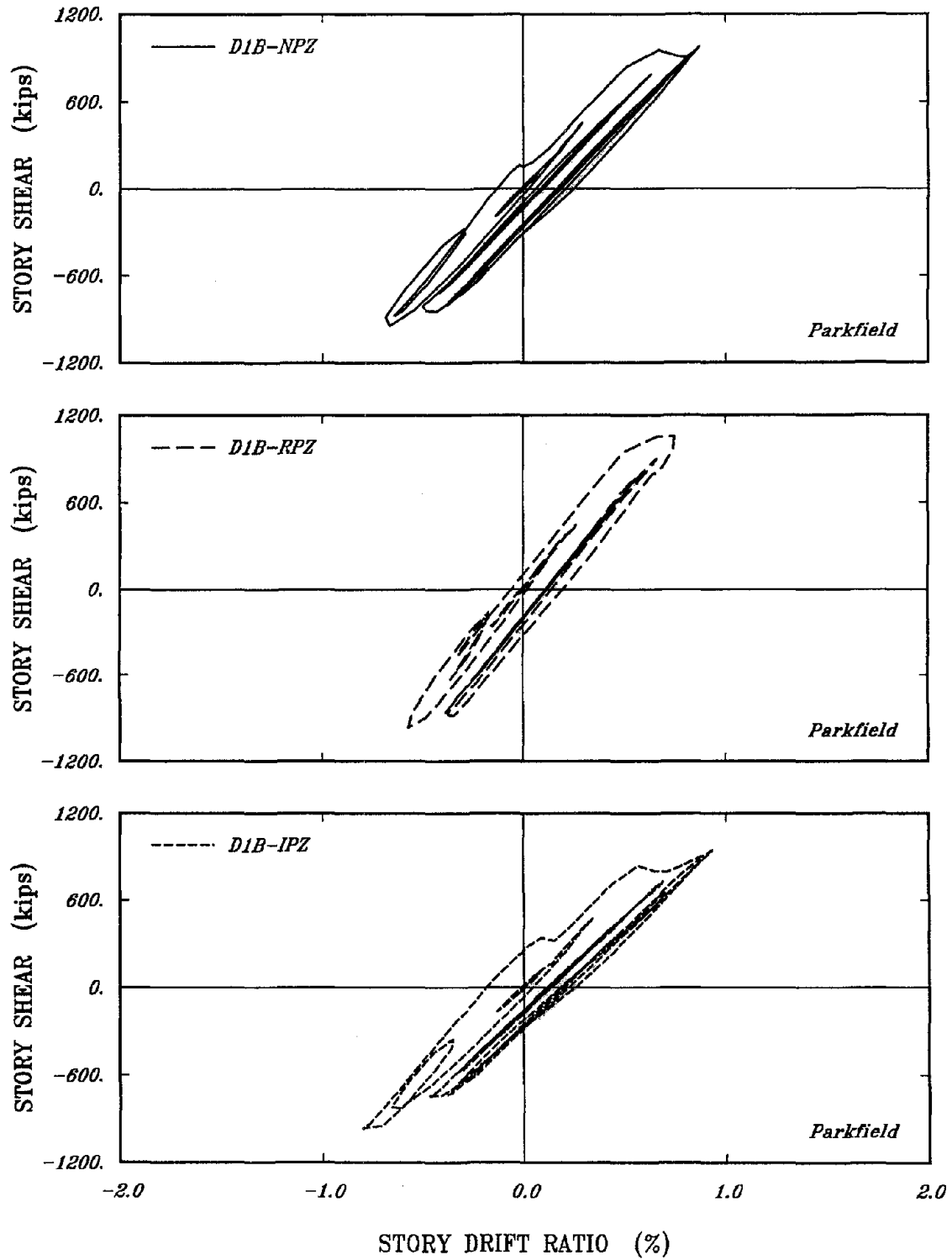


FIGURE 4.8 Shear-Drift Histories of First Story for Different Connection Modelling of D1B Frame Subjected to Parkfield



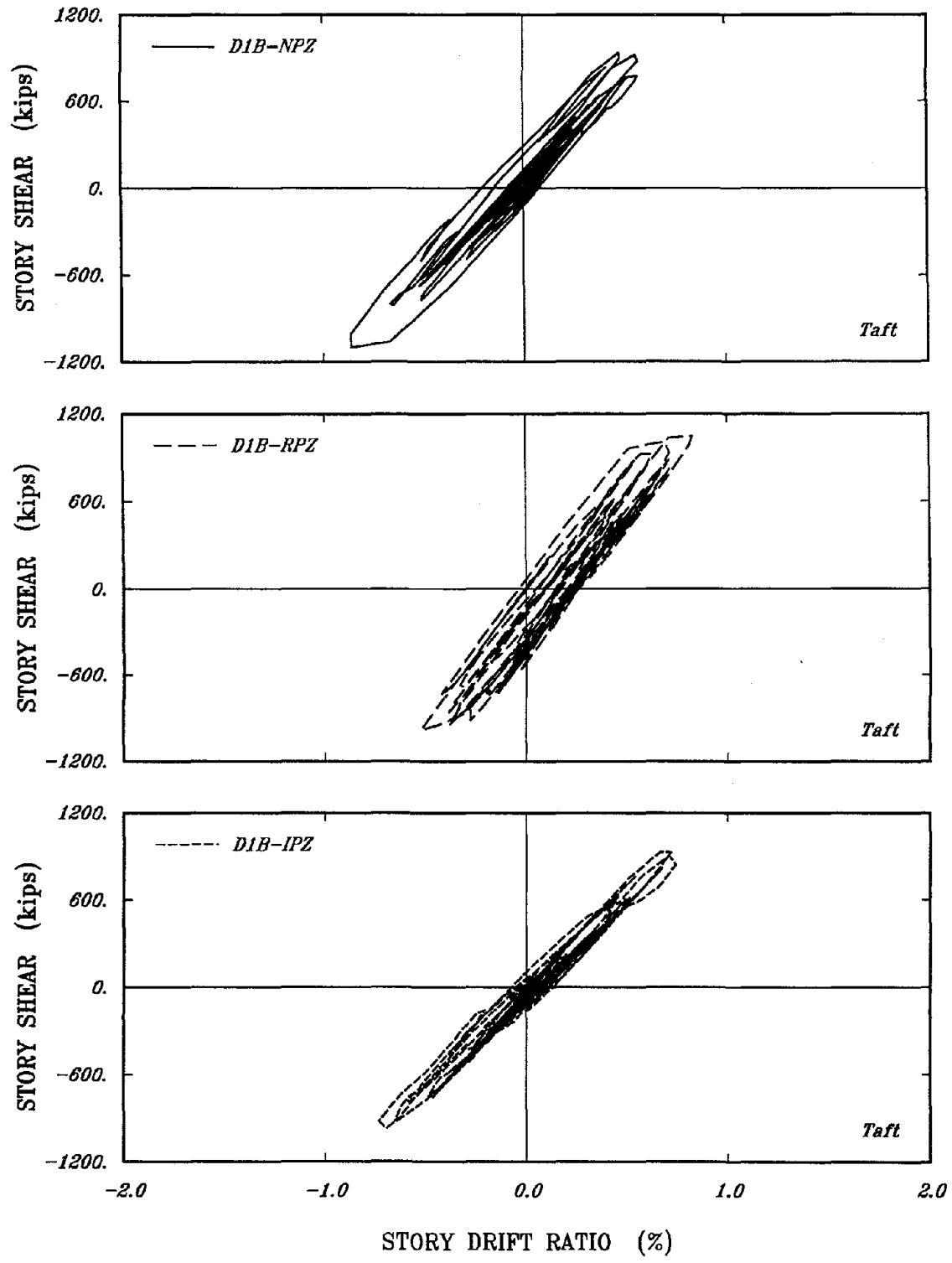


FIGURE 4.9 Shear-Drift Histories of First Story for Different Connection Modelling of D1B Frame Subjected to Taft

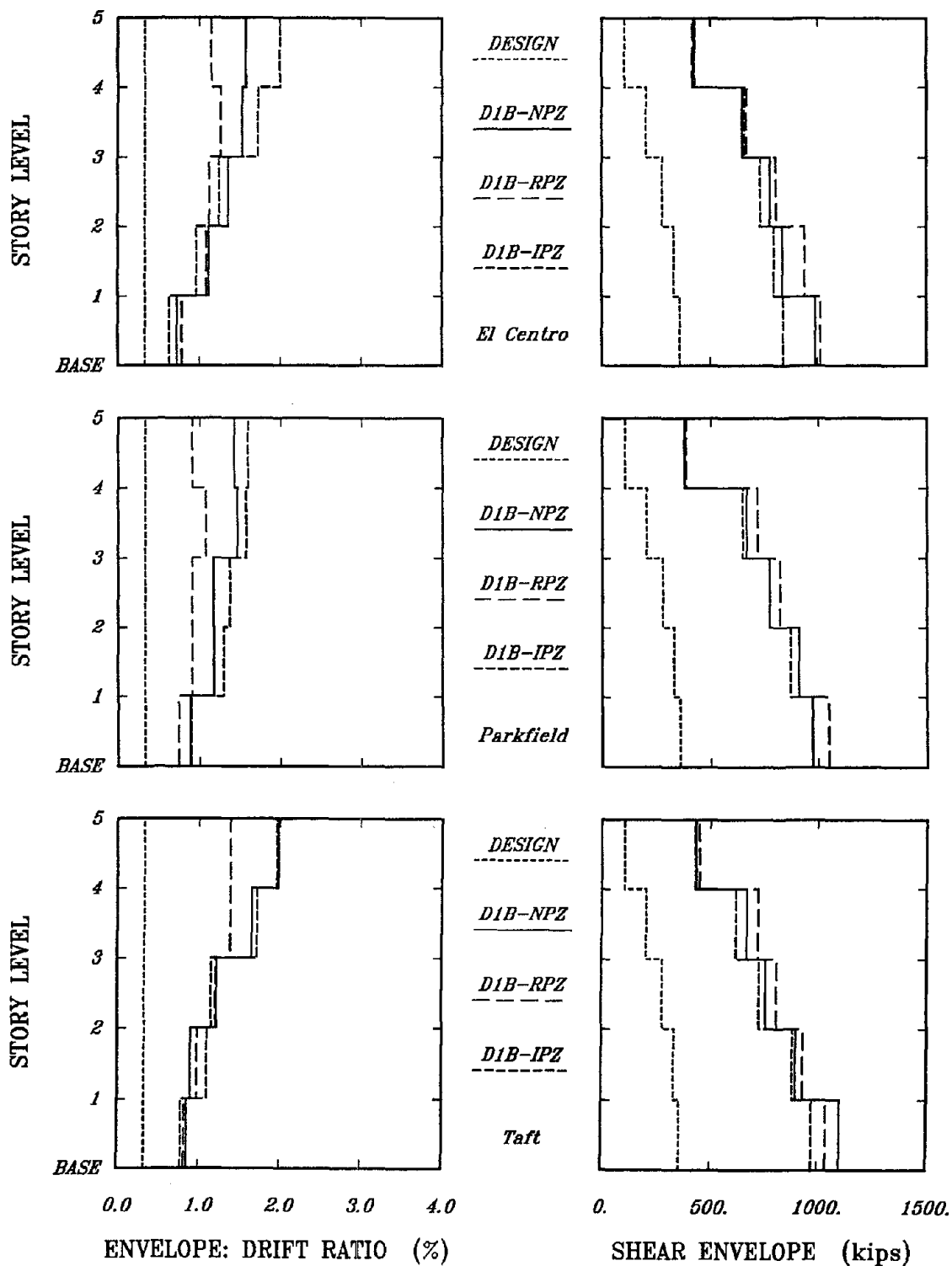


FIGURE 4.10 Story Drift and Shear Envelopes for Different Connection Modelling of D1B Frames Subjected to Three Earthquakes

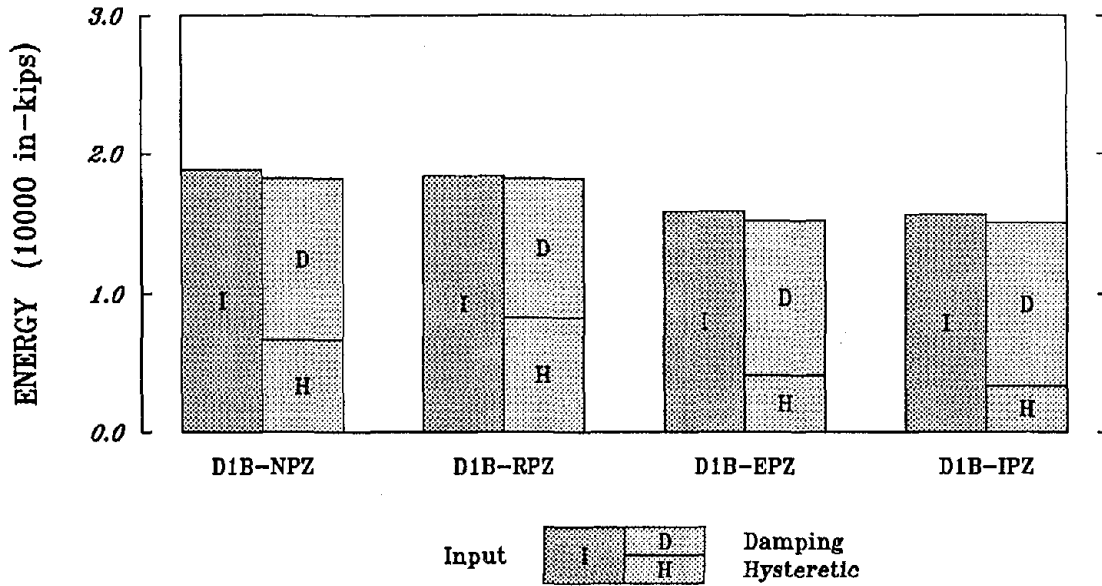


FIGURE 4.11a Cumulative Energy Quantities for Different Connection Modelling of D1B Frame Subjected to El Centro

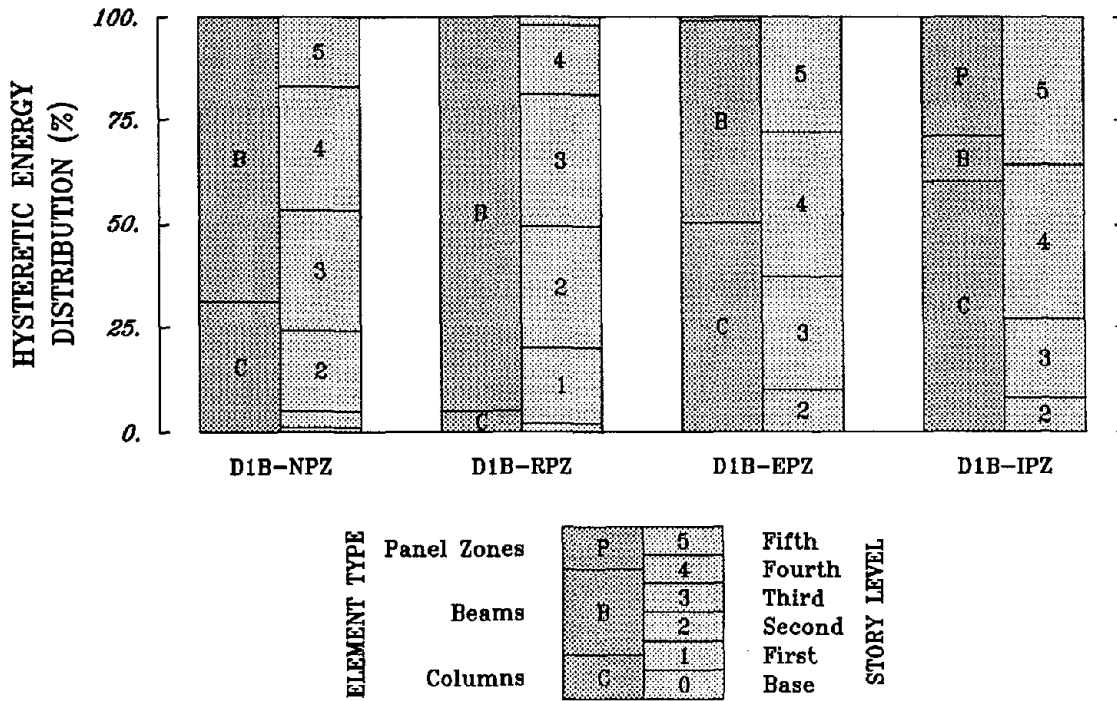
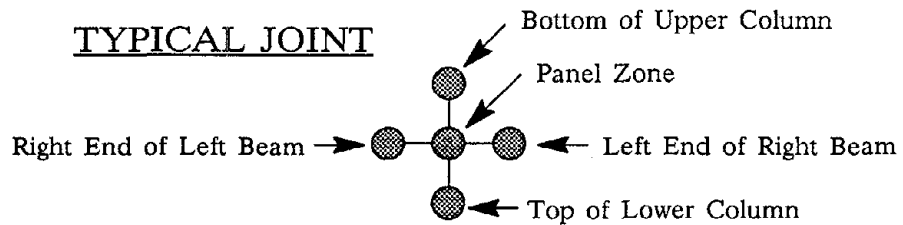
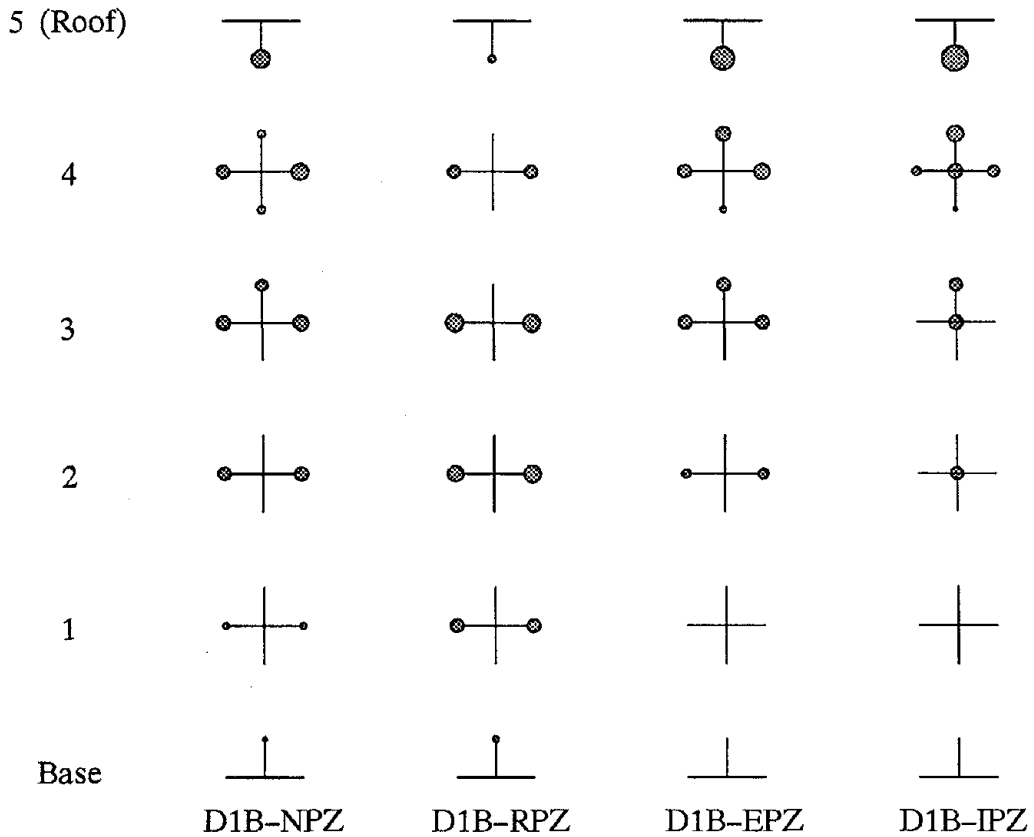


FIGURE 4.11b Hysteretic Energy Distributions for Different Connection Modelling of D1B Frame Subjected to El Centro



Note: Areas proportional to percentage of hysteretic energy dissipated at location.

FIGURE 4.11c Hysteretic Energy Dissipations for Different Connection Modelling of D1B Frame Subjected to El Centro

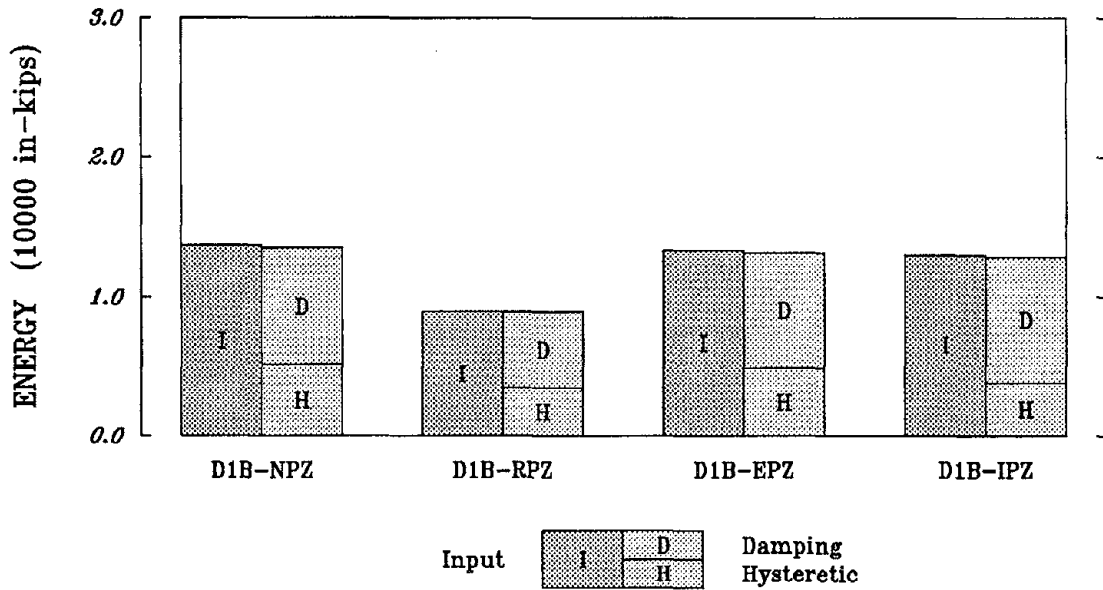


FIGURE 4.12a Cumulative Energy Quantities for Different Connection Modelling of D1B Frame Subjected to Parkfield

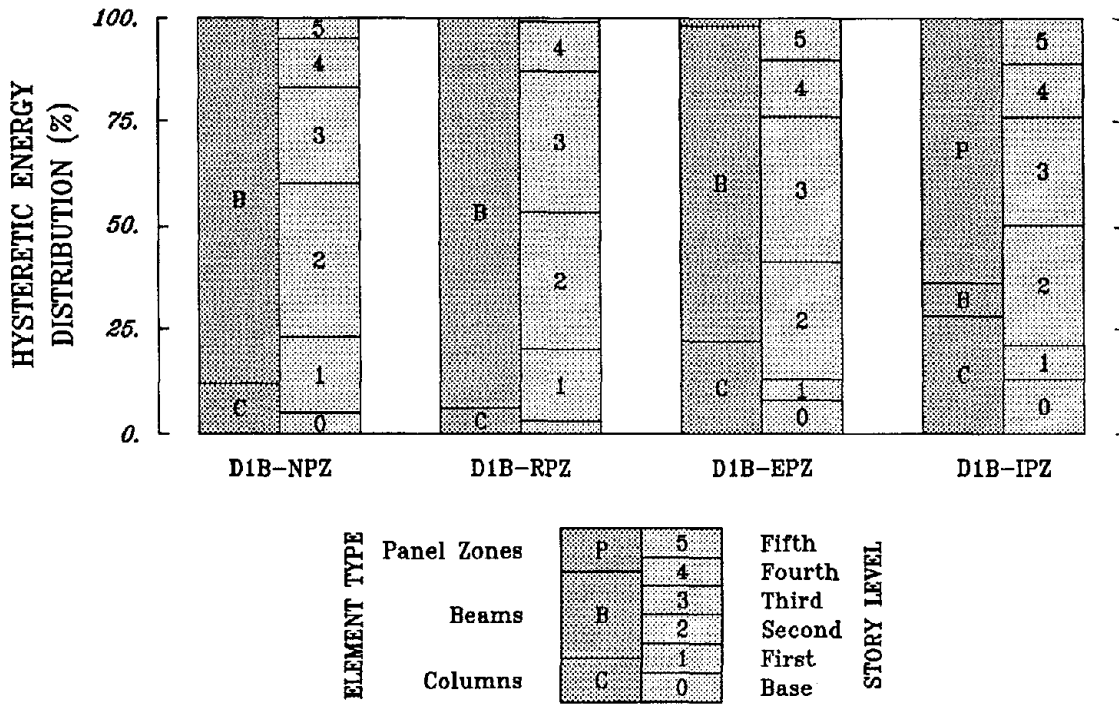
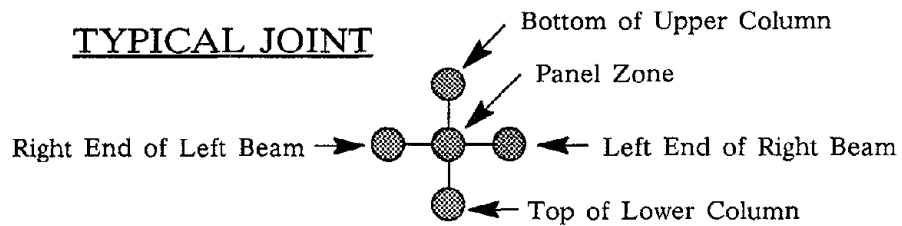
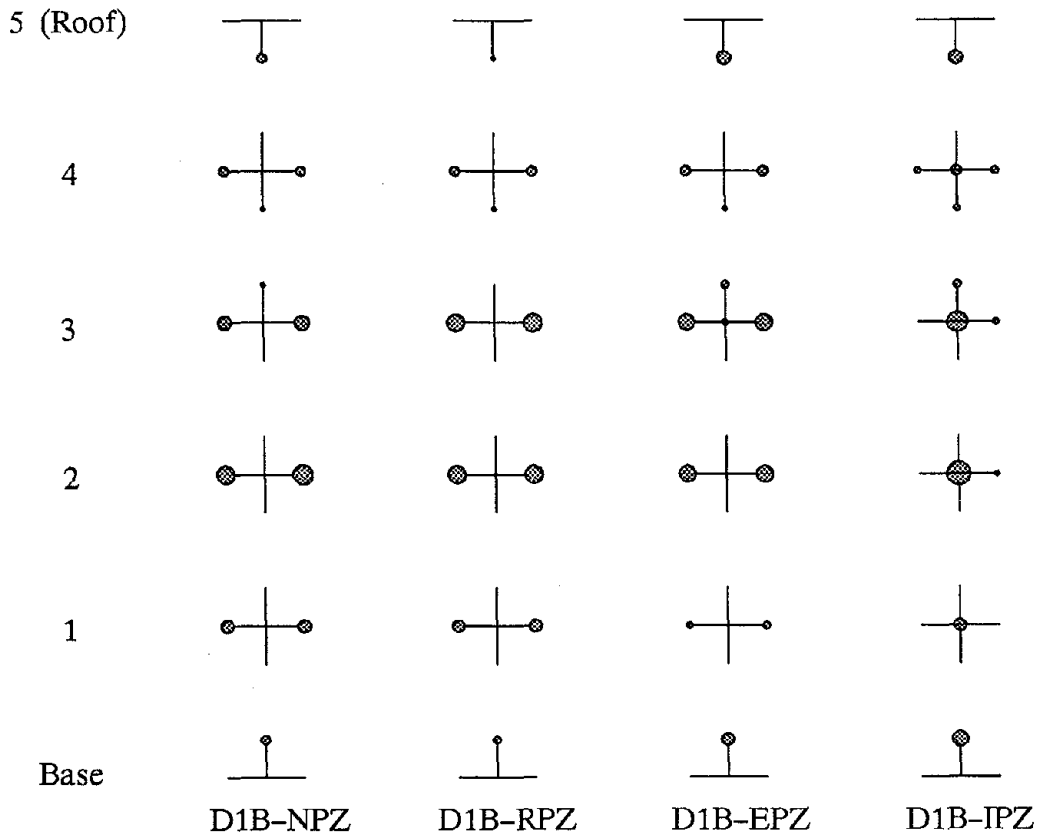


FIGURE 4.12b Hysteretic Energy Distributions for Different Connection Modelling of D1B Frame Subjected to Parkfield



Note: Areas proportional to percentage of hysteretic energy dissipated at location.

FIGURE 4.12c Hysteretic Energy Dissipations for Different Connection Modelling of D1B Frame Subjected to Parkfield

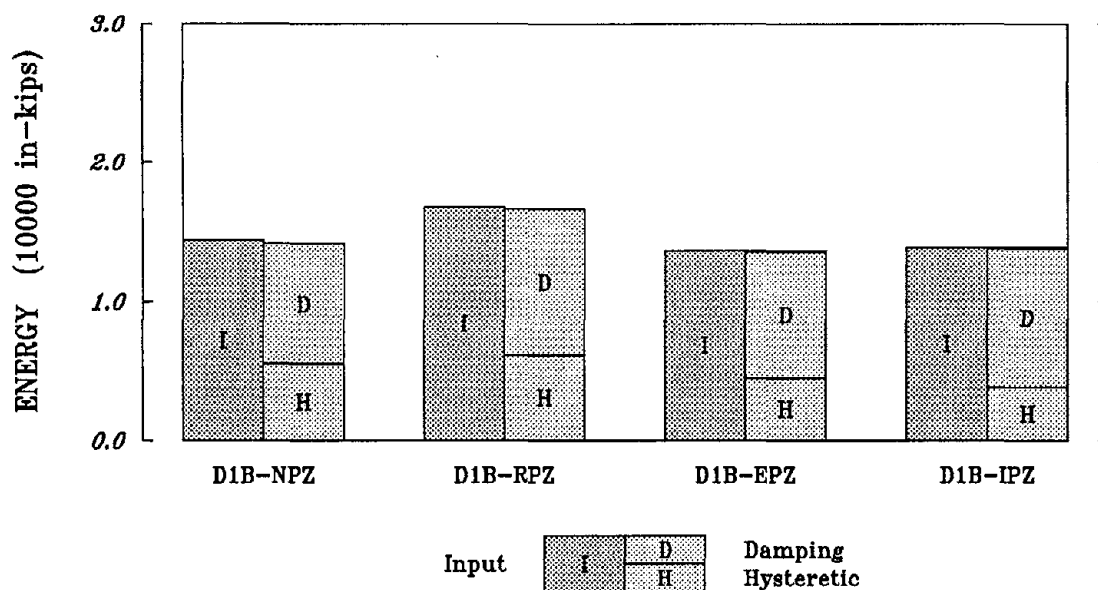


FIGURE 4.13a Cumulative Energy Quantities for Different Connection Modelling of D1B Frame Subjected to Taft

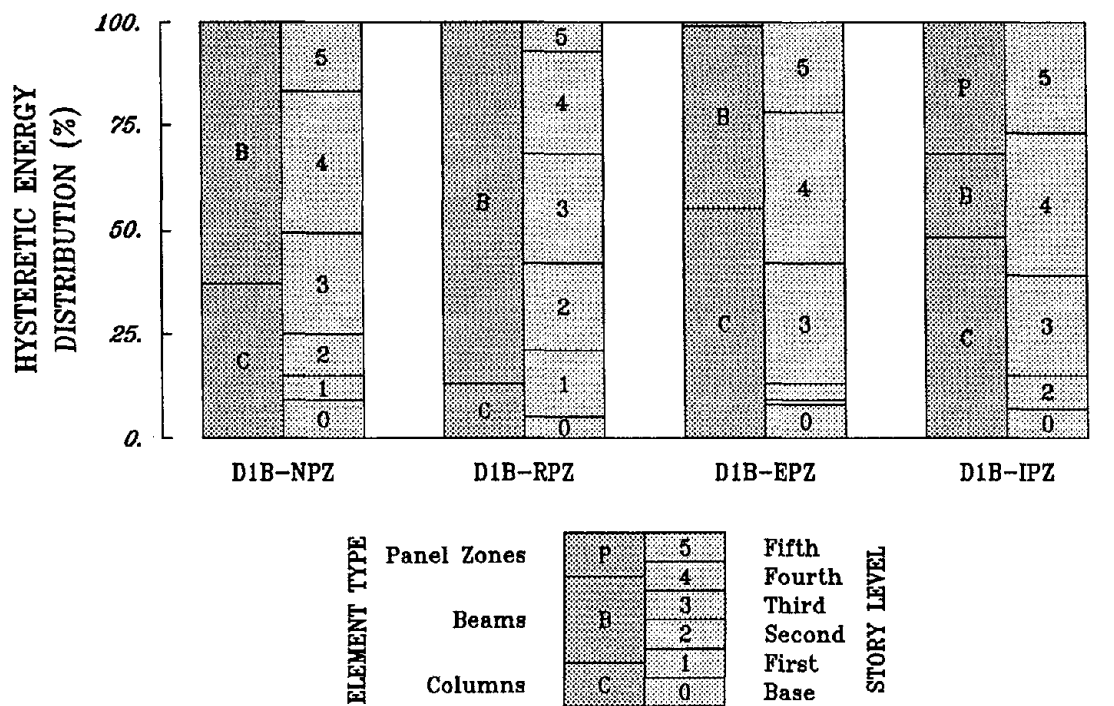
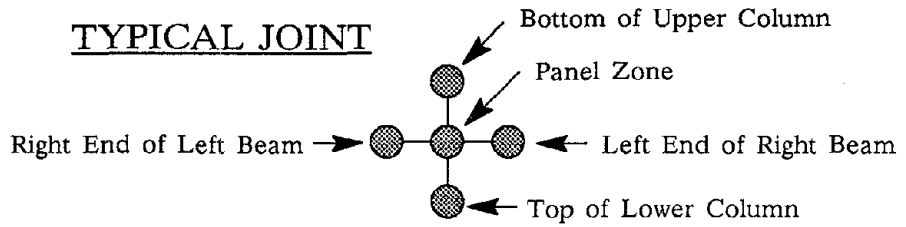
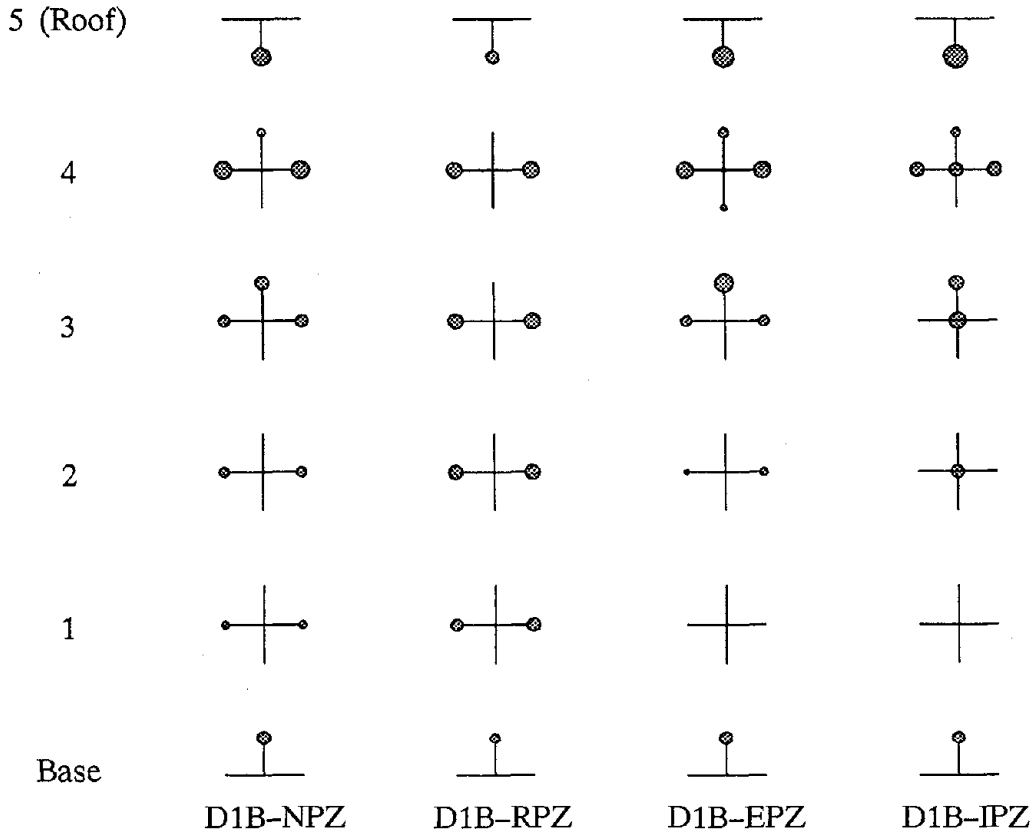


FIGURE 4.13b Hysteretic Energy Distributions for Different Connection Modelling of D1B Frame Subjected to Taft



Note: Areas proportional to percentage of hysteretic energy dissipated at location.

FIGURE 4.13c Hysteretic Energy Dissipations for Different Connection Modelling of D1B Frame Subjected to Taft



#### 4.4.3 Investigation of Nonstructural Element Participation

The provisions in the 1988 edition of the *Uniform Building Code* for the direct design procedure for the lateral force-resisting system of a building do not specifically address the interaction of the nonstructural elements (cladding, interior partitions, mechanical systems, etc.) with the lateral deformation of the bare structural frame. The stiffness contribution of nonstructural elements is indirectly incorporated in the code equation for the estimation of the fundamental period of vibration for a structure. The estimated fundamental period of the building is shorter than the fundamental period of the bare structural frame. However, the strength contribution of the nonstructural elements is ignored.

The provisions in the code regarding the lateral force procedures maintain that the mathematical model of the structure should represent, to the adequacy required to predict the significant contributions to the response, the load-deformation behavior of the structure. However, no recommendations are given in the code regarding the assessment of the lateral stiffness and strength for nonstructural elements or incorporation of nonstructural element participation into the design and analysis of a structure.

At first, simple modelling of the nonstructural elements was employed to determine the significance of these elements in the calculated response. Shear panel elements, modelling nonstructural elements, were added to each story of the standard modelling for the D1B frame. The additional lateral stiffness from the nonstructural elements reduced the calculated fundamental period of the frame model to the estimated value given by the code. The load-deformation behavior of the initial modelling of nonstructural elements

was linear with a failure strain of one-half of a percent, which also corresponds to a one-half of a percent story drift ratio. After studying the response of the frame model using the nonstructural elements with a linear load-deformation behavior and realizing that the influence can be quite profound, an improved model of nonstructural elements was developed. This model had a load-deformation relationship with degradation of stiffness and strength at three deformation levels. The transition to failure for the nonstructural elements of a story was more gentle. A discussion regarding the modelling of nonstructural elements is given in Chapter 3.

In this parametric study, the D1B frame model without nonstructural elements was designated D1B-NNE (No Nonstructural Elements). The D1B frame model containing nonstructural elements with a linear load-deformation relationship was designated as D1B-LNE, while the frame model containing nonstructural elements with a trilinear load-deformation relationship was designated as D1B-TNE. In the D1B-LNE and D1B-TNE models, the stiffness and strength contribution of the nonstructural elements had a greater influence in the upper stories of the frames because the lateral stiffness and strength of the stories decreased from the lower stories to the upper stories, while the lateral stiffness and strength contributions of the nonstructural elements remained relatively constant throughout the height. Therefore the distribution of stiffness and strength, which was fairly uniform, was no longer proportional to the story shears from the equivalent lateral forces.

The comparisons of the time histories for the first story drift for the D1B-NNE, D1B-LNE and D1B-TNE frame models are shown in Figure 4.14. The differences between the traces of the three models from excitation with the

El Centro accelerogram were small as were the differences between the traces from excitation with the Taft record. Although, it should be noted that the nonstructural elements degraded or even failed during the first few cycles of strong excitation. The Parkfield traces of the models with nonstructural elements were roughly the same. However, the general amplitude of the response of the bare structural frame model was larger than the other two. This distinction was attributable to the shifting of frequencies in the models, because the models with nonstructural elements had small drifts in the upper stories during the response from the Parkfield accelerogram. Thus, the general behavior of these frame models was a rigid body movement of the upper stories responding on a soft first story.

The story shear-drift histories from excitation by each earthquake are shown in Figures 4.15, 4.16 and 4.17. The degradation or failure of the nonstructural elements can be seen in these traces by the change in slope of the elastic portion of the hysteresis loops. The inelastic behavior of the models with linear behavior nonstructural elements was greater because of the complete rapid failure of the nonstructural elements in the lower stories. The shear carried by these elements was transferred abruptly to the structure as a shock loading, causing considerable accelerations which consequently lead to large story drifts.

The story drift and shear envelopes of maximum response are plotted in Figure 4.18. The maximum story drifts tended to be of similar magnitude for the lower stories, while the story drifts in the upper stories of the bare structural frame model tended to be larger than in the frame models with nonstructural elements. The addition of nonstructural elements increased the lateral stiffness and strength of the softer upper stories of the bare

structural frame since the nonstructural elements of these stories did not suffer much degradation. In the upper stories, the maximum story drifts for the frame models without nonstructural elements approached or exceeded the expected inelastic drifts, while the maximum story drifts for the frame models with nonstructural elements were smaller than the expected inelastic drifts. The differences between the maximum story drifts of the frame models with and without nonstructural elements were quite different if the nonstructural elements of a story did not fail or suffer much degradation. The maximum story shears, especially for the frame models with nonstructural elements, were considerably larger than the design story shears.

The total input energy quantities and the dissipation thereof are shown in Figures 4.19a, 4.20a, 4.21a. The input energy corresponding to each earthquake usually were within ten percent of each other. As indicated by the hysteretic energy distributions given in Figures 4.19b, 4.20b and 4.21b, the dissipation of hysteretic energy from the El Centro and Taft records was mainly in the upper stories of the D1B-NNE frame model and mainly in the lower stories of the D1B-LNE, while the distribution was more uniform in the D1B-TNE. The hysteretic energy dissipation for both of the frame models with nonstructural elements was really concentrated in the lower stories from excitation with the Parkfield record. The locations of hysteretic energy dissipation also are shown in Figures 4.19c, 4.20c and 4.21c. As shown in these figures, the addition of the nonstructural elements tended to reduce the number of locations for hysteretic energy dissipation.

The participation of nonstructural elements in this study caused a significant change in the dynamic behavior of the model. The nonstructural elements with the linear load-deformation behavior provided a considerable

increase in lateral stiffness and strength, especially as the story drifts approached their failure strain since the bare structural frame had nearly reached its maximum shear capacity at one-half of a percent story drift ratio. Therefore, the distribution of stiffness and strength for the frame models considering the participation of nonstructural elements was not compatible with the assumed distribution of the 1988 UBC. The variance in the maximum drift for a story in a frame model with linear behavior nonstructural elements was dependent on the failure of the nonstructural element for that story. If the nonstructural element of a story failed, the maximum response of the story was roughly the same as the maximum response obtained by the bare structural frame model.

In many buildings, an attempt is made to isolate the nonstructural elements from the bare structural frame. However, because of improper installation of the nonstructural elements or insufficient isolation from the lateral force-resisting system, nonstructural elements will ultimately participate in the response. Depending on the relationship between the lateral stiffness and strength of the bare structural frame and the nonstructural elements, the nonstructural elements can have a substantial influence on the response.

The modelling of the nonstructural elements was rather crude, even for the more refined model with the trilinear load-deformation behavior. Even so, the importance of accounting for the participation of nonstructural elements was evident. If sufficient isolation of the nonstructural elements from the bare structural frame is not provided, the anticipated behavior of the nonstructural elements should be considered in the design for proper assessment as to the adequacy of the lateral force-resisting system.

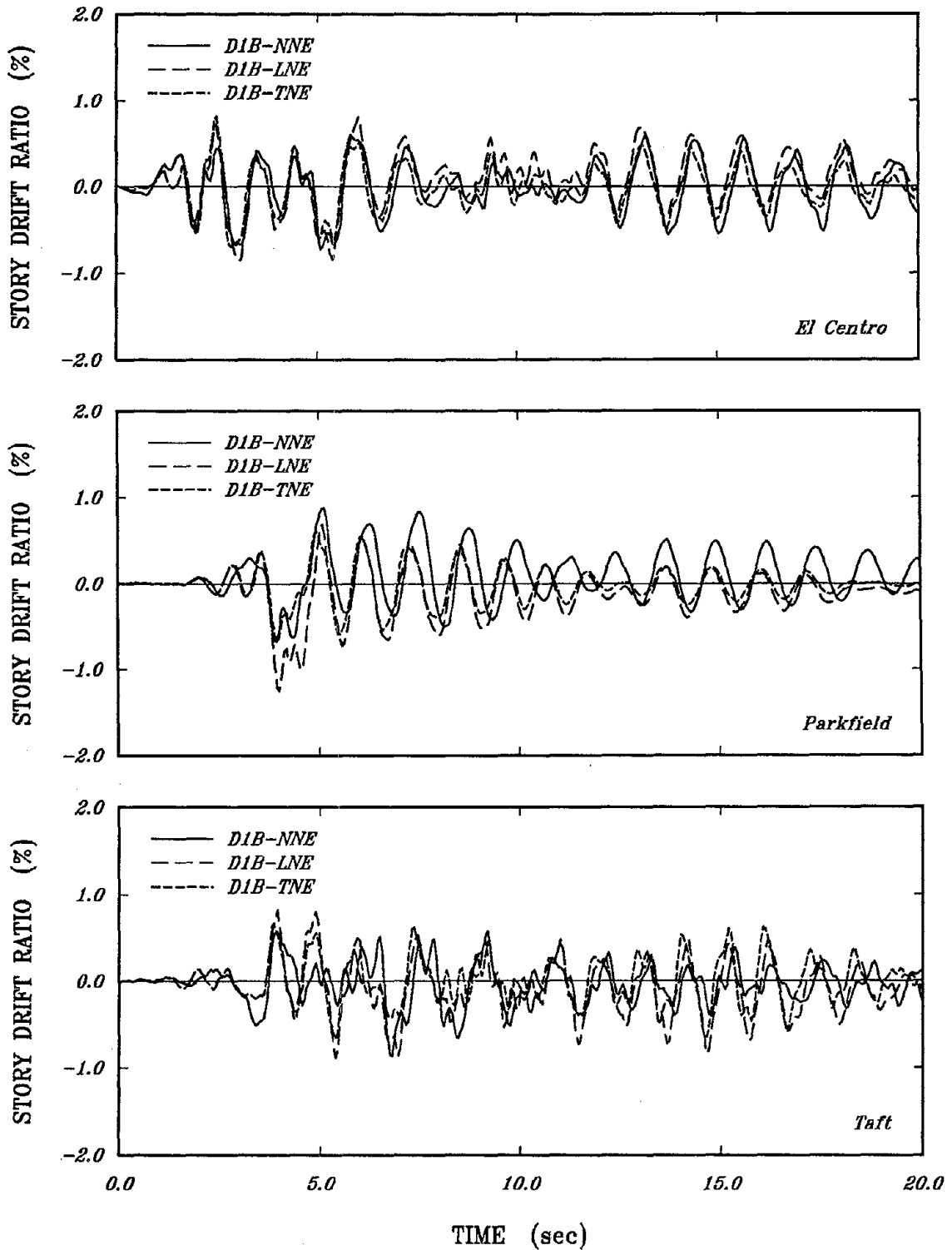


FIGURE 4.14 Drift-Time Histories of First Story for D1B Frame with Nonstructural Elements Subjected to Three Earthquakes

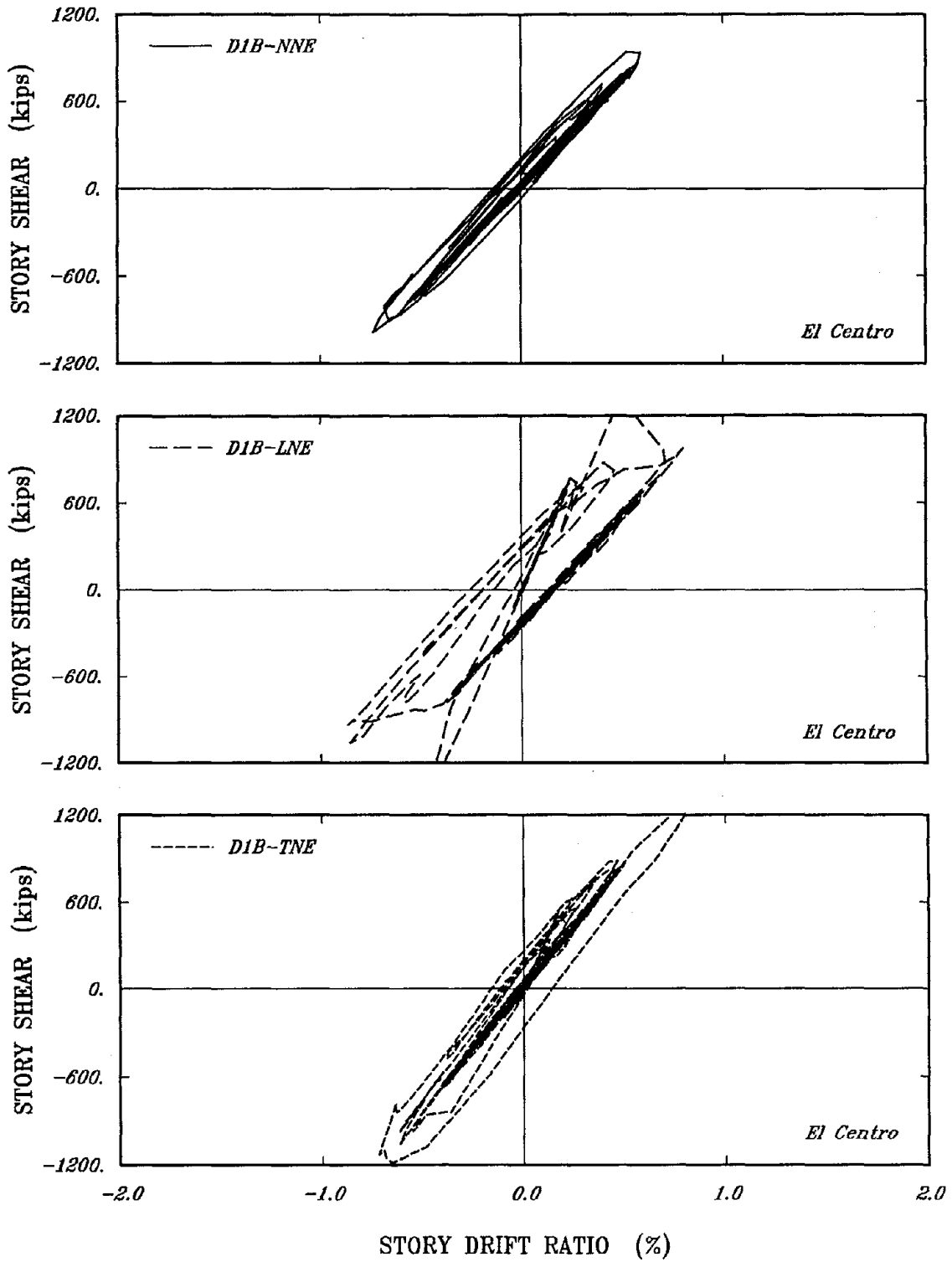


FIGURE 4.15 Shear-Drift Histories of First Story for D1B Frame with Nonstructural Elements Subjected to El Centro

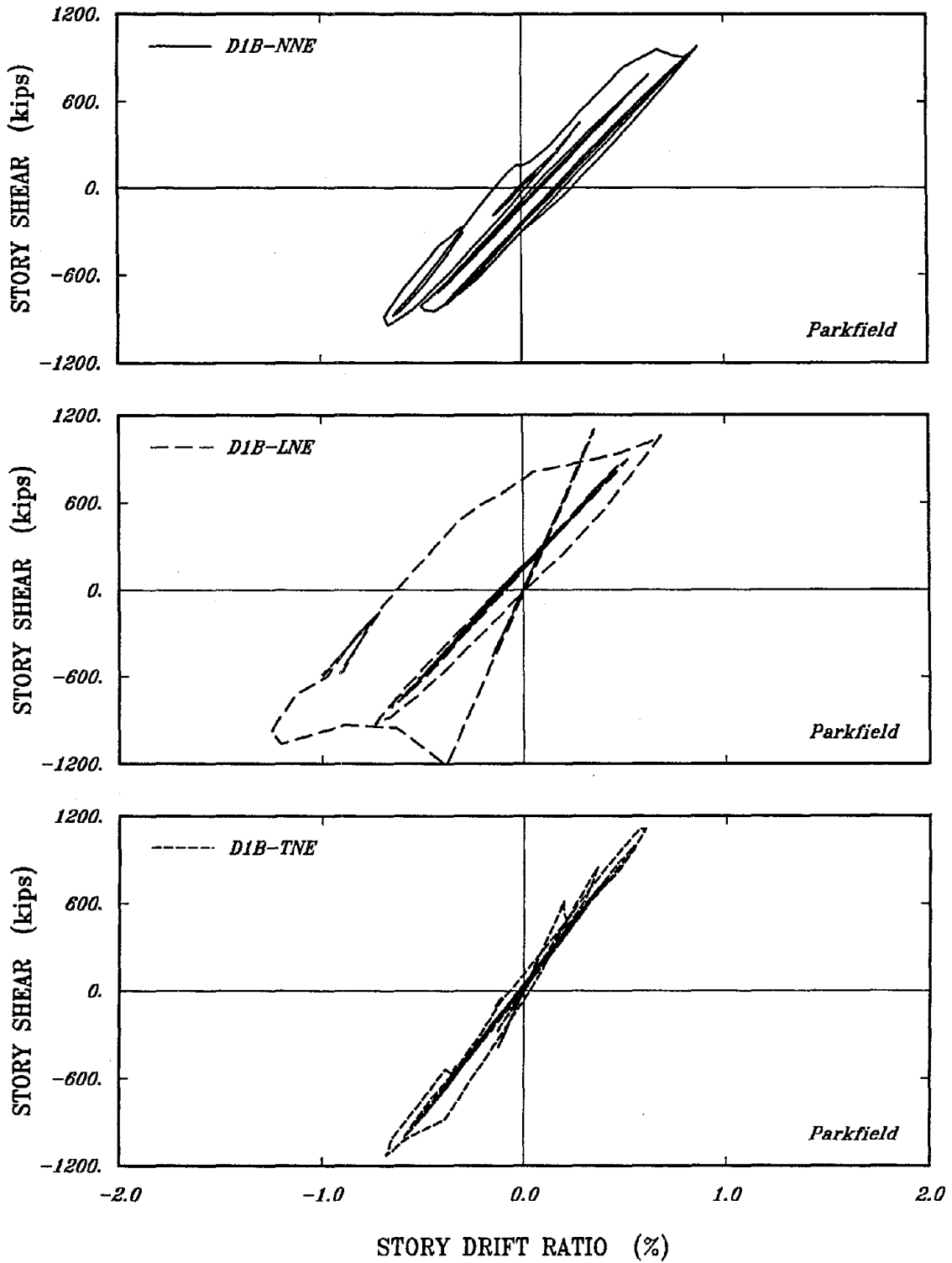


FIGURE 4.16 Shear-Drift Histories of First Story for D1B Frame with Nonstructural Elements Subjected to Parkfield



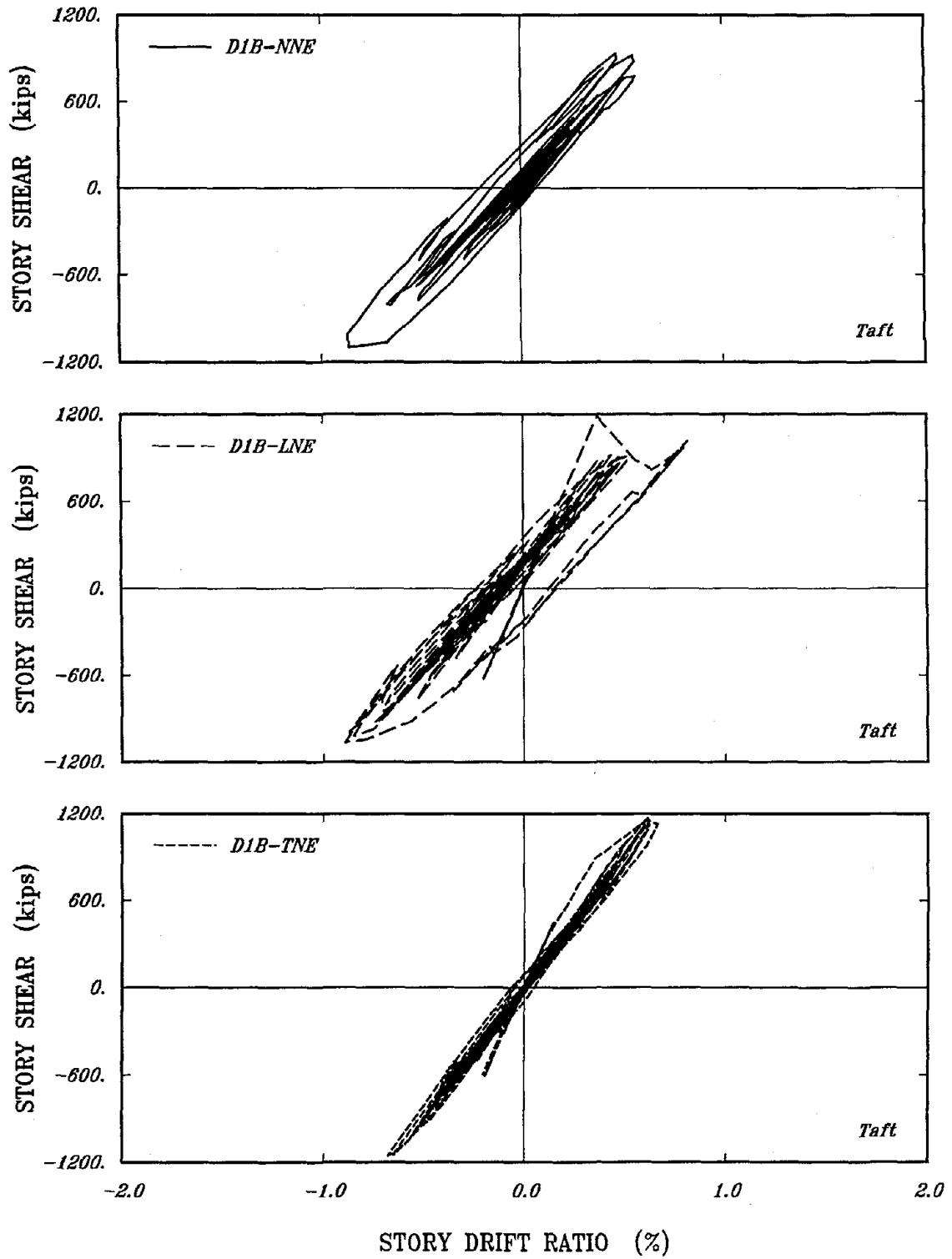


FIGURE 4.17 Shear-Drift Histories of First Story for D1B Frame with Nonstructural Elements Subjected to Taft

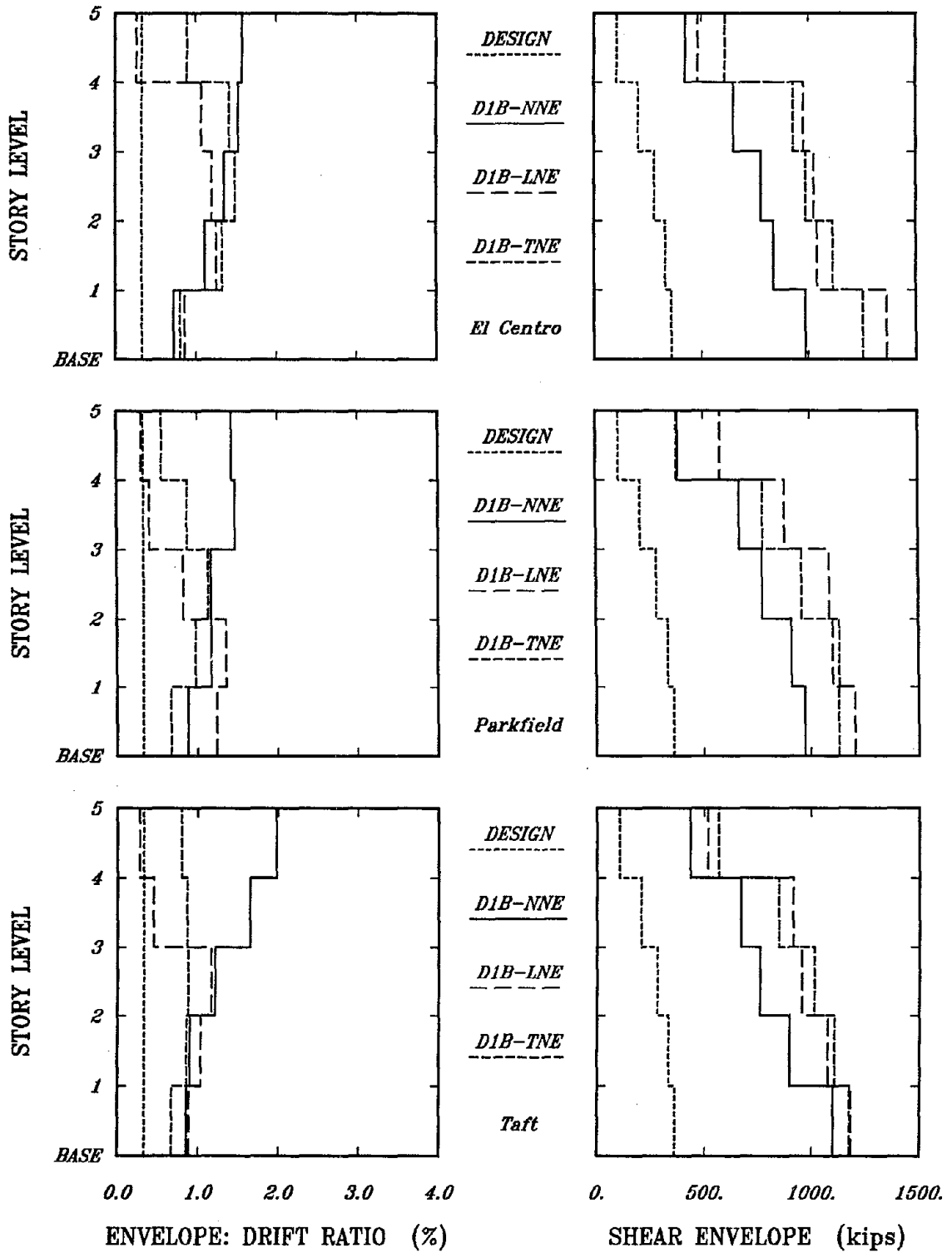


FIGURE 4.18 Story Drift and Shear Envelopes for D1B Frame with Nonstructural Elements Subjected to Three Earthquakes

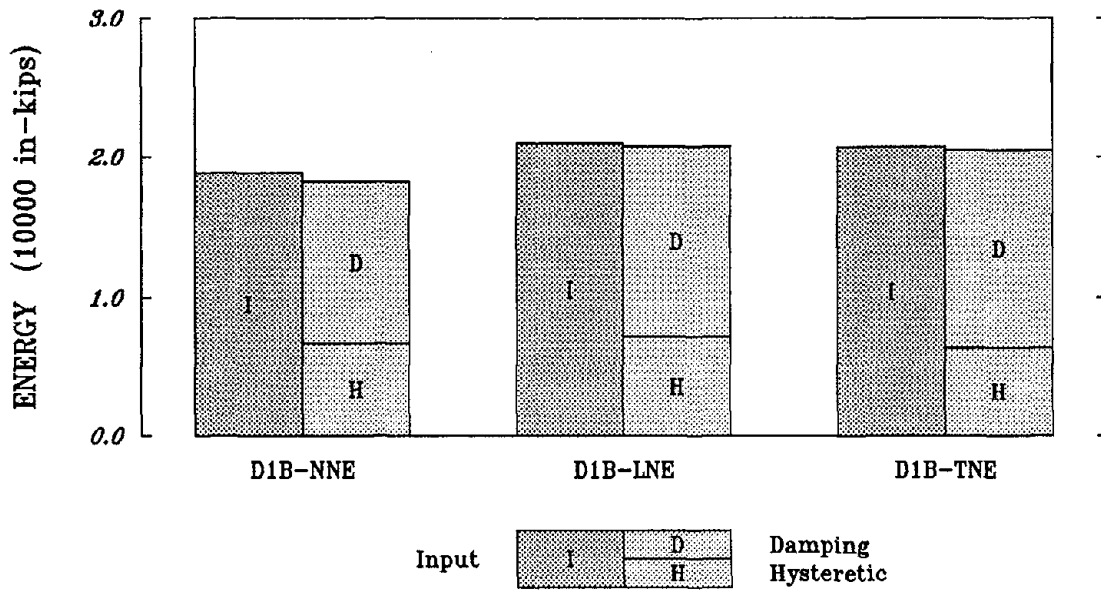


FIGURE 4.19a Cumulative Energy Quantities for D1B Frame with Nonstructural Elements Subjected to El Centro

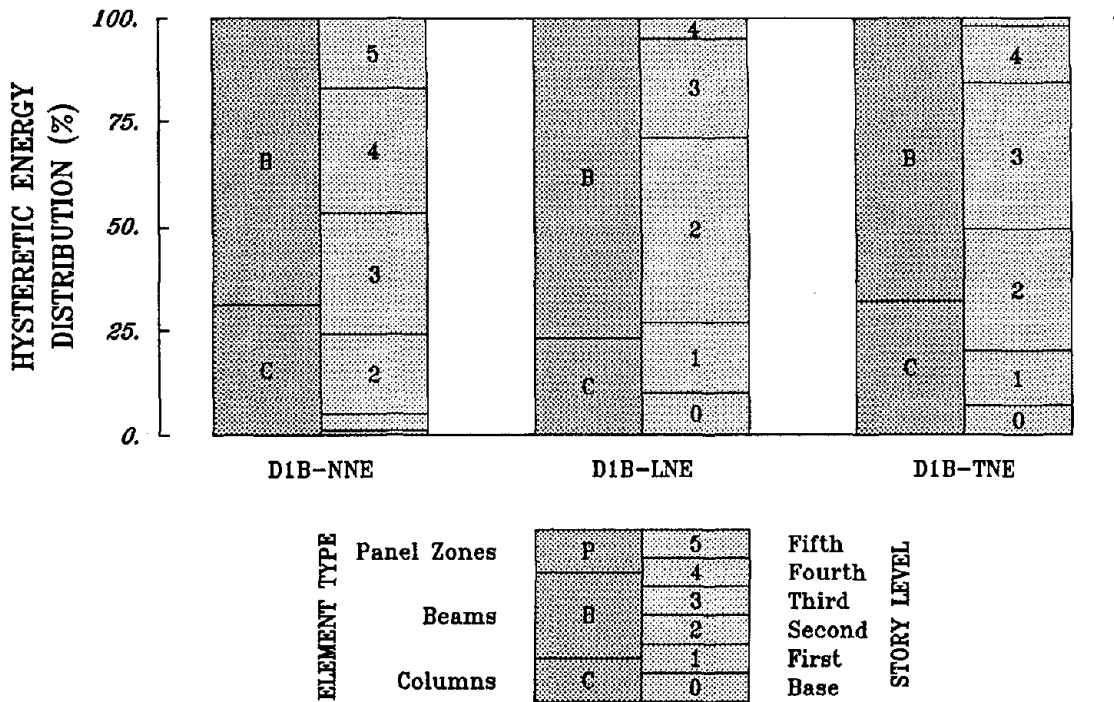
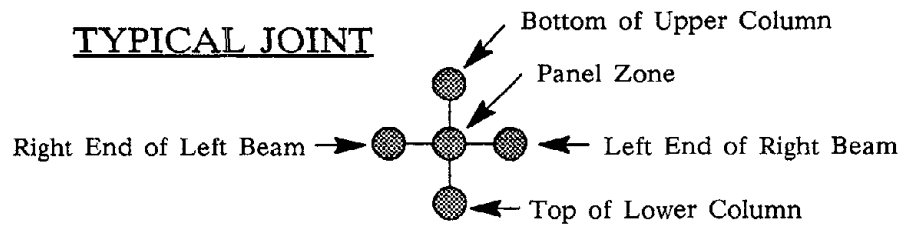
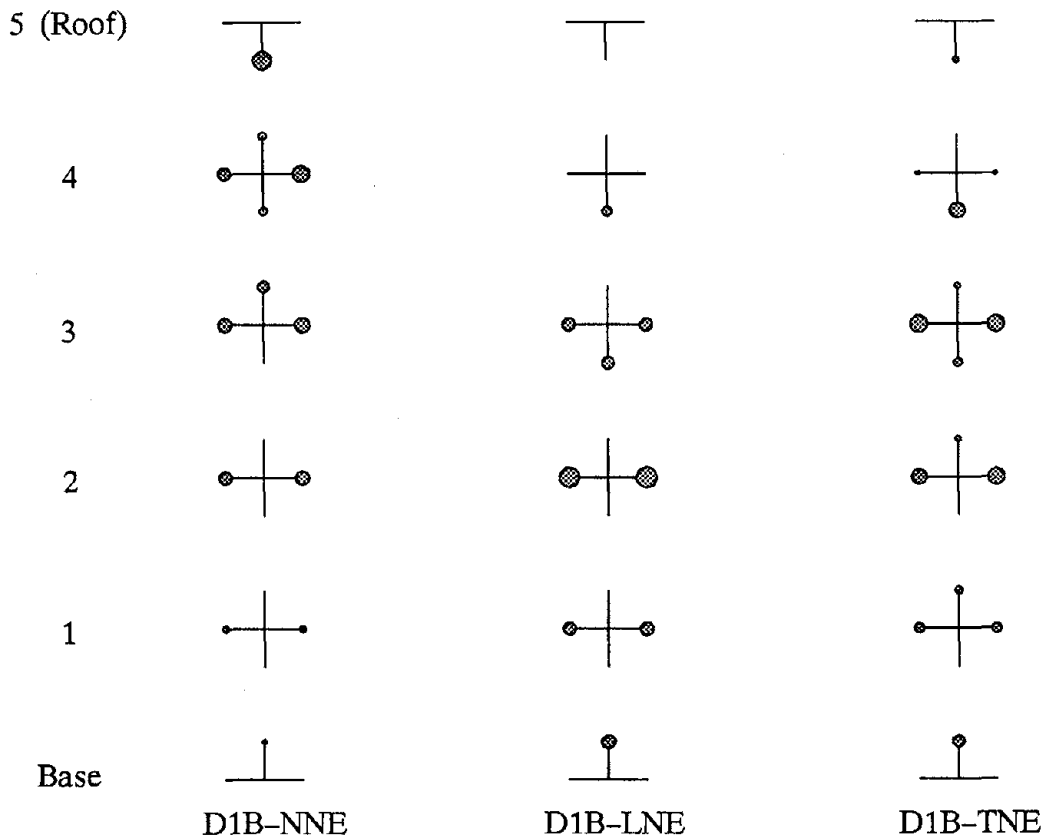


FIGURE 4.19b Hysteretic Energy Distributions for D1B Frame with Nonstructural Elements Subjected to El Centro



Note: Areas proportional to percentage of hysteretic energy dissipated at location.

FIGURE 4.19c Hysteretic Energy Locations for D1B Frame with Nonstructural Elements Subjected to El Centro

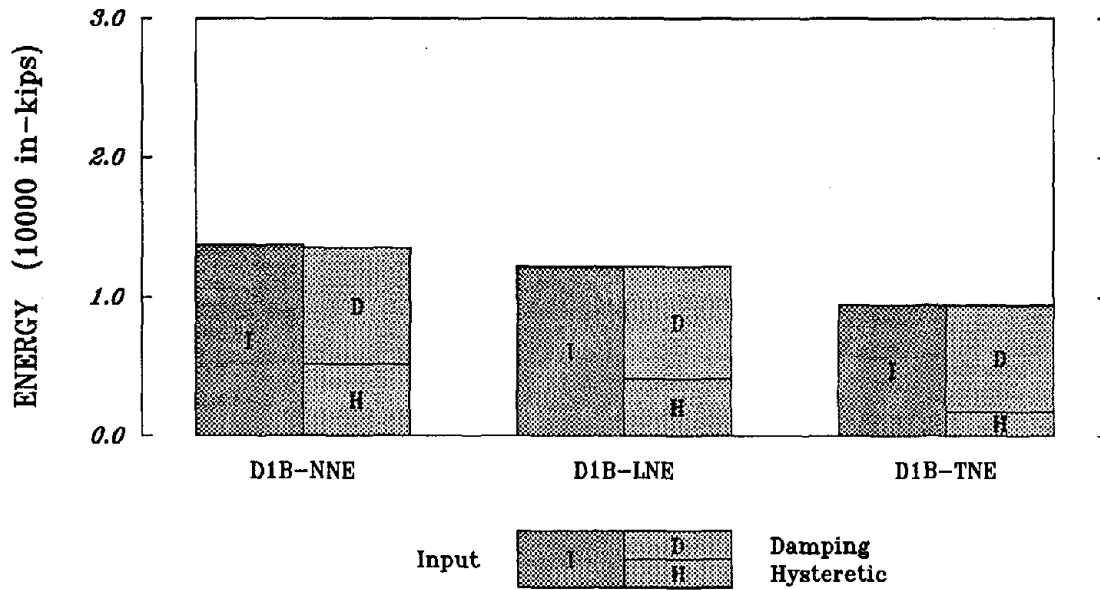


FIGURE 4.20a Cumulative Energy Quantities for D1B Frame with Nonstructural Elements Subjected to Parkfield

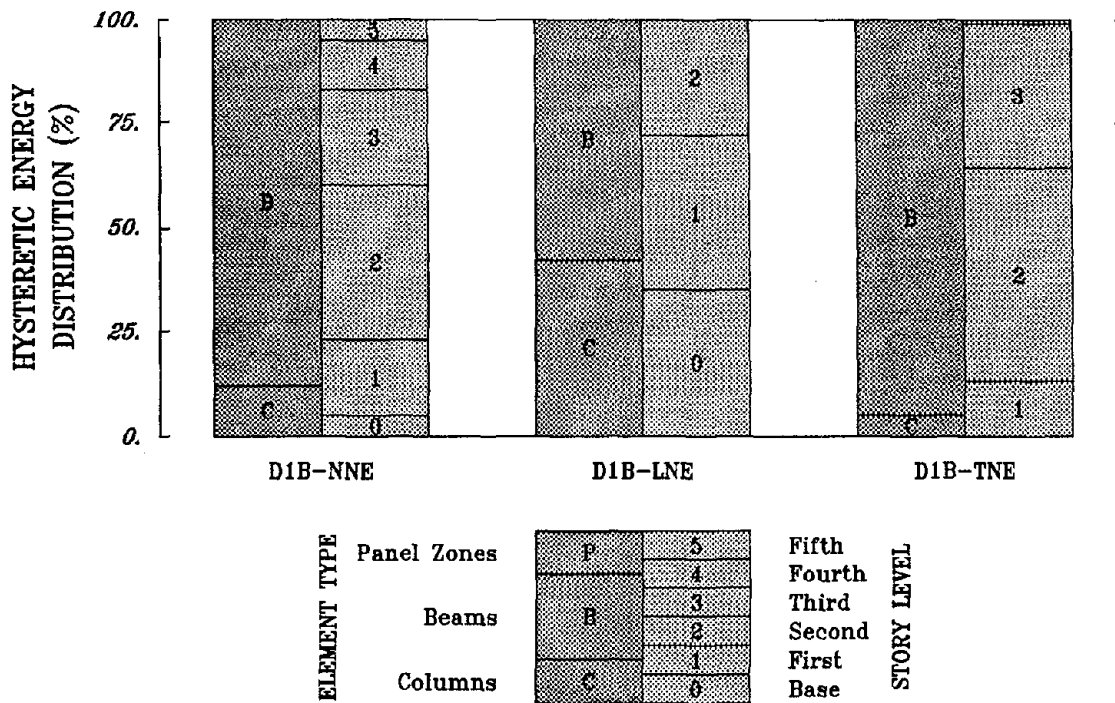
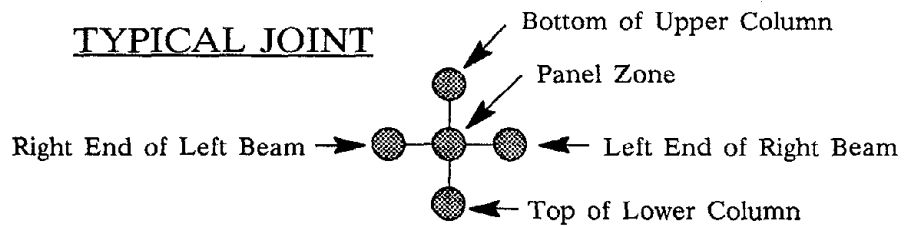
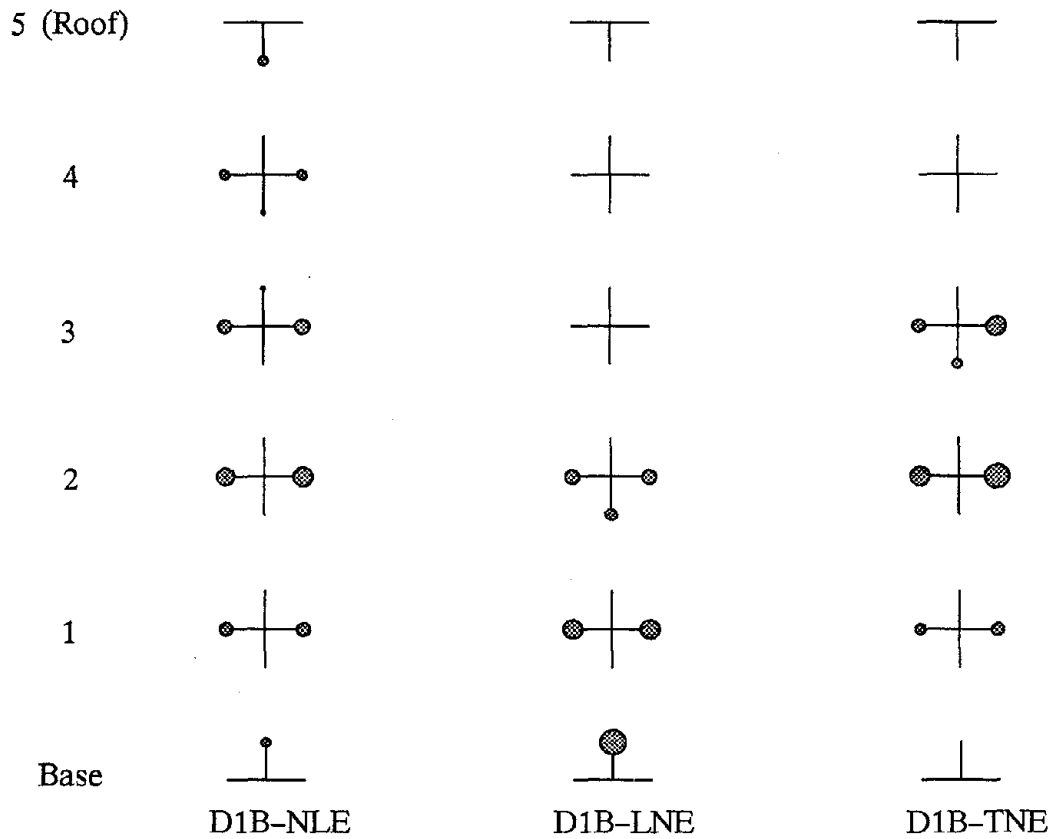


FIGURE 4.20b Hysteretic Energy Distributions for D1B Frame with Nonstructural Elements Subjected to Parkfield



Note: Areas proportional to percentage of hysteretic energy dissipated at location.

FIGURE 4.20c Hysteretic Energy Locations for D1B Frame with Nonstructural Elements Subjected to Parkfield

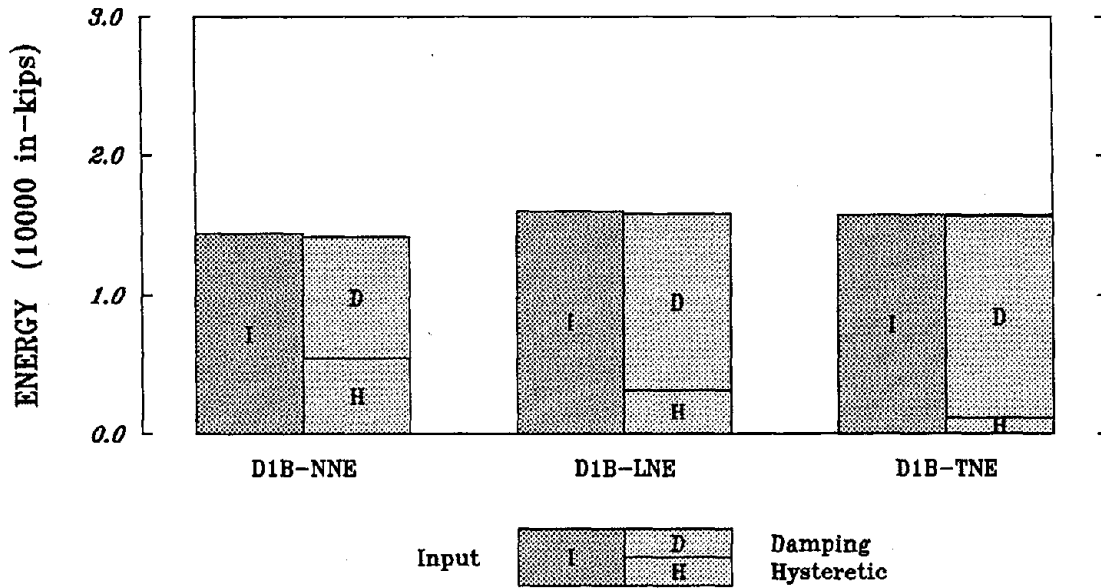


FIGURE 4.21a Cumulative Energy Quantities for D1B Frame with Nonstructural Elements Subjected to Taft

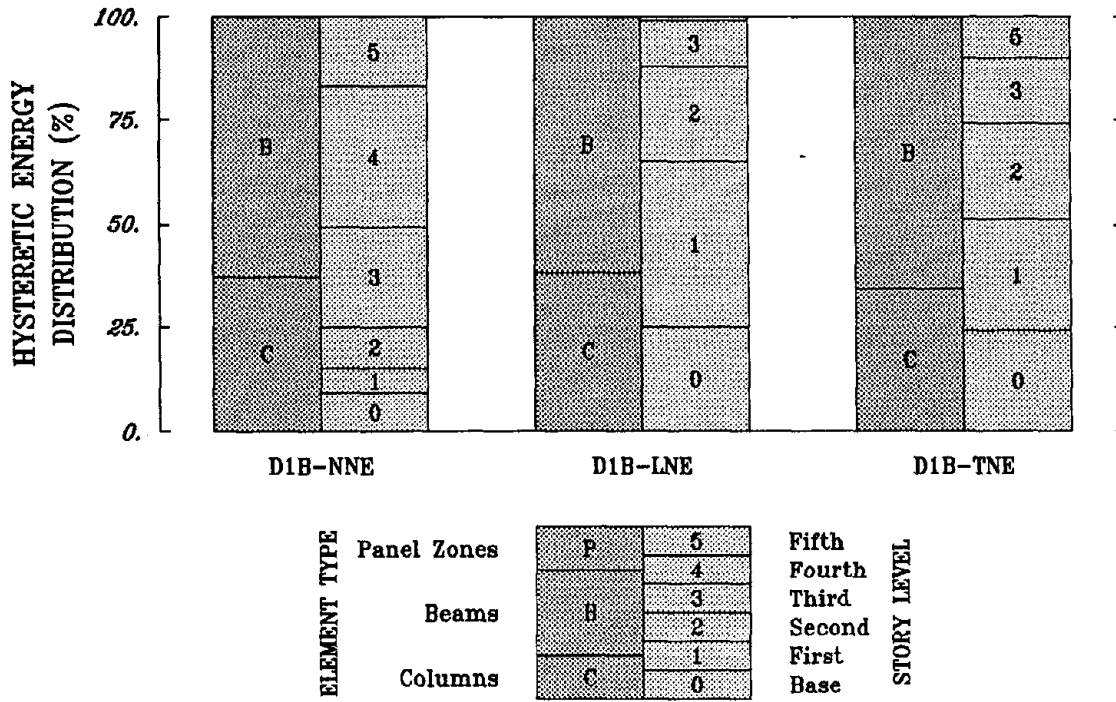
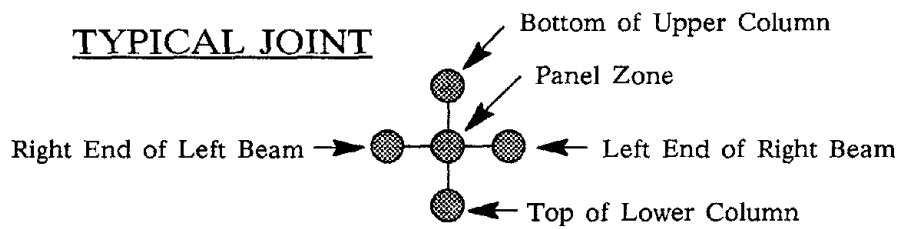
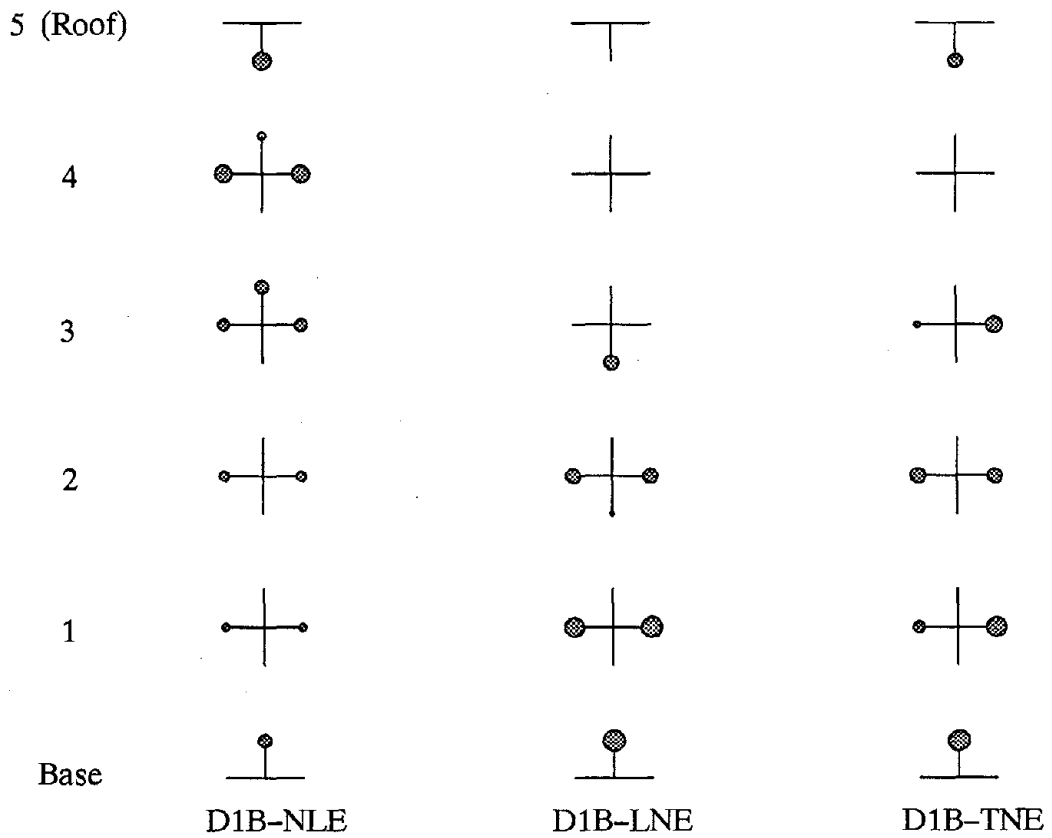


FIGURE 4.21b Hysteretic Energy Distributions for D1B Frame with Nonstructural Elements Subjected to Taft



Note: Areas proportional to percentage of hysteretic energy dissipated at location.

FIGURE 4.21c Hysteretic Energy Locations for D1B Frame with Nonstructural Elements Subjected to Taft



#### 4.4.4 Investigation of Frame Configuration

The calculation for the design base shear used in the direct design procedure is independent of the configuration selected for the lateral force-resisting system of a particular building. Some factors influencing the selection of frame configuration are architectural considerations and open space requirements, and material, fabrication and erection costs. Three different frame configurations for a five-story structure were studied to determine the influence on the inelastic response from severe ground excitation. One frame configuration for this building, designated D2A, had six 18-foot bays in the lateral force-resisting frame to resist lateral forces and stabilize the building (see Figures 2.3 and 2.4). Another frame configuration choice for this building, designated D2B, had five 28.8-foot bays to resist lateral forces (see Figures 2.5 and 2.6). The final selection of a frame configuration for this building, designated D2C, was the same as the D2B frame except that only one of the bays resisted lateral forces (see Figures 2.5 and 2.7).

The same criteria were used in the direct design procedure for each frame configuration. Since the overall building height, story heights and story weights of each frame configuration were the same, the design base shear and distribution of design base shear were identical for each frame. Although, the equivalent lateral forces and allowable story drifts were the same for each frame, the lateral stiffness and especially the strength of the three frames were different because of the requirements for satisfying the provisions of the 1988 UBC. The objective of reconfiguring the lateral force-resisting frames was a reduction in the number of moment-resisting connections and in the total number of members for the columns and beams.

These reductions generally will result in a more economical structure and are becoming a prevalent trend for many structural engineers in California.

The time histories of first story drift, shown in Figure 4.22, were quite similar, except for vertical shifting of the traces during unloading at peak displacements. The lateral strengths of the stories for each of the frame configurations were not the same because the frame designs were based on allowable stresses which are determined from the effective lengths of the members in a frame. In addition, the ability to match closely the stiffness and strength requirements was dependent on the available rolled I-sections. Therefore, the strengths of a story for each of the frame configurations were different even though the design story shear for that story was the same. The frequency content of first story drift traces associated with each earthquake record is similar, since the fundamental period of vibration for the different frame configurations was nearly the same as a result of drift controlling the design of each frame.

The shear-drift histories for the first story of the three frame configurations are plotted in Figures 4.23, 4.24 and 4.25 from each of the earthquakes. As evident by the maximum height of the hysteresis loops, the first story of the D2B frame had more elastic strength than the other two frame configurations, while the D2C frame had the least elastic strength. In addition, the slope of the elastic portion of the hysteresis loops is nearly the same since drift controlled the frame designs. The inelastic deformation of the first story generally increased as the yield level of the story decreased, since the elastic stiffness of each frame configuration was roughly the same. The Parkfield accelerogram caused considerable permanent deformation in the first story of the D2A and D2C frame models.

The story drift and shear envelopes given in Figure 4.26 had similar shapes for the maximum response values obtained from each earthquake. In all three frames, the sections used for the columns and beams changed between the third and fourth stories. Thus, the conservatism as a result of using stiffer and stronger sections than required for a story followed the same pattern for each of the frames. This is probably the main reason why the story drifts jumped between the third and fourth stories. The stories that had large drifts in one model usually had large drifts in the other models. The D2C frame design generally had larger story drifts and smaller story shears than the other two frame designs as a result of the smaller yield strength. In fact, the strength of a story in the D2B frame was sometimes thirty percent larger than the same story of the D2C frame. The El Centro accelerogram produced story drifts in the lower stories that were smaller than the maximum expected story drifts by the 1988 UBC, but the drifts in the upper two stories were larger than expected. The story drifts from the Parkfield record generally were larger than the maximum expected drifts. The Taft accelerogram produced fairly even story drifts through the height of the frame which were right around the maximum expected.

The total input energy quantities and distribution thereof are shown in Figures 4.27a, 4.28a and 4.29a for each earthquake. The input energy levels for each earthquake were within five percent of each other. The D2C frame experienced larger inelastic excursions, which made up for the difference between the yield levels of the frames. The distributions of hysteretic energy, given in Figures 4.27b, 4.28b and 4.29b, were different for each earthquake. However in each of the analyses, a disproportional amount of hysteretic energy was dissipated at the base of the first story column. The

locations for hysteretic energy dissipation are given in Figures 4.27c, 4.28c and 4.29c. The nonuniform distribution over the height of the frame for hysteretic energy dissipation, especially from the Taft record, was clearly indicated in these figures.

The advantage of the D2B frame configuration over the D2A frame was both a reduction in moment-resisting connections and members. The advantage of the D2C frame over the D2B frame was a further reduction in the number of moment-resisting connections. Because the bay spacings were longer in the D2B frame design than in the D2A frame, the effective length of the columns also increased in the D2B frame as a result of the more flexible joints. Therefore, the reduction in allowable stresses for the columns in the D2B frame decreased the material efficiency of the sections. In fact, the total weight of the D2B frame was greater than the D2A frame, even though the total length of the columns in the D2A frame was greater.

One interesting aspect from this parametric study was that the total energy levels were nearly identical for each of the frame configurations as were the distributions by stories, even though the load-deformation behavior for each frame was unique. The frame with the smallest yield strengths experienced the largest inelastic deformations in order to dissipate the same amount of hysteretic energy. One disadvantage the reduction in the number of moment-resisting connections is that fewer locations exist for dissipating hysteretic energy, especially when the same amount of hysteretic energy needs to be dissipated. This increases greatly the possibility of connection failure by low-cycle fatigue, since the frames with fewer connections and members are forced to dissipate more energy at each available location.

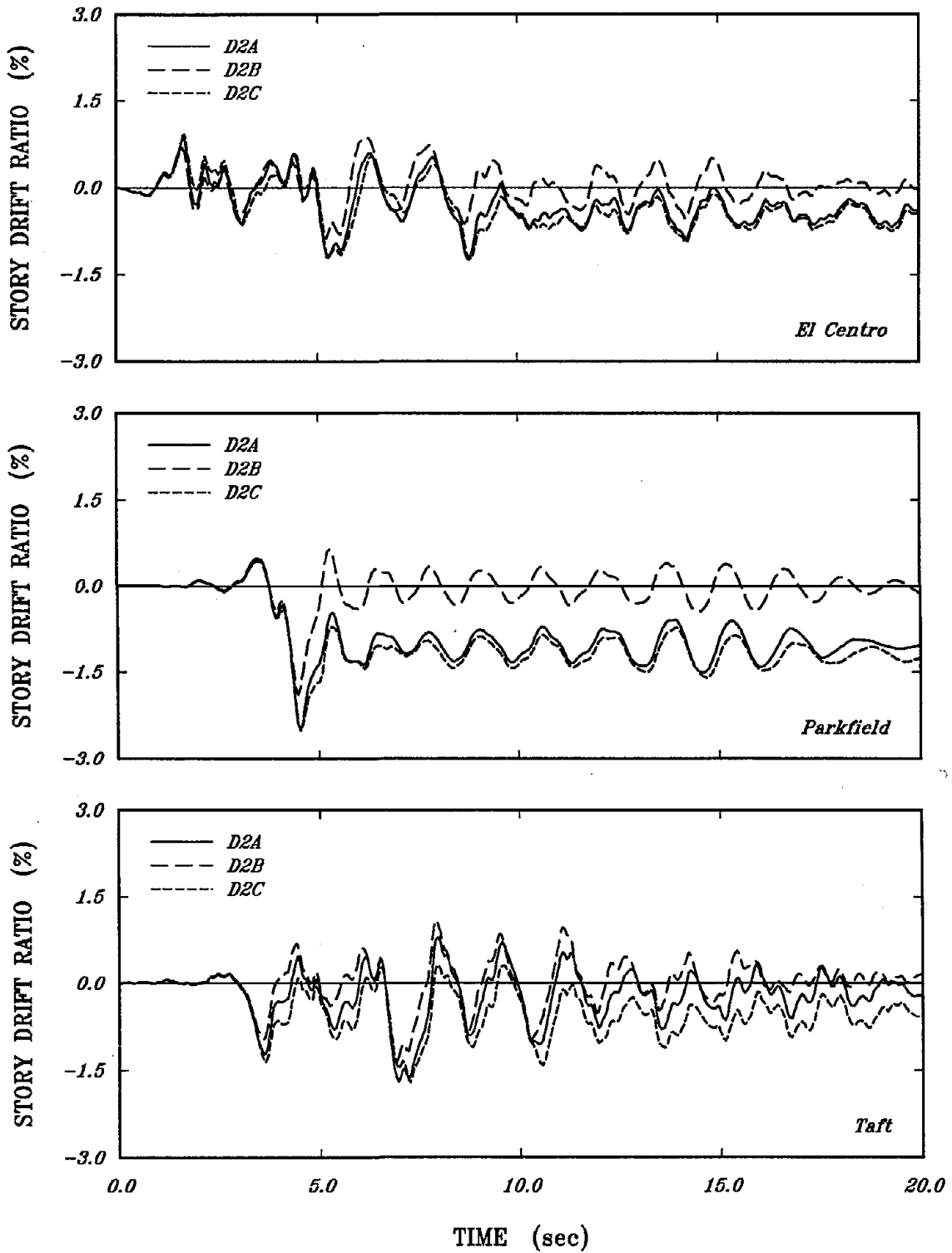


FIGURE 4.22 Drift-Time Histories of First Story for D2A, D2B and D2C Frames Subjected to Three Earthquakes

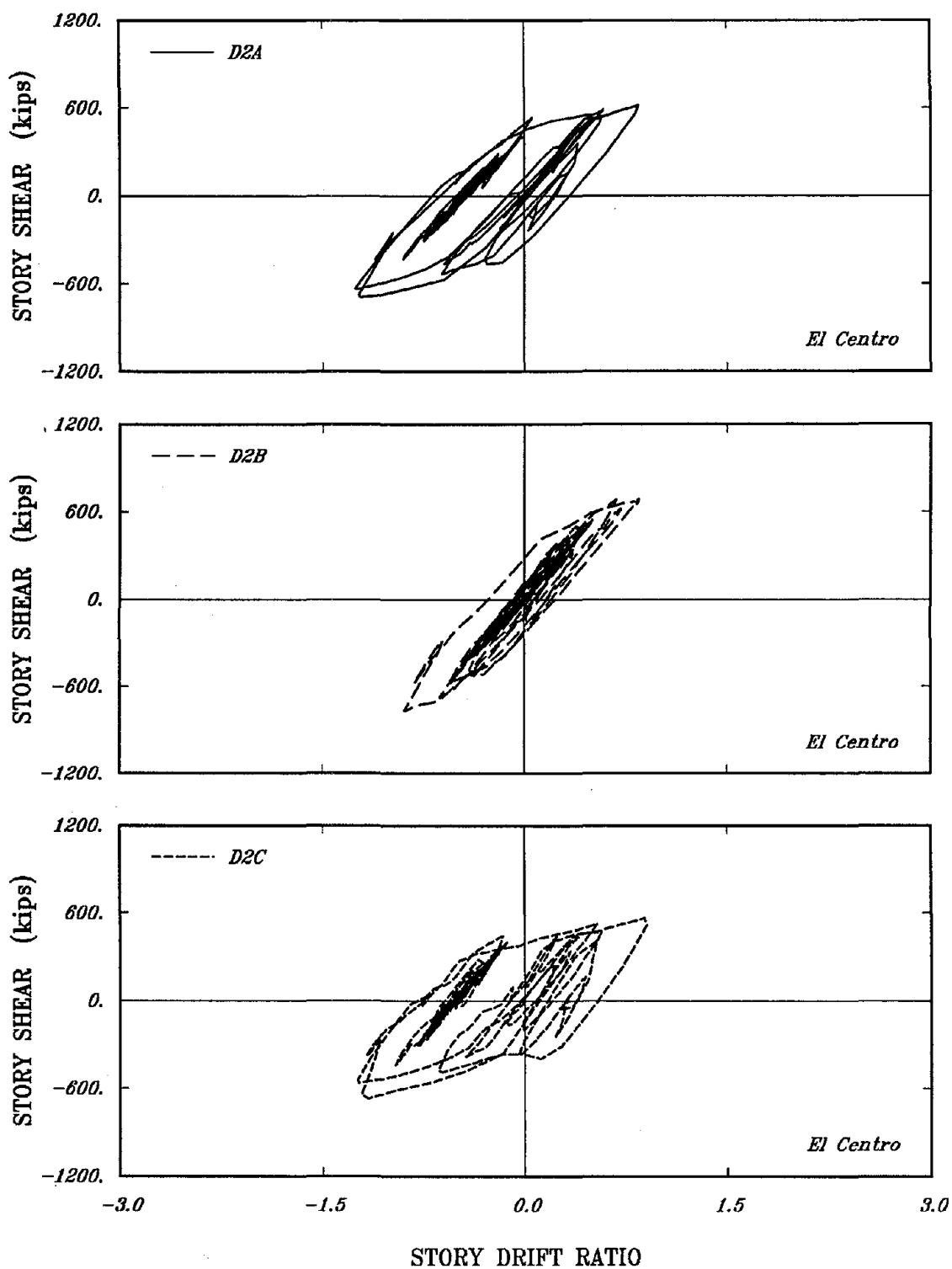


FIGURE 4.23 Shear-Drift Histories of First Story for D2A, D2B and D2C Frames Subjected to El Centro

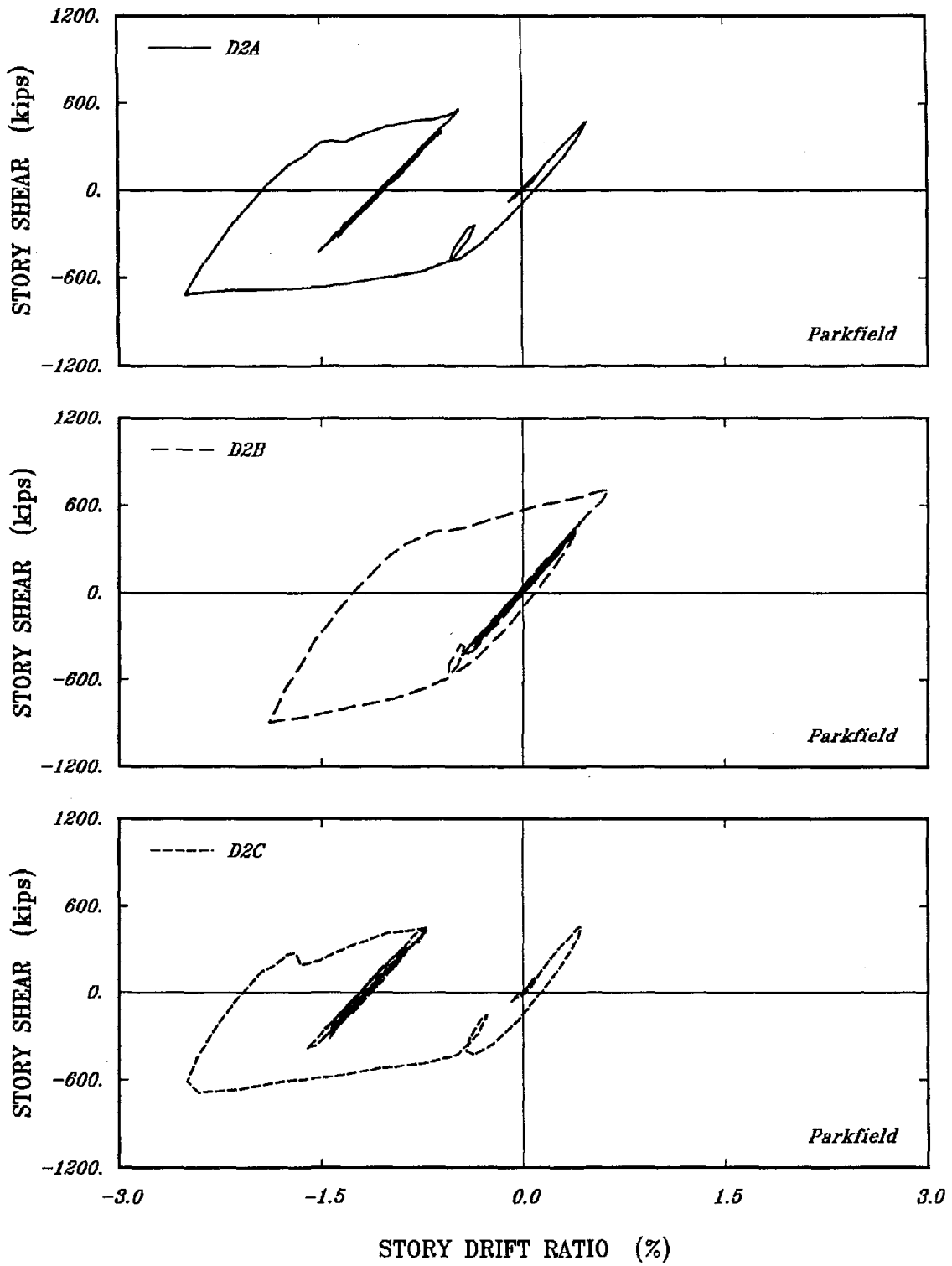


FIGURE 4.24 Shear-Drift Histories of First Story for D2A, D2B and D2C Frames Subjected to Parkfield

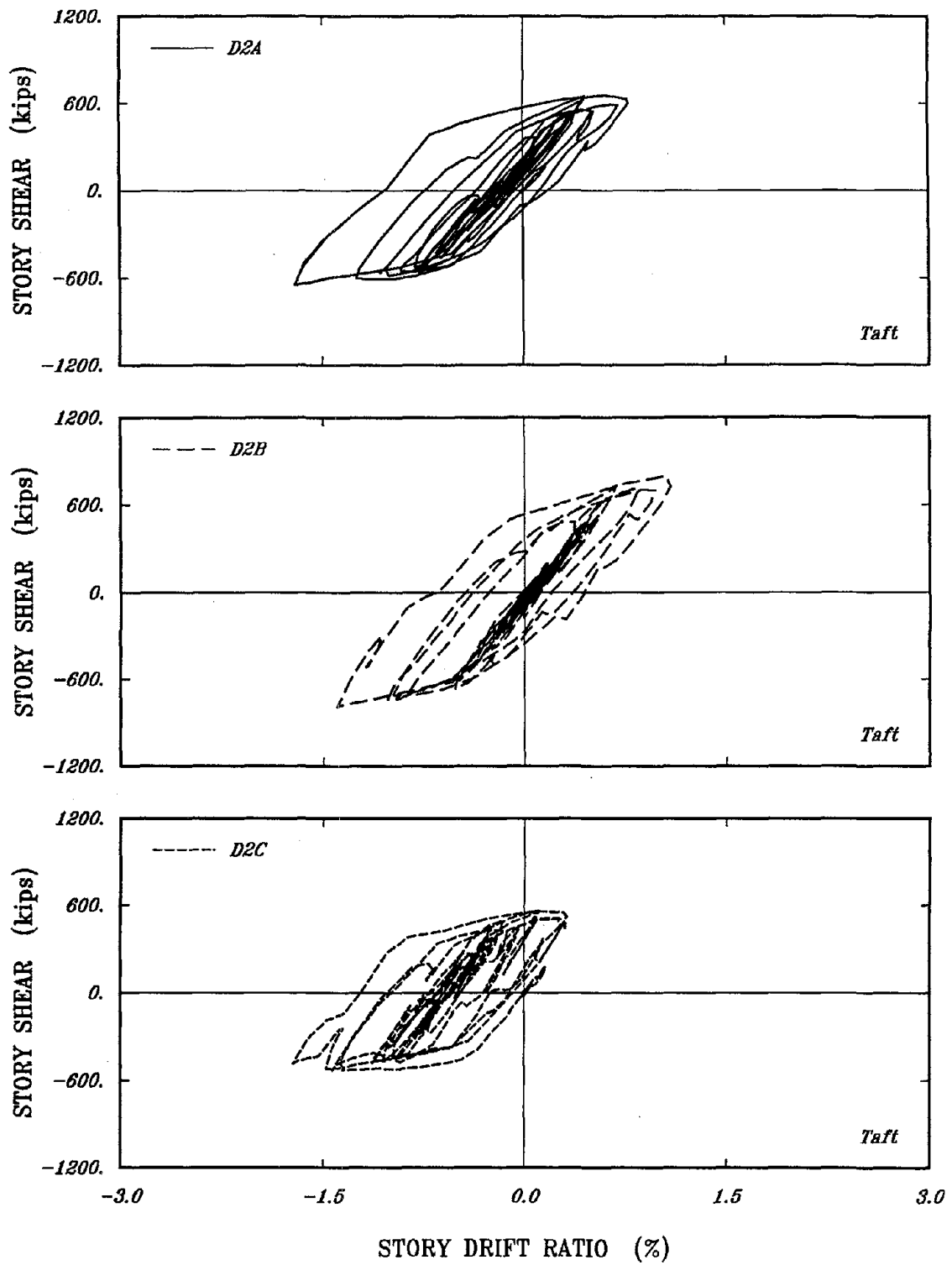


FIGURE 4.25 Shear-Drift Histories of First Story for D2A, D2B and D2C Frames Subjected to Taft



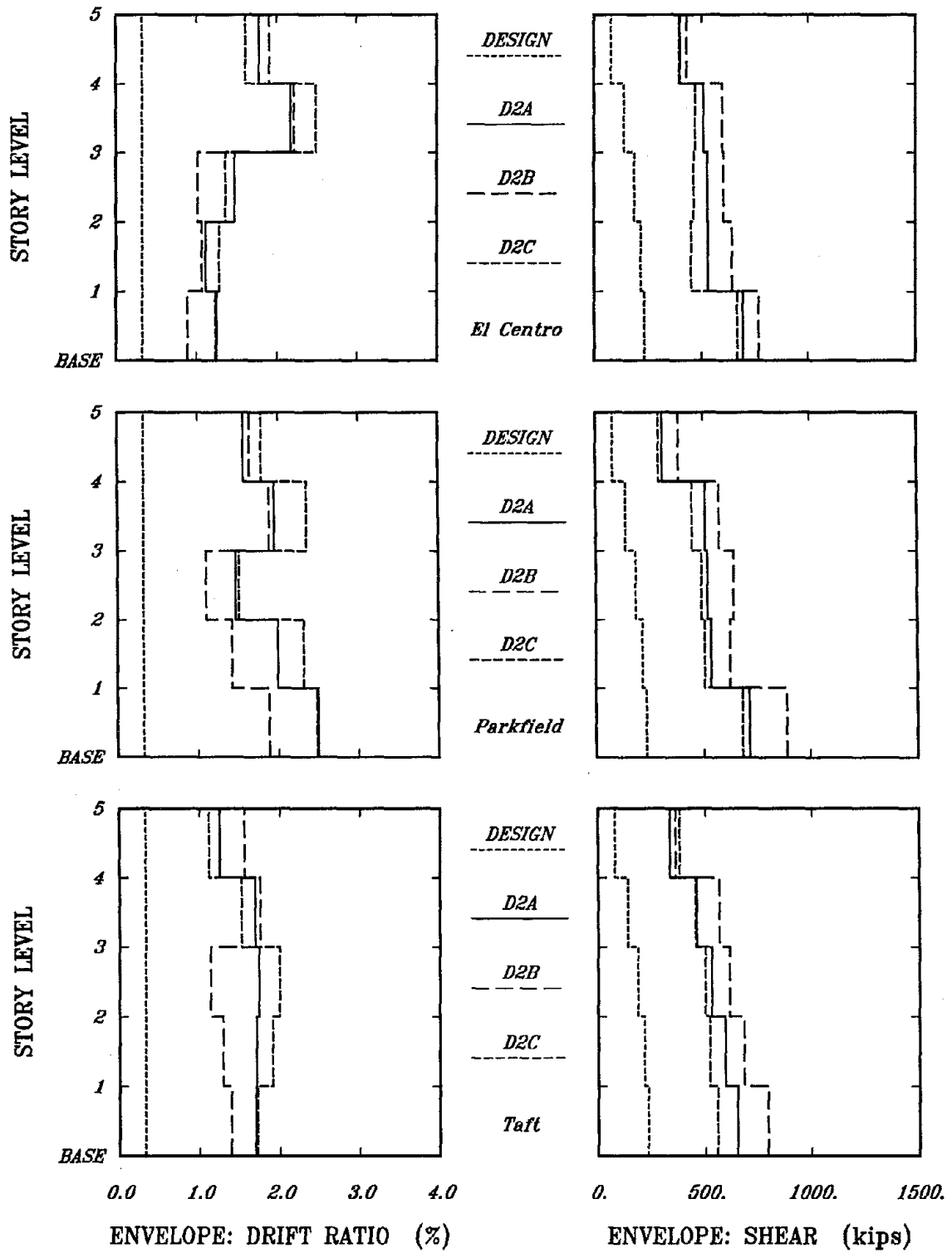


FIGURE 4.26 Story Drift and Shear Envelopes for D2A, D2B and D2C Frames Subjected to Three Earthquakes

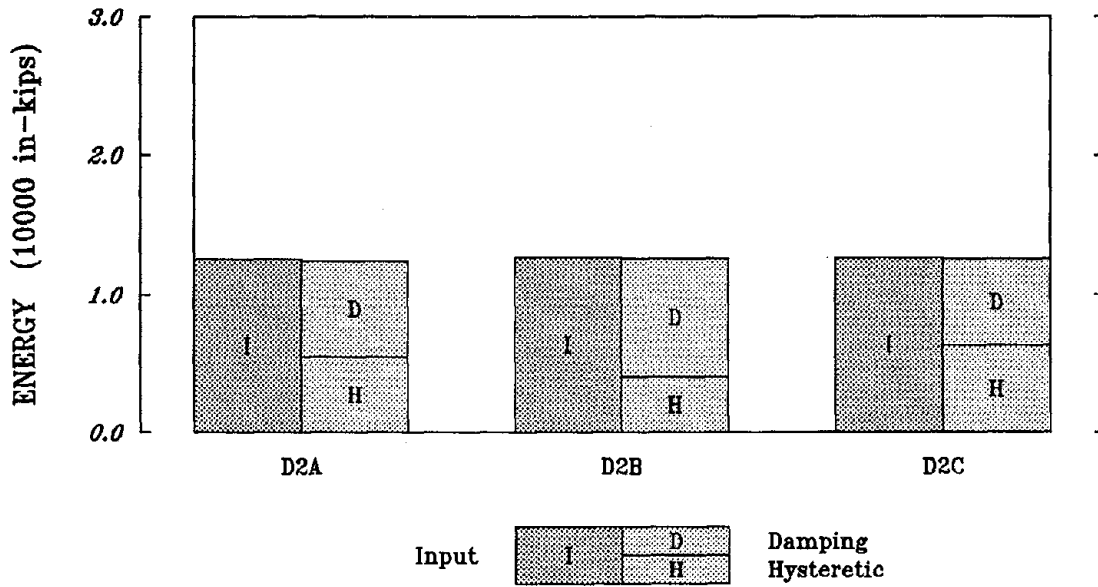


FIGURE 4.27a Cumulative Energy Quantities for D2A, D2B and D2C Frames Subjected to El Centro

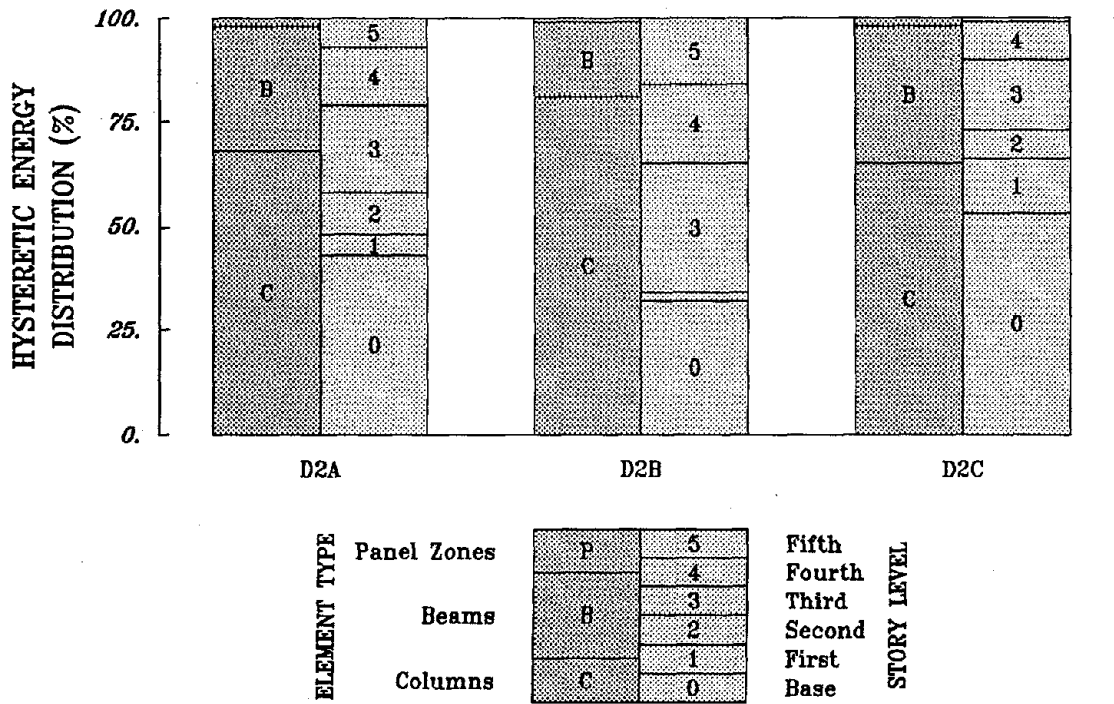
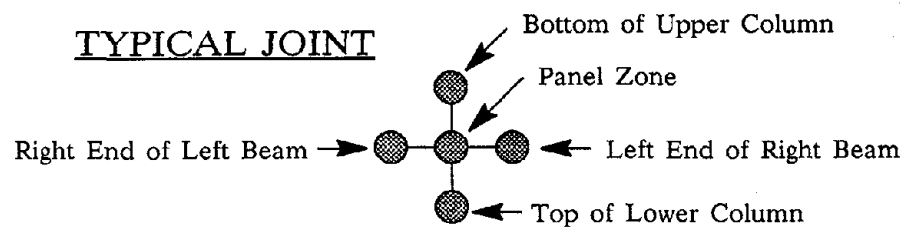
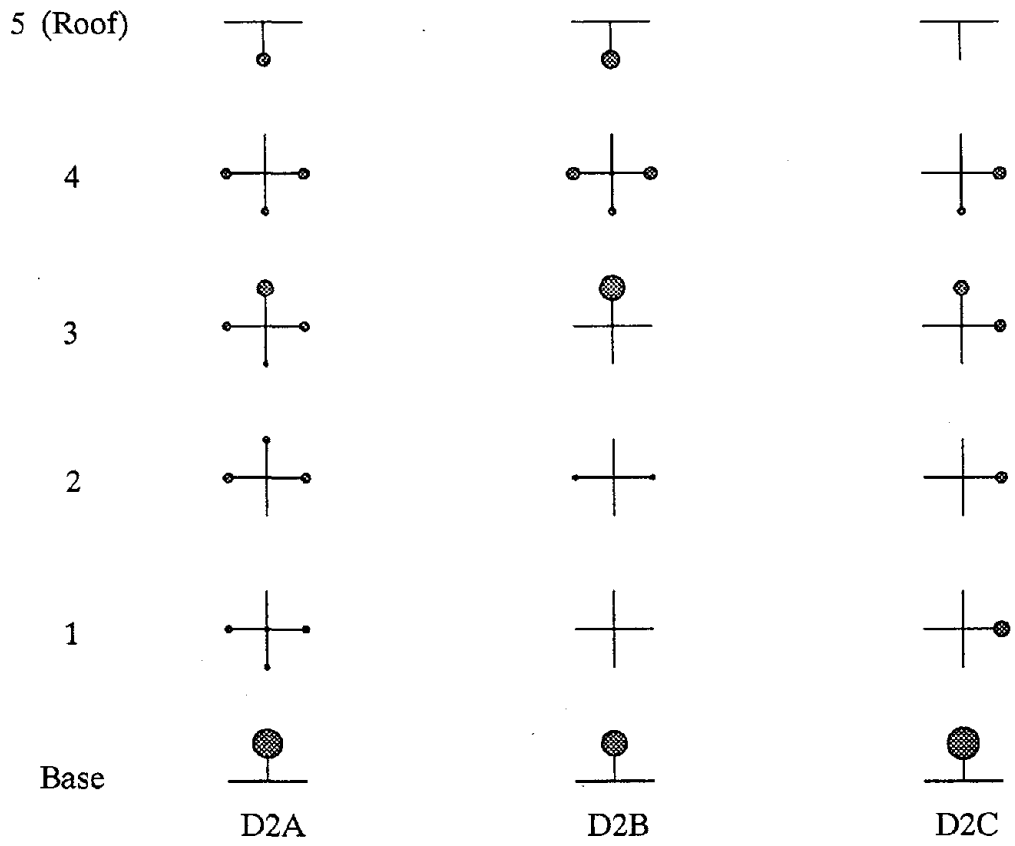


FIGURE 4.27b Hysteretic Energy Distributions for D2A, D2B and D2C Frames Subjected to El Centro



Note: Areas proportional to percentage of hysteretic energy dissipated at location.

FIGURE 4.27c Hysteretic Energy Locations for D2A, D2B and D2C Frames Subjected to El Centro

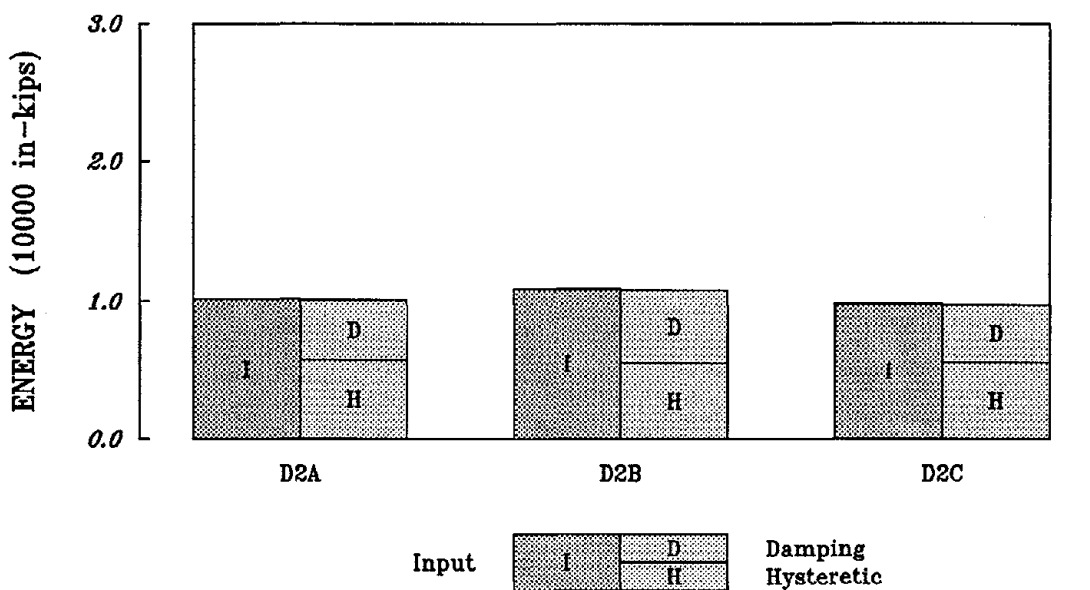


FIGURE 4.28a Cumulative Energy Quantities for D2A, D2B and D2C Frames Subjected to Parkfield

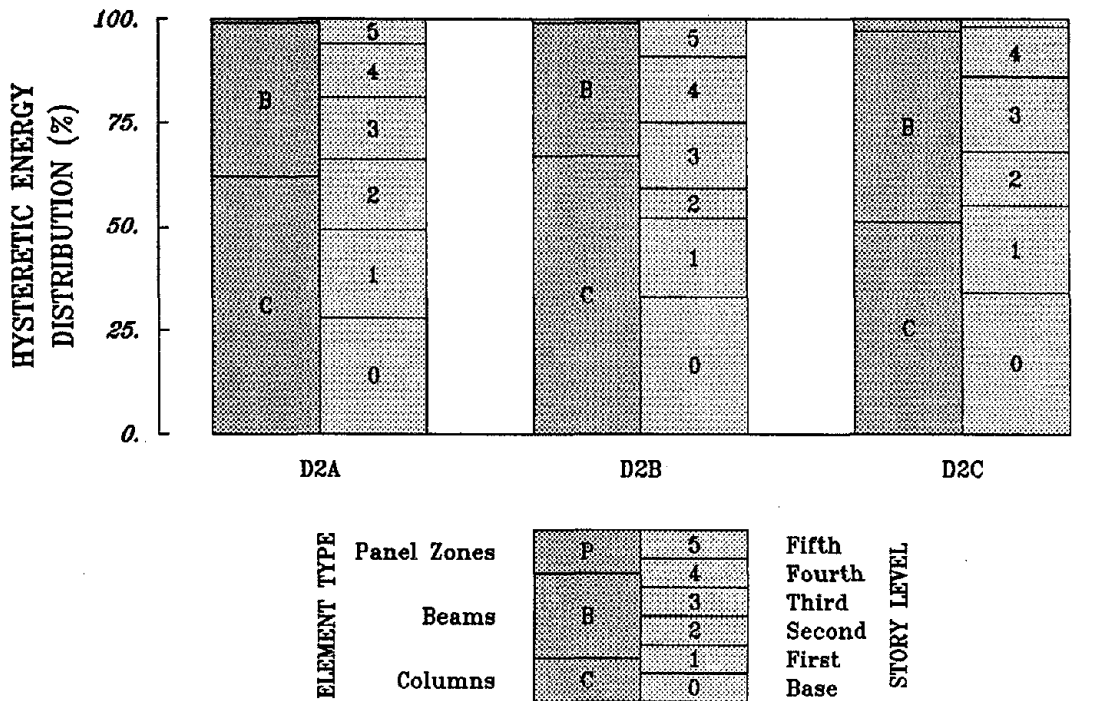
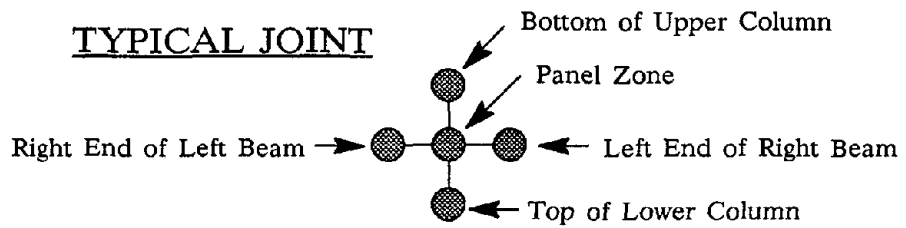
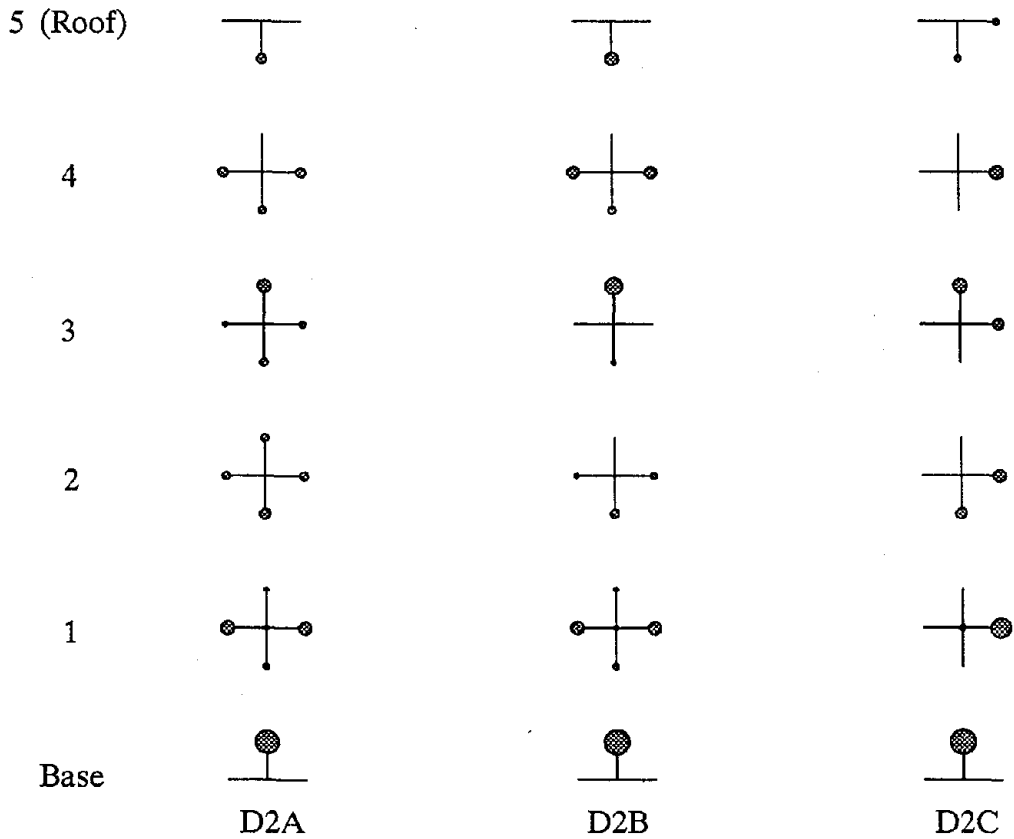


FIGURE 4.28b Hysteretic Energy Distributions for D2A, D2B and D2C Frames Subjected to Parkfield



Note: Areas proportional to percentage of hysteretic energy dissipated at location.

FIGURE 4.28c Hysteretic Energy Locations for D2A, D2B and D2C Frames Subjected to Parkfield

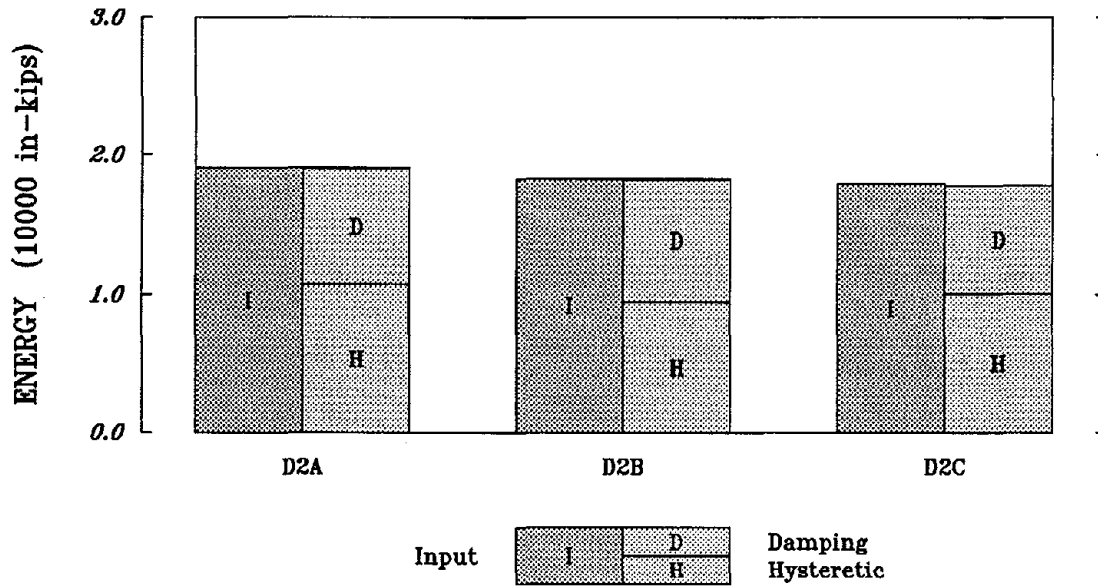


FIGURE 4.29a Cumulative Energy Quantities for D2A, D2B and D2C Frames Subjected to Taft

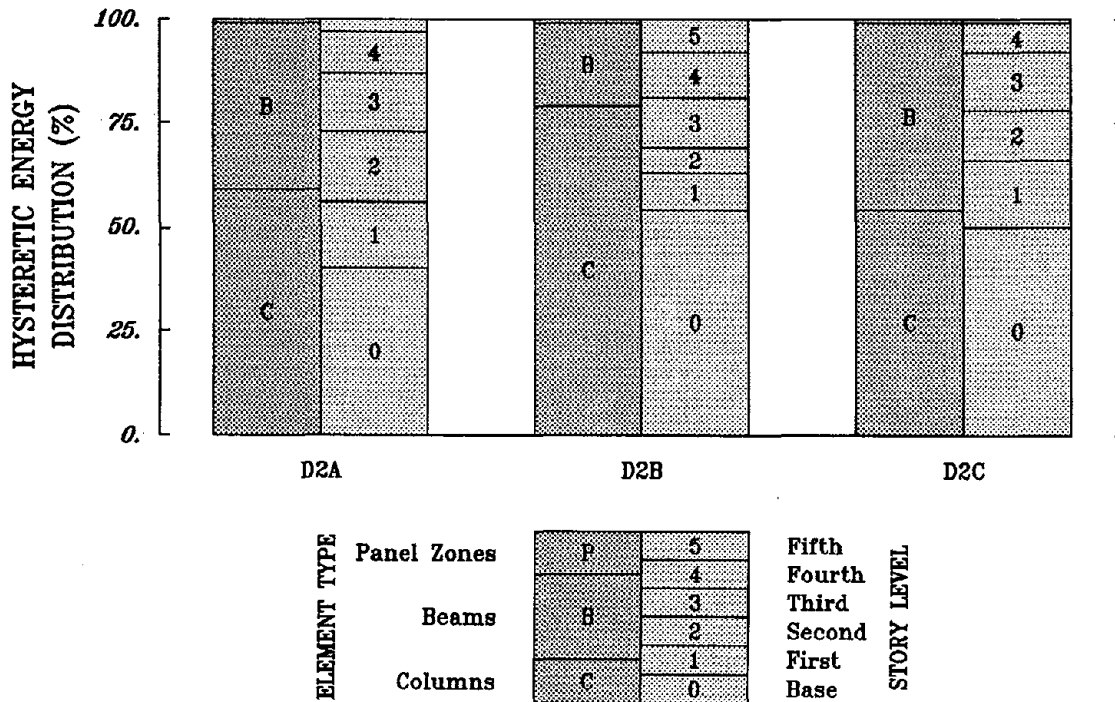
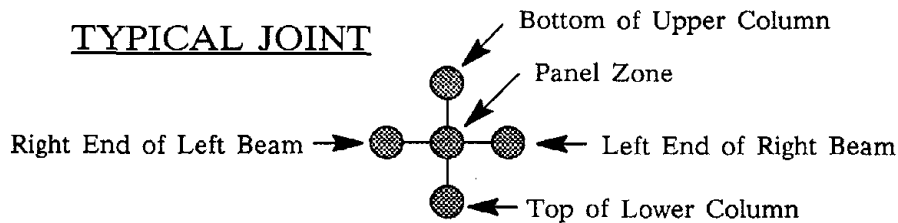
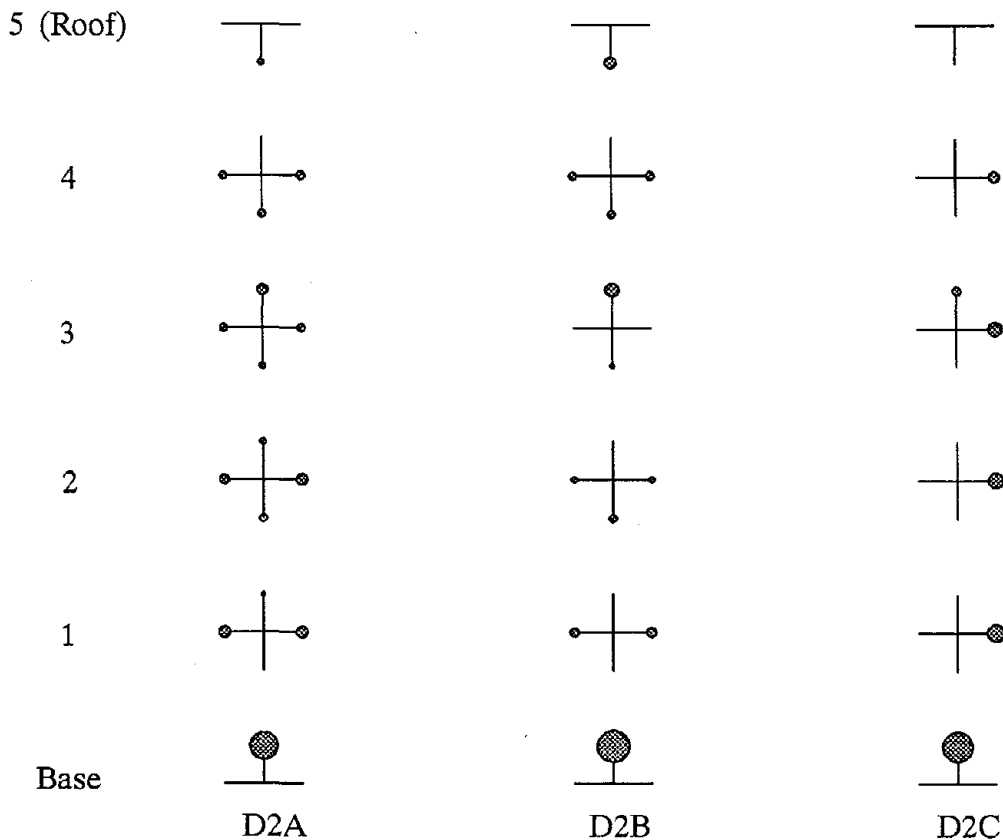


FIGURE 4.29b Hysteretic Energy Distributions for D2A, D2B and D2C Frames Subjected to Taft



Note: Areas proportional to percentage of hysteretic energy dissipated at location.

FIGURE 4.29c Hysteretic Energy Locations for D2A, D2B and D2C Frames Subjected to Taft

#### 4.4.5 Investigation of Design Base Shear and P-Delta

The design base shear for a frame can be significantly different depending on the provisions followed in the direct design procedure of the 1988 edition of the *Uniform Building Code*. The design base shear for the D1B frame design, which had six 18-foot bays, was related to the absolute maximum value required by the code. The D2A frame design, which had the same configuration as the D1B frame design, had a design base shear based on the estimated fundamental period of the structure. The code also allows the design process to be "recycled" by using a better approximation for the fundamental period - generally the fundamental period of the structure from a trial design is used. The better approximation generally will result in a longer fundamental period, which will lead to a smaller design base shear. The response of the D2C frame design, which had a single 28.8-foot bay providing lateral resistance in the perimeter moment-resisting frame, was compared to the response of the D3 frame design, which had a design base shear established from the calculated fundamental period of the D2C frame.

In addition to the comparisons between the calculated responses of the two sets of frame designs with different design base shear, the P-Delta effects and participation of nonstructural elements also were studied for frames of different stiffness and strength. The design base shear is directly related to the required lateral stiffness and strength of a frame. Therefore, the usage of a smaller design base shear produces more flexible and weaker frame design. If the "response" spectra for an earthquake was uniform over the range of natural frequencies corresponding to the dominate modes of frame models based on different design base shears, the inelastic response of a frame model would increase as the design base shear decreased.



Comparisons of the time histories of the first story drift for the D1B and D2A frame models are shown in Figure 4.30. The time histories for each earthquake accelerogram were different, although the same general trends appeared in the traces for the excitation arising from each accelerogram. The P-Delta effects are shown in Figure 4.31 for the D1B frame model and in Figure 4.32 for the D2A frame model. The P-Delta effects in the D1B frame model were hardly perceivable. However as the story drifts increased as in the D2A frame model, the P-Delta effects gave rise to vertical shifting of the time histories.

The story shear-drift histories for the first stories of the D1B and D2A frame designs are given in Figure 4.33. The elastic strength, as indicated by the height of the hysteresis loops, of the D1B frame design was around fifty percent greater. The amount of inelastic deformation increased considerably in the first story as the design base shear was reduced and in some cases lead to sizeable permanent deformations.

The story drift and shear envelopes for the maximum response are given in Figure 4.34. The shape of the story drift envelopes associated with each earthquake tended to be different for the D1B and D2A models, but the same general shape existed between a model with and without P-Delta effects. In addition, the story drifts for the D2A frame design generally exceeded the expected inelastic drifts of one and a half percent of the story height. In fact, story drifts exceeded two percent for several locations and even reached two and a half percent for the first story drift under the Parkfield excitation. The story shear envelopes were almost identical for the frame models with and without P-Delta effects. However as expected, the maximum story shears for the D1B frame were larger than the D2A frame.

The total input energy quantities and distribution thereof, given in Figure 4.35a, corresponding to the El Centro and Parkfield accelerograms were larger for the D1B frame design, while the input energy corresponding to the Taft accelerogram was larger for the D2A frame design. In all cases, the hysteretic energy levels were larger for the D2A frame design even though this structure was not as strong as the D1B frame. This was a reflection of the much larger story drifts experienced by the D2A frame as previously mentioned. The hysteretic energy distributions are shown in Figure 4.35b. The D1B frame design dissipated most of the hysteretic energy in the upper stories, while the D2A frame design dissipated a large percentage of energy in the base and a fairly uniform amount in the upper stories. This same information is conveyed in Figure 4.35c.

The comparisons of the time histories for the first story drift for the D2C and D3 frame models are shown in Figure 4.36 and for the D2C and D3 frame models with nonstructural elements are shown in Figure 4.37. The same modeling of the nonstructural elements was used for both frame models. The differences between the traces were greater for the frame models without nonstructural elements because the addition of nonstructural elements tended to lessen the difference between the stiffness and strength of the D2C and D3 frame models.

The story shear-drift histories for the first story are given in Figures 4.38 and 4.38 for the frame models with and without nonstructural elements. The first story of the D3 frame had larger inelastic deformations than the first story of the D2C frame. However, the inelastic deformations of the first story of the D3-TNE frame were not necessarily larger than the D2C-TNE frame as a result of the interaction between the structure and the

ground motion. In fact, the permanent deformations for the D2C and D3 frame models were in the opposite direction as the frame models with nonstructural elements.

The maximum response quantities plotted in the story drift and shear envelopes, shown in Figure 4.40, were surprising in that the story shears were much more uniform over the height of the structure than the story drifts. Many of the story drifts exceeded by as much as twice the expected inelastic drifts of one and a half percent of the story height. In general, the addition of nonstructural elements significantly reduced the story drifts in the upper stories of the D3 frame because of the additional stiffness and strength. As evident by the maximum shear envelopes, the addition of nonstructural elements to the D3 frame increased the shear capacity beyond the capacity of the bare structural D2C frame, which was stronger than the D3 frame.

The total input energy quantities and distribution thereof are given in Figures 4.41a and 4.42a. The total input energies for the D2C and D3 frames subjected to each earthquake were fairly close, especially for the models with nonstructural elements. The amount of hysteretic energy dissipated with the addition of nonstructural elements, even though the addition of these elements increased the maximum story shears. The distributions of hysteretic energy are given in Figures 4.41b and 4.42b. The D3 frame had a more even distribution of hysteretic energy by stories than the D2C frame. As shown in Figure 4.41c, the locations of hysteretic energy dissipation for the D2C and D3 frame models were generally the same. The addition of the nonstructural elements forced the majority of hysteretic energy dissipation into the lower stories. In fact, at least fifty percent of the hysteretic

energy was dissipated as the base of the first story columns as shown in Figure 4.42c.

The results from this parametric study indicated that the level of inelastic response increased as the design base shear decreased. Some of the calculated story drifts for the most conservative frame design (D1B) approached the expected inelastic story drifts, but the calculated story drifts of the other frame designs repeatedly exceeded the expected story drifts. The expected story drifts of one and a half percent of the story height are quite large, but to have even larger story drifts would cause additional instability of structure and deformation incompatibilities. In addition, the frames that experienced larger than expected deformations may also undergo larger than desired deformations during a more moderate earthquake. The increased story drifts could lead to more nonstructural damage and possibly structural damage, which is to be avoided for a moderate earthquake.

The influence of P-Delta effects generally were not that significant. The inclusion of P-Delta effects caused more displacements towards the end of a large inelastic excursion. However, P-Delta effects also tended to oppose the motion of the structure as the structure returned back to the undisplaced configuration and, therefore, acted to slow the structure down. The inclusion of P-Delta effects should produce a more realistic calculated response, since the effect of P-Delta forces are actually present in the real structure under excitation. Fortunately, the approximation of P-Delta effects can easily be incorporated into a DRAIN-2D time-history analysis, although there may not be any significant differences in the calculated responses of models with and without P-Delta effects.

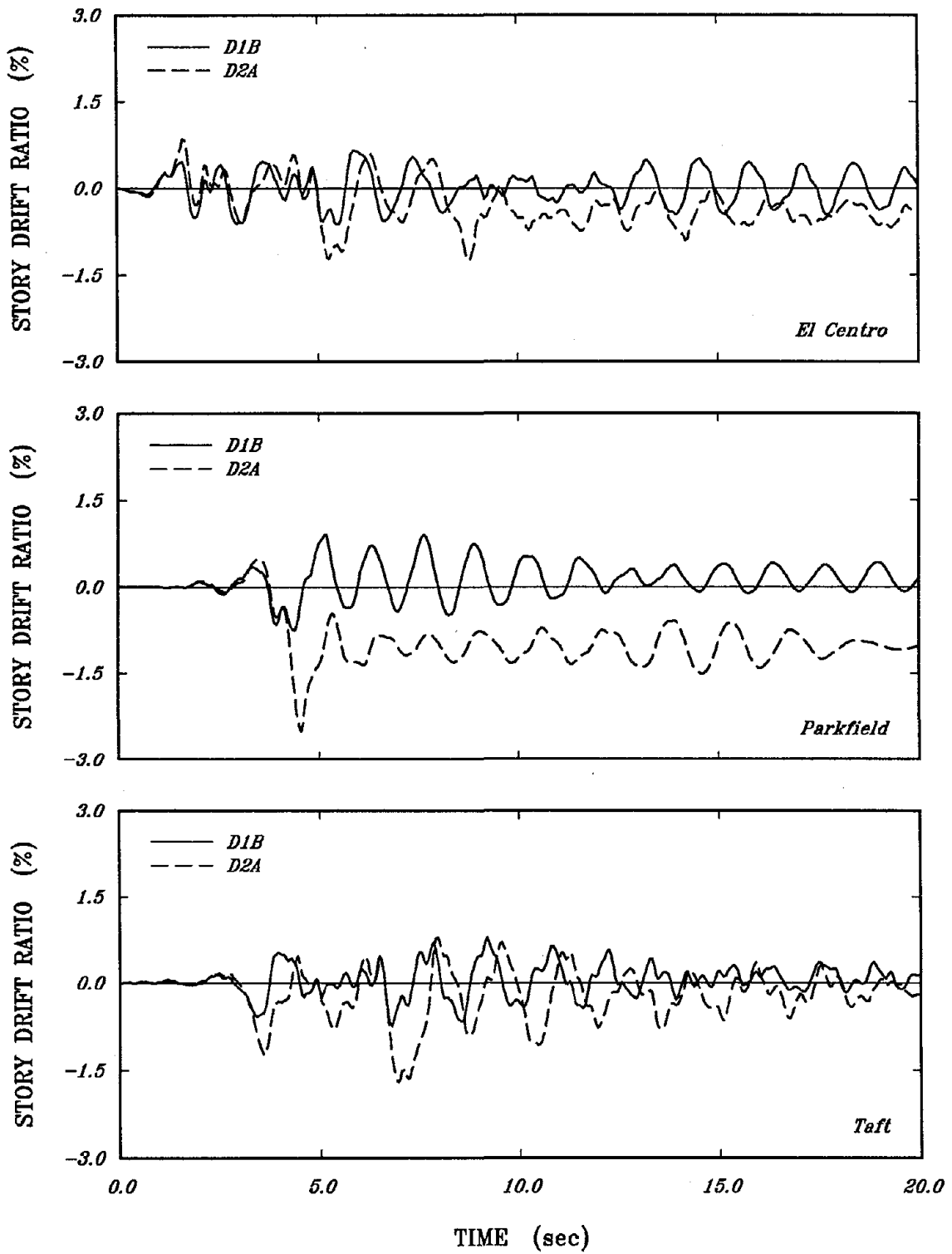


FIGURE 4.30 Drift-Time Histories of First Story for Similar Modelling of D1B and D2A Frames Subjected to Three Earthquakes

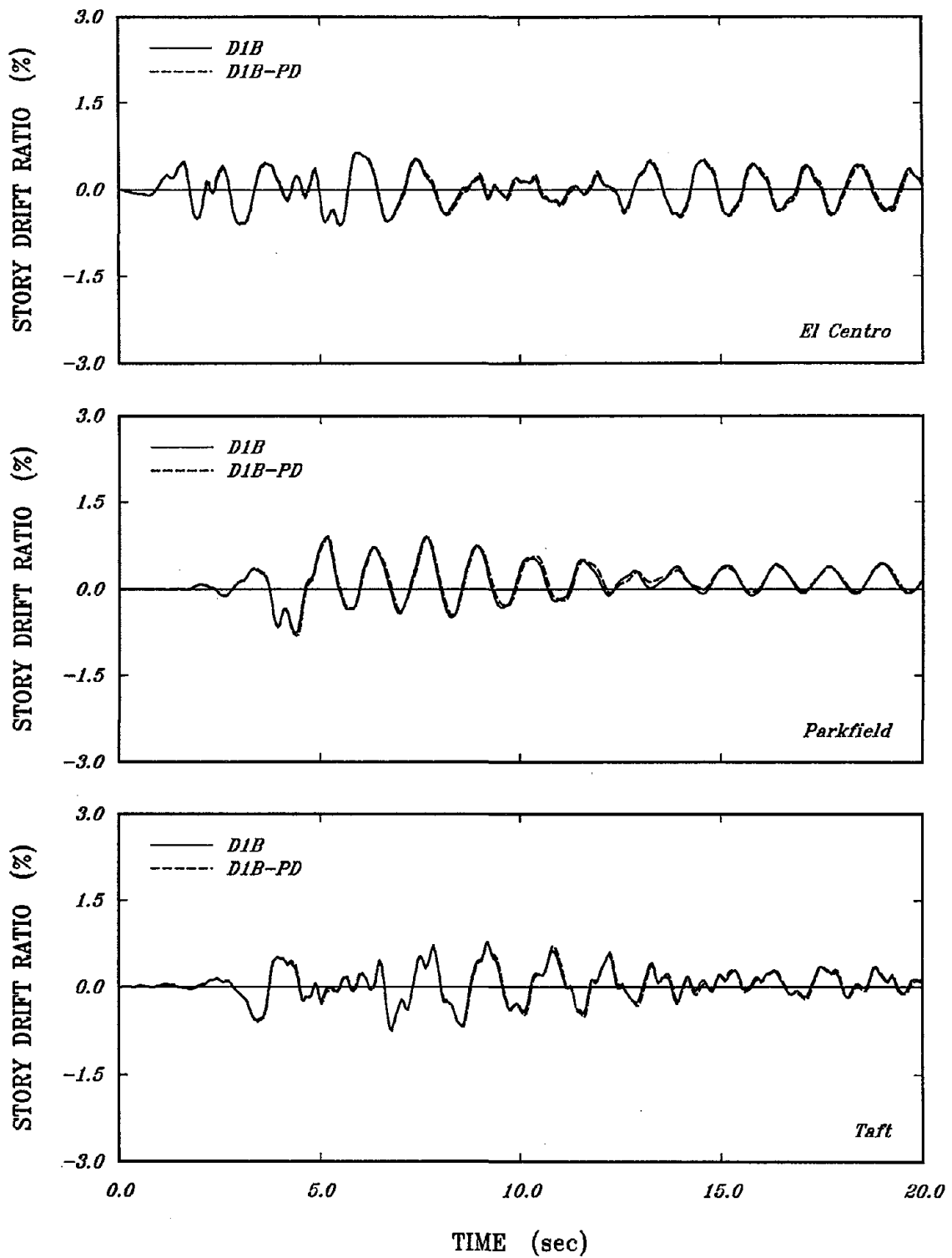


FIGURE 4.31 Drift-Time Histories of First Story for D1B and D1B-PD Frames Subjected to Three Earthquakes

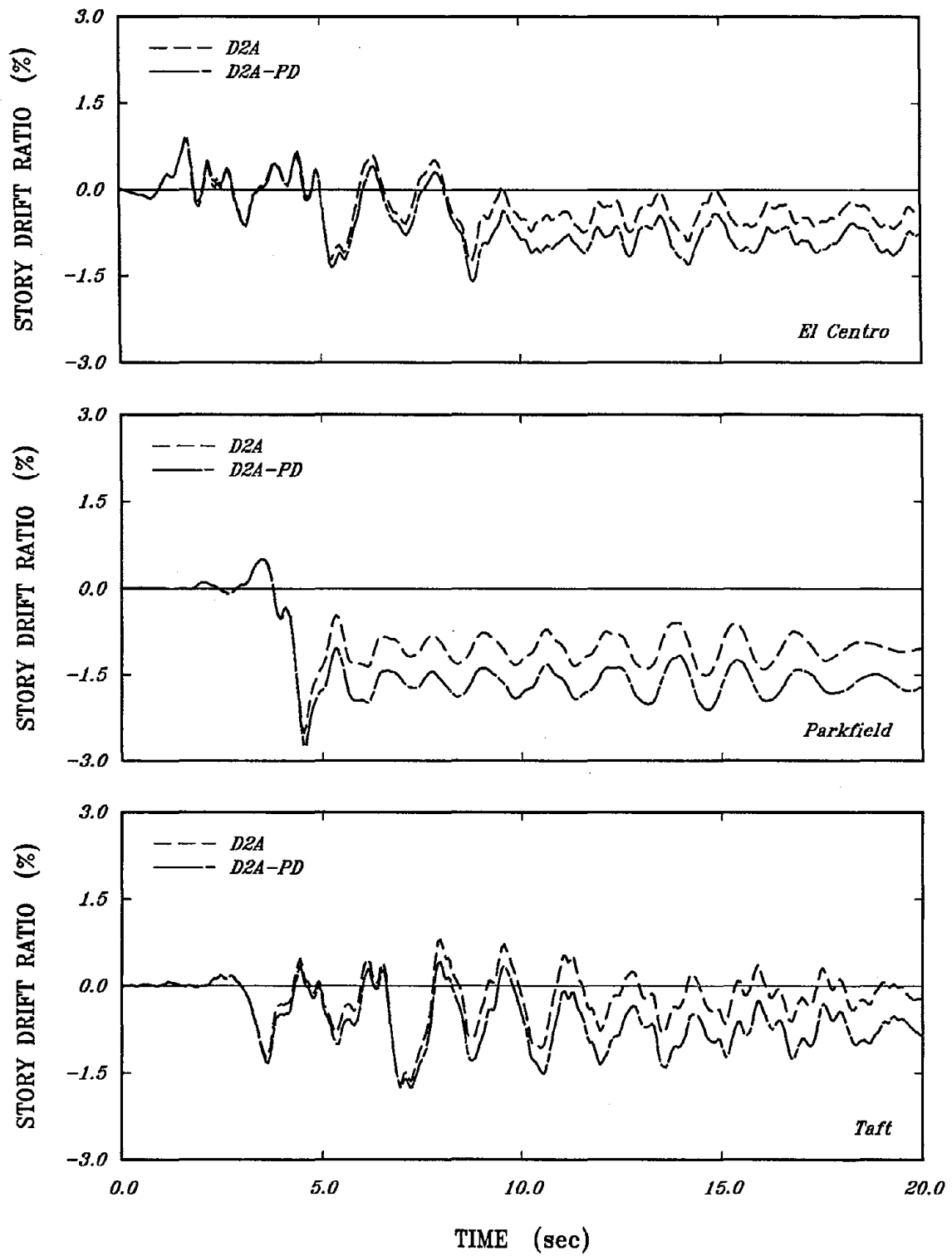


FIGURE 4.32 Drift-Time Histories of First Story for D2A and D2A-PD Frames Subjected to Three Earthquakes

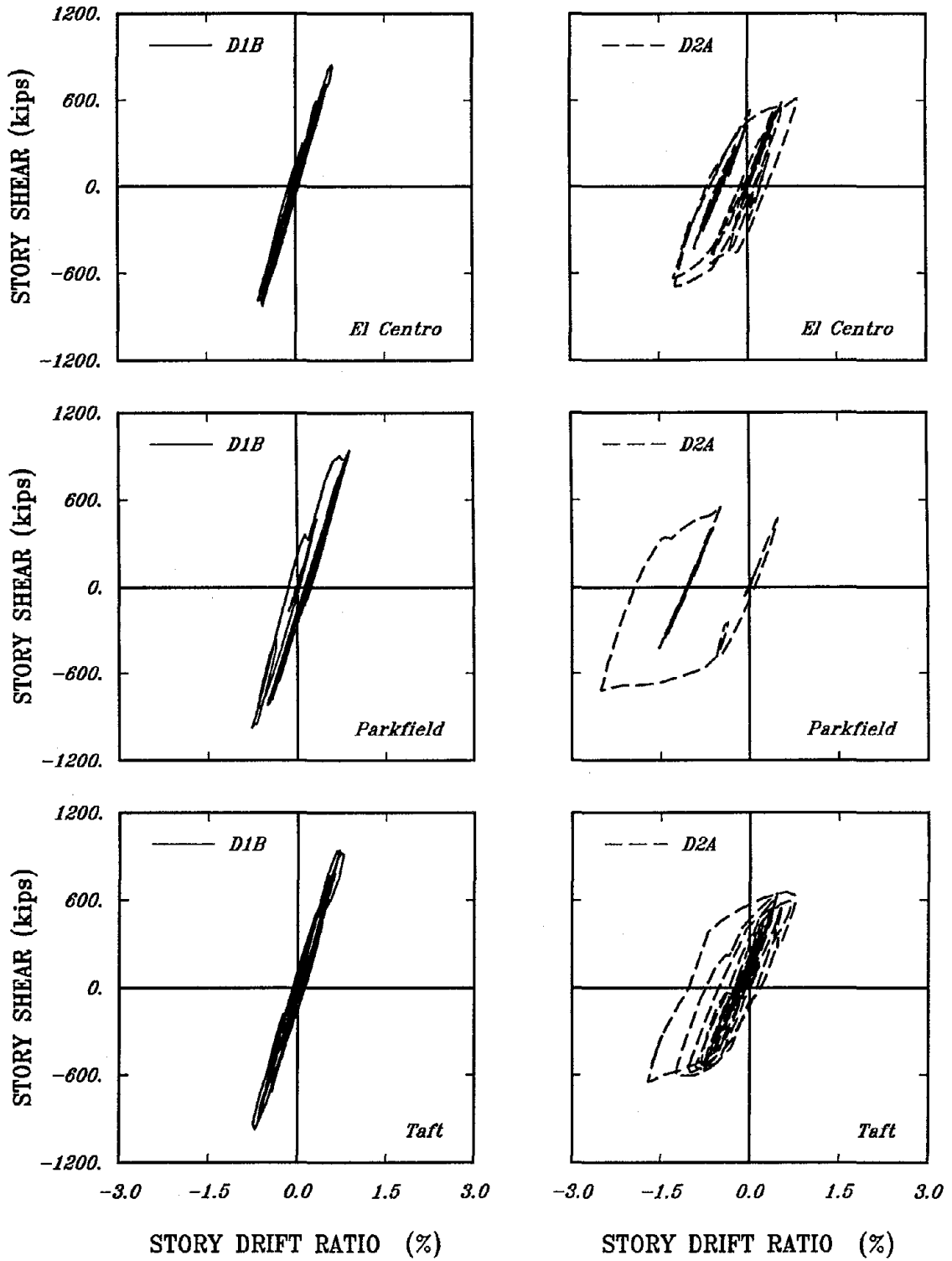


FIGURE 4.33 Shear-Drift Histories of First Story for Similar Modelling of D1B and D2A Frames Subjected to Three Earthquakes



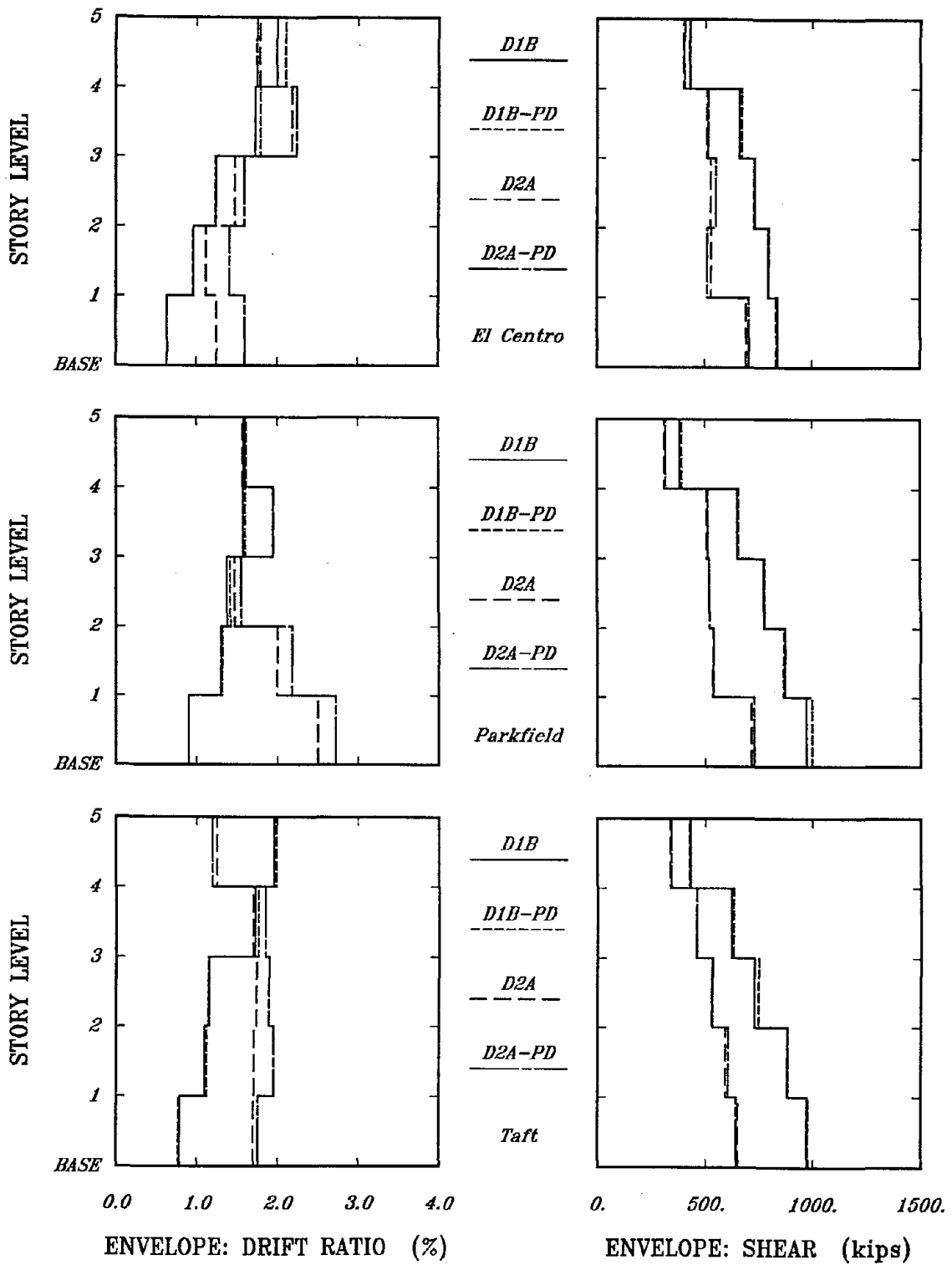


FIGURE 4.34 Story Drift and Shear Envelopes for Similar Modelling of D1B and D2A Frames Subjected to Three Earthquakes

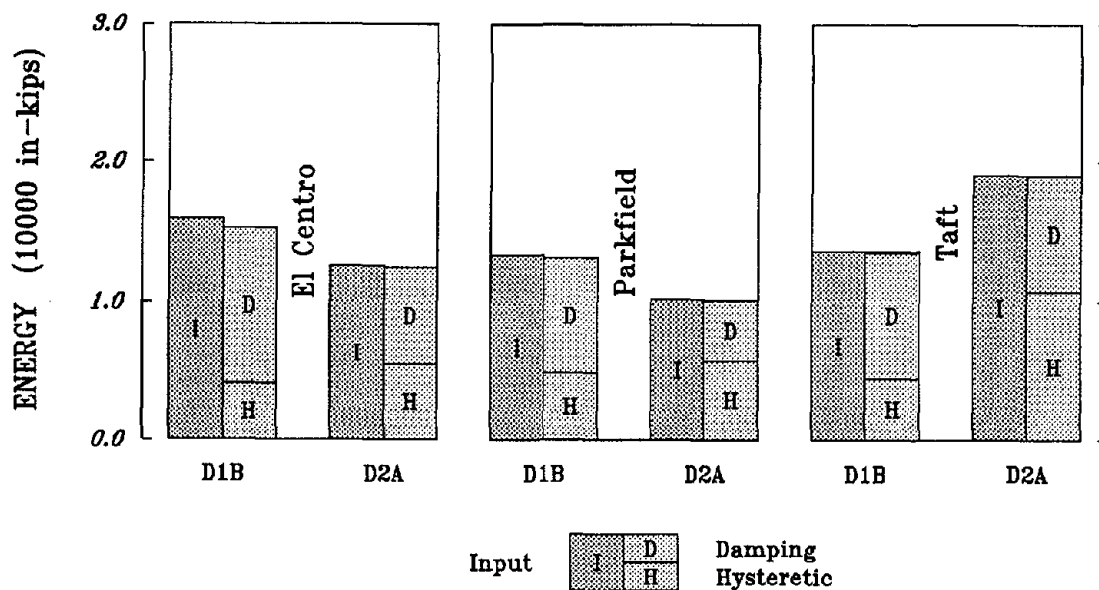


FIGURE 4.35a Cumulative Energy Quantities for Similar Modelling of D1B and D2A Frames Subjected to Three Earthquakes

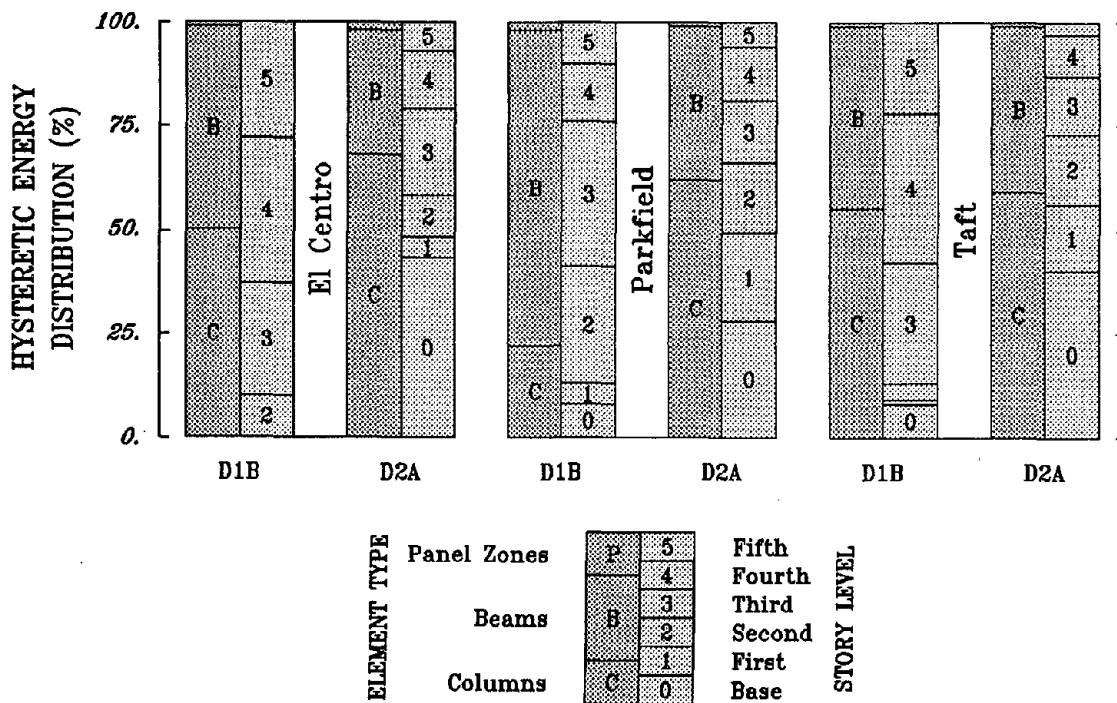
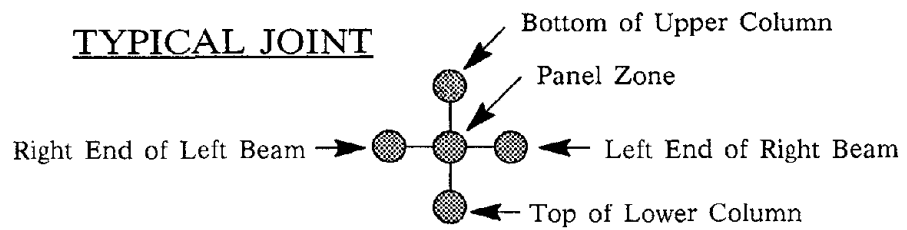
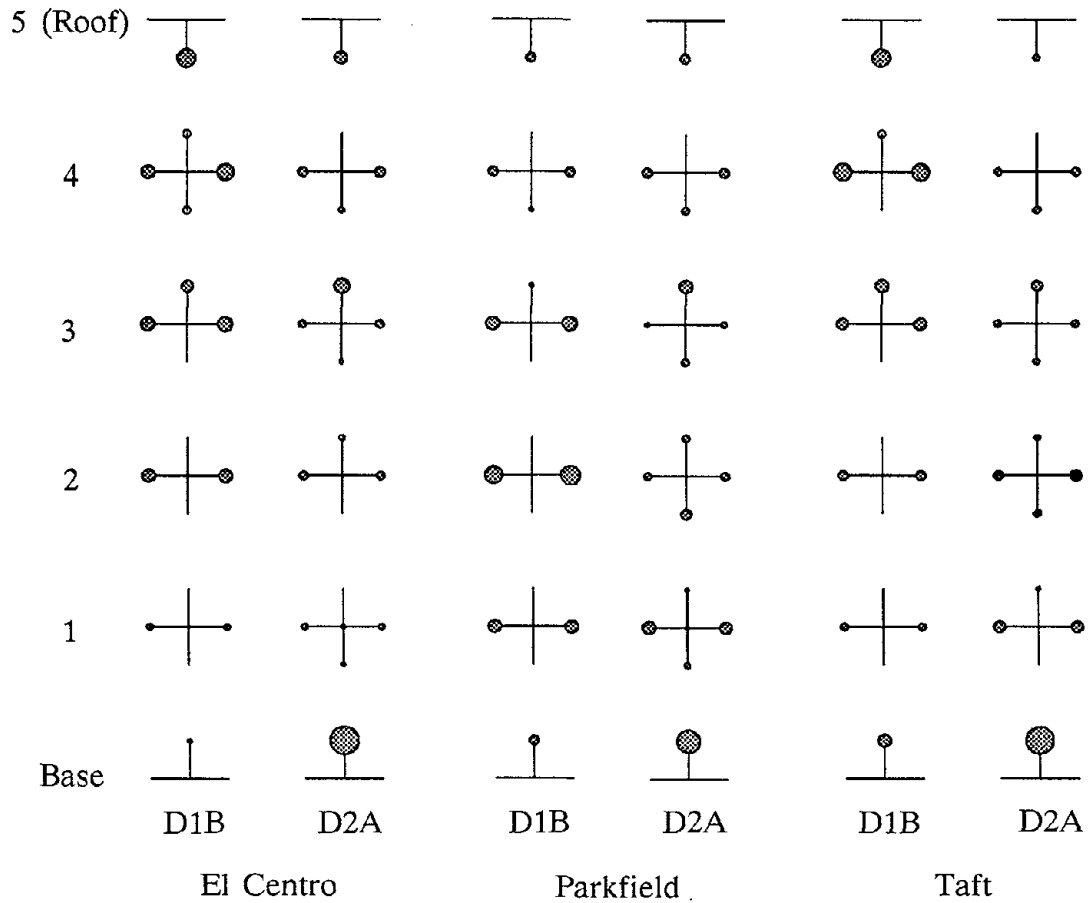


FIGURE 4.35b Hysteretic Energy Distributions for Similar Modelling of D1B and D2A Frames Subjected to Three Earthquakes



Note: Areas proportional to percentage of hysteretic energy dissipated at location.

FIGURE 4.35c Hysteretic Energy Locations for Similar Modelling of D1B and D2A Frames Subjected to Three Earthquakes

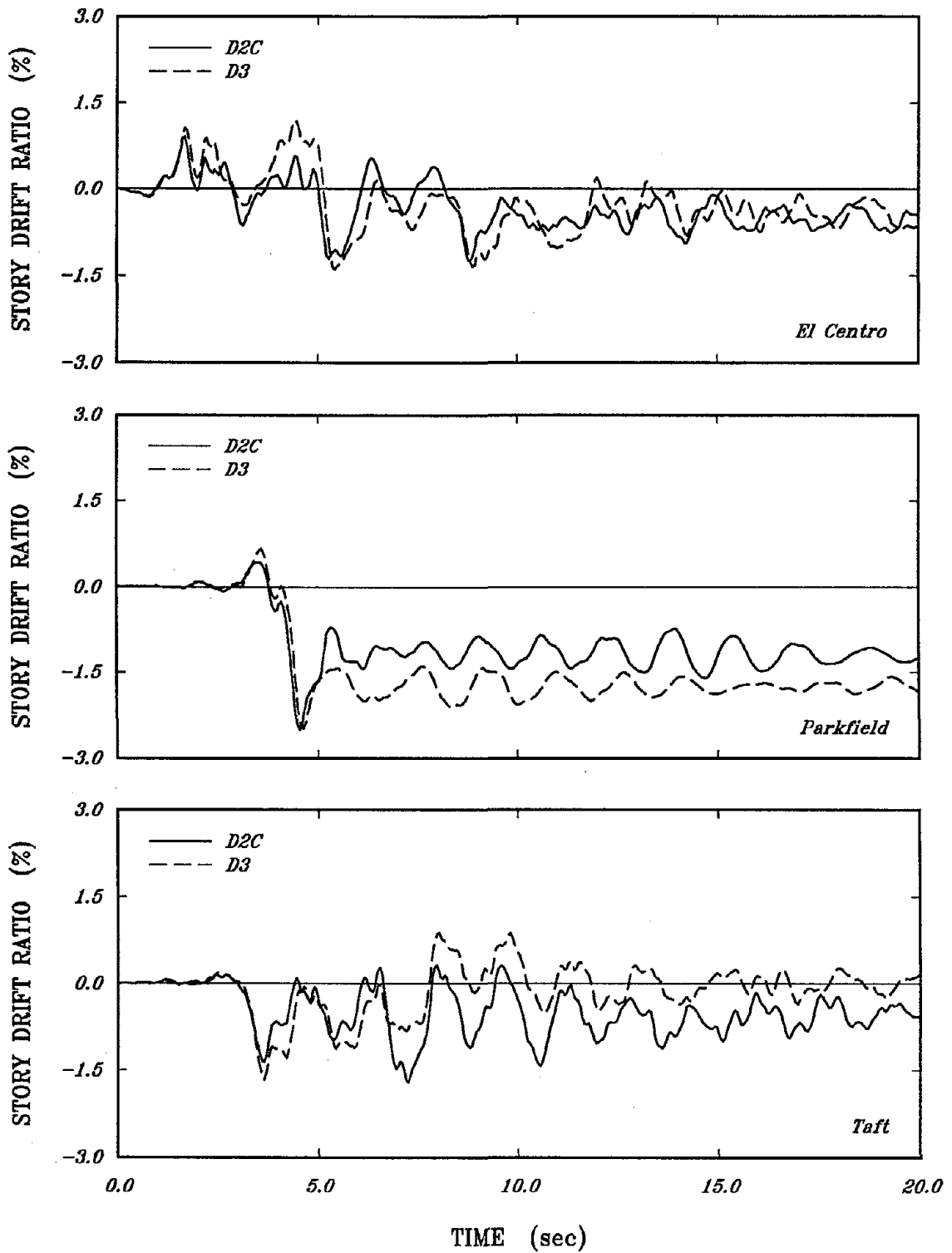


FIGURE 4.36 Drift-Time Histories of First Story for Similar Modelling of D2C and D3 Frames Subjected to Three Earthquakes

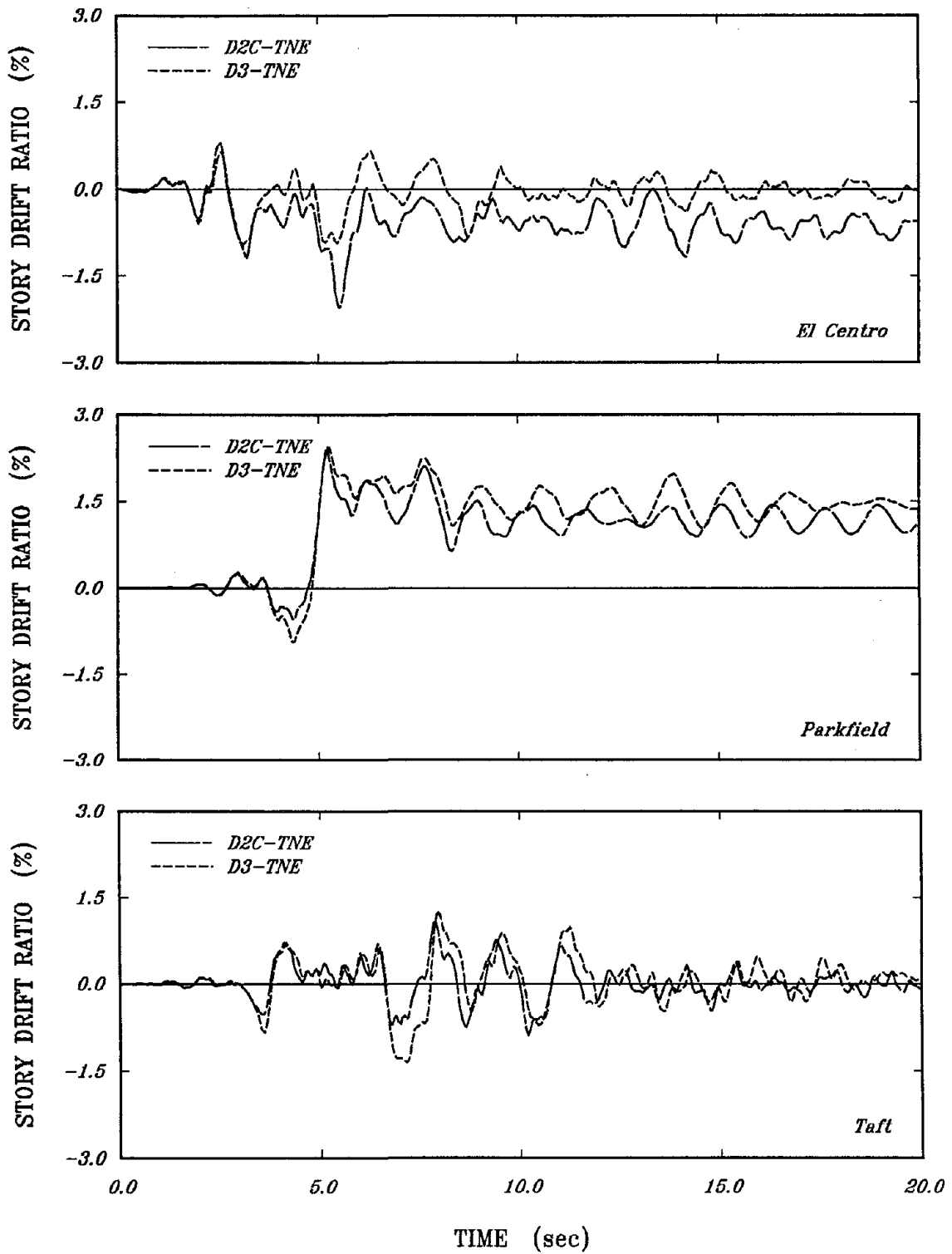


FIGURE 4.37 Drift-Time Histories of First Story for Similar Modelling of D2C-TNE and D3-TNE Frames Subjected to Three Earthquakes

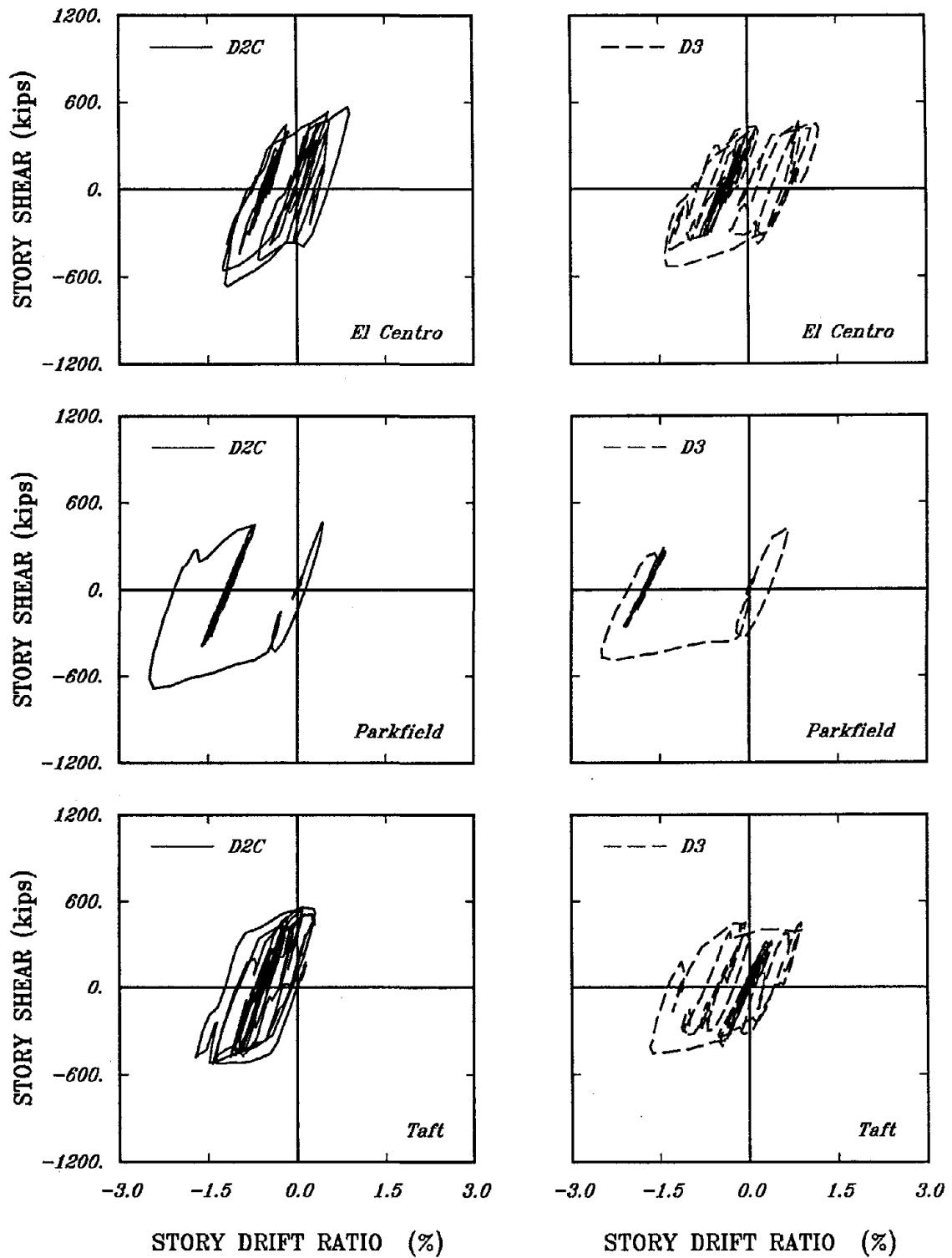


FIGURE 4.38 Shear-Drift Histories of First Story for Similar Modelling of D2C and D3 Frames Subjected to Three Earthquakes

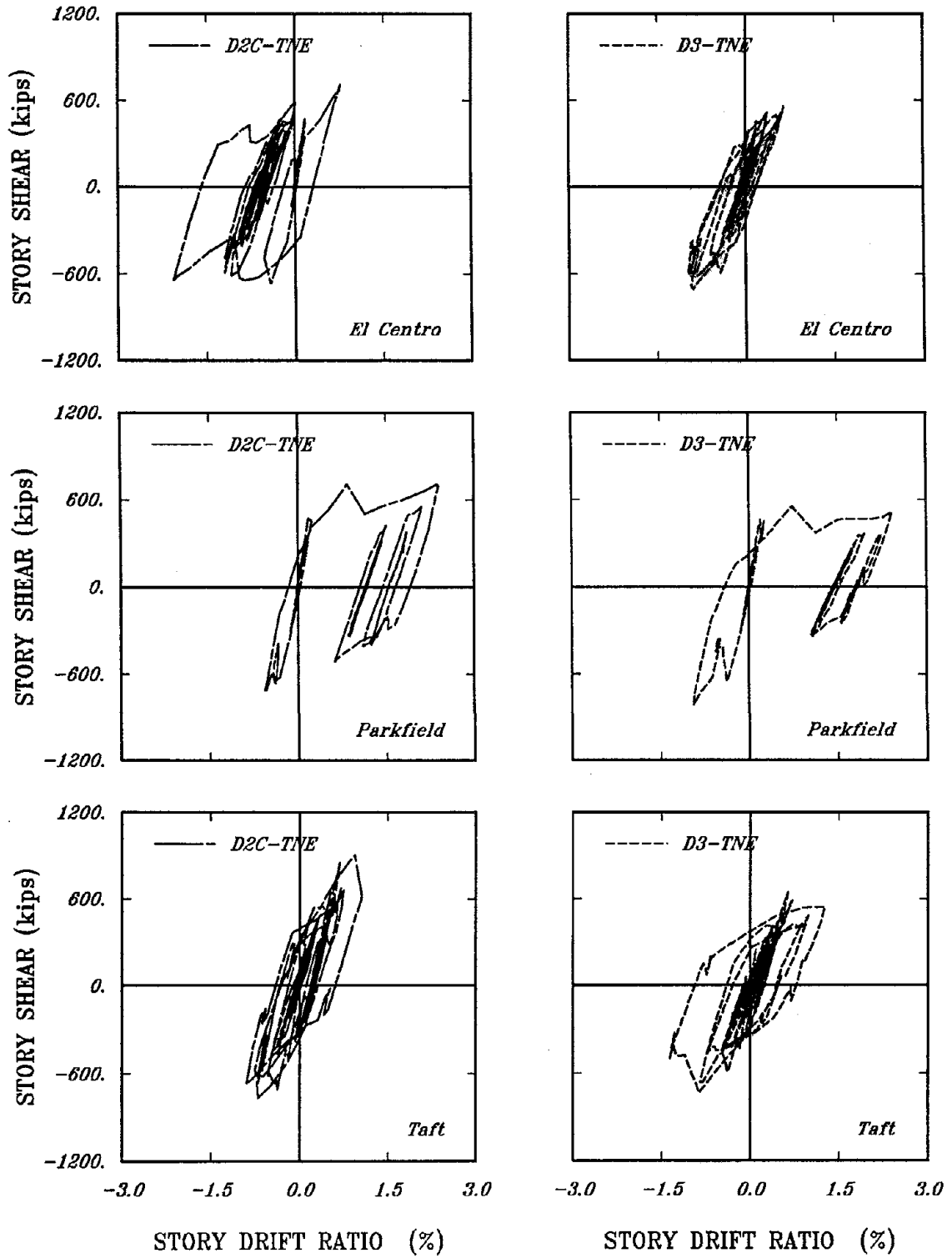


FIGURE 4.39 Shear-Drift Histories of First Story for Similar Modelling of D2C-TNE and D3-TNE Frames Subjected to Three Earthquakes

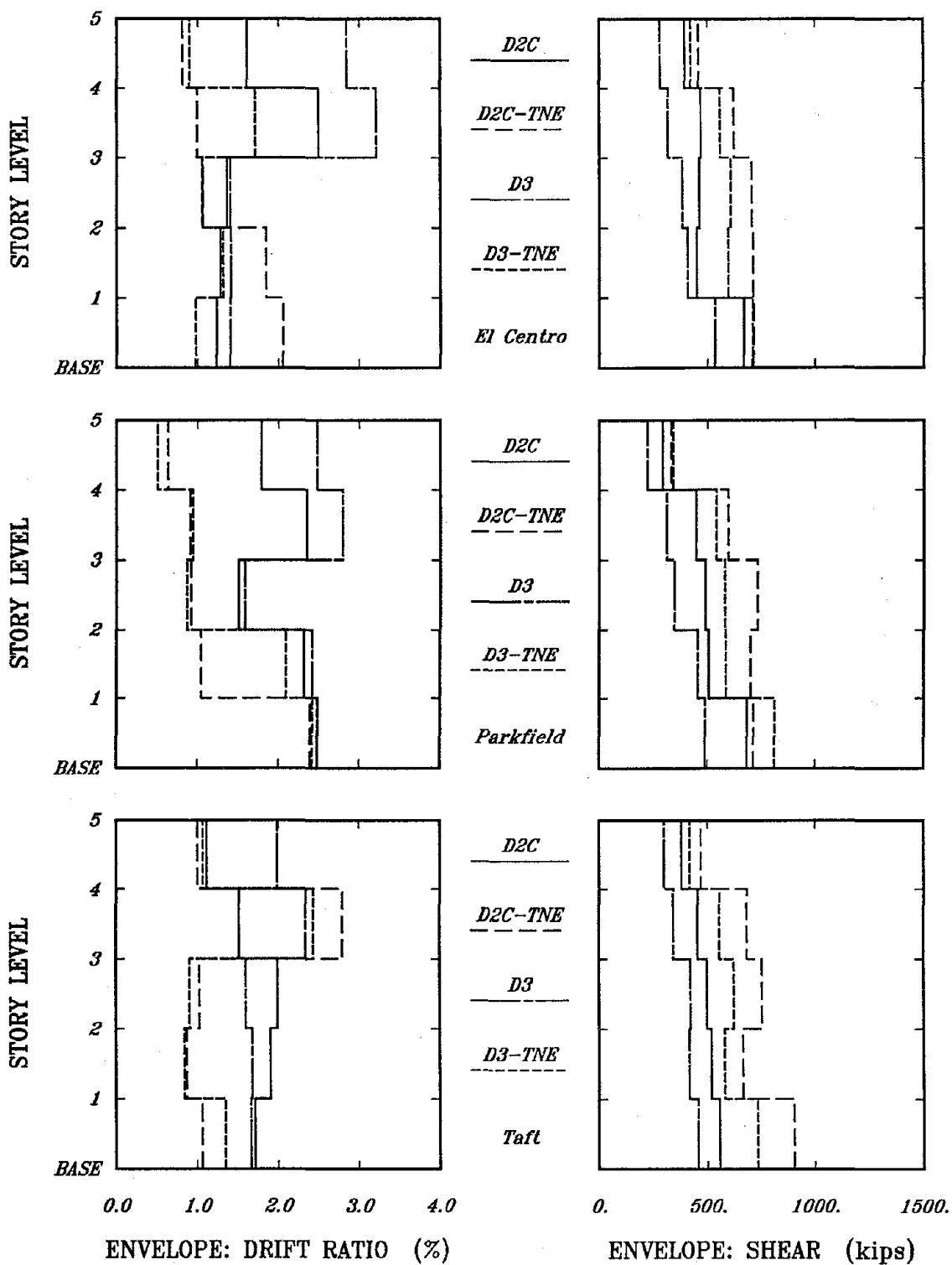


FIGURE 4.40 Story Drift and Shear Envelopes for Similar Modelling of D2C and D3 Frames Subjected to Three Earthquakes



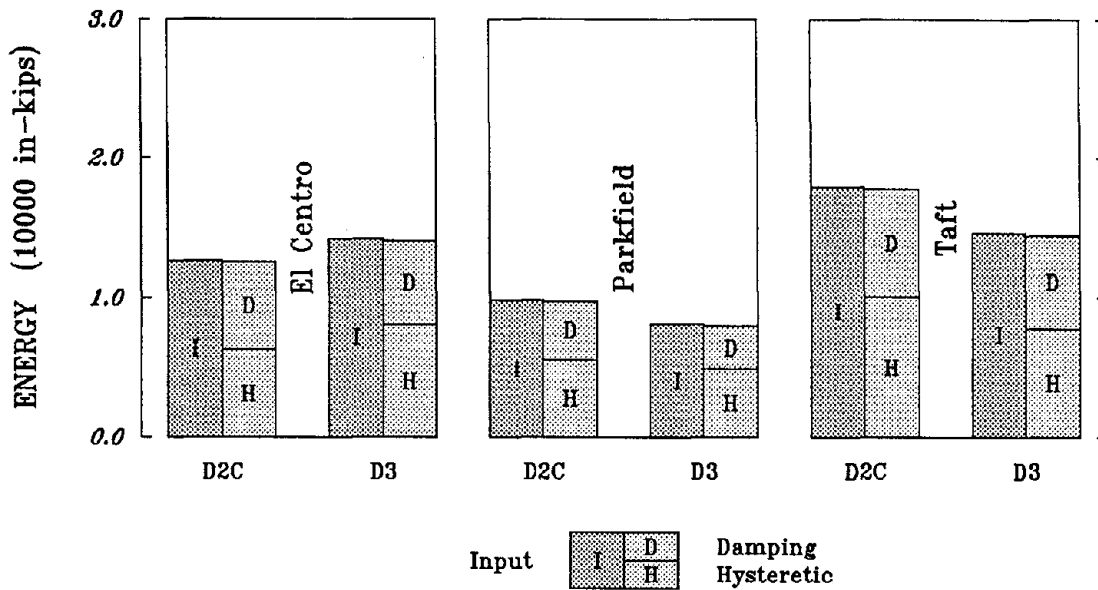


FIGURE 4.41a Cumulative Energy Quantities for Similar Modelling of D2C and D3 Frames Subjected to Three Earthquakes

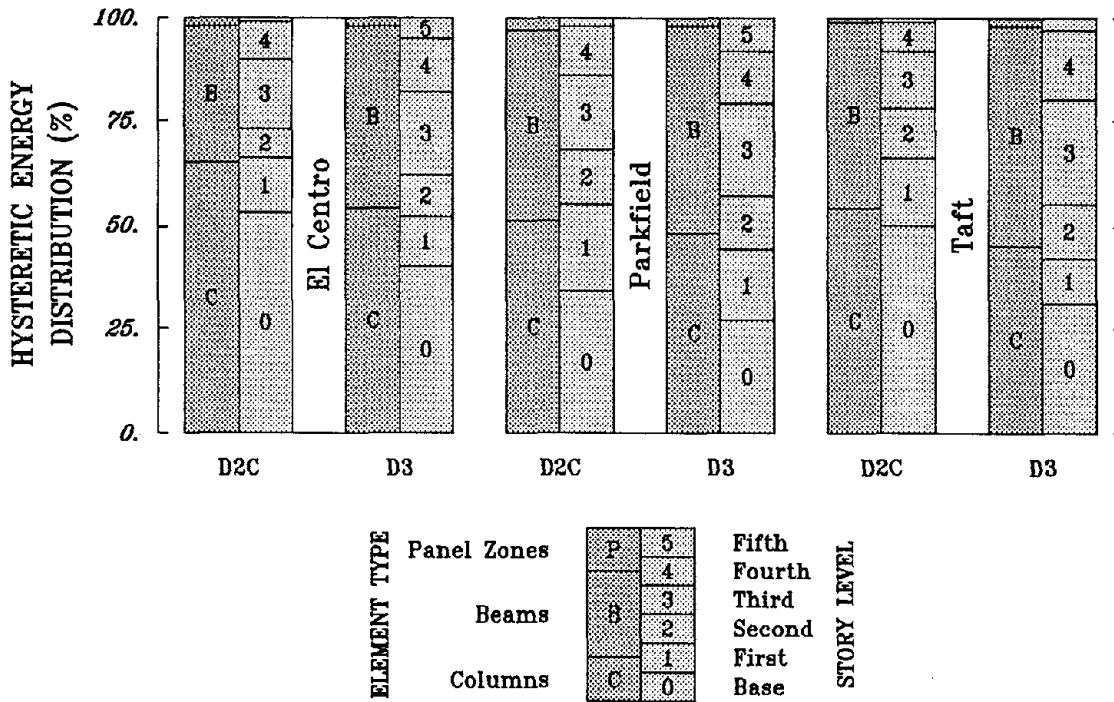
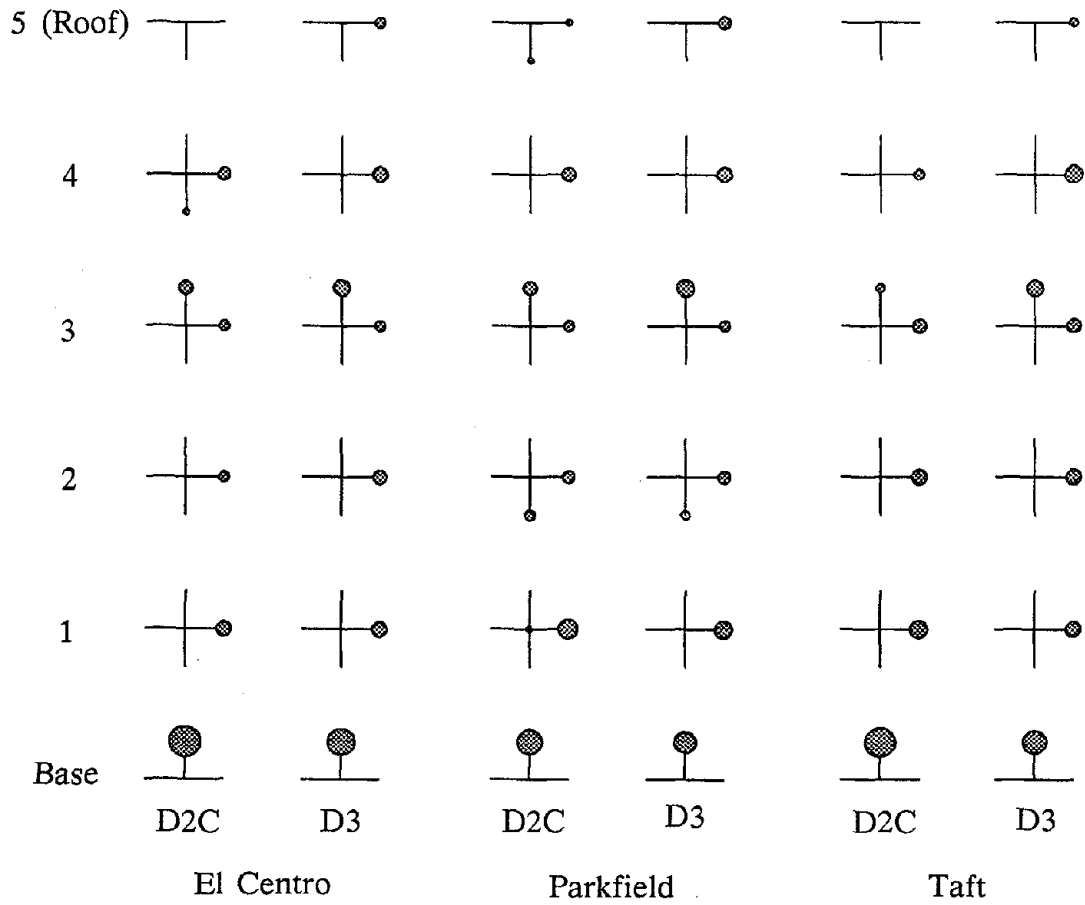
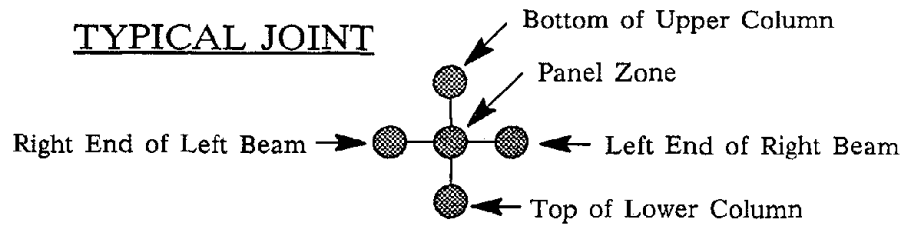


FIGURE 4.41b Hysteretic Energy Distributions for Similar Modelling of D2C and D3 Frames Subjected to Three Earthquakes



D2C



Note: Areas proportional to percentage of hysteretic energy dissipated at location.

FIGURE 4.41c Hysteretic Energy Locations for Similar Modelling of D2C and D3 Frames Subjected to Three Earthquakes

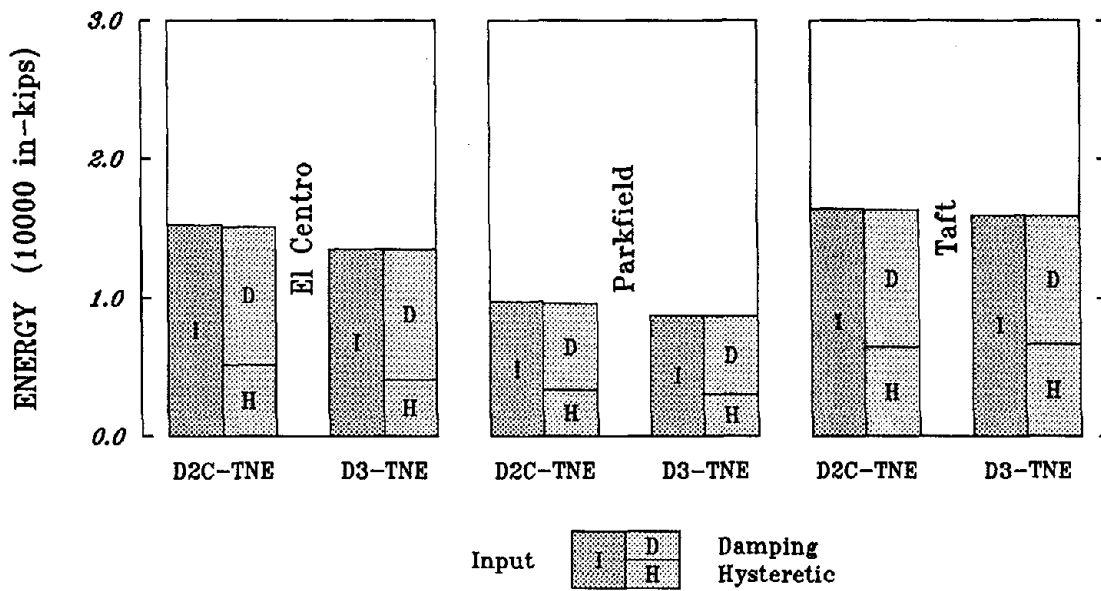


FIGURE 4.42a Cumulative Energy Quantities for Similar Modelling of D2C-TNE and D3-TNE Frames Subjected to Three Earthquakes

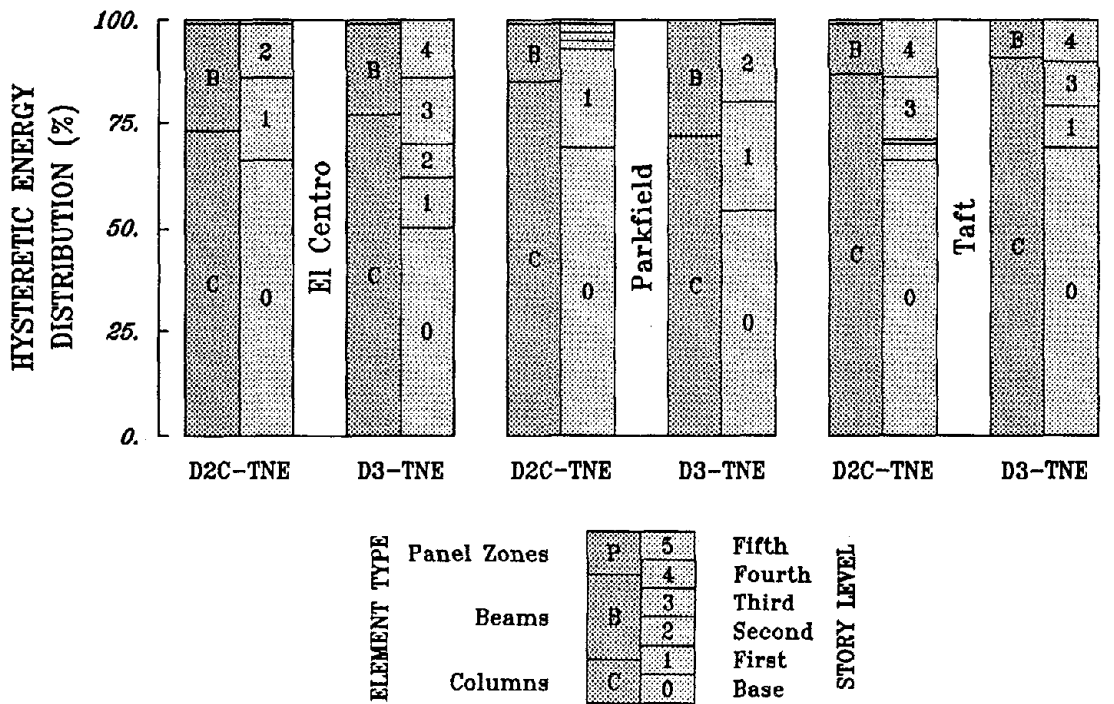
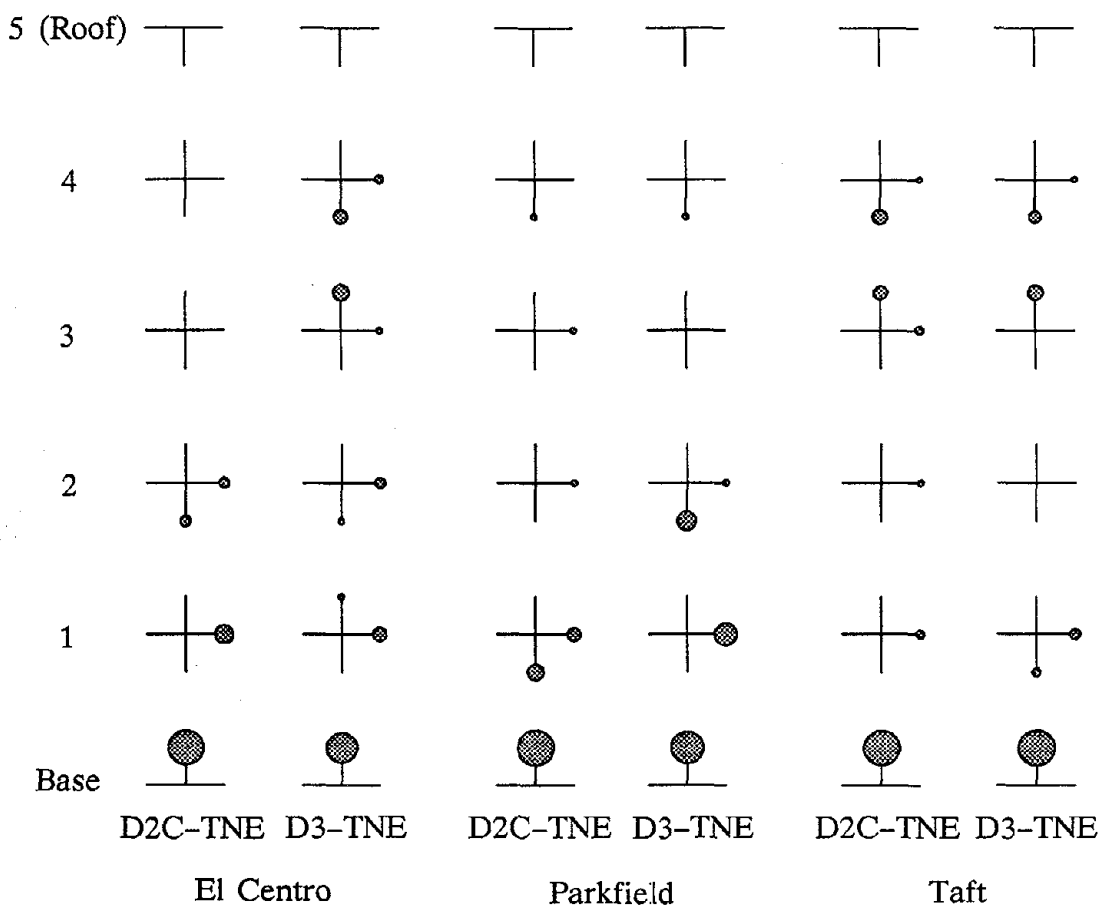
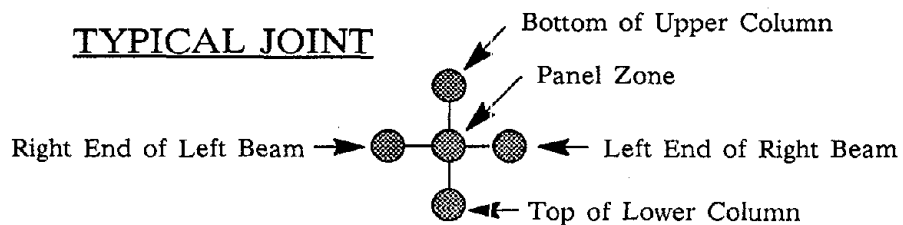


FIGURE 4.42b Hysteretic Energy Distributions for Similar Modelling of D2C-TNE and D3-TNE Frames Subjected to Three Earthquakes



D2C



Note: Areas proportional to percentage of hysteretic energy dissipated at location.

FIGURE 4.42c Hysteretic Energy Locations for Similar Modelling of D2C-TNE and D3-TNE Frames Subjected to Three Earthquakes

#### 4.4.6 Investigation of Defective Connections

The D2C frame had only one bay in the frame resisting lateral forces and, consequently, had just two moment-resisting connections per story (see Figure 2.7). Since a few members of the D2C frame were required to provide all of the lateral resistance and stability, the I-sections used for these members were large with flange widths of up to one and a half inches thick. The fabrication of this size members is quite difficult, especially to maintain the ability to transfer the necessary forces through the "rigid" connection after inelastic deformation of the joint. Therefore, the D2C-D frame which was essentially identical to the D2C frame except that one beam-to-column connection in each of the first and third stories was assumed to be initially defective (poor quality). A pinned connection, instead of a moment-resisting connection was placed in the frame model.

The intention of this parametric study was to investigate what would be the influence on the inelastic response of a frame without much redundancy if some of the moment-resisting connections were defective. Because of the limitations of the DRAIN-2D program, the connections had to be assumed to be defective from the beginning of the analysis. However, a more realistic study would have been possible if the connection model would have degraded as a result of low-cycle fatigue after a period of excitation.

The time histories of the first story drift are plotted in Figure 4.43 for the D2C and D2C-D frames. The differences between the time histories were not that different because the same connections that were assumed defective in the D2C-D frame yielded in the D2C frame. Therefore, the end result was the same - the inability to transfer moment from the beams to the columns. As shown in the story shear-drift histories of the first story

given in Figure 4.44, the Parkfield accelerogram, which generally excited the lower stories, caused larger inelastic excursions in the first story for the frame with defective connections. However, the inelastic deformations for the defective frame subjected to El Centro and Taft were not any larger. One reason for this is that the D2C-D frame was less stiff initially and, therefore, attracted less base shear than the D2C frame.

In Figure 4.45, the story drift and shear envelopes of maximum response are shown for the two frame models. The shape of the envelopes were roughly the same for the two models. The maximum drifts, especially in the lower stories of the frames subjected to the Parkfield accelerogram and in the fourth story of the frames subjected to the El Centro and Parkfield accelerograms, significantly exceeded the maximum expected story drifts. However, the excess deformations were not solely related to the defective connection because the D2C frame experienced large deformations.

The total input energy quantities and distribution thereof, given in Figure 4.46a, were similar in magnitude for each earthquake. As expected, the percentage of hysteretic energy, shown in Figure 4.46b, distributed in the stories with the defective connection were smaller than the percentages of the D2C frame. The locations of hysteretic energy dissipation are shown in Figure 4.46c. The dissipation of hysteretic energy in the beams of the first through fourth stories was relatively uniform for the D2C frame, but not so for the D2C-D frame since the distribution of stiffness and strength was not uniform.

The presence of defective connections can influence the response under certain conditions. However if yielding of the connection at a particular location is expected, then the impact of having a defective connection at

the same location is lessened. Of course, the influence of having defective connections may be more important in the response from a moderate earthquake where significant inelastic deformations of the structural frame are not expected. Therefore a moment-resisting connection is not likely to yield and the difference between the response from a frame having an undamaged connection and a frame having a defective connection could be significant. One important fact that is brought out by this investigation is the ability to redistribute the forces. Even though one of the connections was assumed to be defective the structure was able to maintain some lateral resistance. Therefore it is essential for redundancy to exist to ensure stability in the event of a premature failure of a member or connection.

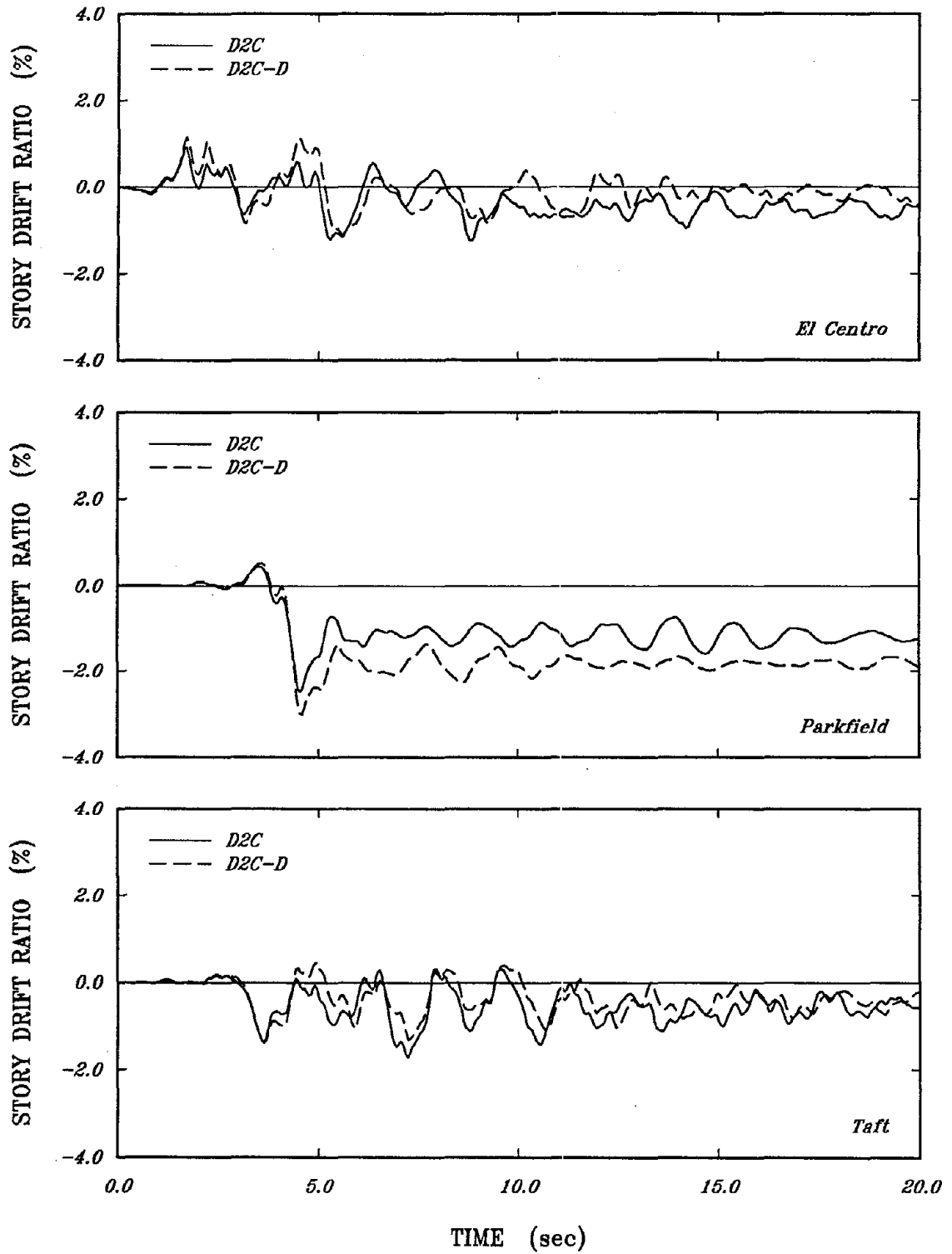


FIGURE 4.43 Drift-Time Histories of First Story for D2C and D2C-D Frames Subjected to Three Earthquakes



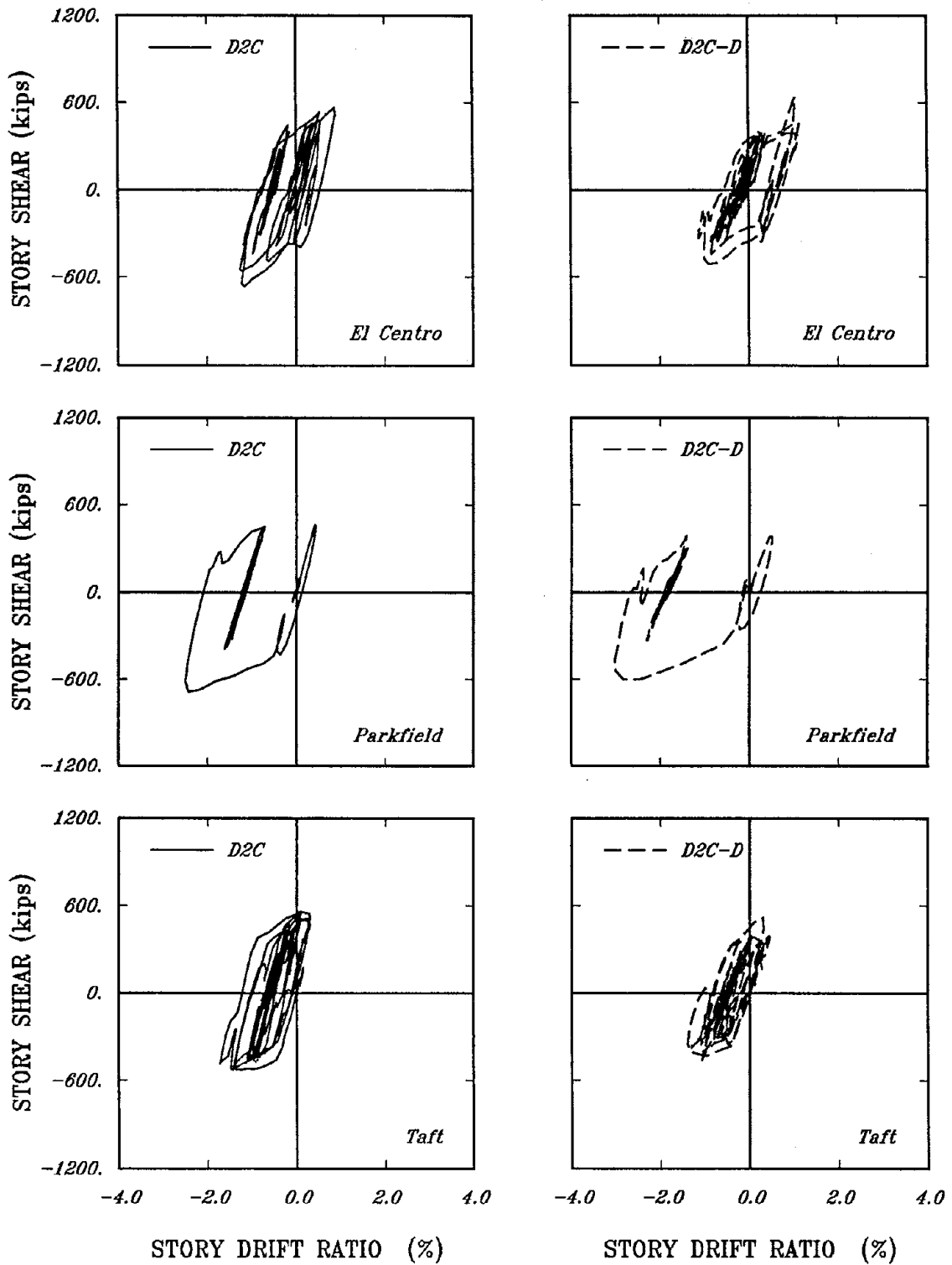


FIGURE 4.44 Shear-Drift Histories of First Story for D2C and D2C-D Frames Subjected to Three Earthquakes

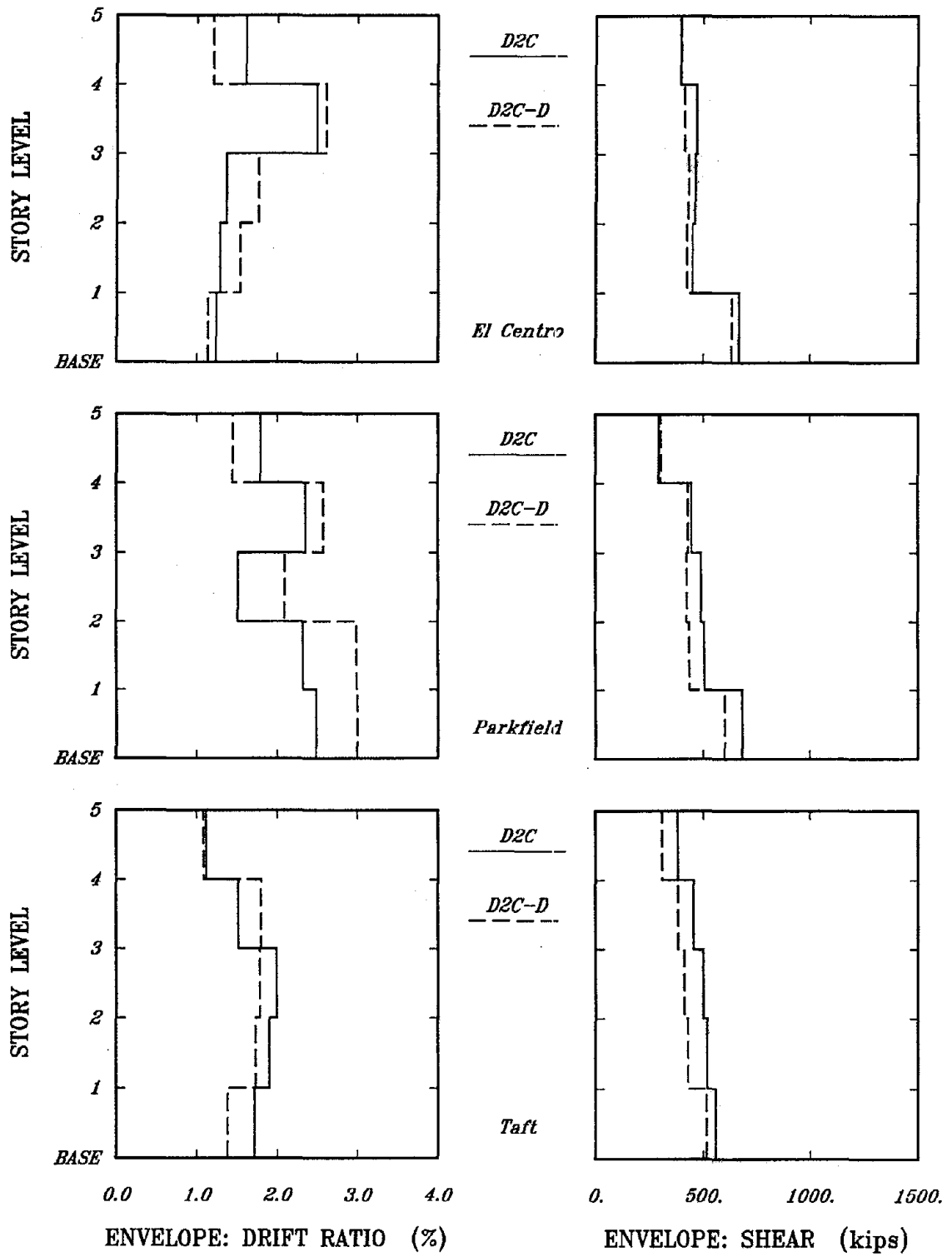


FIGURE 4.45 Story Drift and Shear Envelopes for D2C and D2C-D Frames Subjected to Three Earthquakes

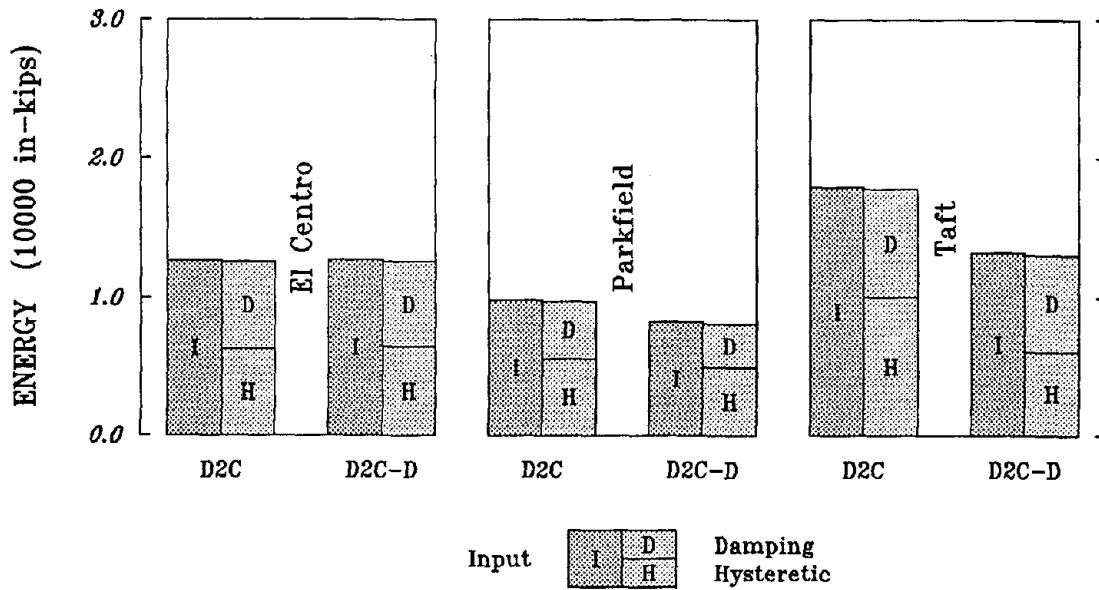


FIGURE 4.46a Cumulative Energy Quantities for D2C and D2C-D Frames Subjected to Three Earthquakes

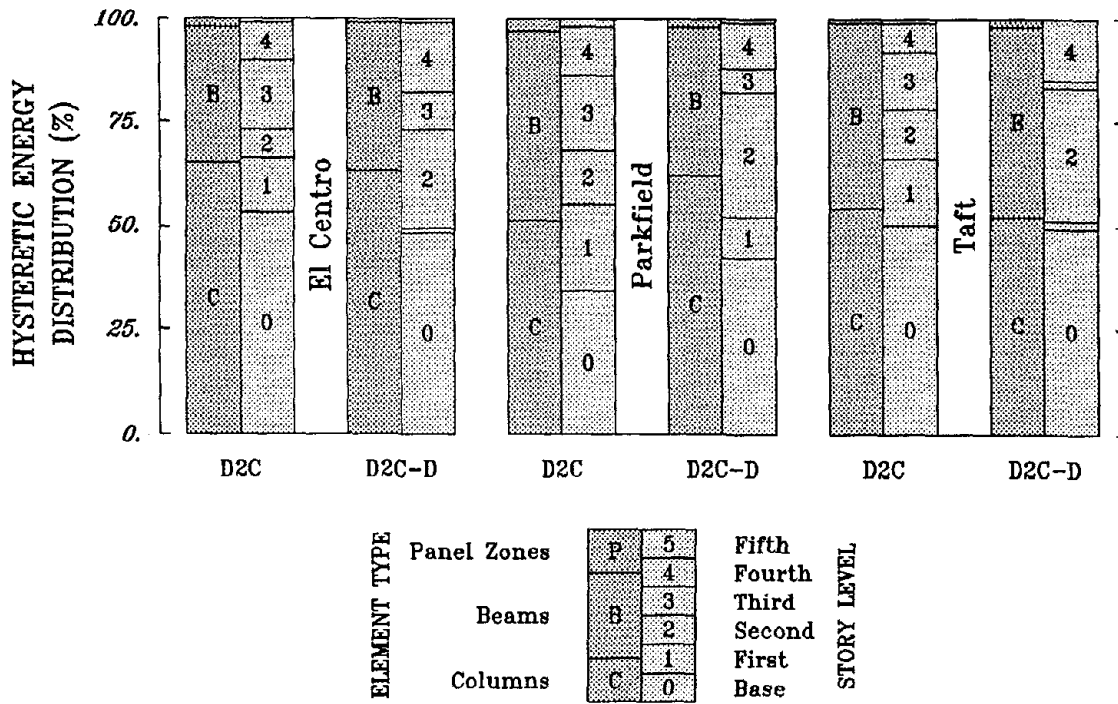
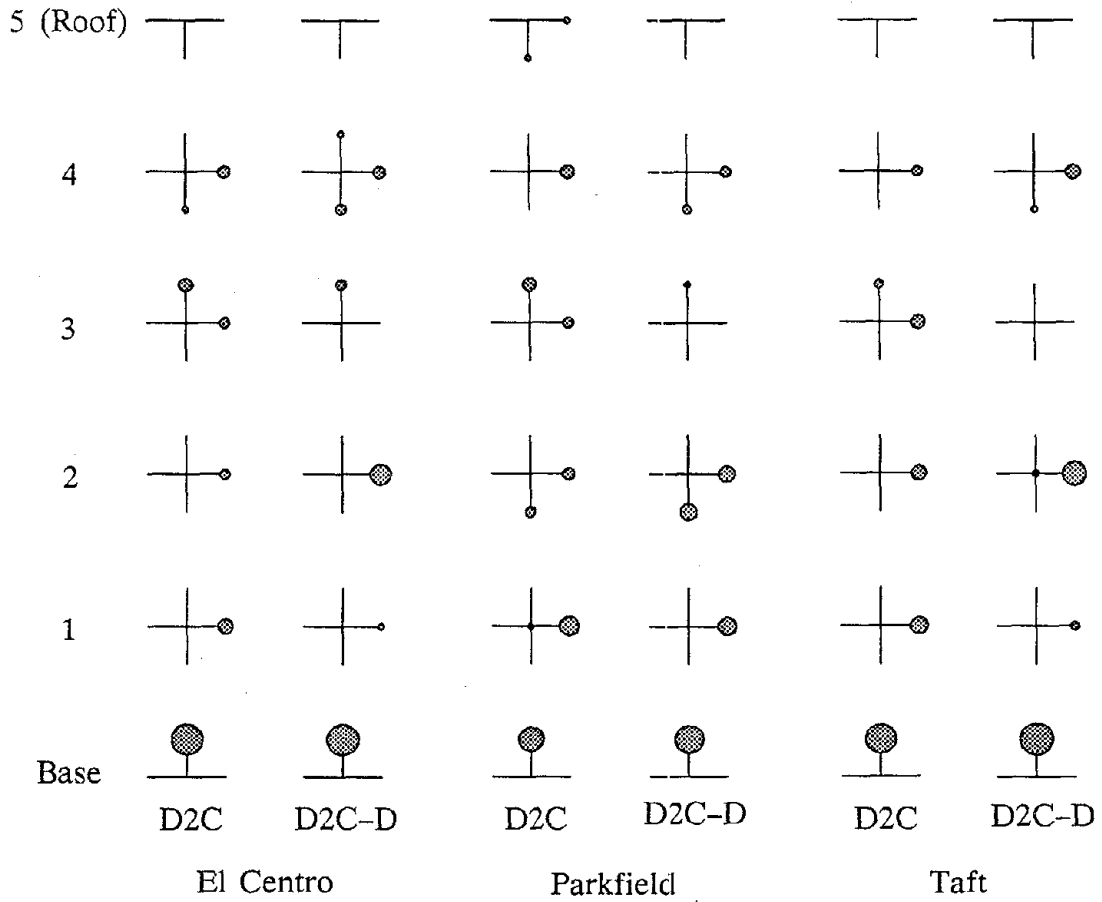
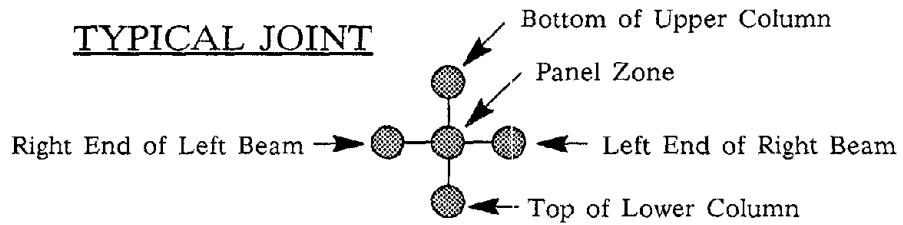


FIGURE 4.46b Hysteretic Energy Distributions for D2C and D2C-D Frames Subjected to Three Earthquakes



D2C



Note: Areas proportional to percentage of hysteretic energy dissipated at location.

FIGURE 4.46c Hysteretic Energy Locations for D2C and D2C-D Frames Subjected to Three Earthquakes

#### 4.4.7 Investigation of Building Height

In the direct design procedure of the 1988 edition of the *Uniform Building Code*, an equation is given to estimate the fundamental period of a structure. This equation is dependent on the building height and type of lateral force-resisting system. The frame configuration of the two-story frame design is the same as the D2B frame design, except that there are only two stories instead of five stories (see Figure 2.8). The calculation of the design base shear for both of these two frame designs was based on the estimated fundamental period of the structure. However, the estimated fundamental period for the two-story frame design resulted in a design base shear equal to the upper limit of the design spectrum for this study (9.2 percent of building weight).

The shear panel elements modelling the trilinear load-deformation behavior for nonstructural elements that were used in the D2B frame model were added to this two-story model. The fundamental period of the bare structural frame model was around one second and was reduced to one-half of a second with the addition of the nonstructural elements. The two-story frame model was designated D4 and designated D4-TNE with the addition of nonstructural elements. The lateral stiffness and strength contribution of nonstructural elements were greater for this two-story model than for the five-story models, because the lateral stiffness and strength of the bare structural frame were less for the two-story building.

Comparisons of the time histories for the first story drift of the D4 and D4-TNE frame models are given in Figure 4.47. Degradation of the nonstructural elements occurred within the first few cycles of strong excitation. The same general trends in the pattern of story drift trace, as

in the five-story frames, were prevalent in the response of the two-story frame as a result of excitation with each earthquake.

As shown in the story shear-drift histories for the first story given in Figure 4.48, the El Centro and Taft accelerograms produced many inelastic excursions, while the Parkfield accelerogram resulted in one large inelastic excursion. The nonstructural elements in the first story eventually reached total failure during the excitation with each of the earthquake records. The hysteresis loops for the bare structural frame were more regular than the frame model with brittle nonstructural elements.

The story drift and shear envelopes of the maximum responses are shown in Figure 4.49. The story drifts for the first and second stories were more uniform for the bare structural frame model than story drifts of the frame model with nonstructural elements. Although, the lateral stiffness of the second story and the strength of the members exceeded the requirements because the same sections as in the first story were used. The maximum drifts for both stories of the bare frame model were about twenty percent more than the expected maximum story drifts. However, the story drifts for the second story of the frame model with nonstructural elements was less than the expected drifts. The maximum story shears for the D4 frame model were almost three times as large as design story shears and the maximum story shears for the D4-TNE model were even larger.

As shown in Figure 4.50a, the total input energy quantities and distribution thereof produced by the El Centro accelerogram were almost twice as much as the quantities from the Parkfield accelerogram, while the quantities from the Taft accelerogram were between the two. Apparently, the fundamental period of vibration for the two-story structure was in a region

were the response spectra for the three earthquakes had notable differences in the maximum accelerations. The addition of nonstructural elements to the frame model eliminated the inelastic behavior of the second story as shown in the hysteretic energy distributions given in Figure 4.50b. In addition, most of the hysteretic energy is dissipated in the column end at the base connection of both models. In fact, more than least seventy percent of the hysteretic energy was dissipated at base connections.

It would not seem unreasonable to envision that the behavior of the two-story frame would be closer to the expected behavior of the code than the five-story since the code behavior is based, in part, on the response of a single-degree-of-freedom system. However, this was not the case, since obtained uniform story drifts for the two-story frame were derived from a frame whose lateral stiffness and strength were not proportional to the design story shears.

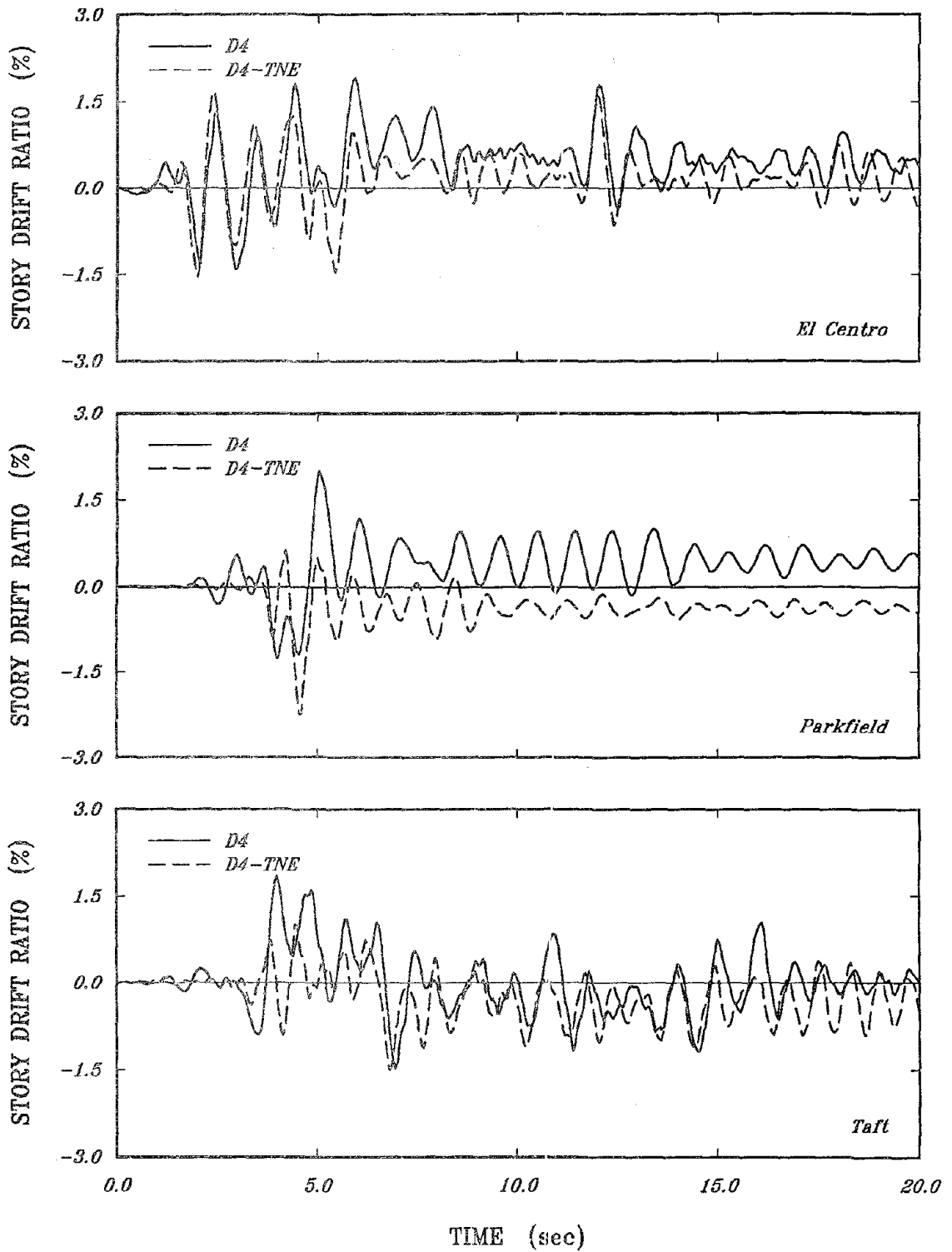


FIGURE 4.47 Drift-Time Histories of First Story for D4 and D4-TNE Frames Subjected to Three Earthquakes



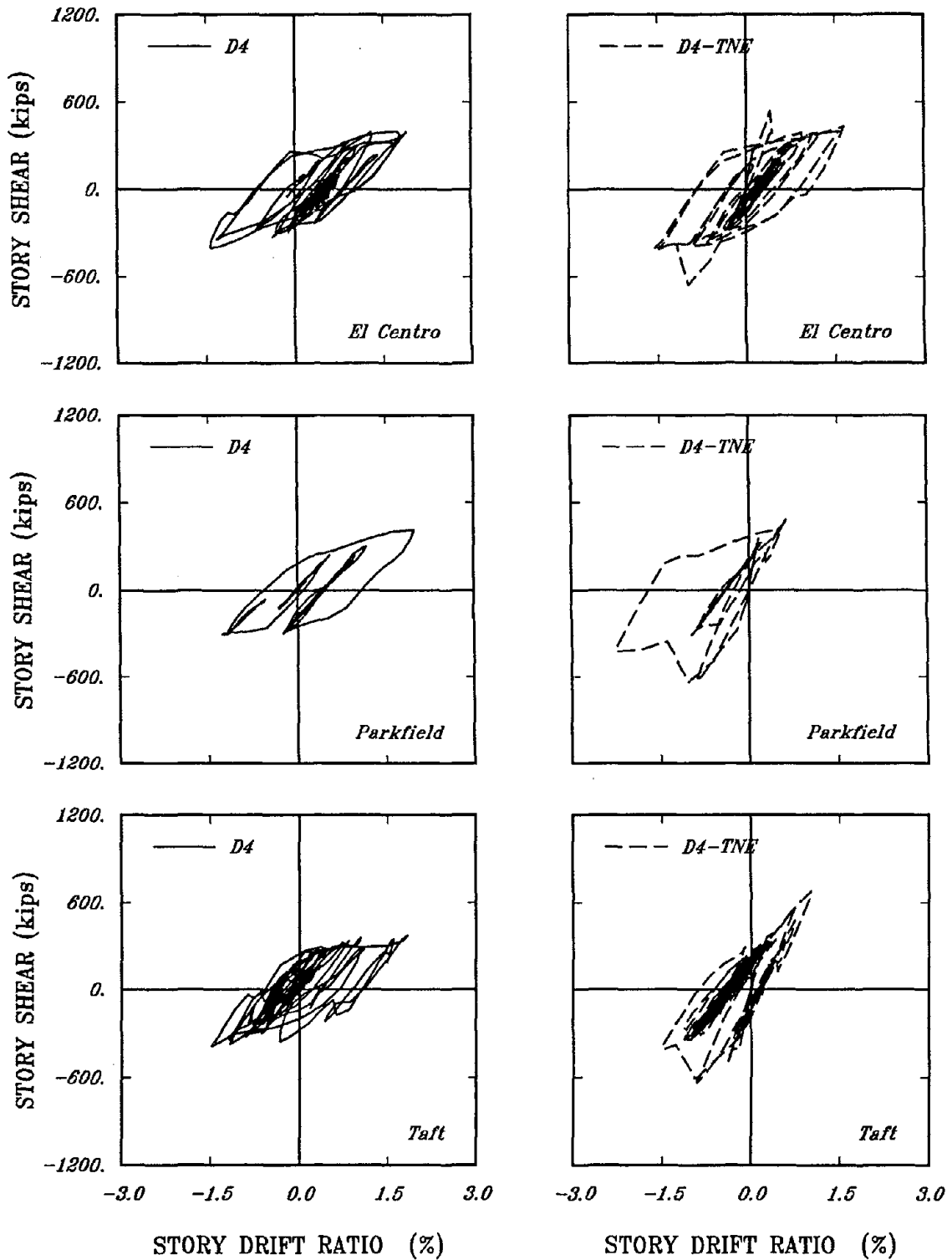


FIGURE 4.48 Shear-Drift Histories of First Story for D4 and D4-TNE Frames Subjected to Three Earthquakes

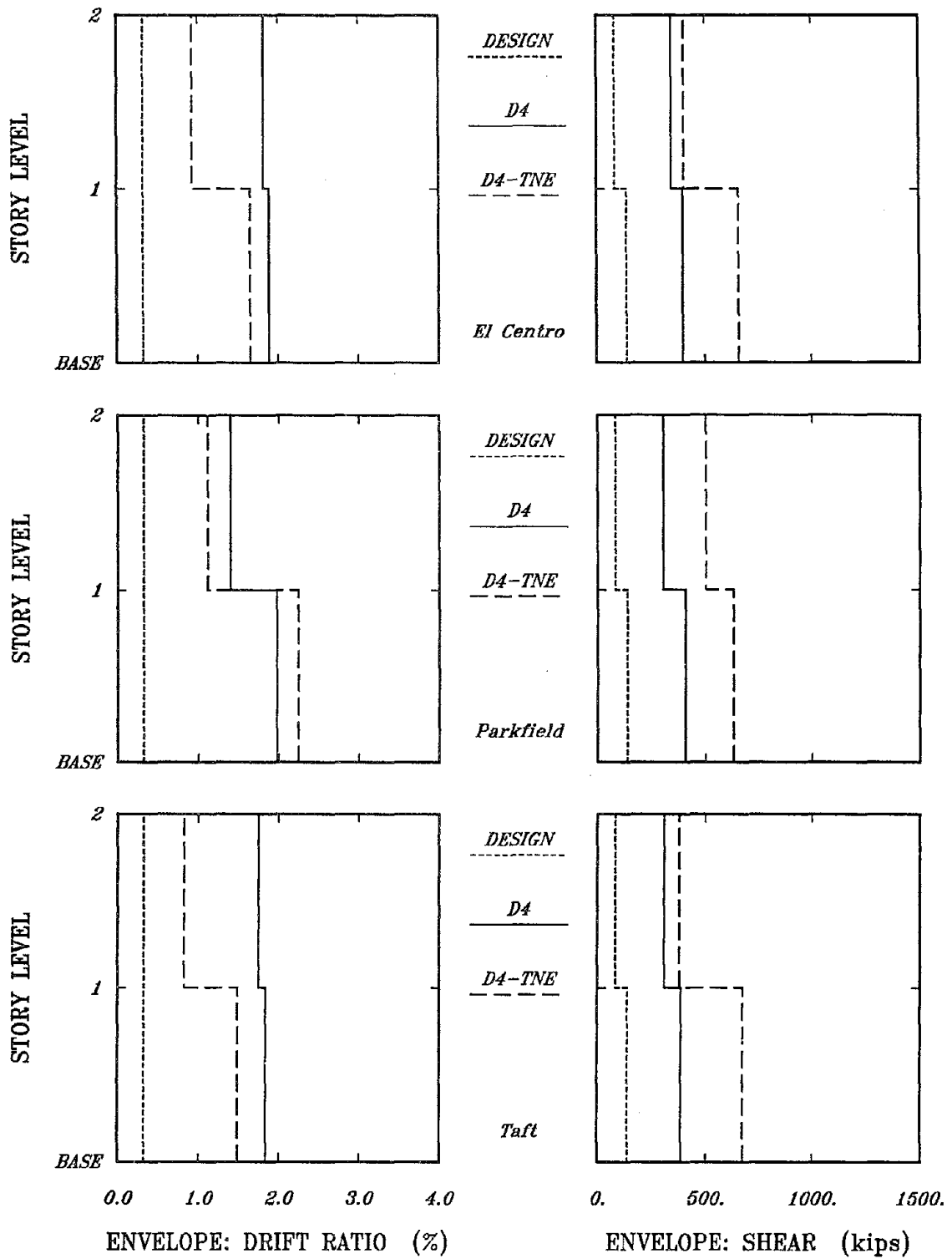


FIGURE 4.49 Story Drift and Shear Envelopes for D4 and D4-TNE Frames Subjected to Three Earthquakes

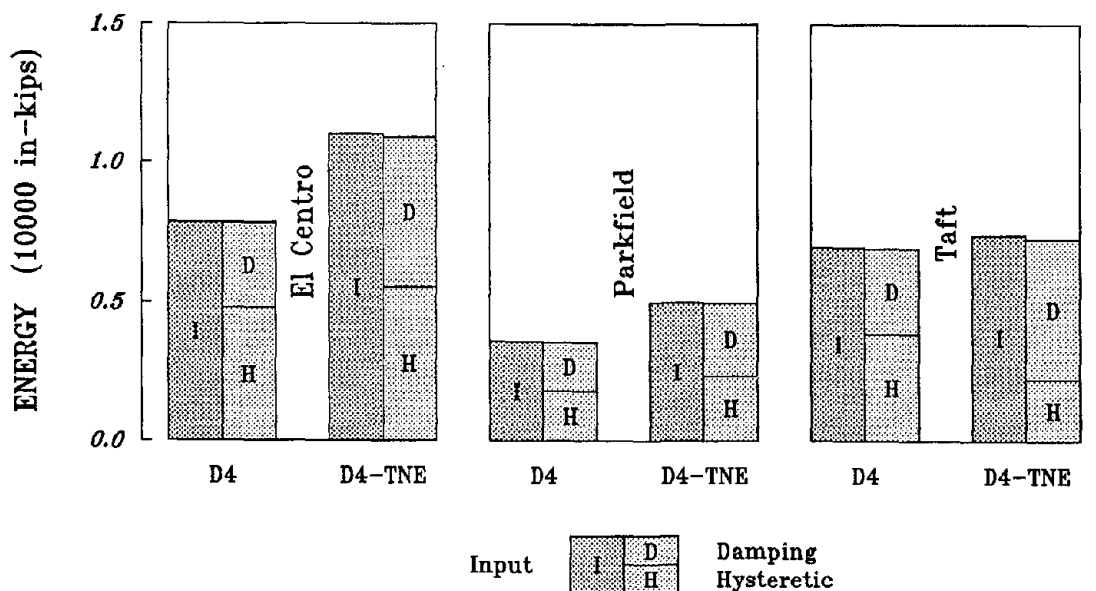


FIGURE 4.50a Cumulative Energy Quantities for D4 and D4-TNE Frames Subjected to Three Earthquakes

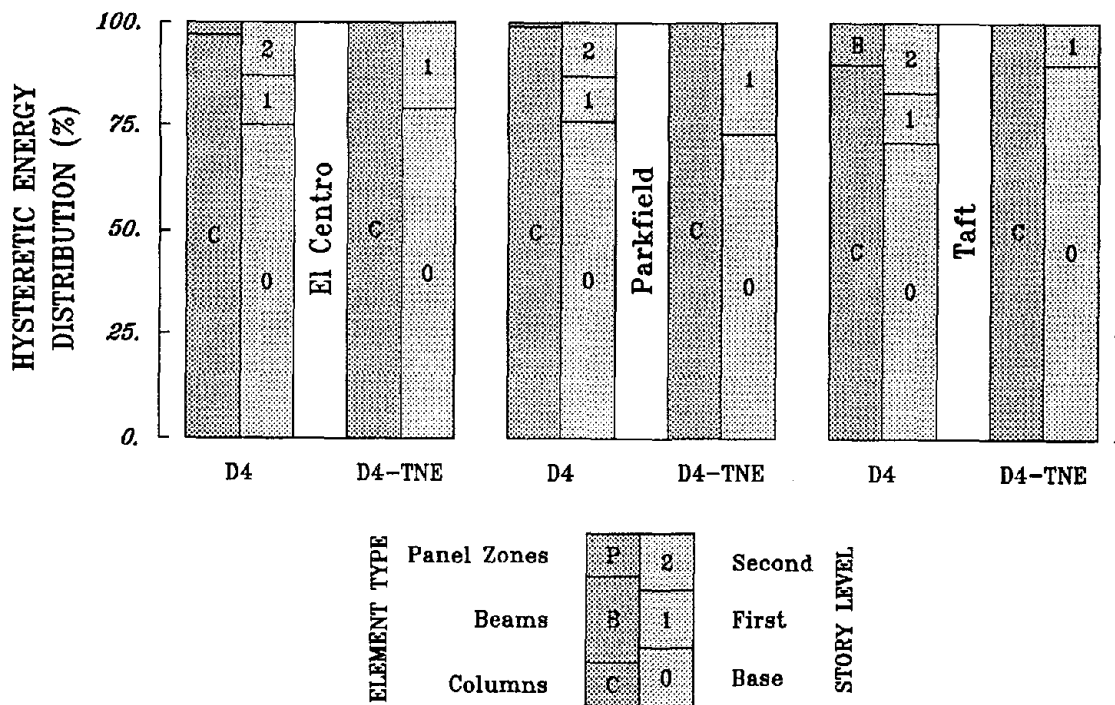


FIGURE 4.50b Hysteretic Energy Distributions for D4 and D4-TNE Frames Subjected to Three Earthquakes

#### 4.5 Overall Summary

The inelastic behavior for most of the frame models in this study was not compatible with the behavior assumed by the direct design procedure of the 1988 edition of the *Uniform Building Code*. The story drifts were not uniform over the height of the building and certain stories exceeded the expected inelastic deformations of the 1988 UBC when the frame model was subjected to severe ground excitation. In fact in some cases, the story drifts approached three times the expected level. The larger than expected story drifts are disconcerting, especially when the frame design is based on the assumption that the story drifts will not exceed one and a half percent of the story height.

The results of the parametric study for the strength ratio of the columns and beams indicated that the strength ratio did not influence the maximum story drifts or shears as much as the locations of hysteretic energy dissipation for a perimeter moment-resisting frames. However, the story drifts of the "strong column-weak beam" design usually were smaller than the "strong beam-weak column" design because, the strength of the members for this design generally exceeded by a larger amount the requirements of the code. The column sections chosen for the "strong column-weak beam" design had the same moment of inertia as the corresponding column sections for the "strong beam-weak column" design, but the strength of the column (plastic moment) was larger.

The behavior of the beam-to-column connections generally did not have a significant influence on the story drifts; but again altered the locations for hysteretic energy dissipation. The usage of the two connection models for a flexible panel zone is a rational method to account for deformation in

the panel zone. Of course, the thickness of the panel zone web, including doubler plates, is the controlling factor in determining the yield strength of the panel zone.

The participation of nonstructural elements had a very significant effect on the dynamic behavior of a building. Even though the distribution of stiffness and strength can be rather uniform for the bare structural frame, the addition of nonstructural elements can create a "soft" story in the lower portion of the building. The ductility demand for a soft story can be quite large since most of the hysteretic energy dissipation occurs within that story. Therefore, the deformation in this story tends to be large while the other stories experience small story drifts.

The reduction in the number of elements and connections providing the lateral resistance and stability by choosing different configurations for the lateral force-resisting system lowers the redundancy of the structure. Less redundancy and the inability to redistribute the forces possibly could lead to total collapse of the structure if a few members or connections fail prematurely, since the ductility demand is concentrated in a few locations.

The design base shear parametric study provided some interesting results. The story drifts for the "conservative" design were really not that conservative and, in fact, exceeded the expected drifts in the upper stories. Therefore, it seems rather questionable to use a smaller design base shear for determining the equivalent lateral forces. In the frame designs based on a smaller design base shear, the story drifts were more often than not larger than the expected story drifts. As the story drifts increased, so did the inelastic behavior and nonuniformity in ductility demand over the height of the frame.

The study on defective connections was not that revealing because the defective connections that were assumed to be defective would have yielded if they were not defective. Therefore, the stiffness and strength of the joints with and without a defective connection was basically the same during inelastic excursions. Perhaps the influence of defective connections would be more prominent from the excitation of a moderate earthquake, because the seismic design philosophy assumes that the lateral force-resisting system will not experience much inelastic behavior. The lateral stiffness of the structure is very important in limiting the story drifts during excitation when significant inelastic behavior of the lateral force-resisting system is not expected.

The limited investigation of a two-story structure resulted in the same deficiencies in the structural performance as in the five-story building. The story drifts were slightly larger than expected for both stories. The addition of nonstructural elements forced all of the inelastic behavior to occur in the first story.

All these parametric studies revealed the difficulty in determining the demand on a building during a major earthquake. In fact, without having an accurate prediction of the expected demand, it is extremely difficult to provide the necessary supply of stiffness and strength in the seismic design of a building. Of course, the design process needs to come "full circle", in that the supply of stiffness and strength for a building must be in agreement with the assumptions made in determining the demand, so that the structure can withstand the demand from a major earthquake.

## CHAPTER 5

## CONCLUSIONS AND DESIGN IMPLICATIONS

## 5.1 Conclusions

The purpose of this investigation was to increase the understanding of the inelastic behavior of ductile steel moment-resisting frames designed in accordance with modern design specifications and accepted design practice. The perimeter moment-resisting frames considered in this study, which were required to provide all of the lateral force resistance and stability, were designed in accordance with the direct design procedure adopted in the 1988 edition of the *Uniform Building Code*. This direct design procedure is a convenient and simple method to obtain equivalent lateral forces for seismic design and does not require extensive calculations beyond that for normal static analysis for vertical (gravity) loads. The direct design procedure is based, in part, on principles related to structural dynamics and past performance of buildings shaken during major earthquakes. Many parameters comprising the load-deformation behavior of the structure and the direct design procedure were investigated to determine their influence on the inelastic dynamic response of the steel moment-resisting frames arising from strong ground motion.

This investigation has contributed to the understanding of the design, analysis and response, and relationships between them for low-rise steel frame buildings. Of course, some of the findings are directly applicable to other types of lateral force-resisting systems, such as reinforced concrete moment-resisting frames or shear walls, or braced frames. In general, this study has shown the importance of accurate modelling of the dynamic behavior

of a building, so that the results from an analysis are meaningful, because the assumptions made in developing the numerical model for a building can and will influence the response. The calculation of the energy quantities, especially the hysteretic energy, provides another method to assess the anticipated demand on a structure from a given ground motion and the ability of the structure to distribute the demand throughout the entire structure.

Several general conclusions related to the application of the direct design procedure can be drawn from each of the parametric studies developed for this investigation.

#### 1. Design Base Shear

- The usage of a larger design base shear resulted in a more conservative design (smaller deformations and ductility demands), even though the larger design base shear required a stiffer structure that attracted more base shear during excitation. However, the maximum drifts in the upper stories were slightly larger than the expected maximum drifts.
- A reduction in the design base shear as allowed by the 1988 UBC resulted in larger deformations that in some stories exceeded the expected deformations by a factor of two.

#### 2. Configuration of Lateral Force-Resisting Frame

- The selection of the frame configuration, which had fewer members and connections providing the lateral resistance, primarily controlled the number of available locations for hysteretic energy dissipation.
- The inability to match closely the stiffness and strength requirements for a frame configuration when selecting the rolled I-sections for the



columns and beams resulted at times in an additional and unaccounted for factor of safety.

### 3. Participation of Nonstructural Elements

- The stiffness and strength contribution of nonstructural elements had a profound effect on the dynamic behavior of the structure and caused considerable increase in the calculated story shears. The maximum story drifts were quite small, less than one-half of one percent, if the nonstructural elements of a story did not endure much degradation.
- It was shown that under certain excitations the nonstructural elements suffered considerable damage (degradation) in a building with special moment-resisting space frames (SMRSF) as the lateral force-resisting system as a result of the disparity between the stiffness and ductility of the frame and the nonstructural elements.

### 4. Beam-to-Column Connection Behavior

- In general, the assumed connection behavior had little impact on the maximum story drifts and shears, or energy imparted into the building, since yielding at a joint regardless of the location prevented the transfer of moment between the columns and beams and resulted in the same effective stiffness and strength of a joint.
- The connection behavior did control the locations for hysteretic energy dissipation at a joint. In a weak panel zone, the yielding would occur in the panel zone prior to yielding of the columns or beams. Further research into the relationship between hysteretic energy and structural

damage may result in determining the optimum location for hysteretic energy dissipation at a joint.

#### 5. Column-to-Beam Strength Ratio

- For buildings in which a moment-resisting frames are only used along the perimeter to provide the entire lateral force resistance and stability for a building, a "strong beam-weak column" design as opposed to a "strong column-weak beam" design for the steel moment-resisting frames had little influence on the maximum deformation, because the stresses caused by the axial forces as compared to the bending moments were relatively small for the columns. Thus the interaction between the axial force acting on a column and the assumed yield moment at the column end was negligible.
- Even though the distribution of mass, stiffness and strength was fairly uniform for the D1A and D1B frame models, the maximum deformations during low levels of inelastic behavior were not that uniform over the height of the building. In fact, the maximum story drifts calculated in some stories were in some cases twice as large as the drifts in other stories. Hence, the dynamic response was not entirely depicted by the fundamental frequency which was assumed to have a linear mode shape, especially as the frame experienced some inelastic behavior.

#### 6. Building Height

- The code provisions to require a greater percentage of the building weight to be used as the design base shear produced results from the

time-history analyses of the two-story structure that were comparable to the five-story structures.

- The addition of nonstructural elements to a less stiff frame lead to a considerable increase in the lateral stiffness and strength. In fact, there was no inelastic behavior in the second story of the two-story frame model.

#### 7. Defective Connections

- The response of the frame models with initially defective connections (the inability to transfer moment) was basically the same as the frame without imperfections (defective connections), since the connections that were assumed defective would have yielded under the strong ground motion. Therefore, the ability to transfer moment between the columns and beams was limited.
- The influence of defective connections may be more substantial in a more moderate earthquake where the expected inelastic behavior of the lateral force-resisting system is much less, if any.

In general, the inelastic behavior for most of the frame models in this study was displeasing because the story drifts and ductility demands were larger than presumed for reliable structural performance and acceptable life safety. The maximum story drifts expected by the 1988 UBC as a result of excitation for the design earthquake are one and a half percent of the story height. At this story drift level, considerable damage to the nonstructural elements will occur if they are forced to conform to the deformations. In fact, if adequate precautions are not taken, the ability of the structural

frame to withstand this drift level may be compromised and premature failure of the elements or connection may result. In addition, it is desired to limit the inelastic story drifts so that second order effects (P-Delta) do not cause additional instability of the building. In general, a building that experiences controlled and limited deformations during severe ground excitation will survive without collapse and possibly be repairable for further occupancy.

The principal reason for the poor structural performance was that the dynamic behavior of the frame models generally was not compatible with the assumed behavior of the 1988 UBC. In other words, the actual supply of lateral stiffness and strength given by the frame model of a building was inconsistent with the demand calculated for the frame model arising from excitation with the design earthquake. One reason for the disparity between the expected response and the calculated response of the frame models can be attributed to the fact that the provisions for the direct design procedure are based, in part, on the past performance of buildings shaken during strong ground motion. It may be unrealistic to expect building designs based on current practice (moment-resisting frames along the perimeter, long bay spacings, smaller design gravity loads, etc.) to have the same general response of past building designs.

In view of the poor structural performance for some of the frame models of the lateral force-resisting system, improvements to the direct design procedure may be necessary. The proper amount of stiffness and strength for a building is necessary to ensure survivability of the structure in the event of a major earthquake. In addition, the design and analysis of a building also should be sensitive to the anticipated behavior of the

structure, so that sound judgement as to the adequacy of the lateral force-resisting system can be made with some reasonable assurance.

## 5.2 Design Implications

On the basis of this study, the suggested improvements to the direct design procedure of the 1988 edition of the *Uniform Building Code* are centered on reducing the inelastic deformations and ductility demands for the lateral force-resisting system of a building. Of course, the first prerequisite for good seismic design is to eliminate those factors that generally have lead to poor performance during past earthquakes; i.e. discontinuous paths for transfer of story shears, nonuniform vertical distributions of mass, stiffness and strength, plan and elevation irregularities, etc. The seismic design provisions in the 1988 UBC recognize that these factors tend to cause uneven ductility demands in a structure and thus disallow the usage of the direct design procedure for the seismic design of said "irregular" buildings.

The advantage of the direct design procedure is the simplicity of the method to obtain lateral forces for the seismic design. However, simplicity of method should not override the objective of meaningful design forces. Usage of the direct design procedure would be severely limited if detailed information about the dynamic behavior of a structure was required and would imply a level of accuracy that really is not warranted considering all of the unknown factors. Thus, any improvements to the direct design procedure should require as little information as possible (that which is readily available) and result in an adequate design regardless of the deviation from the assumed behavior of the structure. Since there are many factors that

influence the behavior of a building and that lead to a deviation from the assumed behavior, the design procedure should be conservative enough, so that the possible range in the behavior of the building will result in satisfactory performance during severe ground excitation.

The principal concern of the seismic design procedures in the 1988 UBC is the protection of life and not mitigation of structural and nonstructural damage from excitation arising from a major earthquake. Since significant inelastic behavior is permitted to occur during a major earthquake, the "ultimate" strength (increase in strength beyond minimum required strength) of the structure, rather than the stiffness, is more of a controlling factor in limiting the overall deformations. In addition, limitations of ductility demands for the various elements of the lateral force-resisting system will reduce the possibility of premature failure of a component due to low-cycle fatigue. The lateral stiffness of the building is important in determining the inertia forces applied to the structure during strong ground motions. The following recommendations are suggested to improve the performance of buildings designed in accordance with the direct design procedures of the 1988 edition of the *Uniform Building Code*.

1. The response modification factor,  $R_w$ , is too large for special moment-resisting space frames (SMRSF). A reduction of twelve from the elastic response level to the design level allows for too much inelastic behavior during severe excitation. In addition, the moment-resisting frames are required to undergo significant deformations to provide the necessary shear resistance thereby forcing failure of the more brittle nonstructural elements. Therefore, the usage of a smaller value of  $R_w$  would lessen the

disparity between the ductility of the lateral force-resisting system and the nonstructural elements. This may even be more important for limiting the nonstructural damage that occurs during a more moderate earthquake.

2. The direct design procedure recognizes the rare occurrence of a major earthquake by permitting inelastic behavior to occur during the event that may even render the structure unusable and necessitate demolition. However, the stress (strength) design for the direct design procedure also accounts for the low probability of having the full load condition for the loading combination of dead, live and earthquake forces by allowing for an additional one-third increase in the allowable stresses. For the design of perimeter moment-resisting frames, the allowable stress increase may be unjustified, because the equivalent lateral forces dominate the loading combination under any circumstance. Thus the allowable stress increase unconservatively reduces the required strength of the structure and induces larger deformations and ductility demands during severe ground excitation.

3. The calculation of the design base shear and subsequent equivalent lateral forces based on a fundamental period of vibration obtained from a trial design is inappropriate, especially when the trial design merely considers the stiffness of the lateral force-resisting system. Only after performing a dynamic analysis which considers the anticipated behavior of the building as a whole and a set of plausible ground acceleration records, could a reduction in the lateral stiffness and strength be justified. As adopted in the 1988 UBC, any type of reduction should not reduce the design

base shear below a specified percentage of the original design base shear for the trial design.

4. Another point of concern for the seismic design of buildings is the increasing trend toward reduction in the number of elements providing the lateral force resistance which in effect reduces the redundancy of the structure and ability to redistribute forces. The premature failure of a few members or connections as a result of defects or low-cycle fatigue could compromise the entire integrity of the lateral force-resisting system of a building and result in its total collapse. Thus, it may be advantageous to increase the margin of safety of a design by increasing the design base shear or reducing the allowable stresses as the redundancy is reduced.

5. The direct design procedure, which typically is dependent on just the stiffness and strength of the lateral force-resisting system, should consider the participation of nonstructural elements. As shown by the results of the parametric studies of this investigation, the nonstructural elements can alter significantly the dynamic behavior of a building if not isolated sufficiently from the lateral force-resisting system. Therefore, the classification of a structure as being regular or irregular should consider the stiffness and strength contribution of the nonstructural elements. Additional research on the behavior of nonstructural elements is required before this can be accomplished.



**APPENDIX A****DETAILS OF DRAIN-2D COMPUTER PROGRAM****A.1 Introduction**

A commercially available version of the DRAIN-2D computer program, which subsequently was modified for this study, was employed to compute the dynamic response of each planar modelling for the lateral force-resisting system of a building. The modifications to DRAIN-2D enabled time histories of story shears and energy related quantities to be calculated. Additional minor modifications altered the format of the input data and output results.

In order to understand the derivation of the energy equations, the beginning sections of this appendix detail the formulation of the mass, damping and stiffness matrices for the DRAIN-2D analyses, the behavior of the finite elements used in the modelling of the frames and the solution procedure implemented in DRAIN-2D for the equations of motion. The final section contains the formulation of the energy expressions that were added to the DRAIN-2D computer program.

**A.2 DRAIN-2D Program Capabilities**

DRAIN-2D is a general purpose program for computing inelastic dynamic responses of structures whose behavior can be represented with planar modelling [25,41]. The structural model is an assemblage of planar elements adjoined at nodal points. Each node typically has horizontal, vertical and rotational displacement degrees of freedom. However, nodal constraints can be imposed to eliminate nodal degrees of freedom from the global degrees of freedom and combine nodal degrees of freedom into one global degree of

freedom. The support points of a structure can be excited by independent vertical and horizontal acceleration records. Although, all support points for each of the translations are excited in phase.

### **A.3 Formulation of Mass, Damping and Stiffness Matrices**

The formulation of the mass, damping and stiffness matrices influences the solution procedure for solving the equations of motion at each time step. The latitude on formulation of the mass, damping and stiffness matrices can be very broad for inelastic dynamic analyses. However to improve the efficiency of the program and limit the complexity of the modelling, several restrictions are imposed in the DRAIN-2D program.

#### **A.3.1 Mass Matrix**

The mass of a structure is lumped at the nodes (degrees of freedom). The mass quantity associated with the vertical and horizontal translations and rotation of a node may be different. The displacement constraints are used to map the mass of each nodal degree of freedom to the accumulative mass of the global degrees of freedom. The mass matrix has a diagonal form, as a result of mass being lumped. A diagonal mass matrix eliminates the coupling of degrees of freedom through the mass matrix.

#### **A.3.2 Damping Matrix**

A modal damping formulation is used to obtain a viscous damping matrix for the equations of motion. Although not required for time-history analysis, modal damping is a convenient (physically relatable) form for specifying the damping associated with the structural response [17,44]. The

DRAIN-2D damping matrix is a linear combination of the mass and stiffness matrices and can be expressed as

$$\mathbf{C} = a \mathbf{M} + b \mathbf{K} , \quad (\text{A.1})$$

where  $\mathbf{C}$  is the viscous damping matrix,  $a$  is the mass proportional damping coefficient,  $\mathbf{M}$  is the time independent mass matrix,  $b$  is the stiffness proportional damping coefficient and  $\mathbf{K}$  is the time dependent tangent stiffness matrix.

Damping is time dependent if the damping matrix is proportional to the stiffness matrix. The proportionality constants are determined from the initial stiffness matrix. In a nonlinear analysis, the usage of "damping ratios" to define damping is deceptive. The stiffness of the structure may vary during an analysis and as a consequence the natural frequencies and mode shapes are not constant. As shown by Equation A.1, the damping in the structure is reduced as the structure yields.

A damping matrix proportional only to the mass matrix produces damping ratios which are inversely proportional to the frequencies of vibration. In contrast, stiffness proportional damping is directly proportional to the frequencies of vibration. Since the contribution of the higher modes is not of interest in this study, stiffness proportional damping was used to damp out the higher modes. Using both stiffness and mass proportional allows the damping ratio of two modes of vibration to be exactly specified. The relationship between the damping of a frequency and the proportionality constants for the mass and stiffness matrices is given by

$$\xi_i = \frac{1}{2} \left( \frac{a}{\omega_i} + b\omega_i \right) , \quad (\text{A.2})$$

where  $\omega_i$  is the natural frequency of vibration and  $\xi_i$  is the damping ratio of the  $i^{\text{th}}$  mode.

The damping ratios of the lowest two modes of vibration was specified to be five percent, since the so-called design spectrum for the direct design procedure in each of the various building codes are based on five percent damping [4,16,43]. The equations for five percent damping in the lowest two modes of vibration are derived from Equation A.2 and may be written as

$$\xi_1 = 0.05 = \frac{1}{2} \left( \frac{a}{\omega_1} + b\omega_1 \right) \quad (\text{A.3a})$$

$$\text{and } \xi_2 = 0.05 = \frac{1}{2} \left( \frac{a}{\omega_2} + b\omega_2 \right) . \quad (\text{A.3b})$$

From the above equations, the coefficients,  $a$  and  $b$ , are dependent on the frequency of vibration of the two modes. The solution of Equations A.3a and A.3b for the proportionality constants gives

$$a = \frac{0.1\omega_1\omega_2}{\omega_1 + \omega_2} \quad (\text{A.4a})$$

$$\text{and } b = \frac{0.1}{\omega_1 + \omega_2} . \quad (\text{A.4b})$$

### A.3.3 Stiffness Matrix

The stiffness matrix of a model is assembled from the material and geometric (P-Delta) stiffness contribution of each element. The stiffness matrix is formulated and triangulated at the beginning on an analysis. In the inelastic time-history analysis procedure, the structure does not have a stiffness change during a time step. However, a change in stiffness can

occur between any two time steps. When a change in stiffness is detected, the stiffness matrix is reformulated and then triangulated.

#### **A.4 Behavior of Finite Elements**

The finite elements or discrete elements, contained in the DRAIN-2D element library, are representative of building components. Beam-column and beam elements are used to model the behavior of columns and beams. Connection elements, which models the panel zone, transfer moment between the beams and columns framing into each joint. Shear panel elements account for the shear stiffness and strength of the nonstructural elements.

##### **A.4.1 Beam-Column Element**

The three modes of deformation in the beam-column element are axial extension, flexural rotation at one end and flexural rotation at the other end. The axial stiffness and flexural stiffness are defined by the modulus of elasticity, moment of inertia, cross sectional area and length of the prismatic member. Yielding only can occur in concentrated plastic hinges located at the ends of the member.

The location of a plastic hinge can be translated along the member centerline by specifying an end eccentricity. For example, vertical eccentricities at the column connections and horizontal eccentricities at the beam connections can be specified to move the plastic hinge locations from the intersection of the beam and column centerlines to the connection faces of joint (edges of panel zone). As shown in Figure A.1, the physical interpretation of an end eccentricity is a rigid and infinitely strong link between the node and the desired hinge location within the element.

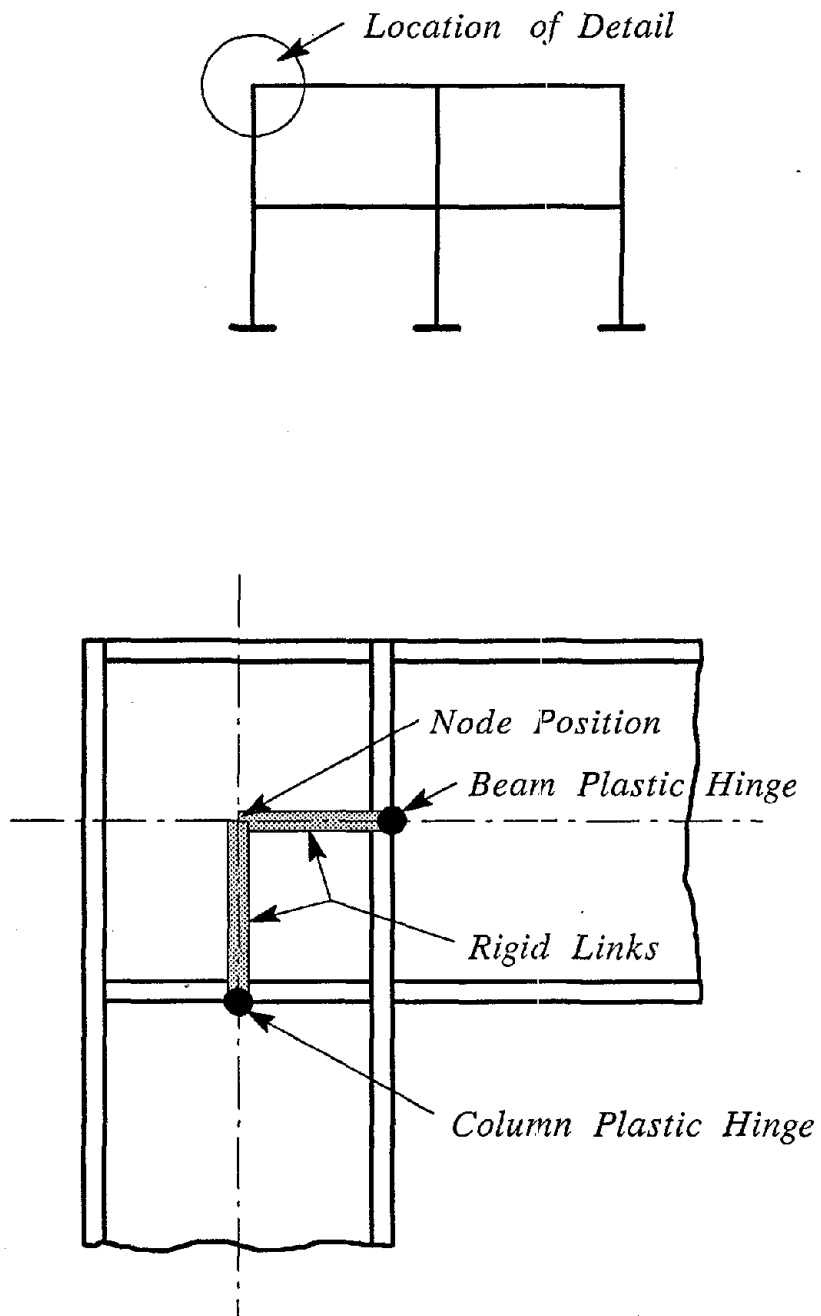
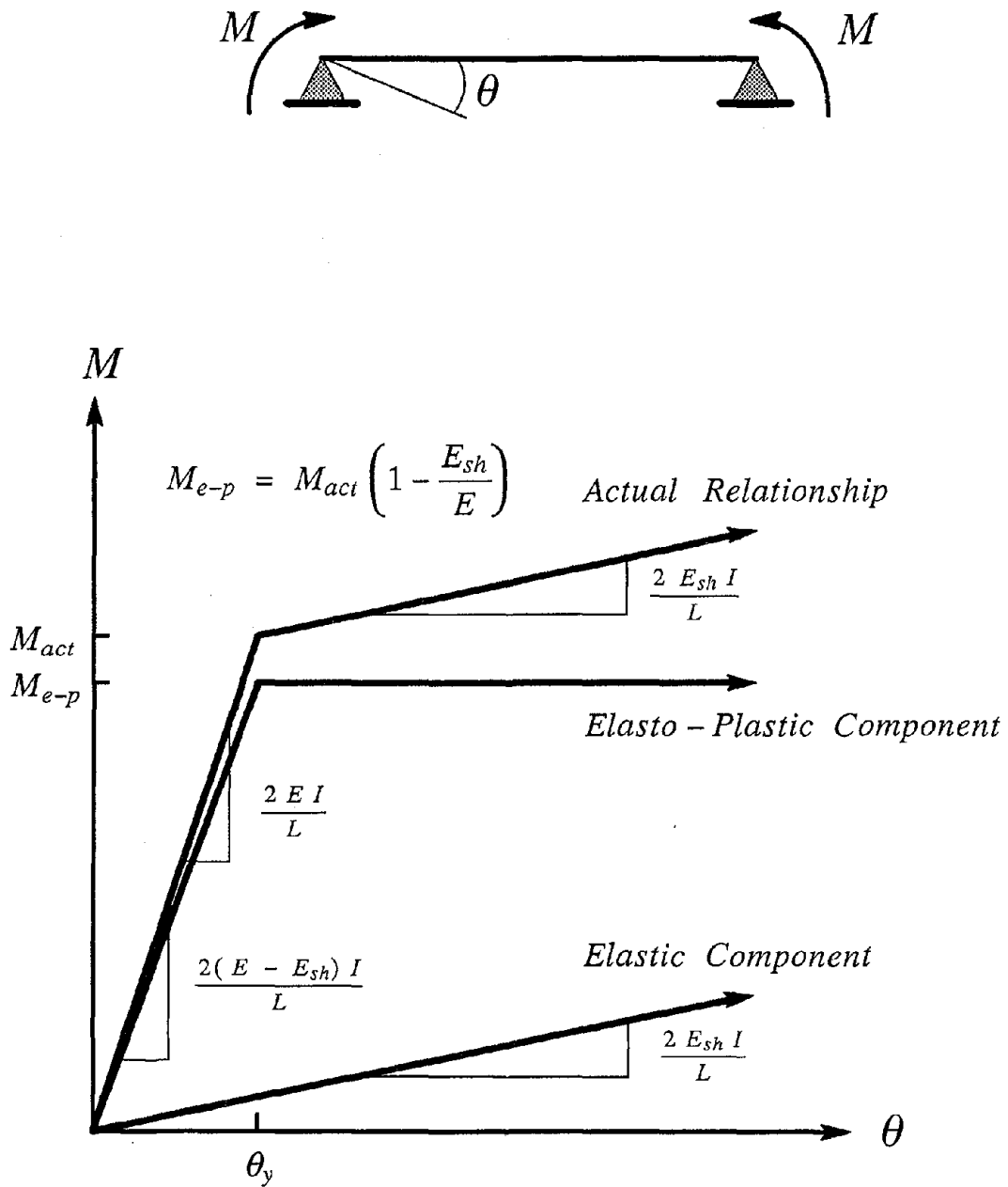


FIGURE A.1 Physical Interpretation of End Eccentricities

A bilinear curve represents the moment-rotation relationship at the ends of the beam-column element. The strain hardening is approximated with elastic and elasto-plastic components acting in parallel. At each member end the rotation of both components is the same. As shown in Figure A.2, the total moment related to the end rotation of a member is equal to the sum of the moments for each component. At a time step, the yield moment for the elasto-plastic component is governed by an interaction surface relating the axial force and bending moment acting on the element. Unloading of the elasto-plastic component occurs along the initial stiffness slope.

The general shape of an interaction surface is shown in Figure A.3a. The maximum positive and negative yield moments, as well as, the maximum tension and compression yield forces can be different. The yield moment coordinate of points *A* and *C* is a specified percentage of the maximum positive yield moment, and the axial force coordinate of each point is the same specified percentage of the respective maximum axial force. The coordinates of points *B* and *D* follow the same rules, except for using the maximum negative yield moment.

As shown in Figure A.3b, a suitable interaction surface for modelling steel I-sections has maximum positive and negative yield moments equal to the plastic moment and tension and compression yield forces equal to the product of the cross sectional area and yield stress. The bending moment coordinate at points *A*, *B*, *C* and *D* is equal to the plastic moment, while the axial force coordinate is equal to fifteen percent of the maximum axial force. This surface mirrors the interaction equations for the codes. That is, if the axial force is less than fifteen percent of the allowable, the interaction between the axial force and moment is ignored [2,4,16,24].



● FIGURE A.2 Decomposition of Moment-Rotation Relationship



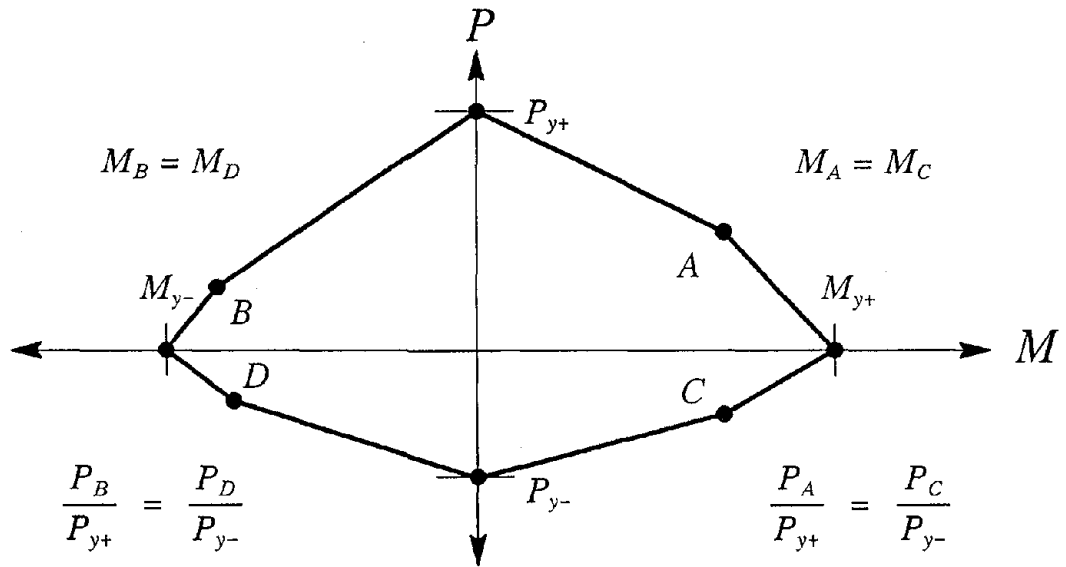


FIGURE A.3a General Shape of Interaction Surface

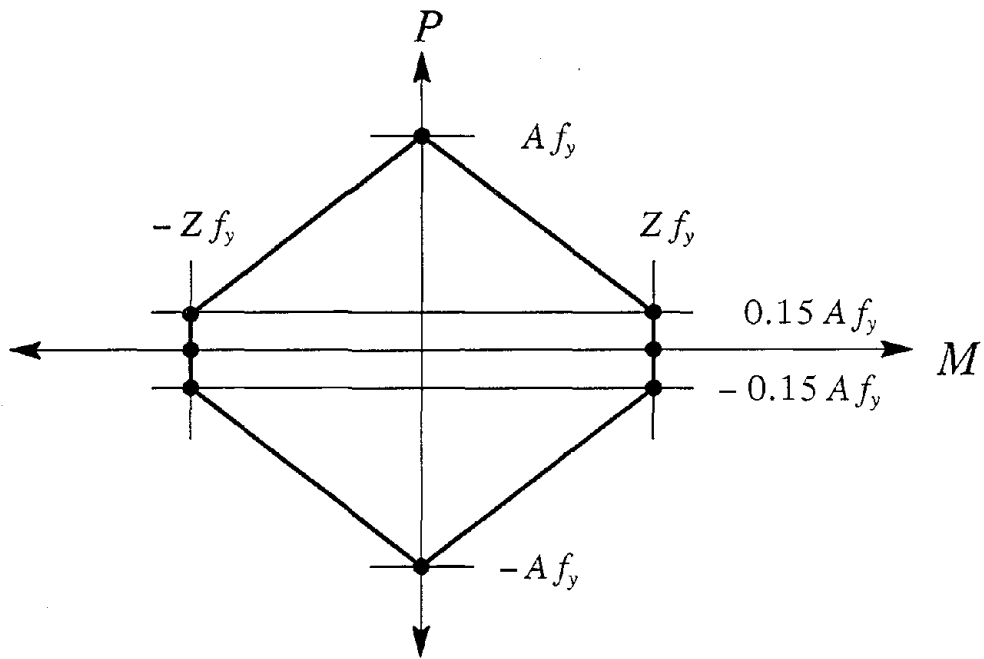


FIGURE A.3b Interaction Surface for Steel I-Section

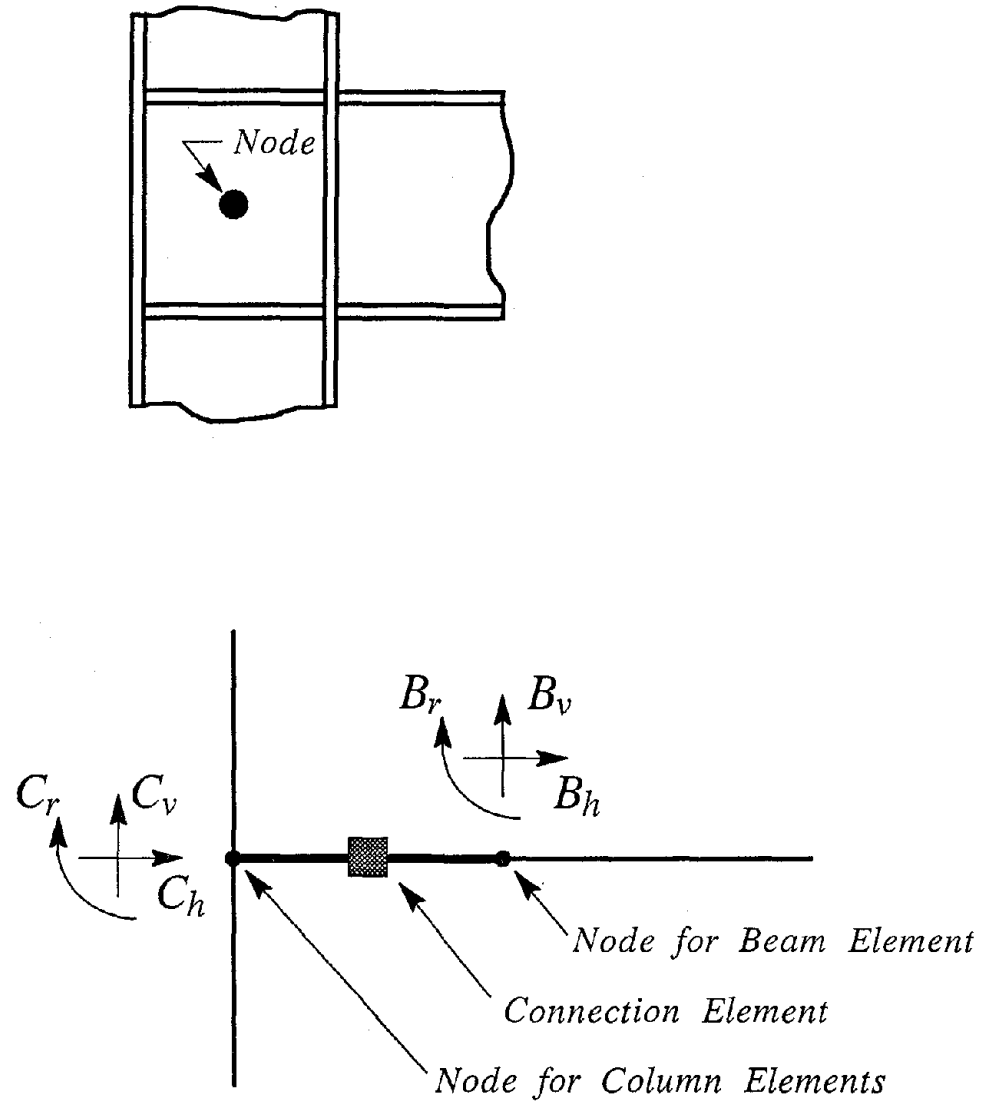
In the beam-column element, the geometric stiffness contribution is a linear approximation, since only the axial force acting on the member and relative lateral displacement of the element ends are considered [32]. When the axial force in the member is compressive, the relative lateral stiffness of the element is reduced, while a tensile force increases the stiffness. The physical interpretation of the geometric stiffness is an additional lateral force couple applied to the ends of the member. The moment from the force couple is equal to the axial force times the relative lateral displacement. The geometric stiffness matrix of an element is assembled at the start of an analyses using the static axial force acting in the member.

#### A.4.2 Beam Element

The properties of the beam element are identical to the beam-column element, except for a constant yield moment (independent of the axial force acting in member). If an interaction surface was used it would be a set of parallel vertical lines, one intersecting the x-axis at the positive yield moment and the other at the negative yield moment. The beam element is computationally more efficient than the beam-column element, because an interaction surface is not needed to determine the yield moment. The results from this study would be the same regardless of using beam-column or beam elements to model the beams. The beams had no axial deformation and consequently no axial force, because the horizontal translations of the nodes within each story level were constrained to be identical. The location on the interaction surface would have been at the intersection with the moment axis (x-axis).

#### A.4.3 Connection Element

The connection element is essentially a rotational spring element, which transfers moment between the columns and beams framing into a joint. The connection element is attached to two nodes located at the same point in space. One of these nodes is attached to the element(s) modelling the columns framing into the joint, while the other node is attached to the element(s) modelling the beams. Therefore, the moment transferred by the connection element is related to the relative rotation between the columns and beams framing into a joint. The vertical and horizontal translations of the two nodes are constrained to be identical so that the beam and column ends move together. Therefore, one vertical, one horizontal and two rotational degrees of freedom exist at each joint. The idealization of a typical beam-to-column connection is shown in Figure A.4. The definable properties of a connection element are the rotational stiffness, strain hardening stiffness, and positive and negative yield moment. The inelastic relationship between the rotational moment and relative rotation between the members is represented by a bilinear curve. The strain hardening stiffness also is approximated with elastic and elasto-plastic components acting in parallel. The connection element ignores the actual physical dimensions of the rigid beam-to-column connection.



Notes : Both nodes located at same point in space

Constraints :  $C_h = B_h$

$C_v = B_v$

FIGURE A.4 Idealization of Beam-to-Column Connection

#### A.4.4 Shear Panel Element

The shear panel element is a rectangular four-noded element, having only shear stiffness. The shear resistance is defined by the shear modulus, strain hardening shear modulus, yield shear stress, failure strain and physical dimensions. The relationship between the shear stress and shear strain may be inelastic. Again a bilinear curve represents the shear stress-strain relationship. Shear modulus hardening is approximated with elastic and elasto-plastic components acting in parallel. The element also can fail upon reaching a prescribed failure strain. Failure results in either complete loss of stiffness and strength or retainment of only the elastic component of the stiffness and strength.

#### A.5 Equations of Motion

For inelastic nonlinear time-history analysis, the solution procedure can be thought of as a series of solutions for a linear structure with varying stiffness. The response quantities at the end of each time step become the initial conditions for the succeeding time step. The stiffness matrix is reevaluated at the end of each time step based on the calculated displacements. If yielding or hardening of a member has occurred, the stiffness matrix is updated, and residual forces are applied to the nodes to maintain equilibrium at the end of the time step. The residual forces are added to the nodal forces of the succeeding time step. The magnitude of the residual forces should remain small in comparison to the other nodal forces in order to maintain the accuracy of the analysis.

The solution of the incremental equations of motion is simply the change in displacement, velocity and acceleration of the structure from one

time step to the next resulting from the change in external loading (ground excitation). The incremental form of the equations of motion is given by

$$\mathbf{M} \Delta \ddot{\mathbf{U}} + \mathbf{C} \Delta \dot{\mathbf{U}} + \mathbf{K} \Delta \mathbf{U} = -\mathbf{M} \Delta \ddot{\mathbf{Y}} + \mathbf{P} + \mathbf{R} , \quad (\text{A.5})$$

where  $\Delta \mathbf{U}$  is the incremental relative displacement vector (dots over variable indicating derivatives with respect to time, namely velocity and acceleration),  $\Delta \ddot{\mathbf{Y}}$  is the incremental ground acceleration vector,  $\mathbf{P}$  is the time independent external nodal force vector and  $\mathbf{R}$  is the residual force vector.

The solution procedure uses Newmark's Beta Method, a step by step integration procedure, to solve the incremental equations of motion [34]. The  $\beta$  value of  $\frac{1}{4}$ , which has an physical interpretation of constant average acceleration (average of acceleration at beginning and end of time step) through the time step interval is imbedded within the program. The acceleration, velocity and displacement within a time step is expressed by the following three equations:

$$\ddot{\mathbf{U}}(t+\tau) = \frac{1}{2} \left\{ \ddot{\mathbf{U}}(t) + \ddot{\mathbf{U}}(t+\Delta t) \right\} ; \quad (\text{A.6})$$

$$\dot{\mathbf{U}}(t+\tau) = \dot{\mathbf{U}}(t) + \frac{\tau}{2} \left\{ \ddot{\mathbf{U}}(t) + \ddot{\mathbf{U}}(t+\tau) \right\} ; \quad (\text{A.7})$$

$$\mathbf{U}(t+\tau) = \mathbf{U}(t) + \tau \dot{\mathbf{U}}(t) + \frac{\tau^2}{4} \left\{ \ddot{\mathbf{U}}(t) + \ddot{\mathbf{U}}(t+\tau) \right\} , \quad (\text{A.8})$$

where  $\tau$  is between zero and  $\Delta t$ , the time step increment.

The velocity and displacement at the end of a time step are found from Equations A.7 and A.8, when  $\tau$  equals  $\Delta t$ . The incremental accelerations and velocities as a function of the current response quantities and incremental

displacements are found by rearrangement of Equations A.7 and A.8, and can be written as

$$\Delta \ddot{\mathbf{U}} = -2 \ddot{\mathbf{U}}(t) - \frac{4}{\Delta t} \dot{\mathbf{U}}(t) + \frac{4}{\Delta t^2} \Delta \mathbf{U} \quad (\text{A.9})$$

$$\text{and } \Delta \dot{\mathbf{U}} = -2 \dot{\mathbf{U}}(t) + \frac{2}{\Delta t} \Delta \mathbf{U} . \quad (\text{A.10})$$

The equations of motion are rewritten in terms of the unknown incremental displacements by substitution of Equations A.9 and A.10 into Equation A.5, namely

$$\begin{aligned} \mathbf{M} \left\{ -2 \ddot{\mathbf{U}}(t) - \frac{4}{\Delta t} \dot{\mathbf{U}}(t) + \frac{4}{\Delta t^2} \Delta \mathbf{U} \right\} + \mathbf{C} \left\{ -2 \dot{\mathbf{U}}(t) + \frac{2}{\Delta t} \Delta \mathbf{U} \right\} + \mathbf{K} \Delta \mathbf{U} \\ = -\mathbf{M} \Delta \ddot{\mathbf{Y}} + \mathbf{P} + \mathbf{R} . \end{aligned} \quad (\text{A.11})$$

The above equation can be expressed as a set of equations reassembling the displacement method of analysis for static forces using the form:

$$\bar{\mathbf{K}} \Delta \mathbf{U} = \bar{\mathbf{P}} ; \quad (\text{A.12})$$

in which,

$$\bar{\mathbf{K}} = \mathbf{K} + \frac{4}{\Delta t^2} \mathbf{M} + \frac{2}{\Delta t} \mathbf{C} \quad (\text{A.13})$$

$$\text{and } \bar{\mathbf{P}} = \mathbf{P} + \mathbf{M} \left\{ -\Delta \ddot{\mathbf{Y}} + 2 \ddot{\mathbf{U}}(t) + \frac{4}{\Delta t} \dot{\mathbf{U}}(t) \right\} + 2 \mathbf{C} \dot{\mathbf{U}}(t) + \mathbf{R} . \quad (\text{A.14})$$

$\bar{\mathbf{K}}$  is usually called the effective stiffness matrix or the pseudo-static stiffness matrix, while  $\bar{\mathbf{P}}$  is called the effective load vector or the pseudo-static load vector, since the form of Equation A.12 resembles the formulation for a static analysis of a system.

Since the form of the damping matrix is a linear combination of the mass and stiffness matrices, the substitution of Equation A.1 into Equations A.13 and A.14 results in equations of the form:

$$\bar{\mathbf{K}} = \left(1 + \frac{2b}{\Delta t}\right) \mathbf{K} + \left(\frac{4}{\Delta t^2} + \frac{2a}{\Delta t}\right) \mathbf{M} \quad (\text{A.15})$$

$$\text{and } \bar{\mathbf{P}} = \mathbf{P} + \mathbf{M} \left\{ -\Delta \ddot{\mathbf{Y}} + 2 \ddot{\mathbf{U}}(t) + \left(\frac{4}{\Delta t} + 2a\right) \dot{\mathbf{U}}(t) \right\} + 2b \mathbf{K} \dot{\mathbf{U}}(t) + \mathbf{R} . \quad (\text{A.16})$$

During a time history analysis,  $\bar{\mathbf{K}}$  only needs to be reformulated after a change in stiffness, since  $\mathbf{K}$  is the only time dependent variable in the equation. However,  $\bar{\mathbf{P}}$  must be reformulated at every time step, since there are several time dependent variables. The time required to determine  $\bar{\mathbf{P}}$  is increased considerably with inclusion of stiffness proportional damping, since a vector-matrix multiplication is required. The vector-matrix multiplication is eliminated if the following transformation is introduced:

$$\Delta \bar{\mathbf{U}} = \Delta \mathbf{U} + b \Delta \dot{\mathbf{U}} = \left(\frac{2b}{\Delta t} + 1\right) \Delta \mathbf{U} - 2b \dot{\mathbf{U}}(t) . \quad (\text{A.17})$$

Equation A.17 maybe recast in another form, namely

$$\Delta \mathbf{U} = \frac{\Delta t}{2b + \Delta t} \left\{ \Delta \bar{\mathbf{U}} + 2b \dot{\mathbf{U}}(t) \right\} . \quad (\text{A.18})$$

Substitution of Equation A.18 into Equation A.11 leads to the following:

$$\bar{\mathbf{K}} \Delta \bar{\mathbf{U}} = \bar{\mathbf{P}} ; \quad (\text{A.19})$$

in which,

$$\bar{\mathbf{K}} = \mathbf{K} + \left(\frac{4 + 2a\Delta t}{4b\Delta t + \Delta t^2}\right) \mathbf{M} \quad (\text{A.20})$$



$$\text{and } \bar{P} = P + M \left\{ -\Delta \ddot{Y} + 2 \ddot{U}(t) + \left[ \frac{4}{\Delta t} + 2a + \frac{8b + 2ab\Delta t}{2b\Delta t + \Delta t^2} \right] \dot{U}(t) \right\} + R . \quad (\text{A.21})$$

The solution procedure for the incremental response of the current time step is:

- 1) Reformulate  $\bar{K}$ , if stiffness update has occurred (Equation A.20);
- 2) Reformulate  $\bar{P}$  for the current time step (Equation A.21);
- 3) Solve for  $\Delta \bar{U}$  (Equation A.19);
- 4) Transform  $\Delta \bar{U}$  into  $\Delta U$  (Equation A.18);
- 5) Calculate  $\Delta \ddot{U}$  and  $\Delta \dot{U}$  (Equations A.9 and A.10).

The total response at the end of the current time step is the total response from the previous time step plus the incremental quantity or in equation form:

$$U(t+\Delta t) = U(t) + \Delta U ; \quad (\text{A.22a})$$

$$\dot{U}(t+\Delta t) = \dot{U}(t) + \Delta \dot{U} ; \quad (\text{A.22b})$$

$$\ddot{U}(t+\Delta t) = \ddot{U}(t) + \Delta \ddot{U} . \quad (\text{A.22c})$$

The elemental forces are calculated from the nodal displacements. If the current yield state of an element is not compatible with the elemental forces, the stiffness matrix is updated and residual loads are applied to maintain equilibrium.

## A.6 Energy Expressions

An energy balance expression is obtained by integration of the terms (inertia, damping, resisting and external forces) in the equations of motion through the displacements [48]. The set of forces obtained from the

solution to the equations of motion maintains equilibrium at each degree of freedom or in others words, the sum of the forces in the set is equal to zero. The integration of this set of forces through the same distance gives zero energy. However, the energy quantities associated with the individual integration of each nodal force through the displacement provides additional information to evaluate the response of a structure.

Instead of integration of the forces through the nodal displacements, a more advantageous integration is possible by substituting  $\dot{U}dt$  for  $dU$ . The energy balance at any time,  $T$ , is given by

$$\begin{aligned} & \int_0^T \dot{U}^T(t) M \ddot{U}(t) dt + \int_0^T \dot{U}^T(t) C \dot{U}(t) dt + \int_0^T \dot{U}^T(t) K U(t) dt \\ & = -\int_0^T \dot{U}^T(t) M \ddot{Y}(t) dt + \int_0^T \dot{U}^T(t) P dt + \int_0^T \dot{U}^T(t) R dt . \end{aligned} \quad (\text{A.23})$$

The individual integration of the three terms on the left hand side of the Equation A.23 represent the kinetic, damping and elastic strain plus plastic strain (hysteretic) energies. The terms on the right hand side represent the energy imparted into a structure from ground acceleration, external nodal forces and residual forces. The energy associated with the residual forces is insignificant when the residual forces remain small.

The kinetic and elastic strain energies are recoverable (stored in the vibrating structure), while the damping and hysteretic energies are dissipated by the structure during the excitation. The accumulative kinetic and elastic strain energies can be calculated at the end of any time step, because they are instantaneous quantities (function of the current state of response). However, the input, damping and hysteretic energies must be

calculated as the sum of the incremental quantities of each time step. The incremental energy quantities can be integrated, because the value of  $\beta$  in Newmark's method determines the variation of acceleration, velocity and displacement through an individual time step interval. In the case of  $\beta$  equal to  $\frac{1}{4}$  (constant acceleration), the change in velocity within a time step is linear (first order), and change in displacement is parabolic (second order).

The incremental input energy (taken from Equation A.23) for each time step is expressed as

$$\Delta IE = -\int_t^{t+\Delta t} \dot{U}^T(\tau) \mathbf{M} \ddot{\mathbf{Y}}(\tau) d\tau + \int_t^{t+\Delta t} \dot{U}^T(\tau) \mathbf{P} d\tau + \int_t^{t+\Delta t} \dot{U}^T(\tau) \mathbf{R} d\tau . \quad (\text{A.24})$$

Since the mass matrix is diagonal, Equation A.24 to be expanded as

$$\begin{aligned} \Delta IE &= \sum_{i=1}^n \left[ -\int_t^{t+\Delta t} \dot{u}_i(\tau) m_{i,i} \ddot{y}_i(\tau) d\tau + \int_t^{t+\Delta t} \dot{u}_i(\tau) p_i d\tau + \int_t^{t+\Delta t} \dot{u}_i(\tau) r_i d\tau \right] \\ &= \sum_{i=1}^n \int_t^{t+\Delta t} \dot{u}_i(\tau) \left[ -m_{i,i} \ddot{y}_i(\tau) + p_i + r_i \right] d\tau , \end{aligned} \quad (\text{A.25})$$

where  $n$  equals the number of degrees of freedom and the subscripted terms are individual terms within the various matrices.

The above equation can be integrated by using Equations A.6 and A.7, which give the variation of acceleration and velocity through a time step. The incremental input energy as a function on the initial and incremental response quantities is given by

$$\Delta IE = \Delta t \sum_{i=1}^n \left[ \dot{u}_i(t) + \frac{1}{2} \Delta \dot{u}_i \right] \left[ -m_{ii} \left[ \ddot{y}_i(t) + \frac{1}{2} \Delta \ddot{y}_i \right] + p_i + r_i \right] . \quad (\text{A.26})$$

The input energy calculation added to the DRAIN-2D program disregards the residual term, and as a consequence the energy expression does not balance when numerical instabilities occur in an analysis. The energy balance is used as a check to determine the adequacy of the modelling of the structure and time step increment in the solution procedure.

The kinetic energy at time,  $T$ , is expressed as

$$KE(T) = \int_0^T \dot{\mathbf{U}}^T(t) \mathbf{M} \ddot{\mathbf{U}}(t) dt . \quad (\text{A.27})$$

Since the mass matrix is diagonal, Equation A.27 may be rewritten in summation notation as

$$KE(T) = \sum_{i=1}^n \int_0^T \dot{u}_i(t) m_{ii} \ddot{u}_i(t) dt . \quad (\text{A.28})$$

Equation A.28, which is uncoupled by the diagonal mass matrix, can be directly integrated using partial integration. The integrated expression for kinetic energy, which is a function of the initial and final velocities of each of the lumped masses is written as:

$$KE(T) = \frac{1}{2} \sum_{i=1}^n \left[ \dot{u}_i(t) m_{ii} \dot{u}_i(t) \Big|_0^T \right] . \quad (\text{A.29})$$

If the structure is initially at rest, Equation A.29 can be rewritten as

$$KE(T) = \frac{1}{2} \sum_{i=1}^n \left[ \dot{u}_i(T) m_{i,i} \dot{u}_i(T) \right] . \quad (A.30)$$

As shown by the above equation, kinetic energy is no longer stored in the structure after the excited structure comes to rest. However, during an analysis the kinetic energy fluctuates as the structure responds.

The incremental viscous damping energy dissipated within a time step is given by

$$\Delta DE = \int_t^{t+\Delta t} \dot{U}^T(\tau) C \dot{U}(\tau) d\tau . \quad (A.31)$$

At this point Equation A.30 can be rewritten in the following expanded form:

$$\Delta DE = \sum_{i=1}^n \sum_{j=1}^n \int_t^{t+\Delta t} \dot{u}_i(\tau) c_{i,j} \dot{u}_j(\tau) d\tau . \quad (A.32)$$

The above equation can be integrated by using Equations A.6 and A.7, which give the variation of acceleration and velocity through a time step. The incremental damping energy as a function on the initial and incremental response quantities is expressed as

$$\begin{aligned} \Delta DE = \Delta t \sum_{i=1}^n \sum_{j=1}^n c_{i,j} \left[ \dot{u}_i(t) \dot{u}_j(t) + \frac{1}{2} \left[ \dot{u}_i(t) \Delta \dot{u}_j + \dot{u}_j(t) \Delta \dot{u}_i \right] \right. \\ \left. + \frac{1}{3} \Delta \dot{u}_i \Delta \dot{u}_j \right] . \end{aligned} \quad (A.33)$$

Since the damping matrix is proportional to the mass and stiffness matrices, Equation A.33 can be restated as

$$\begin{aligned}
\Delta DE = & a\Delta t \sum_{i=1}^n m_{i1} \left[ \dot{u}_i(t) \dot{u}_i(t) + \dot{u}_i(t) \Delta \dot{u}_i + \frac{1}{3} \Delta \dot{u}_i \Delta \dot{u}_i \right] \\
& + b\Delta t \sum_{i=1}^n \sum_{j=1}^n k_{ij} \left[ \dot{u}_i(t) \dot{u}_j(t) + \frac{1}{2} \left[ \dot{u}_i(t) \Delta \dot{u}_j + \dot{u}_j(t) \Delta \dot{u}_i \right] \right. \\
& \left. + \frac{1}{3} \Delta \dot{u}_i \Delta \dot{u}_j \right] .
\end{aligned} \tag{A.34}$$

If  $\beta$  equals zero, the incremental damping energy expression can be simplified to

$$\begin{aligned}
\Delta DE = & \frac{a\Delta t}{3} \sum_{i=1}^n m_{i1} \left[ \dot{u}_i(t) \dot{u}_i(t) + \dot{u}_i(t) \dot{u}_i(t+\Delta t) \right. \\
& \left. + \dot{u}_i(t+\Delta t) \dot{u}_i(t+\Delta t) \right] .
\end{aligned} \tag{A.35}$$

The damping energy is calculated in one of two methods. If the damping matrix is proportional to the stiffness matrix, the damping energy is calculated as the difference between the input energy and the sum of the kinetic, elastic strain and hysteretic energies. Otherwise, the damping energy is calculated with Equation A.35.

The incremental elastic strain and hysteretic energy of a time step is given by

$$\Delta SE + \Delta HE = \int_t^{t+\Delta t} \dot{U}^T(\tau) \mathbf{K} \mathbf{U}(\tau) d\tau . \tag{A.36}$$

One shortcoming with Equation A.36 is that the strain and hysteretic energy quantities cannot be separated. Instead of using the Equation A.36, the strain and hysteretic energy may be calculated individually for each

element. Since the elastic strain energy is an instantaneous quantity, the calculation of elastic strain energy need not be on an incremental basis.

The elastic strain energy associated with only bending of either a beam-column or beam element is given by

$$SE = \int_0^L \frac{M^2(x)}{2EI} dx , \quad (A.37)$$

where  $M(x)$  is the variation of bending moment along the member,  $E$  is Young's modulus and  $I$  is the moment of inertia.

Since the stiffness ( $EI$ ) is constant and the variation of moment is linear over the length of the beam, the integration of Equation A.37 gives an equation of the form:

$$SE = \frac{L}{6EI} \left[ M^2(0) + M(0)M(L) + M^2(L) \right] . \quad (A.38)$$

where  $M(0)$  is the bending moment at one end and  $M(L)$  is the bending moment at the other end.

The elastic strain energy associated with the elasto-plastic and elastic components of the bilinear decomposition is given by the following two equations:

$$\hat{SE} = \frac{L}{6(E-E_{sh})I} \left[ \hat{M}^2(0) + \hat{M}(0)\hat{M}(L) + \hat{M}^2(L) \right] ; \quad (A.39a)$$

$$\tilde{SE} = \frac{L}{6E_{sh}I} \left[ \tilde{M}^2(0) + \tilde{M}(0)\tilde{M}(L) + \tilde{M}^2(L) \right] , \quad (A.39b)$$

where  $E_{sh}$  is the strain hardening modulus. The variables with carats are associated with the elasto-plastic component, while the variables with the

tildes are associated with the elastic component. The maximum value of  $M(0)$  and  $M(L)$  in Equation A.39a is the yield moment of the elasto-plastic component.

The elastic strain energy from rotation of a connection element is expressed as

$$SE = \frac{M^2}{2K}, \quad (A.40)$$

where  $M$  is the bending moment and  $K$  is the rotation stiffness of the connection element.

The elastic strain energy associated with the elasto-plastic and elastic components of the bilinear decomposition is given by the following two equations:

$$\hat{SE} = \frac{\hat{M}^2}{2(K-K_{sh})}; \quad (A.41a)$$

$$\tilde{SE} = \frac{\tilde{M}^2}{2K_{sh}}, \quad (A.41b)$$

where  $K_{sh}$  is the strain hardening stiffness.

The elastic strain energy from shear deformation of a shear panel element is given by

$$SE = \frac{V \tau^2}{2G}, \quad (A.42)$$

where  $\tau$  is the shear stress,  $G$  is the shear modulus and  $V$  is the volume of the shear panel element. It should be noted that the shear panel element only can resist shear forces.



The elastic strain energy associated with the elasto-plastic and elastic components of the bilinear decomposition is given by the following two equations:

$$\hat{S}E = \frac{V \hat{\tau}^2}{2(G-G_{sh})} ; \quad (A.43a)$$

$$\tilde{S}E = \frac{V \tilde{\tau}^2}{2G_{sh}} , \quad (A.43b)$$

where  $G_{sh}$  is the strain hardening shear modulus.

The incremental hysteretic energy from plastic hinge rotation of both ends of either the beam-column or beam element is given by

$$\Delta HE = \Delta\theta(0) \hat{M}_y(0) + \Delta\theta(L) \hat{M}_y(L) , \quad (A.44)$$

where  $\Delta\theta$  is the incremental plastic end rotation and  $\hat{M}_y$  is the yield moment of the elasto-plastic component.

The incremental hysteretic energy from inelastic rotation of the connection element is expressed as

$$\Delta HE = \Delta\theta \hat{M}_y . \quad (A.45)$$

The incremental hysteretic energy from inelastic deformation of the shear panel element is given by

$$\Delta HE = h l w \Delta\gamma \hat{\tau}_y , \quad (A.46)$$

where  $h$  is the height,  $l$  is the length and  $w$  is the width of the shear panel element,  $\Delta\gamma$  is the incremental plastic shear strain and  $\hat{\tau}_y$  is the yield shear stress of the elasto-plastic component.

The elastic strain and hysteretic strain energies, calculated from the two components of the decomposition of the load-deformation relationship of any of the elements, are an approximation to the energies associated with the bilinear curve of the actual relationship. As shown in Figure A.2, the yield moment for the elasto-plastic component is less than the yield moment of actual relationship. The calculated hysteretic energy is the area enclosed within the load-deformation loops of the elasto-plastic component. For small values of strain hardening, the difference between the energies associated with the actual relationship and the bilinear decomposition is negligible.

**LIST OF REFERENCES**

1. Anderson, J. C. and V. V. Bertero, 1987, "Uncertainties in Establishing Design Earthquakes," *Journal of the Structural Division*, Vol. 113, No. 8. New York, American Society of Civil Engineers.
2. American Institute of Steel Construction, 1980, *Manual of Steel Construction*, Eighth Edition. New York, American Institute of Steel Construction.
3. American National Standard Institute, Inc., 1982, *American National Standard - Minimum Design Loads for Buildings and Other Structures*, ANSI A58.1-1982. New York, American National Standard Institute.
4. Applied Technology Council, 1978, *Tentative Provisions for the Development of Seismic Regulations for Buildings*, Report No. ATC 3-06. Redwood City, California, Applied Technology Council.
5. Axley, J. W. and V. V. Bertero, 1979, *Infill Panels: Their Influence on Seismic Response of Buildings*, UBC/EERC-79/28. Berkeley, California, Earthquake Engineering Research Center.
6. Becker, R., 1975, "Panel Zone Effect on the Strength and Stiffness of Steel Rigid Frames," *Engineering Journal*, Vol. 12, No. 1. New York, American Institute of Steel Construction.
7. Becker, R., 1976, *Practical Steel Design for Buildings 2-20 Stories*. New York, American Institute of Steel Construction.
8. Berg, G. V., 1983, *Seismic Design Codes and Procedures*. El Cerrito, California, Earthquake Engineering Research Institute.
9. Bertero, V. V., 1986, *Implications of Recent Earthquakes and Research on Earthquake-Resistant Design and Construction of Buildings*, UBC/EERC-86/03. Berkeley, California, Earthquake Engineering Research Center.
10. Bertero, V. V., 1986, "Lessons Learned from Recent Earthquakes and Research and Implications for Earthquake-Resistant Design of Building Structures in the United States," *Earthquake Spectra*, Vol. 2, No. 4. El Cerrito, California, Earthquake Engineering Research Institute.
11. Bertero, V. V. and R. W. Clough, 1986, "Interdependence of Dynamic Analysis and Experiment," *Dynamic Response of Structures*, ed. G. C. Hart and R. B. Nelson. New York, American Society of Civil Engineers.
12. Biggs, J. M., M. J. Holley and R. J. Hansen, 1977, "On Methods of Structural Analysis and Design for Earthquake," *Structural and Geotechnical Mechanics*, ed. W. J. Hall. Englewood Cliffs, New Jersey, Prentice-Hall.

13. Brokken, S. T. and V. V. Bertero, 1981, *Studies on Effects of Infills in Seismic R/C Construction*, UBC/EERC-81/12. Berkeley, California, Earthquake Engineering Research Center.
14. Cruz, E. F. and A. K. Chopra, 1985, *Simplified Methods of Analysis for Earthquake Resistant Design of Buildings*, UBC/EERC-85/01. Berkeley, California, Earthquake Engineering Research Center.
15. de Buen, O., 1980, "Steel Structures," Chapter 4 in *Design of Earthquake Resistant Structures*, ed. E. Rosenblueth. New York, Halsted Press.
16. Building Seismic Safety Council, 1986, *NEHRP Recommended Provisions for the Development of Seismic Regulations for New Buildings*, 1985 Edition, 3 Volumes, Federal Emergency Management Agency Earthquake Hazards Reduction Series 17, 18, and 19. Washington, D. C., U. S. Government Printing Office.
17. Clough, R. W. and J. Penzien, 1975, *Dynamics of Structures*. New York, McGraw-Hill.
18. Degenkolb, H. J., 1987, "A Study of the PA Effect," *Earthquake Spectra*, Vol. 3, No. 1. El Cerrito, California, Earthquake Engineering Research Institute.
19. Earthquake Engineering Research Institute, 1986, "Engineered Buildings," Chapter 3 in *Reducing Earthquake Hazards: Lessons Learned From Earthquakes*, Publication No. 86-02. El Cerrito, California, Earthquake Engineering Research Institute.
20. Freeman, S. A., 1985, "Drift Limits: Are they Realistic?," *Earthquake Spectra*, Vol. 1, No. 2. El Cerrito, California, Earthquake Engineering Research Institute.
21. Hall, W. J. and N. M. Newmark, 1980, "Earthquake Resistant Design Considerations." Presented at the EERI Seminar on Intra-Plate Earthquakes, Salt Lake City, Utah.
22. Housner, G. W., 1959, "Behavior of Structures During Earthquakes," *Journal of the Engineering Mechanics Division*, Vol. 85, No. EM4. New York, American Society of Civil Engineers.
23. International Conference of Building Officials, 1985, *Uniform Building Code, 1985 Edition*. Whittier, California, International Conference of Building Officials.
24. International Conference of Building Officials, 1988, *Uniform Building Code, 1985 Edition*. Whittier, California, International Conference of Building Officials.

25. Kanaan, A. and G. H. Powell, 1985, *General Purpose Computer Program for Inelastic Dynamic Response of Plane Structures*, UBC/EERC-73/06. Berkeley, California, Earthquake Engineering Research Center.
26. Klingner, R. E. and V. V. Bertero, 1976, *Infilled Frames in Earthquake-Resistant Construction*, UBC/EERC-76/32. Berkeley, California, Earthquake Engineering Research Center.
27. Krawinkler, H., V. V. Bertero and E. P. Popov, 1971, *Inelastic Behavior of Steel Beam-to-Column Subassemblages*, UBC/EERC-71/07. Berkeley, California, Earthquake Engineering Research Center.
28. Krawinkler, H., V. V. Bertero and E. P. Popov, 1975, "Shear Behavior of Steel Frame Joints," *Journal of the Structural Division*, Vol. 101, No. ST11. New York, American Society of Civil Engineers.
29. Krawinkler, H., 1978, "Shear in Beam-Column Joints in Seismic Design of Steel Frames," *Engineering Journal*, Vol. 15, No. 3. New York, American Institute of Steel Construction.
30. Krawinkler, H. and E. P. Popov, 1982, "Seismic Behavior of Moment Connections and Joints," *Journal of the Structural Division*, Vol. 108, No. ST2. New York, American Society of Civil Engineers.
31. Larson, M. A., 1987, "Needed Improvements in Aseismic Design," *Earthquake Spectra*, Vol. 3, No. 1. El Cerrito, California, Earthquake Engineering Research Institute.
32. Montgomery, C. J. and W. J. Hall, 1977, *Studies on the Seismic Design of Low-Rise Steel Buildings*, Civil Engineering Studies, Structural Research Series No. 442. Urbana, Illinois, University of Illinois.
33. Nau, J. M. and W. J. Hall, 1982, *An Evaluation of Scaling Methods for Earthquake Response Spectra*, Civil Engineering Studies, Structural Research Series No. 499. Urbana, Illinois, University of Illinois.
34. Newmark, N. M., 1959, "A Method of Computation for Structural Dynamics," *Journal of the Engineering Mechanics Division*, Vol. 85, No. EM3. New York, American Society of Civil Engineers.
35. Newmark, N. M., et al., 1977, "Seismic Design and Analysis Provisions for the United States", *Proceedings of the Sixth World Conference on Earthquake Engineering*, Vol. II. New Delhi, India.
36. Newmark, N. M., 1979, "Earthquake Resistant Design and ATC Provisions." Presented at the Third Canadian Conference on Earthquake Engineering, Montreal, Quebec.
37. Newmark, N. M. and W. J. Hall, 1982, *Earthquake Spectra and Design*. El Cerrito, California, Earthquake Engineering Research Institute.

38. Popov, E. P., 1983, *Seismic Moment Connections for Moment-Resisting Steel Frames*, UBC/EERC-83/02. Berkeley, California, Earthquake Engineering Research Center.
39. Popov, E. P., et al., 1985, "Cyclic Behavior of Large Beam-Column Assemblies," *Earthquake Spectra*, Vol. 1, No. 2. El Cerrito, California, Earthquake Engineering Research Institute.
40. Popov, E. P., 1986, "On California Structural Steel Seismic Design," *Earthquake Spectra*, Vol. 2, No. 4. El Cerrito, California, Earthquake Engineering Research Institute.
41. Powell, G. H., 1973, *DRAIN-2D User's Guide*, UBC/EERC-73/22. Berkeley, California, Earthquake Engineering Research Center.
42. Rivero, C. E. and W. H. Walker, 1982, *An Analytical Study of the Interaction of Frames and Infill Masonry Walls*, Civil Engineering Studies, Structural Research Series No. 502. Urbana, Illinois, University of Illinois.
43. Seismology Committee, 1985, *Recommended Lateral Force Requirements and Commentary*. Sacramento, California, Structural Engineers Association of California.
44. Thomson, W. T., 1981, *Theory of Vibration with Applications*, Second Edition. Englewood Cliffs, New Jersey, Prentice-Hall.
45. Wang, M. L., 1986, *Nonstructural Element Test Phase*, National Science Foundation Earthquake Mitigation Program. Berkeley, California, University of California.
46. Wang, M. L., 1986, "Full Scale Tests of Cladding Components," *Dynamic Response of Structures*, ed. G. C. Hart and R. B. Nelson. New York, American Society of Civil Engineers.
47. Wang, M. L., 1987, "Cladding Performance on a Full-Scale Test Frame," *Earthquake Spectra*, Vol. 3, No. 1. El Cerrito, California, Earthquake Engineering Research Institute.
48. Zahrah, T. F. and W. J. Hall, 1982, *Seismic Energy Absorption in Simple Structures*, Civil Engineering Studies, Structural Research Series No. 501. Urbana, Illinois, University of Illinois.